

Investigating mechanisms of Epstein-Barr virus reactivation in epithelial cells

Stefanie Žentelis

A thesis submitted for the degree of
Doctor of Philosophy

St Cross College
Nuffield Department of Clinical Medicine
University of Oxford

Trinity Term 2018

Abstract

Investigating mechanisms of Epstein-Barr virus reactivation in epithelial cells

Stefanie Žentelis
St Cross College
DPhil in Clinical Medicine
Trinity Term 2018

Approximately 10% of all gastric cancer cases worldwide are associated with Epstein-Barr virus (EBV) infection. This subgroup differs from non-infected equivalents through a distinct mutational and epigenetic signature, which is crucial for the establishment and maintenance of the viral latent state. Disruption of the latent state and subsequent induction of the lytic cycle, called reactivation, can be used as a therapeutic strategy for this cancer type through either combination with antiviral agents or by induction of an EBV-specific immune response.

In this study, epigenetic inhibitors were tested for their potential to reactivate EBV using a novel screening method based on the expression of Zebra, a key regulator of EBV reactivation. Histone deacetylase inhibitors (HDACis), more specifically benzamide-based HDACis, were the most potent group of reactivating agents in this screen. Those HDACis induced the expression of lytic cycle genes as well as targeted cell killing in combination with antiviral agents. Moreover, the reactivation through those agents was sufficient to activate cytotoxic T-cells and thereby ensured a supportive role of the immune system in targeted cell killing. In an additional screen, topoisomerase inhibitors and other chemotherapeutic agents showed synergistic effects on Zebra expression together with HDACis, which was linked to the induction of p53 expression through those compounds. While p53 is known to be involved in the expression of Zebra, the viral DNA processivity factor Ea-D and the viral DNA binding protein DNBI were identified as a potential novel binding protein of p53 and could thus point towards a novel role of p53 in EBV lytic replication.

Taken together, this study identifies potential novel therapeutic compound combinations for the treatment of EBV-associated epithelial cancers that could be translated into the clinic after further assessment.

Declaration

The material presented in this thesis is the result of my own work, except for the following sections:

1. All high-throughput screening experiments (Chapters 3.2.4 and 5.2.1.) have been performed in cooperation with the Target Discover Institute (TDI) Cellular High Throughput Screening Facility, Oxford. While members of the screening facilities were responsible for all robotic handling of the screening plates for seeding, treatment and imaging, I performed the staining for all plates manually. Val Millar generated a protocol to analyse the generated images regarding cell numbers and Zebra expression. Final analysis to identify hits was performed by me.
2. Computational analysis of compound classifications was performed by Dr Felix Zhou, University of Oxford (Chapters 3.2.4 and 5.2.1.).
3. The flow cytometry experiments performed in chapter 4.2.4 were performed together with Dr Thomas Partridge, University of Oxford. The cell culture part of the experiment and the staining were performed by me and Dr Thomas Partridge performed the actual flow cytometry of the experiments. Analysis of obtained data was performed by me.
4. The T-cell experiments in Chapter 4.2.5 were performed together with Dr Carol Leung, University of Oxford. We performed all parts including design of the experiment, cell culture and the enzyme-linked immunosorbent assays (ELISAs) in collaboration.
5. Two experiments analysing the p53 interactome by mass spectrometry were performed in collaboration with Dr Thomas Leissing (Chapter 5.2.6). The cell culture part of the experiment was performed by me, but the collection of the cells and the sample preparation were performed together. Mass spectrometry was performed at the Advanced Proteomics Facility of the TDI, Oxford by Dr Roman Fischer and Georgina Berridge. Analysis of the generated results was executed by Dr Thomas Leissing.

Contributions by the stated colleagues are clearly indicated in the text of the thesis where relevant. The work presented in this thesis has not been accepted or submitted for any other degree, diploma or other qualification at the University of Oxford or elsewhere. This thesis does not exceed 50,000 words, exclusive of bibliography, as required by the Nuffield Department of Medicine.

Acknowledgements

I would like to express my gratitude to my supervisor Prof. Xin Lu for her support during the last four years and for giving me the opportunity to complete my DPhil in her laboratory. I also wish to acknowledge the financial support I received from the Ludwig Cancer Research Institute, without which this DPhil would not have been possible.
I would like to extend my gratitude to my examiners Professors Paul Brennan and Paul Farrell for their time and effort.

I am thankful to past and present members of the Lu lab and other laboratories of the Ludwig Institute for providing a supportive, fun and educational environment to work in. In particular thanks go to Imogen Roth, Thomas Leissing, Michael White, Richard Owen, Ludo Buti, Carlos Ruiz Puig, Felix Zhou, David Severson, Carol Leung, Gopi Sutendra, Zinaida Dedeic, Khatoun Al Moussawi, Thomas Carroll and Michael McClellan.
I wish to acknowledge the colleagues who helped me during various stages of my DPhil: Thomas Partridge and Carol Leung for suggestions and help with immune cell assays and Ludo Buti, Thomas Leissing, Michael McClellan, Carol Leung and in particular Imogen Roth for useful suggestions on sections of my thesis.

Thanks must also be given to Mark Shipman, for his help with microscopy and image analysis, the TDI Cellular High Throughput Screening Facility for help in planning and performing high-throughput screening experiments and the Advanced Proteomics Facility for help with mass spectrometry experiments. Special thanks go to Claire Beveridge for critical reading of this thesis. Many thanks to Ludwig's past and present support and administration team including Alex Ward, Jan Twitchen, James Hall, Stan Ng, Carly Morris, Stephen Fisher, Jo Wainwright and David Bartle. I want to especially thank Veronica Counsell for her help and for being a constant source of support and encouragement.

I must thank my family; my parents Kerstin and Stefan, my sister Sandra, my grandparents Dorle and Franz as well as Renate and Horst for their love, encouragement and support. I am very grateful to my parents for always believing in me and supporting me no matter where my plans took me.

Special thanks must also go to my great friends Agata and Julia. Your friendship has made all the difference during my journey in Oxford and my sincere gratitude is beyond words.

Last but not least, my deepest gratitude goes to my husband Mindaugas for his unconditional love, tireless patience, support and endless supply of tissues. You have helped me to stay positive and excited during sometimes frustrating and demanding times. I also want to thank my in-laws for an endless supply of encouragement and Lithuanian treats.

I am indebted to you all for your invaluable contributions without which this DPhil would not have been achievable. Thank you all very much.

Table of contents

Abstract i

Declaration ii

Acknowledgements iii

Table of contents iv

Glossary of acronyms viii

List of figures xi

List of tables xiv

Chapter 1: Introduction 1

1.1 Introduction to cancer 1

1.2 The role of infectious agents in cancer 2

1.3 Viruses and cancer 4

1.3.1. RNA tumour viruses 7

1.3.2. DNA tumour viruses 8

1.3.3. Herpesvirus family 9

1.4 EBV 10

1.4.1. The EBV genome 11

1.4.2. General biology of EBV 13

1.5 The life cycle of EBV 17

1.5.1. Life cycle in B-cells 18

1.5.2. Life cycle in epithelial cells 20

1.5.3. The role of epigenetic marks in the life cycle of EBV 22

1.6 EBV lytic proteins 23

1.6.1. IE proteins 23

1.6.2. The key regulator Zebra 26

1.6.3. Early proteins 27

1.6.4. Late proteins 30

1.7 Immune evasion of EBV 31

1.7.1. Immune evasion during latency I/II 32

1.7.2. Immune evasion by lytic gene products 35

1.8 Reactivation of EBV 38

1.8.1. Physiological induction of the lytic cycle 38

1.8.2. Pharmacological reactivation 40

1.8.3. Antiviral cancer therapies 41

1.9 EBVaGC 44

1.9.1. Infection in gastric cancer 44

1.9.2. Genetic and epigenetic properties of EBVaGC 45

1.10 Aims of the study 47

Chapter 2: Materials and methods 48

2.1 Materials 48

2.1.1. Reagents for cell culture 48

2.1.2. Materials for cell-based assays 56

2.1.3. Reagents for DNA- and RNA-based techniques 58

2.1.4. Reagents for protein-based techniques 61

2.2 Methods 65

2.2.1. Cell culture methods 65

2.2.2. Cell-based assays 67

2.2.3. DNA- and RNA-based methods 71

2.2.4. Protein-based methods 75

Chapter 3: Inhibition of HDACs by benzamides induces Zebra expression in epithelial cells 77

3.1 Introduction 77

3.2 Results 81

3.2.1. Only HDACis induce Zebra expression in a panel of epigenetic inhibitors 81

3.2.2. Benzamide HDACis are more potent in inducing Zebra expression than other HDACi classes 86

3.2.3. The differences between groups of HDACis are not caused by differential histone H3 acetylation or HDAC expression 91

3.2.4. Benzamide-containing HDACis, but not all benzamides, induce Zebra expression 94

3.3 Summary and brief discussion 99

Chapter 4: Characterisation of two novel HDACis and their potential to reactivate EBV 101

4.1 Introduction 101

4.2 Results 104

4.2.1. Chidamide and CXD101 induce Zebra expression in a panel of epithelial cell lines 104

4.2.2. Expression of the whole lytic cascade is induced by HDAC inhibition 108

4.2.3. The combination of HDACi treatment with antiviral compounds leads to increased cell death 111

4.2.4. Reactivation by HDACi treatment downregulates HLA class I expression 114

4.2.5. Reactivation through HDACi treatment is sufficient to activate cytotoxic T-cells 117

4.3 Summary and brief discussion 119

Chapter 5: The role of p53 in the induction of Zebra expression 124

5.1 Introduction 124

5.2 Results 126

5.2.1. Topoisomerase inhibitors increase Zebra expression in combination with chidamide 126

5.2.2. Not all chemotherapeutic agents induce Zebra expression together with chidamide 135

5.2.3. Induction of p53 increases the level of Zebra expression induced by HDACi treatment 138

5.2.4. Knockdown of p53 abolishes the reactivation potential of HDACis 145

5.2.5. Protein levels of p53 and Sp1 influence the level of Zebra expression 147

5.2.6. Identification of novel interactions between p53 and lytic EBV proteins 149

5.2.7. Differential effect of combinatorial treatment on cell viability in gastric cancer cells 154

5.3 Summary and brief discussion 158

Chapter 6: Different patterns of viral lytic gene expression upon drug treatment 164

6.1 Introduction 164

6.2 Results 165

6.2.1. Combination of chidamide with epirubicin treatment induces abortive lytic cycle expression 165

6.2.2. Effects of topoisomerase inhibitors on viral DNA replication 169

6.2.3. Epirubicin and chidamide treatment together increases the occurrence of modified Zebra 172

6.3 Summary and brief discussion 177

Chapter 7: Final discussion and perspectives 182

7.1 Overview 182

7.2 Role of class I HDACs and histone acetylation in EBV reactivation 183

7.3 Mechanisms of drug-induced reactivation 185

7.3.1. The involvement of p53 in Zebra induction 185

7.3.2. Potential role of the cell cycle state in EBV reactivation 186

7.3.3. Potential role of the DNA damage response in EBV reactivation 188

7.3.4. Effect of posttranslational Zebra modifications on EBV reactivation 193

7.3.5. A potential role of p53 in the lytic replication of EBV 195

7.3.6. Alternative compound classes with an effect on EBV reactivation 197

7.4 Potential lytic induction therapy for EBV-associated epithelial malignancies 199

7.4.1. Potential novel treatment combinations for the treatment of EBV-related epithelial cancers 200

7.4.2. The role of the immune system in lytic induction therapy 201

7.4.3. Implications of the latent EBV pool in B-cells for lytic induction therapy 202

7.5 Final remarks 203

Bibliography 204

Appendix 257

Appendix tables 257

Appendix figures 263

ImageJ macro for the quantification of the Zebra signal per cell 267

Glossary of acronyms

Abbreviation	Name
5-Aza	5-azacytidine
5-FU	5-Fluorouracil
ACV	Acyclovir
ATF2	Activating transcription factor 2
ATM	Ataxia-telangiectasia mutated protein
ATP	Adenosine triphosphate
BARTs	*Bam*HIA rightward transcripts
BCL-2	B-cell lymphoma 2
BCR	B-cell receptor
BET	Bromodomain and extra-terminal
BLIMP1	B-lymphocyte-induced maturation protein 1
BSA	Bovine serum albumin
bZIP	Basic leucine zipper
CBP	CREB-binding protein
cDNA	Complementary DNA
CK2	Casein kinase II
CMV	Cytomegalovirus
CR1/2	Complement receptor 1/2
CREB	cAMP response element-binding protein
CSF-1	Colony stimulating factor-1
CTL	Cytotoxic T-cell
CXCL-11	C-X-C motif chemokine 11
DAPI	4’,6-diamidino-2-phenylindole dihydrochloride
DMSO	Dimethyl sulfoxide
DNA	Deoxyribonucleic acid
DNA-PK	DNA-dependent protein kinase
dNTP	Deoxyribonucleotide triphosphate
DSB	Double-strand break
E	Early lytic genes
Ea-D	Early antigen diffuse component
EBER1/2	EBV-encoded RNA 1/2
EBNA1	EBV nuclear antigen 1
EBV	Epstein-Barr virus
EBVaGC	EBV-associated gastric carcinoma
EBV-PK	EBV protein kinase
EDTA	Ethylenediaminetetraacetic acid
ELISA	Enzyme-linked immunosorbent assay
EphA2	Ehrin type-A receptor 2
ER	Endoplasmic reticulum
FBS	Foetal bovine serum
FDA	Food and Drug Administration
GAPDH	Glyceraldehyde 3-phosphate dehydrogenase
GCV	Ganciclovir
GFP	Green fluorescent protein
HAT	Histone acetyltransferases

HBV	Hepatitis B virus
HCC	Hepatocellular carcinoma
HCMV	Human cytomegalovirus
HCV	Hepatitis C virus
HDAC	Histone deacetylase
HDACi	Histone deacetylase inhibitor
HHV	Human herpesvirus
HIV	Human immunodeficiency virus-1
HLA	Human leukocyte antigen
HPV	Human papillomavirus
HRP	Horseradish peroxidase
HSV	Herpes simplex virus
HTLV-1	Human T-cell lymphotropic virus type-1
IARC	International Agency for Research on Cancer
IE	Immediate-early lytic genes
IFNγ	Interferon γ
IL	Interleukin
IKKα/β	Iκ kinase α/β
IRF	Interferon regulatory factor
JNK	c-Jun N-terminal kinase
KS	Kaposi's sarcoma
KSHV	Kaposi sarcoma herpesvirus
L	Late lytic genes
LCL	Lymphoblastoid cell line
LMP1	Latent membrane protein 1
mAb	Monoclonal antibody
MCV	Merkel cell polyomavirus
mDBP	Major DNA binding protein
MDM2	Mouse double minute 2 homolog
MEF2D	Myocyte enhancer factor 2D
meZRE	Methylated Zebra-response element
mRNA	Messenger ribonucleic acid
MHC	Major histocompatibility complex
MS	Mass spectrometry
NAD	Nicotinamide adenine dinucleotide
NF-κB	Nuclear factor-κB
NK	Natural killer
NPC	Nasopharyngeal Carcinoma
oriLyt	Origin of lytic DNA replication
panH3ac	Acetylated histone H3
PBMCs	Peripheral blood mononuclear cells
PBS	Phosphate-buffered saline
PCR	Polymerase chain reaction
PD-L1	Programmed death-ligand 1
PEL	Primary effusion lymphoma
PI3K	Phosphoinositide-3-kinase
PKR	Protein kinase R
PTEN	Phosphatase and Tensin homolog

PTM	Posttranslational modification
RNA	Ribonucleic acid
Rp	Rta promoter
RPMI	Roswell Park Memorial Institute
RT-qPCR	Real-time quantitative PCR
SAHA	Suberoylanilide hydroxamic acid
SB	Sodium butyrate
SDS	Sodium dodecyl sulfate
SGC	Structural Genomics Consortium
siRNA	Small interfering RNA
Sp1	Specificity protein 1
STAT	Signal transducers and activators of transcription
SV40	Simian vacuolating virus 40
TAE	Tris-acetate-EDTA
TAP	Transporter associated with antigen processing
TBS	Tris-buffered saline
TBS-T	TBS-Tween
TDI	Target Discovery Institute
TGFβ	Transforming growth factor β
TLR	Toll-like receptor
TNFα	Tumour necrosis factor α
TRs	Terminal repeats
TSA	Trichostatin A
UV	Ultraviolet
VCA	Viral capsid antigen
vIL-1	Viral IL-10
VPA	Valproic acid
VZV	Varicella-Zoster virus
XBP-1	X-box binding protein 1
YY1	Ying yang protein 1
ZBP-89	Zinc-finger DNA-binding protein 89
ZEB1/2	Zinc finger E-box binding homeobox 1/2
Zp	Zebra promoter
ZRE	Zebra-response element

List of figures

Figure 1 The seven classes of virus distinguished by genome replication and encapsidation strategies defined in the Baltimore classification. 7
Figure 2 Structure of the herpesvirus virion. 9
Figure 3 Diagram showing the location and transcription of EBV latent genes on the double-stranded viral DNA episome. 12
Figure 4 Models of primary B-cell infection by EBV. 16
Figure 5 Model of EBV entry into B-cells. 18
Figure 6 Life cycle of EBV infection in epithelial cells. 19
Figure 7 Model of EBV entry into epithelial cells. 21
Figure 8 Transcription factors with known roles in the regulation of Zp and Rp, the promoters of *BZLF1* and *BRLF1,* respectively. 24
Figure 9 Model of replication complex formation at oriLyt after the induction of the lytic phase of EBV's life cycle. 28
Figure 10 Immune evasion mechanisms in latent EBV infection. 33
Figure 11 Immune evasion mechanisms in lytic EBV infection. 36
Figure 12 Model of lytic induction therapy. 42
Figure 13 Overview of histone modifications and epigenetic readers, writers and erasers. 78
Figure 14 Zebra-based screening method for EBV reactivation in epithelial cells. 81
Figure 15 Example of nuclear identification by an ImageJ macro used for the analysis of immunofluorescence images. 82
Figure 16 Epigenetic inhibitor screening for EBV reactivation in YCCEL1 cells. 84
Figure 17 Zebra expression induced by epigenetic inhibitor treatment in YCCEL1 cells analysed by western blot. 85
Figure 18 Structural comparison of HDACi classes. 86
Figure 19 Comparison of the EBV reactivation potential of hydroxamates and benzamide HDACi. 88
Figure 20 Comparison of Zebra expression levels upon HDACi treatment by western blot. 90
Figure 21 Comparison of histone H3 acetylation upon HDACi treatment. 92
Figure 22 Western blot comparison of HDAC class I expression levels upon HDACi treatment. 93
Figure 23 Western blot validation of hits identified in the high-throughput screen. 96
Figure 24 Comparison of potential hits with benzamide HDACi controls as well as benzamide-based compounds included in the FDA-approved library screen. 98
Figure 25 Western blot analysis of Zebra expression upon HDACi treatment in a panel of epithelial cell lines. 104
Figure 26 Quantification of Zebra expressing cells upon HDACi treatment in different cell lines by immunofluorescence. 106
Figure 27 Western blot analysis of Zebra expression upon HDACi treatment in a panel of B-cell lines. 107
Figure 28 Comparison of lytic RNA expression levels upon HDACi treatment in different cell lines. 109

Figure 29 Quantification of VCA expression levels in different cell lines by immunofluorescence. 110
Figure 30 BGLF4 expression and cell killing by antiviral compounds in HDACi-treated cells. 113
Figure 31 HLA class I expression levels upon HDACi treatment in epithelial cell lines analysed by flow cytometry. 115
Figure 32 Changes in HLA class I expression levels relative to Zebra levels upon HDACi treatment in different cell lines analysed by flow cytometry. 116
Figure 33 Measurement of INF-γ secretion by ELISA in co-culture of HDACi treated epithelial cells with a T-cell clone specific to the lytic protein BMLF1. 118
Figure 34 Distribution of compound classifications in the extended FDA library and in the identified hits. 128
Figure 35 Induction of Zebra expression by topoisomerase inhibitor treatment alone or in combination with chidamide in YCCEL1 cells. 134
Figure 36 Zebra expression induced by chemotherapeutic treatment in combination with chidamide. 137
Figure 37 Zebra expression levels upon HDACi treatment in combination with Nutlin-3a assessed by western blot in a panel of EBV-positive epithelial cell lines. 139
Figure 38 Quantification of Zebra-expressing cells in different epithelial cell lines treated with chidamide and CXD101 alone or in combination with Nutlin-3a. 140
Figure 39 Zebra expression levels upon HDACi treatment in combination with Nutlin-3a treatment assessed by immunofluorescence staining in YCCEL1 cells. 142
Figure 40 Percentage of Zebra-expressing cells in YCCEL1 cells upon treatment with a panel of HDACis with or without Nutlin-3a. 144
Figure 41 Comparison of Zebra expression levels upon HDACi treatment in combination with Nutlin-3a and epirubicin in epithelial and B-cell lines. 145
Figure 42 Zebra expression after p53 knockdown in a panel of epithelial cells treated with either chidamide or CXD101 with Nutlin-3a. 146
Figure 43 Zebra expression after p53 knockdown in YCCEL1 cells treated with doxorubicin or epirubicin in combination with chidamide. 147
Figure 44 Influence of Sp1 and p53 levels on Zebra expression in YCCEL1 cells treated with different HDACis and Nutlin-3a. 149
Figure 45 Western blot analysis of p53 interactome samples used for MS analysis. 150
Figure 46 Comparison of identified and previously reported p53 interactors and examples of their detected abundance. 152
Figure 47 EBV proteins identified to bind p53 after 24 h of compound treatment and their normalised abundance. 154
Figure 48 BGLF4 expression and cell killing in combination therapy together with antiviral agents. 156
Figure 49 EBV lytic gene expression upon different combinatorial treatments with chidamide assessed by qPCR. 167

Figure 50 Zebra and Ea-D expression induced by chemotherapeutic treatment in combination with chidamide. 169
Figure 51 Examination of viral DNA amplification upon treatment with epirubicin and Nutlin-3a alone or in combination with chidamide. 170
Figure 52 Examination of viral DNA amplification upon treatment with different topoisomerase inhibitors and Nutlin-3a alone or in combination with chidamide. 171
Figure 53 Modifications of Zebra detected by western blot in YCCEL1 cells treated with topoisomerase inhibitors in combination with chidamide. 173
Figure 54 Modifications of Zebra detected by western blot in YCCEL1 cells treated with chemotherapeutic agents in combination with different HDACis. 175
Figure 55 Time course of the occurrence of Zebra modifications by western blot in YCCEL1 cells treated with epirubicin or Nutlin-3a in combination with chidamide. 176
Figure 56 Model of the synergistic effect of HDACi and topoisomerase inhibitor treatment on EBV lytic cycle induction. 192
Figure 57 Model of the role of Zebra modifications in EBV lytic cycle induction by treatment with different compounds. 194
Figure 58 Model of the role of p53 in lytic DNA replication of EBV. 196

Appendix Figure 1 Percentage of Zebra-expressing cells induced by topoisomerase inhibitor treatment at different concentrations. 263
Appendix Figure 2 Comparison of identified and previously reported p53 interactors with examples of their detected abundance. 264
Appendix Figure 3 EBV proteins identified to bind p53 after 48 hours of compound treatment and their normalised abundance. 265
Appendix Figure 4 Percentage of Zebra-expressing cells induced by decitabine treatment at different concentrations. 266

List of tables

Table 1 Cancer cases attributed to infection in 2012. 4
Table 2 Global deaths associated with EBV-positive malignancies in 2010. 11
Table 3 EBV latency expression profiles and associated malignancies. 15
Table 4 List of epithelial cell lines used in this study. 48
Table 5 List of lymphoid cell lines used in this study. 49
Table 6 List of compounds used in this study. 51
Table 7 List of compounds and their concentrations used for the extended SGC screen. 52
Table 8 List of HDACi concentrations used in this study. 53
Table 9 List of topoisomerase inhibitors and their concentrations used in this study. 54
Table 10 List of DNA primers used in this study. 59
Table 11 List of siRNA oligos used in this study. 60
Table 12 List of Taqman™ probes used for quantification of the EBV load per cell. 60
Table 13 List of primary antibodies used in this study 61
Table 14 List of secondary antibodies used in this study. 61
Table 15 Recipes for the preparation of stacking and resolving SDS-polyacrylamide gels. 63
Table 16 Composition of RT-qPCR reactions. 71
Table 17 Composition of the PCR reaction for the amplification of *TP53* cDNA. 72
Table 18 Cell numbers used for reverse transfection in 24-well plates. 73
Table 19 Composition of qPCR reactions for the quantification of the EBV genome load per cell. 74
Table 20 Classification of HDAC members into four classes. 79
Table 21 Table summarising the Zebra expression and cellular toxicities of a panel of HDACis in YCCEL1 cells. 89
Table 22 Hits of FDA-approved compound screen. 95
Table 23 Benzamide compounds contained in the FDA-approved library. 97
Table 24 HDACis approved for clinical use. 102
Table 25 Top 10 hits identified in a high-throughput screen of an extended FDA library with or without the addition of chidamide in YCCEL1 cells. 130
Table 26 Top 10 topoisomerase inhibitors included in the extended FDA library based on their Zebra expression in combination with chidamide treatment. 132
Table 27 Overview of different types of DNA damage and the DNA repair pathways they induce. 189

Appendix Table 1 Extended SGC compound library information. 257
Appendix Table 2 Biochemical inhibition of HDAC1-9 by HDACis (Ki [nM]). 258
Appendix Table 3 Additional compounds of extended FDA-approved library. 259
Appendix Table 4 Complete list of screening hits alone or in combination with chidamide treatment. 261
Appendix Table 6 *TP53* status in different cell lines. 262

Chapter 1: Introduction

1.1 Introduction to cancer

Cancer is one of the leading causes of mortality worldwide, accounting for 8.8 million deaths in 2015 (Boyle & Levin, 2014). Over the next two decades, the number of new cancer cases is expected to rise by around 70% (Ferlay *et al*., 2013). The most common forms of cancer are lung, female breast, bowel and prostate cancer, which together comprised 53% of UK cancer cases in 2015 (Ferlay *et al*., 2013; Cancer Research UK, 2018).

Cancer is a disease of deregulated cell growth in which a subpopulation of cells disregards the rules of cell division (reviewed in Dominguez-Brauer *et al.*, 2015). This is commonly caused by mutations of the deoxyribonucleic acid (DNA) sequence or epigenetic dysregulation, collectively changing cellular gene expression and thereby enabling proliferation (You & Jones, 2012). In the early 90s, Vogelstein and colleagues proposed that the acquisition of the necessary mutations for the development of colorectal cancer occurs in a stepwise manner (Fearon & Vogelstein, 1990; Cho & Vogelstein, 1992). This is the basis for the adenoma–carcinoma sequence in which a benign tumour develops towards a highly malignant stage through the stepwise accumulation of a defined set of genetic mutations.

One group of commonly mutated genes in cancer are so-called tumour suppressor genes, which induce a selective growth advantage when inactivated by mutation or other mechanisms (Vogelstein *et al*., 2013). One example of a tumour suppressor gene is *TP53*, which is mutated in over 50% of human cancers and plays an important role in apoptosis, DNA repair and cell cycle regulation (reviewed in Herrero *et al.*, 2016). Another group of genes implicated in tumour development are oncogenes, which lead to a selective growth advantage when activated by mutation (Vogelstein *et al.*, 2013). A commonly cited example are gain-of-function mutations of the *RAS* oncogene or in the RAS signalling pathways,

which have been shown to promote carcinogenesis in multiple cancer types (reviewed in Fernández-Medarde and Santos, 2011).

In 2000, Weinberg and Hanahan defined the hallmarks of cancer including characteristics such as evasion of apoptosis, self-sufficiency in growth signals, insensitivity to antigrowth signals, tissue invasion and metastasis, as well as sustained angiogenesis (Hanahan & Weinberg, 2000). In a follow-up study, these hallmarks were expanded to include deregulated cellular energetics, the escape of immune destruction, genome instability and tumour-promoting inflammation (Hanahan & Weinberg, 2011).

In summary, the acquisition of mutations and features of different cancer hallmarks spontaneously and over time is believed to lead to the development of malignancies.

1.2 The role of infectious agents in cancer

In the late 1800s, three different theories for the causes of cancer were debated, one of which suggested that cancer was caused by infectious or parasitic agents (reviewed in Blackadar *et al.*, 2016). Even though a broad range of microbes were identified in cancerous growths, none of them could be used to induce cancer reproducibly (reviewed in Chang and Parsonnet, 2010). In 1911, Ferguson reported a case study of *Schistosoma haematobium* and bladder cancer in Egypt (Ferguson, 1911). Another parasitic fluke, *Opisthorchis viverrini*, is endemic in Thailand and was suspected to be linked to bile duct cancer in 1931 (reviewed in Sripa *et al.*, 2011). The bacterium *Helicobacter pylori*, which is known to cause chronic inflammation in the stomach called gastritis, was linked to cancer around 50 years later (Marshall & Warren, 1984; Marshall *et al.*, 1985; Morris & Nicholson, 1987; Morris *et.al.*, 1991). It is believed that the chronic inflammation caused by infection with certain mycoplasma, bacteria or viruses can promote tumour development and is therefore associated with increased cancer risk (Grange *et al.*, 2011).

The widespread occurrence of most infections and the long periods required for malignant transformation were some of the reasons for the difficulties in identifying carcinogenic functions of pathogens (reviewed in zur Hausen, 2009). As a consequence, the process of identifying carcinogenic infections is still far from completed. Nevertheless, today it is believed that around 20% of the global cancer burden worldwide is associated with infectious agents (Vandeven & Nghiem, 2014). The parasites *O. viverrini*, *Chlonorchis sinensis* and *S. haematobium*, as well as the bacterium *H. pylori*, have been named as biological carcinogenic agents in the last report of the International Agency for Research on Cancer (IARC) (Table 1) (IARC Working Group on the Evaluation of Carcinogenic Risks to Humans, 2012).

Table 1: Cancer cases attributed to infection in 2012. Adapted from Epstein *et al.*, 1964; Ferguson, 1911; Marshall & Warren, 1984; Blackadar *et al.*, 2016; Plummer *et al.*, 2016.

	Infectious agents	Year of discovered link to cancer	Number of new cancer cases	Proportion of new cases attributable to each infectious agent
Viruses	Hepatitis B virus Hepatitis C virus	1981 1989	420,000 170,000	19.2% 7.8%
	Human papillomavirus	1987	640,000	29.5%
	Epstein-Barr virus	1964	120,000	5.5%
	Kaposi sarcoma herpesvirus	1994	44,000	2.0%
	Human T-cell lymphotropic virus 1	1980	3,000	0.1%
Bacteria/ parasites	*H. pylori*	1984	770,000	35.4%
	O. viverrini or *C. sinensis*	1966-1973	1,300	0.1%
	S. haematobium	1911	7,000	0.3%
	All infectious agents		2,200,000	100%

1.3 Viruses and cancer

The first evidence for a role of viral infection in carcinogenesis was shown more than 100 years ago (reviewed in Blackadar *et al.*, 2016). In 1908, Ellermann and Bang showed that filtered extracts from chicken leukaemia cells could pass leukaemia on to healthy chickens (Ellermann & Bang, 1908). In 1911, Francis Peyton Rous was able to show that, in chickens, sarcomatous chest tumours could be transmitted through cell-free tumour extracts and thus must be caused by a small transmissible agent, hypothesised to be a virus (Rous, 1911). Richard Edwin Shope described the first mammalian tumour

virus, the cottontail rabbit papillomavirus, in 1933 (Shope & Hurst, 1933). In 1960, Sweet and Hilleman discovered a new virus in cultures of rhesus monkey kidney cells, named Simian vacuolating virus (SV40) (Sweet & Hilleman, 1960). The tumourigenic potential of this monkey virus was shown later by injection into newborn hamsters (Eddy *et al.*, 1962; Girardi *et al.*, 1962). The first human tumour virus, Epstein-Barr virus (EBV), was not described until 53 years after Rous' initial experiment. In 1964, EBV particles were shown by electron microscopy in cell lines from African patients with Burkitt's lymphoma (Epstein *et al.*, 1964) . In addition to EBV, six more human cancer viruses have been discovered to date (Table 1). In 2008, Harald zur Hausen received the Nobel Prize for identifying a high-risk human papillomavirus (HPV) strain that accelerates cervical cancer development (Durst *et al.*, 1991; zur Hausen, 2009). This research was the basis for the development of the first virus-based cancer vaccine, which aims to minimise the development of HPV-induced cervical cancer (reviewed in McCormack, 2006). Recently, a novel virus, the Merkel cell polyomavirus (MCV), was detected in Merkel cell carcinoma, a rare type of skin cancer (Feng *et al.*, 2008). While a positive association has been observed between MCV infection and Merkel cell carcinoma, current evidence is not sufficient to classify MCV as a biological carcinogenic agent (IARC Working Group on the Evaluation of Carcinogenic Risks to Humans, 2014).

In their 2012 report, the IARC named the following viruses as biological carcinogenic agents with sufficient evidence to be linked to human cancer in addition to HPV: Hepatitis B virus (HBV), Hepatitis C virus (HCV), Kaposi sarcoma (KS) herpesvirus (KSHV), Human immunodeficiency virus-1 (HIV), Human T-cell lymphotropic virus type-1 (HTLV-1) and EBV (IARC Working Group on the Evaluation of Carcinogenic Risks to Humans, 2012; Martel *et al.*, 2012). In total, 12% of human cancer cases worldwide are associated with oncogenic viruses, 80% of which occur in the developing world (Bouvard *et al*., 2009; Boyle & Levin, 2014).

Certain common traits of viral oncogenesis are shared between different viruses (Bouvard *et al.*, 2009; zur Hausen, 2009). Firstly, oncoviruses are not sufficient for tumourigenesis. Therefore, the cancer incidence is significantly lower than virus prevalence in the human population (reviewed in Mesri *et al.*, 2014). Secondly, viral cancers are mostly connected to persistent viral infections, delaying potential cancer occurrence until years after the original acute infection (Beasley *et al.*, 1981; Wallin *et al.*, 1999).

Viruses can act at different stages in carcinogenesis. They can be part of an early carcinogenic event through viral integration and insertional mutagenesis, as well as virus-induced DNA damage (Chen *et al.*, 2014). In addition, they are able to dysregulate cellular processes through the expression of viral proteins. The first-described viral transforming gene was the tyrosine-protein kinase *v-Src*, which is expressed by the ribonucleic acid (RNA) retrovirus Rous sarcoma virus (Martin *et al.*, 1979). This constitutively active form of human *c-Src* acts as a proto-oncogene and was the first-discovered cellular oncogene (Martin, 2004). Nevertheless, viral infection provides only a subset of the necessary hits within the context of multistep carcinogens and often relies on other factors such as immunosuppression, chronic inflammation or environmental mutagens (Bouvard *et al.*, 2009; zur Hausen, 2009).

Viruses can be divided into seven different classes using the Baltimore classification (Figure 1) (Baltimore, 1971). This is based on differences in viral genome replication as well as the nucleic acids encoding for the viral genome, which are further discussed in Chapters 1.3.1 and 1.3.2.

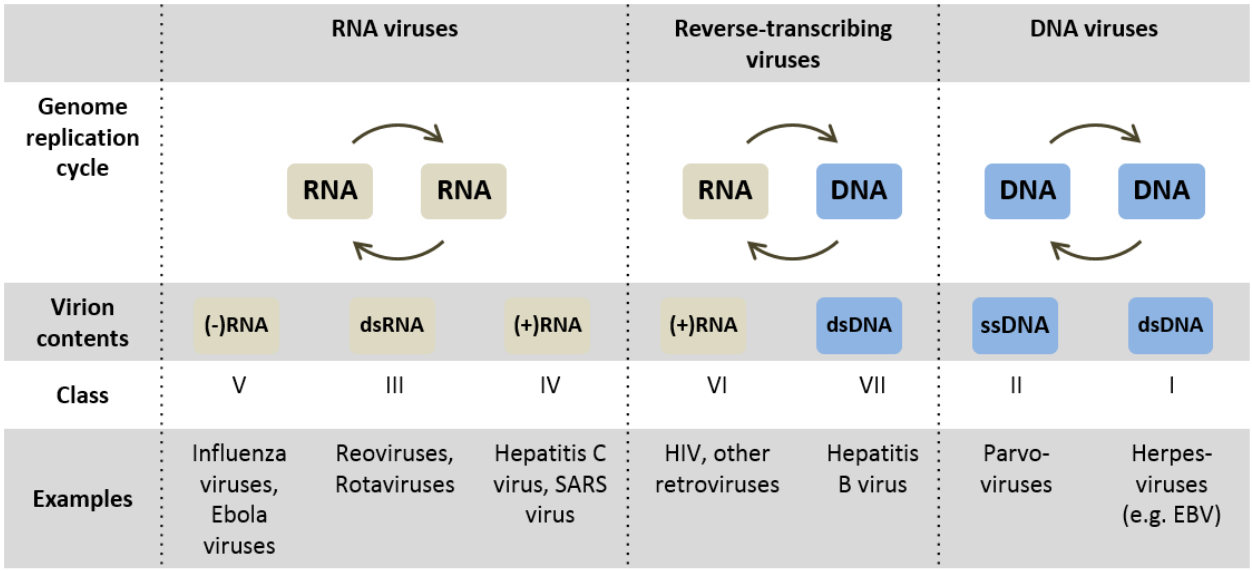


Figure 1: The seven classes of virus distinguished by genome replication and encapsidation strategies defined in the Baltimore classification. (+) RNA, positive-strand RNA, is single-stranded RNA of the same polarity as cellular mRNA that can be used as a template for translation. (-)RNA, negative-strand RNA, is single-stranded RNA of anti-mRNA polarity that needs to be transcribed into mRNA upon viral infection. Reverse-transcribing viruses depend on either DNA or RNA intermediates for the translation of their genetic information within the host cell (adapted from Ahlquist, 2006). dsDNA – double-stranded DNA; dsRNA – double-stranded RNA; EBV – Epstein-Barr virus; HIV – human immunodeficiency virus; SARS – severe acute respiratory syndrome; ssDNA – single-stranded DNA.

1.3.1. RNA tumour viruses

RNA viruses are defined as viruses that use RNA as their genetic material. Several classes of viruses belong to this category. Class III viruses are double-stranded RNA viruses that have segmented genomes such as reoviruses and rotaviruses; this means that their genome is encoded by several molecules of double-stranded RNA (Baltimore, 1971).

In addition, there are several classes of single-stranded RNA viruses that can be further classified according to the polarity of their RNA. Positive-sense RNA is identical to messenger RNA (mRNA) and can therefore be directly translated by the host cell (class IV viruses) (Figure 1). In comparison, negative-sense RNA is antisense RNA that is complementary to mRNA (class V viruses). Thus, besides needing to encode for an RNA-dependent RNA polymerase, these viruses also package the RNA

polymerase in their virions to allow the mRNA to be transcribed upon infection of the host cell. Class IV viruses contain a single positive-sense RNA that serves as mRNA. Examples of this group of viruses are HCV and severe acute respiratory syndrome virus. Influenza and Ebola are examples of class V viruses that contain a single negative-strand RNA, which serves as the template for the production of mRNA by virus-specific enzymes. Retroviruses or class VI viruses such as HIV and HTLV-1 also contain single plus-stranded RNA genomes. This group of viruses requires the inclusion of a viral reverse transcriptase into their virion. Upon infection, this enzyme transcribes the viral RNA into proviral complementary DNA (cDNA), which can then be integrated into the host genome. Thus, the host cell is used to express viral genes and package them into virions.

The RNA viruses that are most commonly associated with tumour occurrence are HCV and HTLV-1. HCV, mostly affiliated with lymphomas and hepatocellular carcinomas (HCCs), is associated with 7.8% of virus-associated cancer cases annually (Plummer *et al*., 2016). In contrast, HTLV-1 correlates with 0.1% of virus-associated cancer cases (Plummer *et al*., 2016).

1.3.2. DNA tumour viruses

DNA viruses are viruses that use DNA as their genetic material. They can be divided into two groups: single- and double-stranded viruses (Figure 1) (Baltimore, 1971). Class I viruses contain a single molecule of double-stranded DNA, such as herpesviruses and adenoviruses. Class II viruses are made of single-stranded DNA that is copied into double-stranded DNA before transcription in the host cell, such as the virus families Reoviridiae and Birnaviridae. Group VII viruses are reverse-transcribing DNA viruses such as HBV. They contain a double-stranded, gapped genome that is transcribed into an RNA intermediate before being used as a template by the viral reverse transcriptase for production of the DNA genome.

Small DNA tumour viruses such as SV40 and adenoviruses have been shown to be associated with mammalian and avian tumours, but association with human tumours has not yet been established (reviewed in Javier and Butel, 2008). In contrast, several DNA viruses have been shown to be associated with human cancer such as HBV with liver cancer; EBV with different lymphomas, nasopharyngeal carcinoma (NPC) and gastric cancer; KSHV with lymphoma; and high-risk HPV with cervical and other cancers (Plummer *et al*., 2016).

1.3.3. Herpesvirus family

Herpesviridae are a large family of DNA viruses that infect several vertebrate hosts and are responsible for human and animal diseases. Herpesviruses are characterised by four distinct morphological features: the core, nucleocapsid, tegument and envelope (Figure 2) (Chen *et al.*, 2016). The double-stranded DNA genome is contained in the core, which itself is located inside an icosadeltahedral nucleocapsid. The tegument consisting of numerous proteins is an amorphous structure located between the nucleocapsid and the viral envelope. The tegument connects the nucleocapsid to the envelope, which is the outermost structure of the herpes virion.

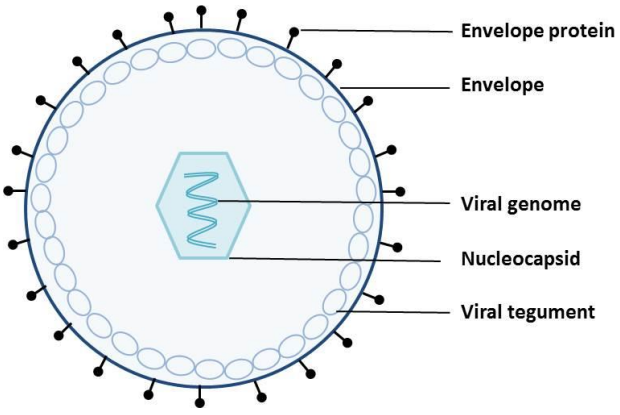


Figure 2: Structure of the herpesvirus virion. Herpesviruses have a unique structure, characterised by a core of double-stranded DNA that is surrounded by the nucleocapsid. The tegument envelops the nucelocapsid and is surrounded by the envelope. The surface of the virion is covered by glycoproteins, the so-called envelope proteins (modified from Chen *et al.*, 2016).

Herpesviruses can be divided into three subfamilies. Alphaherpesvirinae have a variable host range and show a short replicative cycle in the host's mucosal epithelium (reviewed in Van de Walle *et al.*, 2008). Latent infection is established in the sensory ganglia of the nervous system (Smith, 2012). Examples of this neurotropic group of viruses are herpes simplex virus (HSV) 1, HSV-2 and varicella-zoster virus (VZV). In contrast, betaherpesvirinae have a restricted host range with a long reproductive cycle, which often results in the development of a carrier state (reviewed in Jenkins and Hoffman, 2000). Latency can be established in lymphocytes, secretory glands and cells of the kidney, as well as in other cell types (Chen & Hudnall, 2006). Viruses belonging to this group are cytomegalovirus (CMV), human herpesvirus (HHV) 6 and HHV-7. Gammaherpesvirinae have a restricted host range with replication and latency occurring in lymphoid tissues (reviewed in Jenkins and Hoffman, 2000). Viral replication is generally restricted to either T- or B-cells, but lytic cycle expression of some family members has been demonstrated in epithelial, endothelial and fibroblastic cells (Krug *et al.*, 2004; Frangou *et al.*, 2005; Suárez and Van Dyk, 2008). This family can be further subdivided into two genera: *Lymphocyrptovirus*, such as EBV, and *Rhadinovirus*, such as KSHV (Damania, 2004).

EBV and KSHV are the two oncogenic herpesviruses recognised by the IARC and were associated with 5.5 and 2.0% of cancer cases in 2012, respectively (Table 1) (Plummer *et al*., 2016).

1.4 EBV

EBV or HHV-4 is a human gammaherpesvirus that persistently infects more than 90% of the adult population worldwide, residing in the B-lymphocytes in infected individuals (Young and Rickinson, 2004; Young *et al.*, 2016). In developing countries, 90% of children over the age of two are seropositive for EBV (Hjalgrim *et al.*, 2007). In developed countries, infection usually occurs either in young preschool children or during adolescence, at which age acute infection can be either asymptomatic or cause infectious mononucleosis, a self-limiting disease (Hjalgrim *et al.*, 2007).

Even though EBV infection is usually quiescent, it is associated with human proliferative diseases in lymphoid or epithelial cells. The former group of diseases encompasses mainly Burkitt's lymphoma, classical Hodgkin lymphoma and, to a lesser degree, post-transplant lymphoproliferative disease and non-Hodgkin lymphomas in HIV-infected patients. Epithelial cancers linked with EBV infection include NPC and EBV-associated gastric carcinoma (EBVaGC) (Young & Murray, 2003; Young & Rickinson, 2004). Even though EBV is mainly studied in different B-cell lymphomas, the number of EBV-related cancer deaths of epithelial origin is significantly higher (Table 2).

Table 2: Global deaths associated with EBV-positive malignancies in 2010. Adapted from Khan *et al.*, 2014.

Origin	Type of malignancy	Number of cases	Number of cases attributable to EBV	Percentage of EBV-attributed cases
Lymphoid	Burkitt's lymphoma	4,396	2,251	51.2%
	Hodgkin lymphoma	17,718	7,917	44.7%
	Post-transplant lymphoproliferative disease	765	612	80%
Epithelial	Nasopharyngeal carcinoma	64,904	63,118	97.2%
	Gastric cancer	754,891	69,081	9.2%

1.4.1. The EBV genome

EBV has a linear, double-stranded genome that spans 172 kb and encodes more than 80 viral products (Palser *et al.*, 2015). The genome is enclosed in an icosahedral nucleocapsid, surrounded by the viral

tegument and a nuclear membrane-derived lipid envelope (reviewed in Liu and Zhou, 2007). During EBV infection, the linear EBV genome carried by virions undergoes circularisation. The number of terminal repeats (TRs) at the ends of the linear EBV genome is variable and depends on the strain (Figure 3) (Dambaugh *et al*., 1980). Therefore, the resulting circular episomes contain a variable number of TRs, which can be used to determine viral clonality within tumours (Raab-Traub & Flynn, 1986).

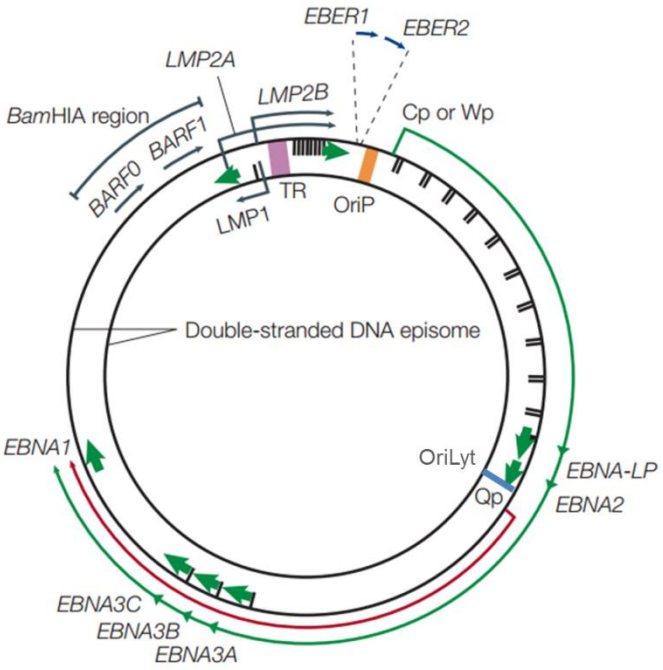


Figure 3: Diagram showing the location and transcription of EBV latent genes on the double-stranded viral DNA episome. The TRs that are generated by circularisation of the viral genome are represented in purple. The origin of plasmid replication is shown in orange and the origin of lytic replication in blue. The blue arrows represent the RNAs EBER1 and EBER2, which are transcribed during all stages of latency. The outer green arrow represents the EBV transcription during latency III. During this latency, all the EBNAs are transcribed from either the Cp or Wp promoter. The red arrow represents the EBNA1 transcript that originates from the Qp promoter during latency I and II (adapted from Young & Rickinson, 2004). EBER1/2 – EBV-encoded RNA 1/2; EBNA – EBV nuclear antigen; LMP – Latent membrane protein; oriLyt – origin of lytic DNA replication; oriP – origin of plasmid replication; TR – terminal repeats.

The first major variation identified in EBV was based on differences in the EBV nuclear antigen 2 (EBNA2) gene (Dambaugh *et al.*, 1984; Adldinger *et al.*, 1985). In contrast to most EBV genes

that differ by less than 5% in sequence, EBNA2 clearly separates into type 1 and type 2, with only 70% identity at the nucleotide level. The main functional difference between these two EBV types is an increased efficacy in *in vitro* immortalisation of B-cells by type 1 EBV compared to type 2 (Rickinson *et al.*, 1987). The differences in the EBNA2 locus, more specifically the C-terminus of EBNA2, have been mapped to be causal for this effect (Cohen *et al.*, 1989; Cancian *et al.*, 2011). In addition, both types also separate geographically. Type 1 is the main variant prevalent worldwide, but in sub-Saharan Africa type 2 is equally abundant (Tzellos & Farrell, 2012).

Although the virus infects the entire world population, tumours show a clear geographical distribution. Burkitt's lymphoma is endemic in equatorial Africa and NPC is common in South-East Asia (Orem *et al.*, 2007; Mahdavifar *et al.*, 2016). EBV-associated T-cell lymphomas are mostly found in Japan, while natural killer (NK) cell tumours occur in South-East Asia (Knipe & Howley, 2013). This geographical distribution can be partly explained by the existence of multiple virus subtypes with different properties that are found in distinct, restricted areas (Palser *et al.*, 2015). Additional factors known to be linked to the distribution of EBV-related cancers are the age of infection, environmental factors such as smoking and concurrent diseases such as Malaria (Hsu *et al.,* 2009; Jia & Qin, 2012).

1.4.2. General biology of EBV

EBV infections usually persist in the latent state *in vivo* (reviewed in Lieberman, 2014). In this state, the double-stranded EBV genome is maintained as a nuclear episome, which the host machinery processes as an additional chromosome tethered to the host genome and thus gets replicated by the host DNA polymerase once per cell cycle (Hammerschmidt & Sugden, 2013). The episome is highly methylated and in a repressive chromatin state which limits the expression of EBV transcripts. Minimising viral expression is advantageous for long-term viral persistence as it maximises the chance to evade detection by the immune system (Paulson & Speck, 1999).

The latent expression pattern of EBV is malignancy-dependent (Table 3) (Amon & Farrell, 2005). The expression of two groups of non-coding EBV RNAs can be detected in all latency stages, except latency 0 (Weigel *et al.*, 1985; Young & Rickinson, 2004). While the group consisting of the EBV-encoded small RNAs 1/2 (EBER1/2) was initially reported not to be essential for the EBV-induced transformation of primary B-lymphocytes (Swaminathan *et al.*, 1991), recent studies showed that EBER2, but not EBER1, is important for this process (Wu *et al.*, 2007). The second group consists of abundantly expressed transcripts from the *Bam*HIA rightward transcript (BARTs) region of the viral genome. Latency I expression can be found in Burkitt's lymphoma and is characterised by the transcription of EBNA1 (Table 3) (Weigel *et al*., 1985; Rowe *et al.*, 1986; Araujo *et al*., 1996). In latency II, latent membrane protein 1 (LMP1), LMP2A/B, BARF1 and EBNA1 are expressed (reviewed in Young & Rickinson, 2004). This expression pattern or variants thereof can be found in diseases such as Hodgkin lymphoma, NPC and EBVaGC (reviewed in Young *et al.*, 2016). In latency I and II, EBNA1 is expressed from the Qp promoter as shown in Figure 3. However, in latency III, which is also called the growth programme, all EBNAs, not just EBNA1, are transcribed from either the Cp or Wp promoter and generated by splicing (Hughes *et al.*, 2011). Additionally, all other latent EBV transcripts are expressed during this latency stage. This expression pattern can be found in post-transplant lymphoproliferative disorders (Kroll *et al.*, 2011).

Table 3: EBV latency expression profiles and associated malignancies. Adapted from Young *et al.*, 2016. BARTs - *Bam*HIA region of the viral genome; EBER1/2 – EBV-encoded RNA 1/2; EBNA – EBV nuclear antigen; LMP – Latent membrane protein.

Latency type	Expression pattern	Disease
0	No viral gene products	Proposed in peripheral resting memory B-cells
I	EBNA1 EBER1/2 BARTs	Burkitt's lymphoma
II	EBNA1 EBER1/2 BARTs LMP1 LMP2 BARF1	Nasopharyngeal carcinoma Hodgkin lymphoma NK/T-cell lymphoma Gastric cancer
III	EBNAs EBER1/2/3 BARTs LMP1 LMP2A/B BARF1	Post-transplant lymphoproliferative disorders

EBV usually resides within the memory B-cell pool of healthy individuals (Babcock *et al.*, 1998). Two different models have been proposed of how EBV infection is established in memory B-cells. One model suggests that memory B-cells are directly infected with EBV (Figure 4, bottom) (Kurth *et al.*, 2000, 2003). In contrast, the germinal centre model proposes that EBV initially infects naïve B-cells and drives B-cell proliferation by the expression of latency III proteins (Figure 4, top) (Thorley-Lawson & Gross, 2004). When the B-cells enter the germinal centre reaction, EBV limits its expression to a latency II pattern, which is believed to mediate the survival of EBV-infected B-cells and their exit from the germinal centre as memory cells (Roughan & Thorley-Lawson, 2009; Roughan *et al.*, 2010). To avoid

immune recognition, EBV-infected memory B-cells downregulate viral gene expression (latency 0). Activation of EBV-infected memory B-cells can induce their differentiation into plasma cells, a process that is hijacked by EBV to drive cells into lytic cycle expression and subsequent virion production (Laichalk & Thorley-Lawson, 2005).

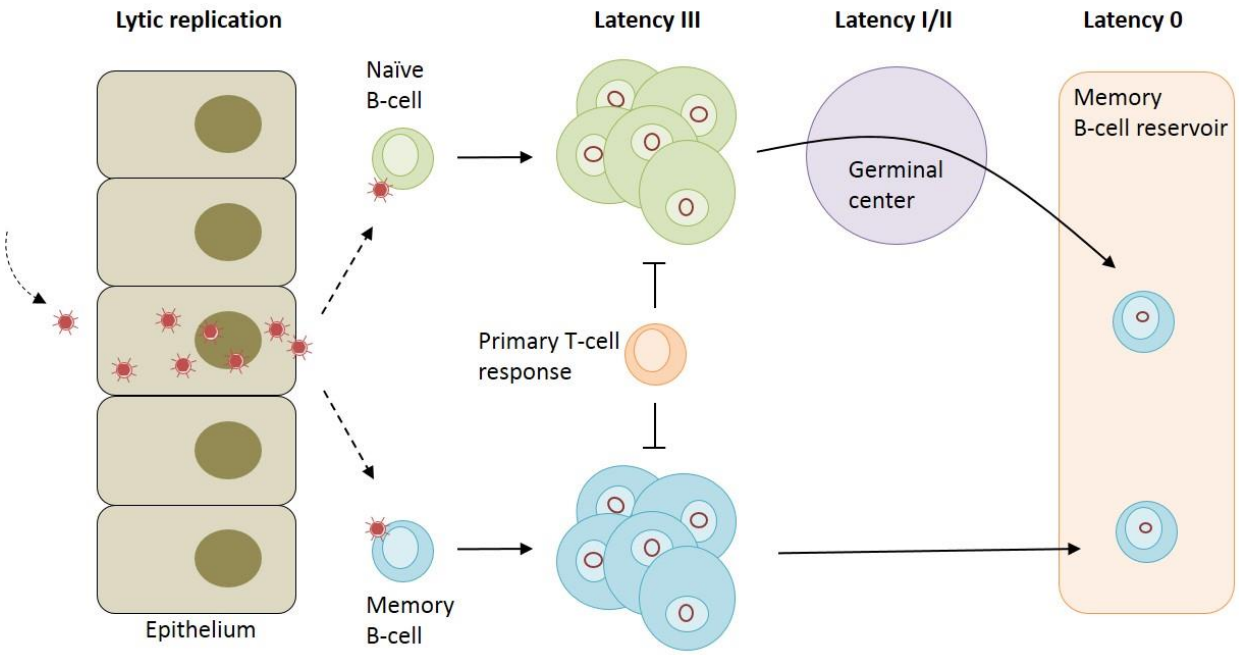


Figure 4: Models of primary B-cell infection by EBV. The incoming virus establishes a primary focus of lytic replication in the oropharynx. The virus then spreads through the lymphoid tissues as a latent growth-transforming infection of B-cells (latency III). The emerging latent antigen-specific primary T-cell response removes most of the proliferating cells. By suppressing viral antigen expression (latency 0), some B-cells escape and establish a stable reservoir of EBV-positive memory B-cells. Two different views of B-cell infection by EBV are shown. In one scenario, the naïve B-cells are the main target for viral infection. This depends on the physiological process of antigen-driven memory cell development during transit through the germinal centre. In an alternative scenario, EBV infects memory B-cells directly and thereby has a direct route into memory (adapted from Young & Rickinson, 2004). EBV-Epstein-Barr virus.

Even though several studies support the germinal centre model, there are some unresolved issues that require further clarification. For example, *in vitro*, naïve and memory B-cells show the same susceptibility to EBV infection, so it is unclear why memory B-cells should be exempted from infection

by EBV *in vivo* (Ehlin-Henriksson *et al.*, 2003). Therefore, further studies are needed to fully characterise the mechanism of B-lymphocytes infection by EBV *in vivo*.

1.5 The life cycle of EBV

The life cycle of EBV is biphasic, consisting of a latent and a lytic phase. Infected cells of EBV-associated malignancies are mainly in the latent state (Amon & Farrell, 2005).

The transition from the latent to the lytic cycle, called reactivation, requires transcription of the two EBV immediate-early (IE) genes, *BZLF1* and *BRLF1*. *BZLF1* and *BRLF1* code for the transcriptional activators Zebra and Rta, respectively. Together, these proteins induce transcription of the entire lytic viral gene programme consisting of early (E) and late (L) viral genes (Feederle *et al*., 2000). In most EBV-positive cell lines, Zebra expression is sufficient to induce reactivation, but particularly in some epithelial cell lines, Rta can also induce the switch to the lytic cycle and lytic DNA replication (Zalani *et al.*, 1996; Ragoczy *et al.*, 1998; El-Guindy *et al.*, 2013).

Additionally, Zebra is able to bind to the lytic origin of replication, oriLyt. This binding is crucial for the formation of an initiation complex necessary for the induction of multiple rounds of replication from the oriLyt (Hammerschmidt & Sugden, 1988; El-Guindy *et al.*, 2007). In contrast to latent episomal replication, this replication process depends on EBV IE and E genes such as *BALF5, BMRF1* and *BBLF4,* rather than on the cellular DNA replication machinery (Fixman *et al.*, 1995). The subsequently transcribed L genes, such as *BcLF1, BDLF1* and *BLLF1,* support viral DNA amplification and produce the structural components required for virion packaging (reviewed in Young *et al.*, 2007b).

1.5.1. Life cycle in B-cells

Upon primary infection, EBV initially replicates in epithelial cells of the oropharynx and then probably infects B-cells in the tonsils (Morgan *et al.*, 1979; Sixbey *et al.*, 1984). Infection of B-cells by EBV requires interaction of the viral gp350/220 protein, the most abundant viral glycoprotein in the EBV envelope, with complement receptor 2 (CR2, CD21) in target cells (Figure 5.A) (Fingeroth *et al.*, 1984; Nemerow *et al.*, 1985; Tanner *et al.*, 1987). CD21-negative B-cells can also be infected through the binding of EBV protein gp350/220 to CR1 (CD35), which is highly expressed in B-lymphocytes as well as follicular dendritic cells (Ogembo *et al.*, 2013). EBV entry into B-cells relies on gp42 forming a complex with viral glycoproteins gH and gL that then binds human leukocyte antigen (HLA) class II (Figure 5.B and C) (Kirschner *et al.* 2006; Sathiyamoorthy *et al.*, 2016). Binding to HLA class II induces widening of a hydrophobic pocket of gp42 that is essential to activate membrane fusion and has been suggested to allow binding to fusion-associated proteins such as gB (Figure 5.D) (Mullen *et al.*, 2002; Silva *et al.*, 2004; Kirschner *et al.*, 2009).

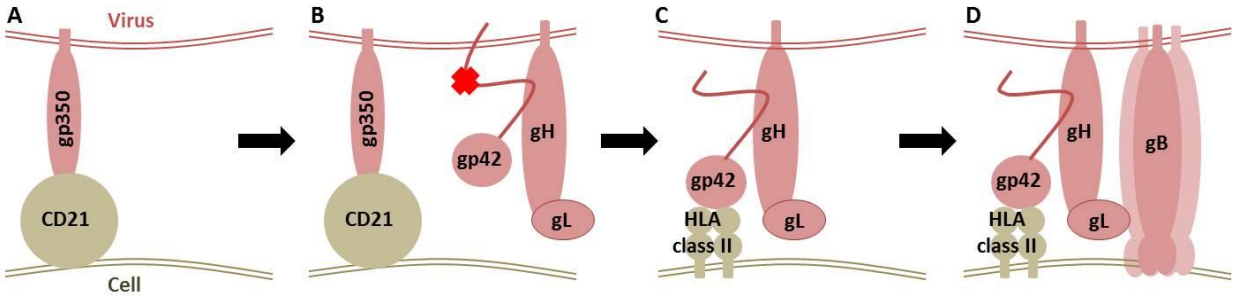


Figure 5: Model of EBV entry into B-cells. A) EBV initially binds to the surface of B-cells via the viral gp350 interacting with CD21. B) Gp42 is then cleaved (indicated by red X) and binds to gH/gL to form the gp42/gH/gL complex. C+D) In the following stage, gp42 binds to HLA class II on the B-cell surface triggering a conformational change, possibly allowing gB interaction. This leads to insertion of the gB fusion loops into the B-cell membrane, resulting in a major refolding of gB into a poorly characterised post-fusion conformation. This induces fusion between the viral envelope and the B-cell endocytic membrane (adapted from Shannon-Lowe & Rowe, 2014). EBV- Epstein-Barr virus; HLA – human leukocyte antigen.

Upon *in vitro* infection, EBV immortalises the B-cell by implementing a virus-encoded programme that results in the unlimited survival and proliferation of infected B-cells (Shannon-Lowe *et al*., 2005). This transformation and the establishment of latent infection have been suggested to occur independently (Price & Luftig, 2014). The details of EBV latency in B-cells are further discussed in Chapter 1.4.2. The viral lytic phase is induced when infected memory B-cells are activated and differentiate into plasma cells (Laichalk & Thorley-Lawson, 2005). During this phase, the viral genome becomes linear, is replicated and new viral particles are assembled and released (Figure 6). The increase of viral expression during the lytic cycle also increases the chances of viral antigen presentation and targeted cell killing by T-cells. The details of the EBV–immune interaction will be further discussed in Chapter 1.7.

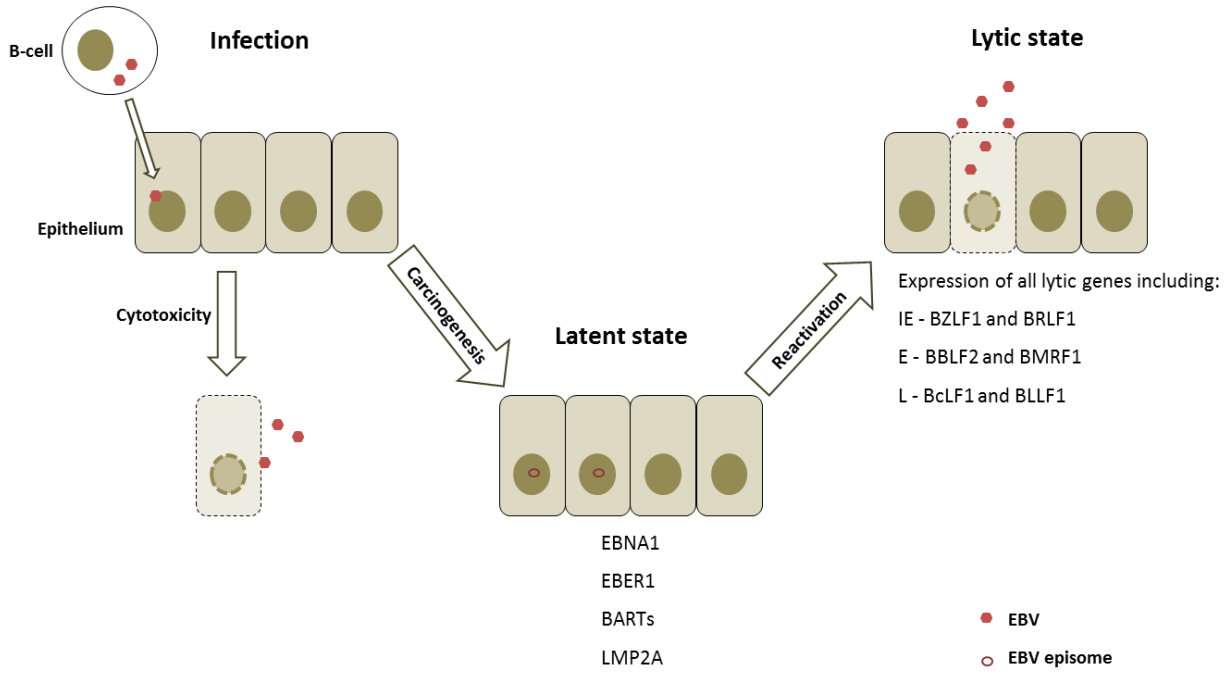


Figure 6: Life cycle of EBV infection in epithelial cells. EBV infection of epithelial cells is a rare event that happens by an unknown mechanism, but it is believed to be mediated by B-lymphocytes. Infection is usually cytotoxic, but in rare cases EBV is able to establish latent infection. In the latent state, EBV only expresses a minimum of viral transcripts such as EBNA1, LMP2A, EBER1 and the BARTs. Through different stimuli, EBV can be reactivated and switched into the lytic state. In this state, immediate early genes are expressed and induce expression of other lytic genes. Early genes are necessary for viral genome replication, which occurs independently of cellular proteins and at a fast rate. The linear viral genome is then packed into new virions and released. The proteins necessary for the virus envelope are expressed by viral late genes (adapted from Uozaki & Fukayama, 2008). BARTs – *Bam*HIA region of the viral genome; E – early lytic genes; EBER – EBV-encoded RNA; EBNA – EBV nuclear antigen; EBV –

Epstein-Barr virus; IE – Immediate-early lytic genes; L – late lytic genes; LMP – latent membrane protein.

1.5.2. Life cycle in epithelial cells

EBV infection of epithelial cells is a rare phenomenon and the exact mechanism of viral entry into epithelial cells is not fully understood yet (reviewed in Shannon-Lowe & Rowe, 2014). Usually, infection is believed to be cytotoxic or to induce productive infection, thereby hindering persistent latent infection in the epithelium (Temple et al., 2014). However, it has been suggested that certain premalignant alterations, such as overexpression of Cyclin D1, are necessary for the establishment of latent EBV infection in nasopharyngel epithelial cells (Tsang et al., 2012).

In vitro evidence indicates that epithelial cells can be more efficiently infected by EBV bound to the cell surface of B-cells (Shannon-Lowe *et al.*, 2006). Even though the exact mechanism of infection through B-cells is not clear yet, the mucosa of oropharyngeal and nasopharyngeal regions is known to be heavily infiltrated by lymphocytes (Jayasurya *et al.*, 2000). Therefore, the cell-to-cell contact mode of EBV infection in epithelial cells might represent a more physiological route of EBV infection of the mucosal epithelium *in vivo.*

The surface molecule CD21 that has been shown to be important for B-cell infection is usually not expressed on epithelial cells (Young *et al.*, 1989). In addition, the entry of EBV into epithelial cells is inhibited by an excess of viral gp42 (Chen *et al.*, 2012b). Instead, it has been suggested that binding of EBV to the epithelial cell surface is based on interactions between viral proteins gHgL and integrins αvβ6 and αvβ8 (Figure 7.A) (Chesnokova *et al.*, 2009; Chesnokova & Hutt-Fletcher, 2011; Chen *et al.*, 2012b). Recent evidence further suggests that EBV then recruits endocytic signalling such as the Ephrin type-A receptor 2 (EphA2) to facilitate EBV internalisation (Zhang *et al.*, 2018). The interaction of the EBV gH/gL/gB complex with EphA2 and integrins is necessary to accomplish successful EBV–endosome

membrane fusion (Figure 7.C) (Chen *et al.*, 2018). These data indicate that the viral tropism for infection of B-lymphocytes versus epithelial cells is controlled by a switch of viral and cellular protein expression.

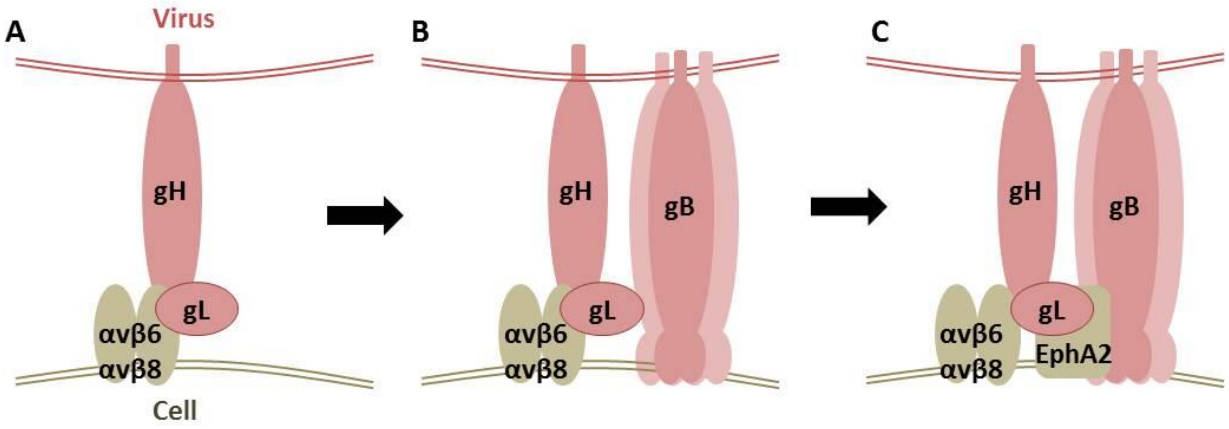


Figure 7: Model of EBV entry into epithelial cells. A) In epithelial cells, the gH/gL complex binds to the epithelial cell surface through integrins such as αvβ6 and αvβ8. B+C) This promotes binding to gB and the recruitment of endocytic signalling, such as EphA2 for EBV internalisation. Interaction of the EBV gH/gL/gB complex with EphA2 as well as integrins leads to the refolding of gB, and thus enables fusion of the EBV envelope with the epithelial cell plasma membrane (adapted from Shannon-Lowe & Rowe, 2014; Chen *et al.*, 2018; Zhang *et al.*, 2018). EBV – Epstein-Barr virus; EphA2 - Ephrin type-A receptor 2.

EBV has been shown to transform mammary epithelial cells (Hu *et al*., 2016), but the same was not observed in nasopharyngeal epithelial cells *in vitro* infected with EBV (Raab-Traub, 2002). Therefore, it is believed that transformation of EBV-positive epithelial cells is a multistep process over a long period of time, involving interplay of EBV gene expression and host gene alterations in pre-malignant cells (Preciado *et al.*, 2002; Chan *et al.*, 2004; Chen *et al.*, 2012c). The mechanism by which EBV induces stable infection is not yet understood, but it has been shown that aberrant methylation of the EBV genome as well as the host genome is associated with latent EBV infection (Paschos *et al.*, 2009; Paulson & Speck, 1999). Aberrant methylation of promoters has been suggested to be involved in the silencing of tumour suppressor genes and thereby potentially in viral-induced carcinogenesis (Li *et al.*, 2014). This is supported by reports that EBV can be detected in most cells of EBV-positive tumours,

indicating that EBV infection is an early event in carcinogenesis of NPC and gastric carcinoma (Pathmanathan *et al.*, 1995; Gulley *et al.*, 1996).

1.5.3. The role of epigenetic marks in the life cycle of EBV

During infection, epigenetically naïve genomic EBV DNA, which does not contain detectable levels of histones or nucleosomes and is free of methylated CpG dinucleotides, enters the cells (Dyson & Farrell, 1985). In this state, EBV is a permissive template for the cellular transcription machinery. Thus, for a short period of time after infection, latent as well as different lytic genes are expressed (Tierney *et al*., 2007; Jochum *et al.*, 2012; Kalla & Hammerschmidt, 2012). Lytic genes are then silenced by chromatinisation through suppressive histone markers including trimethylated histone H3 lysine 27 (H3K27me3), H3K9me2/3 and H4K20me3 at the promoter of the *BZLF1* gene (Zp) of latent cells (Murata *et al.,* 2012; Ramasubramanyan *et al.*, 2012). In addition, host-driven DNA methylation silences EBV lytic genes and thereby stabilises latency of the EBV genome (Flower *et al.*, 2011).

The methylation of CpG islands decreases the binding ability of the lytic activator Rta to DNA (Wille *et al*., 2013). In contrast, Zebra, one of the key transcription factors for the induction of the lytic cycle, can enhance transcription from the EBV genome, which is deeply silenced by CpG methylation, to bring about lytic replication (more details in Chapter 1.6.2) (Dickerson *et al.*, 2009; Bergbauer *et al.*, 2010). Thus, lytic cycle expression can be induced without depending on active demethylation. Viral DNA synthesised from the oriLyt during the lytic cycle is depleted of CpG methylation and histones and will then be incorporated into progeny virus particles (Murata & Tsurumi, 2014).

Through reactivating stimuli, the local acetylation state of histones H3 and H4 around Zp and the *BRLF1* promoter (Rp) is changed to an open state indicated by marks such as H3K27ac, H3K9ac and H4K8ac. The open chromatin allows access by transcription factors and the induction of expression of their gene

products, Zebra and Rta (Jenkins *et al.*, 2000; Countryman *et al.*, 2008; Mansouri *et al.*, 2013). The binding of Zebra to methylated Zebra-response element (meZRE) sites induces epigenetic reprogramming by the removal of nucleosomes and adaption of an open chromatin state (Woellmer *et al.*, 2012). In addition, activating marks such as H3K4me3 are introduced to lytic gene promoters and thus the expression of Zebra target genes is induced (Murata et al., 2012). Overall, it has been shown that high levels of histone acetylation on EBV lytic gene promoters correlate with lytic induction of the virus (Countryman *et al.*, 2008; Ramasubramanyan *et al.*, 2012).

EBV does not just interact with epigenetic enzymes in order to chromatinise the episome, but also to induce other important processes. Zebra and Rta, like many cellular transcription factors, directly interact with histone acetyltransferases (HATs) such as cyclic AMP response element binding protein (CREB) binding protein (CBP) to activate EBV E gene expression (Adamson & Kenney, 1999). The interaction between either Zebra or Rta and CBP enhances the potential of both viral proteins to activate transcription (Swenson *et al.*, 2001). Additionally, Zebra enhances the HAT activity of CBP, especially on dinucleosomes and oligonucleosomes (Chen *et al.*, 2001).

The importance of epigenetic marks and modulators for the reactivation of EBV in different cellular backgrounds led to the adaption of epigenetic inhibitors as viral reactivating agents. The results of those studies will be summarised in Chapter 1.8.2.

1.6 EBV lytic proteins

1.6.1. IE proteins

IE proteins such as Zebra and Rta are proteins that trigger the expression of E genes. Expression of either gene is sufficient for the induction of lytic cycle expression in epithelial and B-cells. Since the two genes also regulate each other's expression, the expression of one gene will lead to the expression of

the other, which is required for full activation of E gene expression (Zalani *et al.*, 1996; Adamson & Kenney, 1998). This enables the virus to amplify weak lytic induction stimuli. Rp contains a direct Zebra-binding site, whereas Zp does not contain a site for direct binding by Rta (Figure 8.A) (Adamson & Kenney, 1998). Rta is able to bind GC-rich motifs in enhancer regions upstream of E gene elements, but such motifs have not been found in Zp (Gruffat *et al.*, 1992a; Gruffat and Sergeant, 1994). A study has suggested that the effect of Rta on Zp is mediated by the activation of c-Jun N-terminal kinases (JNKs) and p38 kinase, allowing Rta to induce Zp transcription through phosphorylation of the activating transcription factor 2 (ATF2) and c-Jun transcription factors (Adamson *et al.*, 2000). Together, Zebra and Rta activate expression of the entire lytic viral gene programme.

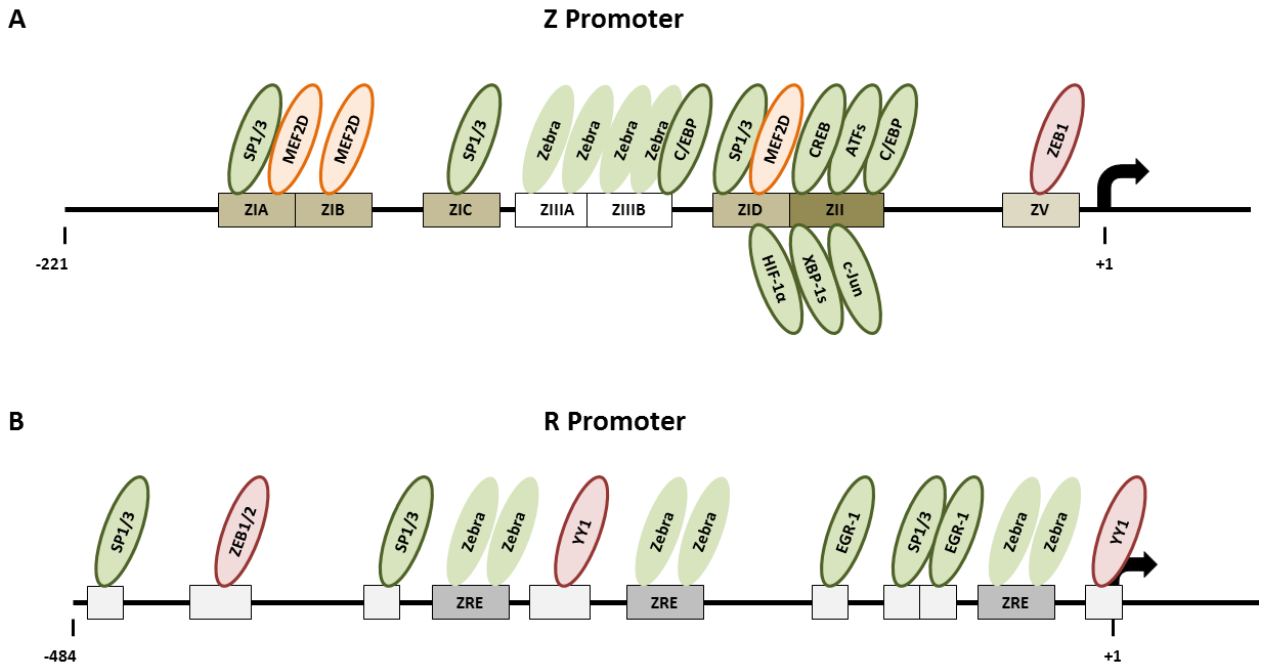


Figure 8: Transcription factors with known roles in the regulation of Zp and Rp, the promoters of *BZLF1* and *BRLF1,* respectively. A) Zp contains four AT-rich motifs, ZIA through ZID, that can be bound by the transcription factors SP1/3 and MEF2D. Inhibitors of Zp activity such as MEF2D can be transformed into activators of Zp through the activation of BCR, a reactivating stimulus. ZII contains a CRE-like motif that is bound by CREB, ATF family members, C/EBPs and the AP-1 family of transcription factors. Additionally, several Zebra binding sites are contained within Zp, located in ZIII. Elements involved in transcriptional silencing are located within ZV and can be bound by ZEB1. B) Rp contains several ZREs and can thus be activated by direct Zebra binding. The expression of BRLF1 can be positively regulated by the binding of SP1/3 and EGR-1, while YY1 and ZEB1/2 have been suggested to suppress Rp activity. Positive regulators are marked in green, regulators with positive and negative effects in orange and negative regulators in red. Outlined transcription factors are of cellular origin,

while transcription factors without an outline are expressed by EBV (adapted from Kenney & Mertz, 2014). ATFs – activating transcriptions factors; BCR – B-cell receptor; C/EBP – CCAAT-enhancer-binding proteins; CREB – cAMP response element binding protein; EGR-1 – early growth response protein 1; HIF-1α – hypoxia-inducible factor 1α; MEF2D - myocyte enhancer factor; SP1/3 – specificity protein 1/3; XBP-1s – X-box-binding protein-1 spliced; YY1 – ying yang 1; ZEB1/2 – Zinc finger E-box-binding homeobox 1/2; ZRE – Zebra-response element.

Cellular transcription factors that regulate the expression of the IE promoters play an important role in determining the level of lytic cycle expression. Several cellular transcription factors have been shown to silence the Zp promoter. Myocyte enhancer factor 2D (MEF2D) binds Zp and represses *BZLF1* gene expression during latency by recruiting type II histone deacetylating complexes (HDACs) to the promoter (Liu *et al.*, 1997; Gruffat *et al.*, 2002a). Through lytic induction stimuli that engage the B-cell receptor (BCR), dephosphorylation of MEF2D is induced and MEF2D thereby converted from a negative to a positive regulator of *BZLF1* transcription (Bryant & Farrell, 2002). Zinc finger E-box-binding homeobox 1 (ZEB1) and ZEB2 bind the Zp promoter at the ZV element and repress *BZLF1* expression (Figure 8) (Kraus *et al.*, 2003; Yu *et al.*, 2007; Ellis *et al.*, 2010). Factors negatively regulating *BRLF1* expression are much less well understood, but it has been suggested that ying yang 1 (YY1) and possibly ZEB1/2 decrease Rp activity (Figure 8.B) (Montalvo *et al.*, 1995; Yu *et al.*, 2007).

The ubiquitously expressed transcription factor specificity protein 1 (Sp1) has been shown to bind to Zp and Rp and induce their transcription (Tsai *et al.*, 2011). Sp1 might play a crucial role in recruiting other transcription factors such as p53 to the promoters in order to increase lytic transcription (Chua *et al.*, 2012). Lytic induction stimuli commonly induce phosphorylation of CREB, ATF-1, AP-1, ATF-2/c-Jun and the spliced variant of X-box-binding protein-1 (XBP-1), which can then activate the expression of *BZLF1* through binding to the ZII element (Sun & Thorley-Lawson, 2007; Shirley *et al.*, 2011). XBP-1 gets activated during plasma cell differentiation and is able to activate both Zp and Rp, and thereby the viral lytic cycle (Bhende *et al.*, 2007; McDonald *et al.*, 2010). Another factor that is important during plasma cell differentiation, B-lymphocyte-induced maturation protein 1 (BLIMP1), has also been shown to

activate transcription from both IE promoters in certain cell lines (Vrzalikova *et al.,* 2011; Reusch *et al.*, 2015).

1.6.2. The key regulator Zebra

The viral *BZLF1* gene encodes the transcription factor Zebra, which plays an important role in the induction of EBV's lytic phase. Zebra is a basic leucine zipper (bZIP) transcription factor consisting of a homodimer of 245 residue subunits. It has a modular structure and contains a basic domain that mediates sequence-specific binding to DNA, a coiled-coil domain for homodimerisation and a transcriptional activation domain (Sinclair, 2003).

Zebra has broader target specificity for the DNA motifs that it binds to than other bZIP transcription factors, such as AP-1 and C/EBP, thereby allowing it to activate many viral and cellular genes (Petosa *et al.*, 2006). Accordingly, Zebra binds to consensus sites for AP-1 and C/EBP as well as motifs divergent from these (Farrell *et al.*, 1989; Kouzarides *et al.*, 1991). In addition to the sequence-specific DNA classes of motifs that Zebra binds, called ZREs, Zebra also binds a second class of DNA motif that contains methylated 5'-cytosine residues, termed meZREs. Binding of both motifs can activate viral promoters that drive lytic genes (Bhende *et al.*, 2004; Karlsson *et al.*, 2008; Dickerson *et al.*, 2009; Bergbauer *et al.*, 2010; Kalla *et al.*, 2010). meZREs are the exclusive Zebra-binding motifs in certain E viral promoters that are essential for the lytic amplification of EBV DNA (Bergbauer *et al.*, 2010). Due to this feature, the methylated epigenome can function as a template for lytic DNA replication without the need of active DNA demethylation.

Zebra orchestrates many functions in the viral life cycle, including as a transcriptional activator of E viral lytic cycle genes. One of Zebra's primary targets is Rp, which encodes the transactivator Rta. The two proteins activate downstream genes synergistically, such as the *BMRF1* gene, and thereby progress the

lytic cascade (Liu & Speck, 2003). Zebra, phosphorylated by casein kinase 2 (CK2), orchestrates the lytic cascade further by temporarily repressing Rta activity on L genes such as *BLRF2* early on during reactivation (El-Guindy & Miller, 2004). In addition, Zebra is able to bind the oriLyt and thus functions as an essential replication protein for lytic DNA replication (Schepers *et al.*, 1996; El-Guindy *et al.*, 2007).

Zebra also interferes with many different cellular pathways. When expressed in EBV-negative cells, Zebra modulates the cell cycle and promotes G1 cell cycle arrest (Wu *et al.*, 2003). Additionally, Zebra has been shown to interact with the tumour suppressor p53 and regulate its activity through both direct and indirect mechanisms (Zhang *et al.*, 1994; Mauser *et al*., 2002). Zebra also influences the host immune response by inhibiting interferon-γ (INF-γ), p65 and tumour necrosis factor alpha (TNFα) (Morrison *et al.,* 2001, 2004; Morrison & Kenney, 2004), and further influences intracellular signalling by activating JNKs and p38 mitogen-activated protein kinases (Adamson *et al*., 2000).

The key role of Zebra during reactivation justifies intensive research efforts into its function and regulation for potential clinical exploitation.

1.6.3. Early proteins

Early proteins are important for the replication of the viral genome. The six core replication proteins expressed during this phase of the life cycle are the following: the polymerase BALF5, the polymerase processivity factor BMRF1, the single-stranded DNA-binding protein BALF2, the helicase BBLF4, the primase BSLF1 and the primase-associated factor BBLF2/3. These proteins have been shown to form a complex and to be required for amplification from the oriLyt, together with Zebra (Hammerschmidt & Sugden, 2013).

Zebra interacts with the helicase/primase/accessory protein complex and recruits it to the oriLyt, which contains Zebra binding sites (Figure 9) (Schepers *et al.*, 1996; El-Guindy *et al.*, 2010). The DNA-binding protein BALF2 then attaches to this pre-priming complex and opens the DNA helix at the oriLyt. The DNA polymerase and its accessory protein subsequently attach to the complex allowing DNA replication to proceed (Fujii *et al.*, 2000). Host cell transcription factors such as Zinc-finger DNA-binding protein 89 (ZBP-89) and Sp1 have been shown to bind the oriLyt and interact with the viral protein complex to stimulate viral DNA replication (Baumann *et al.*, 1999; Hau *et al.*, 2015). This suggests a complementary mechanism by which cellular transcription factors tether the viral replication proteins to the oriLyt.

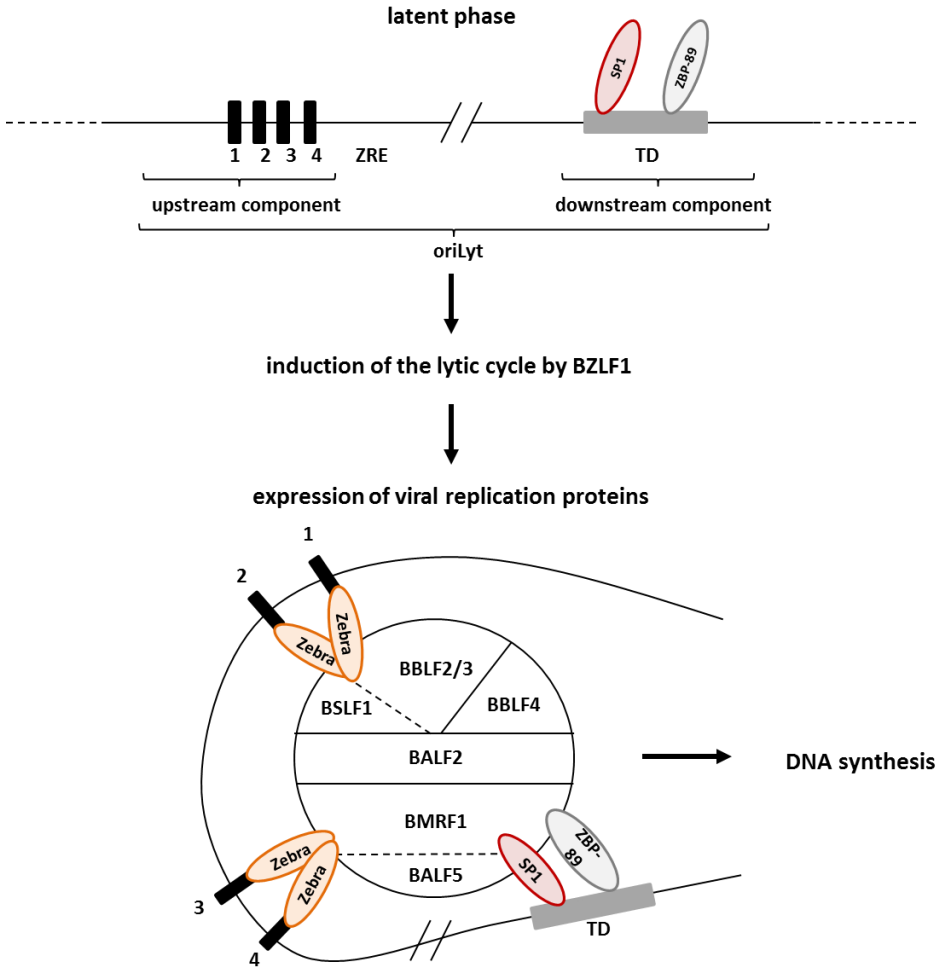


Figure 9: Model of replication complex formation at oriLyt after the induction of the lytic phase of EBV's life cycle. SP1 and ZBP-89 presumably bind to the TD element during the latent as well as lytic

phases of EBV's life cycle. Induction of the lytic cycle through specific stimuli such as 12-O-tetradecanoylphorbol-13-acetate leads to the expression of Zebra, which then activates the expression of viral lytic early genes. Zebra is able to directly bind ZRE motifs within the oriLyt sequence and thereby orchestrates the viral replication complex. Zebra is able to bind several viral proteins involved in DNA replication, such as the DNA polymerase accessory factor BMRF1, the viral helicase BBLF4, the primase subcomplex (composed of BSLF1 and BBLF2/3) and the polymerase BALF5. The single-stranded DNA-binding protein BALF2 binds the helicase–primase subcomplex. The DNA polymerase complex composed of the catalytic subunit BALF5 and BMRF1 interacts with the cellular transcription factors SP1 and ZBP-89. The replication initiation complex is stabilised through the multitude of protein–protein interactions and thereby enables oriLyt-dependent DNA synthesis (adapted from Baumann *et al.*, 1999). oriLyt – origin of lytic replication; Sp1 - Specificity protein 1; ZBP-89 - Zinc-finger DNA-binding protein 89; ZRE – Zebra-response element.

The mRNA export factor ICP27 homologue expressed by the *BMLF1* gene, also called EB2 or SM, shuttles between the nucleus and cytoplasm and thereby promotes the cytoplasmic accumulation of unspliced EBV mRNAs (Semmes *et al.*, 1998; Gruffat *et al.*, 2002b). The importance of this process is underlined by a mutant BMLF1 virus that is no longer able to produce virions (Gruffat *et al.*, 2002a).

EBV encodes two different B-cell lymphoma 2 (BCL-2) homologues to either induce or repress apoptosis: BHRF1 and BALF1. The expression of BHRF1 enhances apoptosis resistance in a number of cell types *in vitro* (Desbien *et al.*, 2009; Kvansakul *et al.*, 2010). This suggests that the main function of BHRF1 *in vivo* may be to delay apoptosis during EBV lytic cycle progression, thereby facilitating virus assembly and release. In contrast, BALF1 has been shown to inhibit the antiapoptotic activity of BHRF1, but not of cellular BCL-2 family members (Bellows *et al.*, 2002). The influence of BALF1 on apoptosis is limited to regulating BHRF1 activity as it does not possess any pro-apoptotic properties (Bellows *et al*., 2002). Notably, the expression of either one of those BCL-2 homologues has been shown to be necessary for B-cell transformation induced by EBV infection as infection with EBV strains lacking those genes induces B-cell apoptosis rather than transformation (Altmann & Hammerschmidt, 2005).

BARF1 is an EBV E gene product that is secreted into the medium of cultured cells and binds to human colony-stimulating factor 1 (CSF-1) (Strockbine *et al.*, 1998; Elegheert *et al.*, 2012). CSF-1 is a pleiotropic cytokine that acts as a modulator of macrophage activation as well as of the immune response against

microbial and viral infections. BARF1 inhibits the proliferative effect of CSF-1 and thereby influences the host immune response towards EBV infection (Strockbine *et al*., 1998; Elegheert *et al*., 2012).

Overall, E genes encode proteins that ensure that the viral genome is rapidly replicated. By modulating the immune response as well as the response to apoptotic stimuli, the virus ensures cell survival until the lytic cycle is completed and virions can be released.

1.6.4. Late proteins

The late phase of the lytic cycle is characterised by the expression of viral structural proteins, the packaging of viral DNA into viral particles and the release of virions.

The capsid is formed by the major capsid protein p160 (encoded by the viral gene BcLF1) together with three small capsid proteins: p18, p23 and p40 (BFRF3, BLRF2 and BdRF1, respectively). The main tegument proteins are BNRF1 and BPLF1. In addition, host cell proteins like β-actin, tubulin, HSP70 and HSP90 can be found in the tegument (Johannsen *et al.,* 2004). The high levels of those proteins in mature virions suggest that cell-encoded proteins are important for virion morphogenesis.

EBV encodes a number of glycoproteins. The best characterised ones are gp350/220 and gH. The N-terminal region of gp350/220 mediates binding of EBV to the B-cell receptor CD21 (Young *et al.*, 2007a, 2008). This interaction induces capping of the receptor, endocytosis of the virus into the cell and triggers intracellular signalling pathways that activate the Wp promoter (Roberts *et al.*, 1996; Sugano *et al.*, 1997). However, a virus deleted of gp350/220 was still able to infect B-cells and epithelial cells, though to a lesser degree than wildtype virus, suggesting that the gp350/220-CD21 interaction is not the only mechanism important for infection (Janz *et al.*, 2000). The alternative mechanism could potentially involve gH/gL/gp42. This heterotrimeric complex of three glycoproteins is involved in B-cell

infection by EBV using cell-surface HLA class II molecules as a co-receptor (Mullen *et al.,* 2002; Kirschner *et al.*, 2006).

Other proteins that are predicted to have multiple membrane-spanning domains are gp60 and BMRF2. BMRF2 can interact with integrins to facilitate the infection of the basolateral surface of epithelial cells by EBV (Tugizov *et al.*, 2003). Gp60, encoded by the BILF1 gene, is a G protein-coupled receptor that has been shown to be involved in viral immune evasion during lytic cycle expression (Zuo *et al.*, 2009).

Another L gene is BCRF1, which is highly conserved between strains and exhibits extensive sequence homology with human cytokine interleukin (IL)-10 (Hsu *et al.,* 1990). It is therefore named viral IL-10 (vIL-10). This cytokine is involved in the deactivation of macrophages and dendritic cells, the inhibition of cytokine synthesis by $CD4^+$ T-cells and the induction of differentiation of activated B-cells (Moore *et al.*, 2001). In contrast to human IL-10, vIL-10 has been shown to oppose the inhibitory effects of T-cells on EBV-induced B-cell transformation (Bejarano & Masucci, 1998). It has further been shown that vIL-10 enhances the viral transformation of B-cells (Miyazaki *et al.*, 1993; Swaminathan *et al.*, 1993).

The expression of vIL-10 with the L genes suggests that cells in the L lytic state produce both virions and vIL-10. This increases the susceptibility of B-cells to EBV-induced transformation, while simultaneously inhibiting the immune response against viral infections. Thereby, EBV increases the chances for successful viral propagation.

1.7 Immune evasion of EBV

The human immune response can be grouped into the adaptive and the innate immune response. The innate immune response is a non-specific defence mechanism that is triggered by the recognition of pathogen-associated molecular patterns by pattern recognition receptors. The adaptive immune

response is antigen-specific and leads to targeted cell killing by cytotoxic T-lymphocytes (CTLs) as well as to antigen-specific antibody production (reviewed in Braciale & Hahn, 2013).

1.7.1. Immune evasion during latency I/II

The expression of viral proteins is severely limited during latent EBV infection to avoid recognition by the host immune system. EBNA1 is the only viral protein that is expressed in all latency stages. The long glycine-alanine repeats within the EBNA1 protein inhibit its proteasomal degradation and thereby enhance its stability (Levitskaya *et al.*, 1997; Dantuma *et al.*, 2000). The decreased protein turnover of EBNA1 aims to minimise viral antigen presentation to $CD8^+$ T-cells (Figure 10) (Yin *et al.*, 2003). An alternative immune-evasive action of EBNA1 is the inhibition of the canonical nuclear factor-κB (NF-κB) pathway by interfering with phosphorylation of the IκB kinases α and β (IKKα/β) (Valentine *et al.*, 2010). By promoting the turnover of Smad2 and thereby reducing the Smad2/4 interaction, EBNA1 has further been shown to have a negative effect on transforming growth factor β (TGFβ) signalling (Wood *et al.*, 2007).

LMP1 is a member of the tumour necrosis factor receptor superfamily and therefore shares many signalling intermediates with Toll-like receptors (TLRs). Accordingly, LMP1 and TLRs both activate NF-κB, a subset of IFN regulatory factors (IRFs) and AP1 (Ning *et al.*, 2003; Song *et al.*, 2004). LMP1 further activates JNK, MAPK, Janus kinase signal transducers and activators of transcription (STAT) and phosphoinositide-3-kinase (PI3K) signalling by mimicking constitutively active CD40 signalling (Izumi & Kieff, 1997; Kieser, 2007; Shair *et al.*, 2007Dawson *et al.*, 2008). Those pathways influence many immunological processes and thereby allow LMP1 to modulate the host immune response. In NPC, increased expression of IL-1α and IL-1β in malignant epithelial cells and increased infiltration of $CD4^+$ T-cells have been detected (Huang *et al.*, 1999; Yip *et al.*, 2009). This upregulation is induced by

LMP1 and can be further enhanced by TNFα stimulation, thereby contributing to tumour growth and lymphocyte infiltration (Huang *et al.*, 2010b).

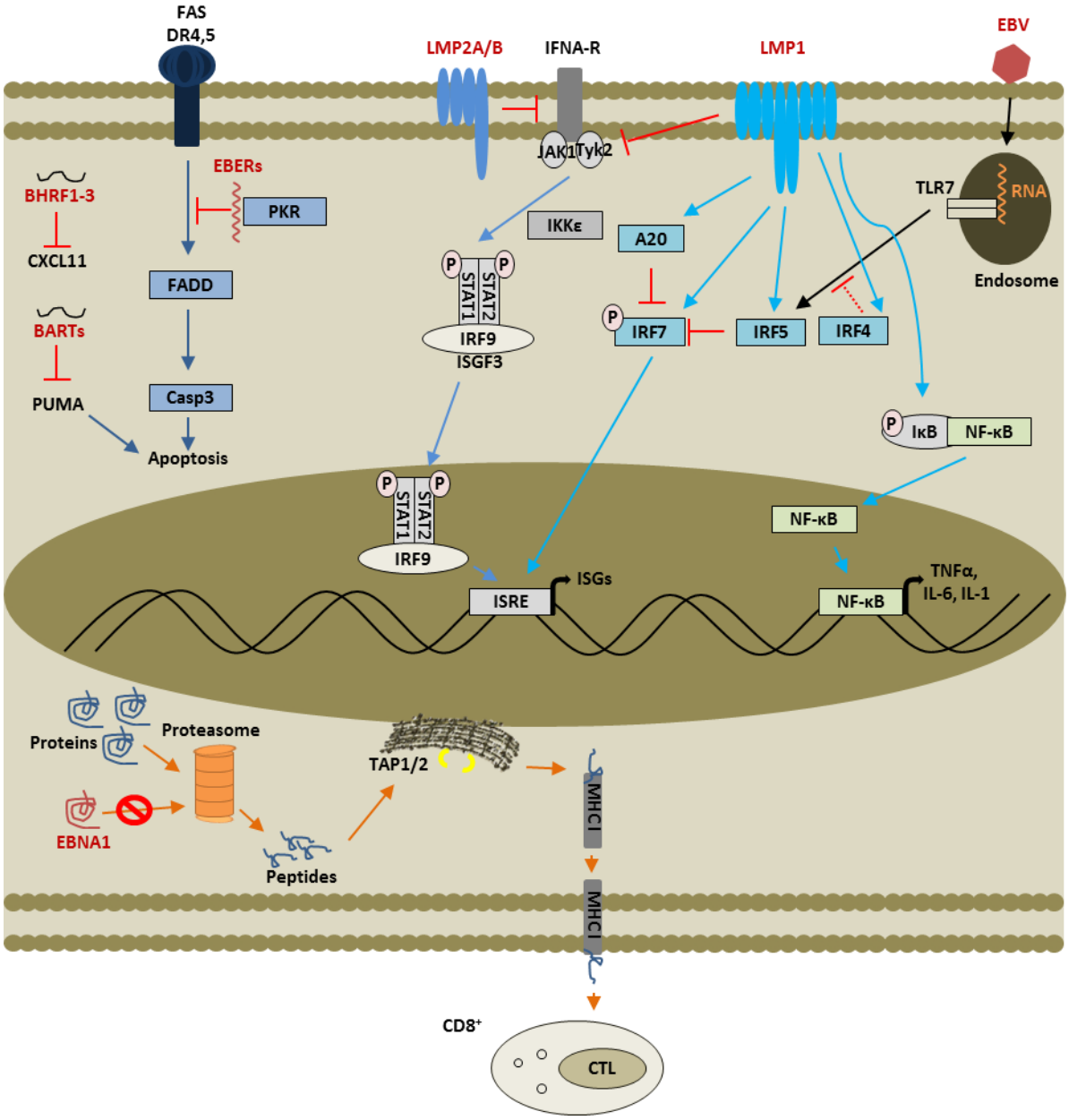


Figure 10: Immune evasion mechanisms in latent EBV infection. LMP1 and LMP2A are able to inhibit IFNA-R signalling and thereby inhibit the expression of downstream IFN-stimulated genes. LMP1 induces NF-κB transcription and thus the expression of a specific set of cytokines such as TNFα and IL-6. The repeats in the EBNA1 protein inhibit its own proteasomal degradation and minimise the presentation of EBNA1 peptides on MHC I molecules and subsequent $CD8^+$ T-cell recognition. The EBV RNAs EBER and BARTs inhibit apoptosis by interfering with different parts of the apoptotic pathway. The microRNA BHRF1-3 targets the T-cell-attracting chemokine CXCL-11 and thereby minimises the T-cell response (adapted from Ning, 2011). BARTs – *Bam*HIA rightward transcripts; BHRF1-3 – *Bam*HIA fragment H rightward open reading frame 1-3; Casp3 – Caspase 3; CTL – cytotoxic T-cell; CXCL-11 – C-X-

C motif chemokine 11; EBER – EBV-encoded RNA; EBNA – EBV nuclear antigen 1; EBV – Epstein-Barr virus; FADD – Fas-associated protein with death domain; IFN – interferon; IKKε – IκB kinase ε; IL – interleukin; IRF – Interferon regulatory factors; ISG – Interferon-stimulated genes; ISRE – Interferon-stimulated response element; JAK1 – Janus kinase 1; MHC – Major histocompatibility complex; NF-κB – nuclear factor-κB; PKR – protein kinase R; STAT – signal transducers and activators of transcription; TAP1/2 – Transporter associated with antigen processing 1/2; TLR7 – Toll-like receptor 7; Tyk2 – Tyrosine kinase 2.

In EBV-positive NPC cells, it has been shown that the immune-suppressive factor programmed death-ligand 1 (PD-L1) is commonly upregulated on the cell surface (Fang *et al.*, 2014; Zhou *et al*., 2017). The constitutive activation of oncogenic pathways induced by LMP1 upregulates PD-L1 expression, which is independent of inflammatory signals in the tumour microenvironment (Fang *et al.,* 2014). In addition, PD-L1 is also induced in response to inflammatory signals such as IFNγ, which are produced during an active anti-viral immune response and thereby dampen this response (Fang *et al.,* 2014).

LMP2A has been shown to inhibit the NF-κB and STAT pathways in carcinoma cells (Figure 10) (Stewart *et al.,* 2004). Both LMP2A and LMP2B attenuate IFNα/β- and IFNγ-mediated transcription by influencing type I and type II IFN-receptor stability (Shah *et al.*, 2009). This leads to a global blockade of IFN signalling.

The ability of LMP1 to induce an antiviral state and to establish latency stands in contrast to the functions of LMP2A/B, which dampen the same responses. Therefore, the balance between those two proteins might be crucial for the establishment of latent infection as well as immune evasion.

EBV-encoded non-coding RNAs have recently also been implicated in immune evasion strategies (reviewed in Ressing *et al.*, 2015). The EBERs have been shown to bind the IFN-inducible double-stranded RNA-dependent protein kinase R (PKR) *in vitro* and to suppress IFNα-induced apoptosis (Clarke *et al.*, 1991; Nanbo *et al.*, 2002). A more recent study suggests that the inhibition of IFNα induction is not mediated by direct binding of the EBERs to PKR (Ruf *et al.,* 2005). By being contained

within exosomes of EBV-transformed cells, EBERs could further support viral immune evasion (Ahmed *et al.*, 2014).

In addition, EBV expresses a number of microRNAs (miRNAs), named the BART and BHRF1 miRNAs. The miRNA BHRF1-3 has been shown to downregulate the T-cell-attracting chemokine C-X-C motif chemokine 11 (CXCL-11) (Xia *et al.*, 2008). BART15 downregulates the alternative inflammasome-activating sensor NLR family Pyrin domain containing 3 (NLRP3) and IL-1 production (Haneklaus *et al.,* 2012). In contrast, the miRNA BART20-5p has been shown to downregulate T-bet and IFNγ, both regulators of IFNγ transcription (Lin *et al.*, 2013; Huang & Lin, 2014).

This shows that most of the transcripts that EBV expresses during latency are involved in immune evasion to ensure cellular, and thereby viral, survival.

1.7.2. Immune evasion by lytic gene products

The expression of major histocompatibility complex (MHC) molecules at the cell surface and the presentation of peptides by them is crucial for the adaptive immune response (reviewed in Wieczorek *et al.*, 2017). Due to the high number of expressed viral proteins, the chances of immune recognition are higher during the lytic state than during the latent state. Thus, EBV has evolved several ways to dampen the $CD4^+$ as well as $CD8^+$ T-cell response in this state (reviewed in Ressing *et al.*, 2015). BILF1, BGLF5 and BNLF2a interfere with the expression of MHC class I, while BGLF5, BZLF1 and gp42 interfere with the expression of MHC class II (Figure 11) (Ressing et al., 2015).

The EBV G protein-coupled receptor homolog BILF1 has been identified as a specific inhibitor for MHC class I presentation on the cell surface (Zuo *et al.,* 2009). BILF1 leads to lysosomal degradation of MHC class I molecules and thus abrogates recognition of lytic cells by immune cells (Zuo *et al.,* 2009). The

gene product of the L gene BDLF3 enhances the internalisation of surface MHC I and II complexes, thereby reducing the rate of their appearance at the cell surface (Quinn *et al.,* 2016). The EBV lytic protein gp42 can occur both in a membrane-bound form that is important for infection by EBV and in a soluble form (Ressing *et al.*, 2005). Soluble gp42 is secreted by the cell and has been shown to inhibit HLA II-restricted antigen presentation to T-cells (Ressing *et al.,* 2005).

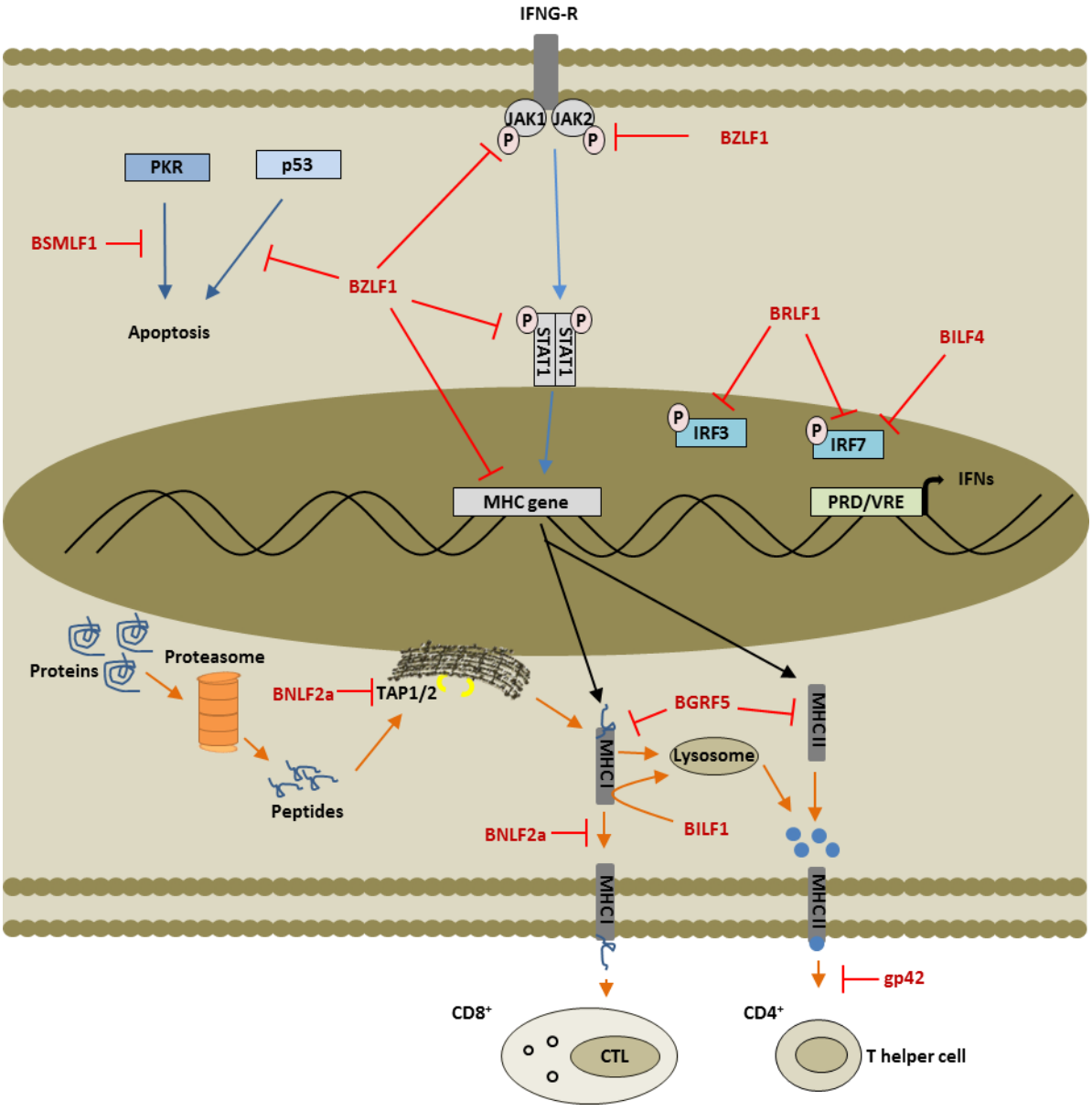


Figure 11: Immune evasion mechanisms in lytic EBV infection. The master regulator of the EBV lytic cycle BZLF1 is involved in several immune evasion mechanisms. Together with BSMLF1, BZLF1 is able to inhibit apoptosis. BZLF1 interferes with IFNG-R signalling at different points and thereby inhibits the expression of MHC on the cell surface. BRLF1 and BILF4 inhibit IRF3 and IRF7, and thus inhibit IFN

expression. MHC I and II stability is decreased by BGRF5 and BILF1, which decreases antigen presentation to immune cells. BNLF2a inhibits MHC I antigen presentation by inhibiting peptide loading onto the MHC by TAP1/2. Soluble gp42 inhibits HLA II-restricted antigen presentation and thereby the $CD4^+$ T-cell response (adapted from Ning, 2011). CTL – cytotoxic T-cell; EBNA – EBV nuclear antigen 1; EBV – Epstein-Barr virus; HLA – human leukocyte antigen; IFN – Interferon; INFG-R – Interferon-γ receptor; IRF – Interferon regulatory factors; JAK – Janus kinase; MHC – Major histocompatibility complex; PKR – protein kinase R; PRD – positive regulatory domain; STAT – signal transducers and activators of transcription; TAP1/2 – transporter associated with antigen presentation 1/2; VRE – virus responsive element.

BGLF5, an EBV-encoded exonuclease, suppresses the expression of MHC class I and II genes and thereby helps EBV to avoid T-cell recognition (Rowe *et al.,* 2007). This effect is mediated by the DNase and RNase activity of BGLF5 (Buisson *et al.,* 2009; Horst *et al.,* 2012). The degradation of RNA by BGLF5 can also affect other immunologically relevant proteins, such as TLR2 and TLR9, that could otherwise sense EBV infection (van Gent *et al.*, 2011, 2015).

The gene product of BNLF2a is inserted into the endoplasmic reticulum (ER) membranes and appears to deplete peptides from the ER through the inhibition of peptide import by the transporter associated with antigen presentation (TAP) (Horst *et al.,* 2011). BNLF2a abrogates the binding of the peptide and adenosine triphosphate (ATP) to the TAP complex and thereby blocks its transporter function (Wycisk *et al.,* 2011). This inhibits the presentation of peptides by the MHC class I complexes and $CD8^+$ T-cell recognition (Croft *et al.,* 2009; Horst *et al.,* 2009).

Zebra interacts with IRF7 and thereby inhibits its transcriptional activity on the IFNα and IFNβ promoters, preventing the induction of an antiviral cell environment (Hahn *et al.*, 2005). The expression of viral Zebra and cellular NF-κB negatively influence each other's expression. As a consequence, higher levels of Zebra during progression of the lytic cycle limit the amount of NF-κB (Morrison & Kenney, 2004). Even though NF-κB is still translocated into the nucleus, Zebra suppresses its transcriptional activity and thereby prevents the induction of an antiviral immune response (Morrison & Kenney, 2004). In addition, Zebra counteracts innate effector molecules by downregulating the receptors for

TNFα and IFNγ, reducing cellular responsiveness to these cytokines (Morrison *et al.,* 2004; Bristol *et al.,* 2010). By impairing IFNγ signalling, Zebra inhibits the activity of the MHC class II transactivator promoter and, as a result, decreases HLA II surface levels (Morrison *et al.,* 2001).

The increased expression of viral proteins during the progression of the lytic cycle could induce a strong antiviral immune response. In order to avoid immune recognition, several viral lytic proteins function to evade the immune system and subsequently enable the production and shedding of new virions.

In summary, EBV has evolved multiple mechanisms of immune evasion in order to avoid immune recognition during all phases of its life cycle. The diversity of the mechanisms underlines the importance of immune modulation for the establishment of latent infection as well lytic cycle propagation. Nevertheless, it is worth noting that those mechanisms of immune evasion do not enable absolute protection from the immune system. Especially during the lytic cycle, when an increased amount of viral proteins is expressed, those mechanism dampen the immune response rather than completely evading it (reviewed in Rowe & Zuo, 2010). This modulation of the immune response plays an important role in the persistence of EBV as a mostly asymptomatic infection.

1.8 Reactivation of EBV

1.8.1. Physiological induction of the lytic cycle

EBV infection in EBV-associated malignancies is mainly latent (reviewed in Young & Rickinson, 2004). Nevertheless, there is evidence that bursts of spontaneous and recurrent reactivation may play a role in EBV persistence (Davies *et al.,* 2010; Phan *et al.*, 2016). Additionally, recurrent chemical reactivation of EBV in NPC cells has been linked to enhanced genome instability and tumour progression (Fang *et al.*, 2009).

The cellular machinery, such as cellular differentiation factors, can regulate spontaneous reactivation (Davies *et al.,* 2010). This effect is usually cell type-dependent. BLIMP1 is a key player in B-cell plasma differentiation that has been shown to facilitate reactivation (Reusch *et al.*, 2015). In epithelial cells, the differentiation factor Krueppel-like factor 4 has been shown to control reactivation (Nawandar *et al.*, 2015). These examples suggest that the reactivation of EBV or the maintenance of the latent state is tightly linked to the differentiation state of the host cell.

Nutritional or environmental factors can also influence the state of EBV in infected cells. N-nitroso compound exposure is increased through the consumption of certain foods in high-risk NPC regions (Ho *et al.*, 1978; Ward *et al.*, 2000). Treatment with N-nitroso compounds led to recurrent EBV reactivation in NPC cells and mouse models, and increased tumourigenicity (Fang *et al.,* 2012). A hypoxic growth environment has also been shown to induce lytic gene expression (Jiang *et al.,* 2006). This is mediated through a hypoxia-inducible factor response element in Zp and thereby induces Zebra expression upon hypoxia (Kraus *et al.,* 2017).

Changes in the cellular microenvironment have also been shown to induce lytic reactivation. Induction of BCR engagement through anti-immunoglobulin G antibodies induces lytic cycle activation by switching MEF2D from a negative to a positive regulator of Zebra expression (Takada & Ono, 1989; Mellinghoff *et al.,* 1991). TGF-β, a cytokine secreted by T-cells, has been shown to activate *BZLF1* expression in some Burkitt's lymphoma cell lines (Fahmi *et al.*, 2000; Iempridee *et al.* , 2011). This effect is believed to be mediated through the downstream activation of Smad2/3/4, which then translocates to the nucleus, where it binds to a series of Smad-binding elements located throughout Zp (Iempridee *et al.*, 2011).

Understanding the mechanism of physiological EBV reactivation could help eliminate potential environmental factors that are associated with EBV-related malignant disease and worse prognosis due to recurrent reactivation.

1.8.2. Pharmacological reactivation

Agents such as radiation and chemotherapeutic compounds have been shown to trigger the reactivation of EBV alone or in combination with other agents such as HDAC inhibitors (HDACis) (Westphal *et al.*, 2000; Feng *et al.*, 2002).

Some, but not all, chemotherapies were shown to reactivate EBV in B-cells. In EBV-transformed B-cells, only gemcitabine and doxorubicin were able to induce lytic expression, while decitabine (5-Aza-2'-deoxycytidine), cisplatin or 5-fluorouracil (5-FU) did not generate the same effect (Feng *et al.*, 2004a). Radiation has been shown to induce lytic cycle expression in EBV-positive gastric cancer (Nandakumar *et al.*, 2017). In lymphoid cells, it has been shown that radiation in combination with ganciclovir (GCV) leads to increased cell killing (Westphal *et al.,* 2000).

Due to the importance of epigenetic marks for the life cycle of EBV, different HDACis have been tested for their reactivation potential in EBV-infected cells (reviewed in Hammerschmidt, 2015). Sodium butyrate (SB) was reported to drastically increase the number of virus-producing cells (Luka *et al.*, 1979). Valproic acid (VPA) has shown synergistic antitumour effects with gemcitabine in NPC cells and patients (Wildeman *et al.*, 2012; Hsu *et al.,* 2015; Stoker *et al.,* 2015). Even though different HDACis have been implicated to be effective reactivating agents, they are not effective in all EBV-positive lymphoid cell lines (Gradoville *et al.*, 2002). The efficacy of HDACis have been shown to be independent of the nucleosomal organisation of Zp and Rp, which is similar in all cell lines (Countryman *et al.*, 2008). This suggests that promoter hyperacetylation is not sufficient to induce the lytic cycle.

The HDACi suberoylanilide hydroxamic acid (SAHA, vorinostat) is able to reactivate EBV in latency II-infected epithelial cells, but not in cells of other tissue backgrounds harbouring EBV in latency II (Hui & Chiang, 2010). In a further study from the same laboratory, it was shown that inhibition of class I HDACs by romidepsin potently induces the EBV lytic cycle and mediates enhanced cell death with GCV

(Hui *et al.*, 2016). In a study in extranodal natural killer/T-cell lymphoma patients, romidepsin's safety and efficacy was assessed (Kim *et al.*, 2016a). The study had to be discontinued after patients developed severe side effects linked to reactivation of EBV and rapidly elevated EBV DNA titres in the blood (Kim *et al.*, 2016a). Therefore, the efficacy of reactivating agents *in vitro* is not necessarily transferable to the patient, and needs to be assessed for their effect on latent EBV in B-cells as well as tumour cells to maximise patient safety.

1.8.3. Antiviral cancer therapies

Conventional cancer therapies include surgery, chemotherapy and radiation therapy. Despite those therapeutic advances, cancer-associated mortality rates are still significant, causing more than one in four of all deaths in the UK in 2011 (Cancer Research UK, 2018). The high proportion of cancer cases that are associated with viral and bacterial infection has led to the development of therapeutic strategies using the infectious agent to specifically target the tumour. The clinical use of antiviral and antimicrobial agents in combination with cancer therapy is called adjuvant antimicrobial therapy (Alibek *et al.*, 2012).

Up to 80% of HCCs are associated with HBV and HCV infection (Plummer *et al*., 2016). Vaccination against HBV, as well as antiviral therapy against HCV, can slow down the progression of liver disease (Shin *et al.,* 2011; Kao, 2015). The efficacy of those antiviral treatments has been shown to be significantly better in patients during early stages of infection (Martin *et al.*, 2016; Mascia *et al.,* 2017).

Human CMV (HCMV), a member of the Herpesviridae family, is commonly associated with brain tumours (Mitchell *et al.*, 2008; Ranganathan *et al.*, 2012). Combination treatment with GCV, an antiviral drug, and celecoxib, a Cyclooxygenase-2 inhibitor, impaired proliferation of HCMV-positive cell lines but had no effect on HCMV-negative medulloblastoma cells (Baryawno *et al.*, 2011). Similar effects were

achieved when cells were treated with acyclovir (ACV), an inhibitor of HCMV thymidine kinase (Söderlund *et al.*, 2010).

KSHV-associated KS and primary effusion lymphoma (PEL) are sensitive to antiviral agents such as GCV, cidofovir and foscarnet, but resistant to others such as cyclovir in pre-clinical studies (Kedes & Ganem, 1997; Medveczky *et al.*, 1997; Fujimuro *et al.*, 2006). The fact that in KSHV- and EBV-positive lymphomas few normal B-cells are infected but nearly all of the tumour cells are infected led to the development of so-called 'lytic induction' therapies. Those therapies are based on a two-step process. The first step aims to efficiently induce viral reactivation, which will trigger recognition of the tumour by immune cells. In the second step, antiviral compounds are administered that can only be metabolised in cells expressing viral lytic cycle proteins and thereby specifically kill them (Figure 12). Targeted cell killing is further aided by activation of the immune system through the presentation of lytic antigens.

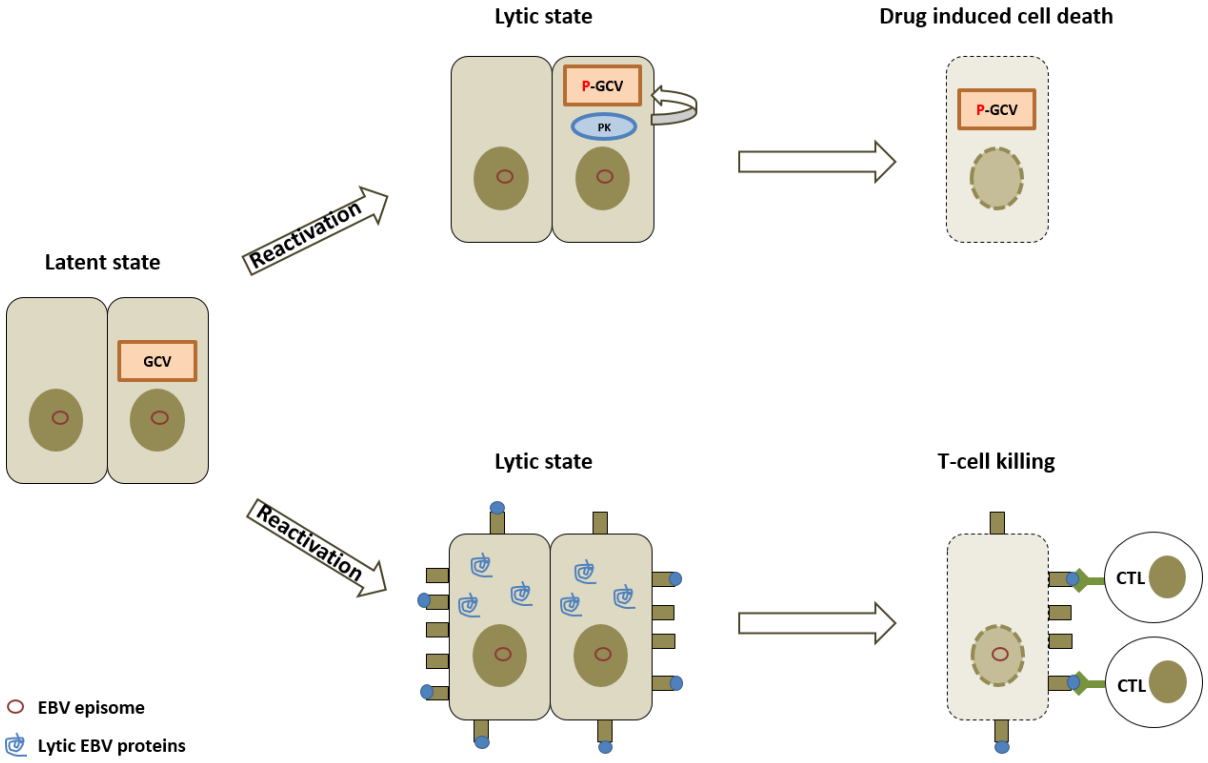


Figure 12: Model of lytic induction therapy. Antiviral agents such as GCV are not toxic for latently infected cells because the pro-drug is not phosphorylated. Upon reactivation through targeted stimuli,

EBV expression of a viral protein kinase is induced. This kinase phosphorylates and thereby activates GCV. Activated GCV can inhibit DNA replication in the cell itself and in surrounding cells, and thus induce cell death in a number of cells. In addition, the increased expression of viral proteins during the lytic cycle increases the number of viral epitopes presented. Those can then be recognised by epitope-specific cytotoxic T-cells, leading to T-cell killing (adapted from Kenney & Mertz, 2014). CTL – cytotoxic T-cell; GCV – Ganciclovir; p-GCV – phosphorylated GCV; PK – viral protein kinase.

In PEL cell lines, it has been shown that the antiviral agent GCV can induce increased cell death and block viral production when combined with the anticonvulsant medication valproate, which has HDACi activity (Klass *et al.*, 2005). This approach has also been shown to be more effective for the inhibition of EBV-driven lymphoproliferative disease in mouse models than chemotherapy alone (Feng, *et al.*, 2004a). In a phase I/II clinical trial of the HDACi arginine butyrate and GCV in patients with EBV-associated lymphoid malignancies, significant antitumour activity was observed (Perrine *et al*., 2007). However, it is worth noting that rapid tumour lysis led to severe adverse events, such as haemorrhage or bowel perforation, in 3 out of 15 patients.

Despite promising data suggesting that a combination of antiviral with reactivating agents might be the future for the treatment of virus-associated cancers, the optimal pharmacological inducer of EBV reactivation has not yet been identified. Therefore, it is necessary to identify novel reactivating agents and characterise their underlying mechanisms of action to minimise side effects in patients. Additionally, the scope of research on lytic induction therapies should be expanded towards EBV-associated epithelial malignancies to overcome the limitations of current studies focussing mostly on EBV infection in B-cell malignancies (reviewed in Ghosh *et al.*, 2012b).

1.9 EBVaGC

Epidemiological data from the World Health Organization suggests that gastric cancer is the fourth most common malignancy in the world and accounts for 6.8% of annual cancer deaths worldwide (Karimi *et al.*, 2014; Shah, 2015).

1.9.1. Infection in gastric cancer

The pathogen most often associated with malignancies within the stomach is *H. pylori*, which confers up to 75% of the attributable risk for gastric cancer (Shah, 2015). The risk of malignancy depends on the extensive genetic diversity and strain-specific proteins of *H. pylori* (McClain *et al.*, 2009). Another pathogen commonly associated with gastric cancer is EBV. About 10% of all gastric cancers are associated with EBV infection, thus over 80,000 patients are estimated to develop EBVaGC annually worldwide (Table 2) (Shibata & Weiss, 1992; Cohen *et al.*, 2011).

The mechanism of EBV infection of the gastric epithelium has not yet been fully elucidated (Chapter 1.5.2). Nevertheless, the increased efficacy of viral infection through direct cell contact with B-cells suggests a crucial role of B-cells in epithelial infection by EBV (Shannon-Lowe *et al*., 2006; Shannon-Lowe & Rowe, 2011). Atrophic gastritis caused by *H. pylori* may induce the infiltration of EBV-carrying lymphocytes and increase the chance of their contact with gastric epithelial cells (de Souza *et al.*, 2014). Therefore, it has been proposed that *H. pylori* infection increases the chances of EBV infection of the stomach epithelium. This is supported by different studies that have shown potential associations of *H. pylori* infection with EBV occurrence (Saxena *et al.*, 2008; de Souza *et al.,* 2014).

Additionally, the gastric inflammation induced by *H. pylori* infection may also produce a cytokine-rich microenvironment that supports clonal growth of EBV-infected epithelial cells (Saiki *et al.*, 1996). It has

been shown that oxidant monochloramine, which is commonly secreted by *H. pylori*, reactivates EBV in gastric epithelial cells (Minoura-Etoh *et al.,* 2006). Increased viral protein expression and DNA replication upon reactivation could potentially explain the observed increased EBV load in the presence of *H. pylori in vivo* (Shukla *et al.,* 2011).

Notably, 58% of EBVaGCs occur in the cardia of the stomach, while *H. pylori*-related adenocarcinomas usually occur in the non-cardia (Singh & Jha, 2017). Therefore, it is likely that the two pathogens do not directly interact with one another but rather influence the microenvironment of the stomach in favour of further infections.

1.9.2. Genetic and epigenetic properties of EBVaGC

EBVaGC shows distinct clinicopathological characteristics compared to EBV-negative gastric cancer such as male predominance and a high proportion of diffuse-type gastric carcinomas, which are usually less well differentiated and associated with a poorer prognosis than other histological groups of gastric cancer (Adachi *et al.*, 2000; Chen *et al.*, 2012a). Recent studies have further shown that EBVaGC differs significantly from other groups of gastric cancers through their genetic and epigenetic signature (Chen *et al.*, 2012a; Cancer Genome Atlas Research, 2014).

EBVaGC has a higher prevalence of DNA hypermethylation than other gastric cancer types in the Cancer Genome Atlas database (Chang *et al.*, 2006; Cancer Genome Atlas Research, 2014). Through interaction with and activation of different DNA methyltransferases, EBV hypermethylates specific promoters, thereby establishing a viral latency expression pattern through the regulation of viral Cp and Wp promoter activity (Paulson & Speck, 1999; Yoshioka *et al.*, 2003; Tsai *et al.,* 2006; Peng *et al.*, 2016). In addition, promoter hypermethylation commonly reduces the expression of cellular tumour suppressor

genes such as p16, p73 and Phosphatase and Tensin homolog (PTEN), and thereby contributes to tumourigenesis (Schneider *et al.*, 2000; Ushiku *et al.,* 2007; Hino *et al.*, 2009).

Moreover, EBVaGC is associated with a specific spectrum of genetic mutations compared to other gastric cancer types (Cancer Genome Atlas Research, 2014). The commonly mutated tumour suppressor p53 has been shown to be rarely mutated in EBVaGC (Cancer Genome Atlas Research, 2014; Ribeiro *et al.,* 2017). In contrast, mutations activating the *PIK3CA* oncogene, which encodes PI3K, were found in up to 80% of EBVaGC cases compared to 3–43% of EBV-negative cases (Lee *et al.*, 2012; Sukawa *et al.,* 2012; Cancer Genome Atlas Research, 2014). Therefore, evaluation of the effect of PI3K inhibition as a potential treatment for EBVaGC might be interesting. Additionally, AT-rich interactive domain-containing protein 1A (ARID1A), a subunit of the mating-type switching (SWI)/sucrose non-fermenting chromatin remodelling (SNF) complex, has been found to be mutated in 55% of EBVaGC cases (Cancer Genome Atlas Research, 2014).

EBVaGC has further been characterised by a robust immune cell presence as well as a strong IL-12-mediated expression signature, which is mainly produced by antigen-presenting cells (Cancer Genome Atlas Research, 2014; Zhang *et al.,* 2016; Jiang *et al*., 2017). The immune suppressive factors PD-L1/2 have been shown to be overexpressed in EBVaGC (Fang *et al.,* 2014; Saito *et al.*, 2017). This strong immune signature of EBVaGC suggests that checkpoint inhibitors might be a promising therapy for this cancer type.

In summary, EBVaGC can be distinguished from other gastric cancer types through EBV infection itself, a distinct genetic and epigenetic signature, and increased immune signalling. Specifically targeting those properties of EBVaGC could aid the development of novel therapies for the treatment of this cancer type.

1.10. Aims of the study

While EBV infection has been intensively studied in the context of B-cell infection and transformation, less is known about the role of EBV infection in epithelial cells and its potential implications for treatment. The distinct properties of EBVaGC, including its epigenetic and genetic signature as well as the high level of immune cell infiltration, could potentially be exploited for targeted therapeutic options. Although treatment with epigenetic inhibitors such as romidepsin has been suggested as the basis for potential lytic induction therapy, the reactivation potential of those compounds has only been shown in a small panel of cell lines and has led to severe adverse effects in patients due to rapid increases of EBV titres in the blood (Hui *et al.*, 2016; Kim *et al.*, 2016a).

This study aimed to identify and characterise novel lytic induction therapies for EBVaGC that specifically target the characteristics of this malignancy. To achieve this aim, a novel imaging-based screening method for the unbiased identification of EBV-reactivating agents was developed. Using this platform, lytic cycle induction through treatment with different pharmacological inhibitors, either alone or in synergy, was examined. The most promising candidates for lytic induction therapy were examined in more detail, especially their effects on cell viability and the immune response towards reactivated cells. In the second part of the study, the identified compound combinations were used to identify key pathways for viral reactivation in epithelial cells and their impact on viral lytic cycle progression.

Chapter 2: Materials and methods

2.1. Materials

2.1.1. Reagents for cell culture

Cell lines

Table 4: List of epithelial cell lines used in this study. EBV – Epstein-Barr virus; GFP – green fluorescent protein.

Name	Tissue type/origin
AGS	Human gastric carcinoma cell line; kindly provided by Dr Christopher Dawson (Birmingham)
AGS rEBV-GFP	Human gastric carcinoma cell line; generated by infecting AGS cells *in vitro* with a modified B95-8 strain of EBV, which contains an inserted GFP gene (Feng *et al.*, 2004b); kindly provided by Dr Christopher Dawson (Birmingham)
C666.1	Human nasopharyngeal carcinoma cell line derived from an EBV-positive tumour; kindly provided by Dr Christopher Dawson (Birmingham)
OE19	Human oesophageal carcinoma cell line; kindly provided by Dr Christopher Dawson (Birmingham)
OE19 rEBV-GFP	Human oesophageal carcinoma cell line; generated by infecting OE19 cells *in vitro* with a modified B95-8 strain of EBV, which contains an inserted GFP gene (Feng *et al.*, 2004b); kindly provided by Dr Christopher Dawson (Birmingham)
SNU719	Human gastric carcinoma cell line derived from an EBV-positive tumour (Oh et al., 2004); kindly provided by Dr Christopher Dawson (Birmingham)
SNU-NCC-24	Human gastric carcinoma cell line derived from an EBV-positive tumour (Ku et al., 2012); this cell line was obtained from the Korean Cell Line Bank
YCCEL1	Human gastric carcinoma cell line derived from an EBV-positive tumour (Kim et al., 2013); kindly provided by Dr Christopher Dawson (Birmingham)

Table 5: List of lymphoid cell lines used in this study. HLA – human leukocyte antigen.

Name	Tissue Type/ Origin
Akata	Burkitt's lymphoma cell line derived from a Japanese patient (Takada et al., 1991); kindly provided by Prof. Paul Farrell (London)
GLC T-cell clone	$CD8^+$ T-cell line against BMLF1 with HLA-A2 restriction (Redchenko & Rickinson, 1999); kindly provided by Prof. Alan Rickinson (Birmingham)
Namalwa	Burkitt's lymphoma cell line; kindly provided by Prof. Paul Farrell (London)
PD LCL	Lymphoblastoid cell line; kindly provided by Prof. Paul Farrell (London)
PLPH LCL	Lymphoblastoid cell line expressing HLA-A2; kindly provided by Pierre Coulie (Brussels)
Raji	Burkitt's lymphoma cell line; kindly provided by Prof. Paul Farrell (London)

Automated cell counting

Pierce 16% formaldehyde (w/v), methanol-free (Life Technologies Ltd, Cat. No. 28908)

Trypan blue solution (Sigma-Aldrich, Cat. No. T8154-100ML)

Cell growth media

Roswell Park Memorial Institute 1640 medium (RPMI 1640) (Thermo Fisher Scientific, Cat. No. 11875093)

10% (v/v) foetal bovine serum (FBS) (Biosera)

2 mM L-glutamine (Thermo Fisher Scientific, Cat. No. 25030)

100 units/mL penicillin and 100 µg/mL streptomycin (Thermo Fisher Scientific, Cat. No. 15140122)

400 µg/mL G418 sulfate (Merck Chemicals Ltd, Cat. No. 345810) was added to the cell culture medium for AGS rEBV-GFP (green fluorescent protein) and OE19 rEBV-GFP cells in order to maintain EBV expression.

Compounds for cell treatment

The following compounds were used for the treatment of cell cultures at the concentrations mentioned in the appropriate figure legends.

Table 6: List of compounds used in this study.

Name	Supplier	Catalogue number
5-fluorouracil	Sigma-Aldrich	F6627-1G
Acycloguanosine	Sigma-Aldrich	A4669-50MG
Actinomycin D	Sigma-Aldrich	A9415-2MG
Adapalene	Sigma-Aldrich	A7486-10MG
Ancitabine hydrochloride	Sigma-Aldrich	A8598-1G
Chlorhexidine dihydrochloride	Sigma-Aldrich	C8527-5G
Cisplatin	Sigma-Aldrich	479306-1G
Daunorubicin hydrochloride	Sigma-Aldrich	D8809-1MG
Decitabine (5'-aza-2'-deoxycytidine)	Sigma-Aldrich	A3656-5MG
Dinaline	Abcam plc	Ab144561-10MG
Dimethyl sulfoxide	Sigma-Aldrich	D2650-100ML
Doxorubicin hydrochloride	Sigma-Aldrich	D1515-10MG
Entinostat (MS-275)	Stratech Scientific Ltd	S1053-SEL-10MG
Epirubicin hydrochloride	Sigma-Aldrich	E9406-10MG
Etoposide	Sigma-Aldrich	E1383-25MG
Ganciclovir	Sigma-Aldrich	G2536-100MG
Mitomycin C	Sigma-Aldrich	M4287-2MG
Mocetinostat (MGCD0103)	Stratech Scientific Ltd	S1122-SEL-5MG
Nutlin-3a	Sigma-Aldrich	SML0580-5MG
Piroctone olamine	Sigma-Aldrich	51872-100MG
Teniposide	Sigma-Aldrich	SML0609-1MG
12-O-Tetradecanoylphorbol-13-Acetate	New England Biolabs	4174S

Table 7: List of compounds and their concentrations used for the extended SGC screen. For extended compound information including mechanism of action see Appendix Table 1. N/A – not applicable; SGC – Structural Genomics Consortium, Oxford.

Name	Supplier	Catalogue number	Concentration 'low' (μM)	Concentration 'high' (μM)
5'-azacytidine	Sigma-Aldrich	A2385-100MG	0.1	0.2
A366	SGC, Oxford	N/A	2.5	5
BAZ2-ICR	SGC, Oxford	N/A	2.5	5
Bromosporine	SGC, Oxford	N/A	2.5	5
CI-994	SGC, Oxford	N/A	5	10
C646	SGC, Oxford	N/A	10	20
Chidamide	Insight Biotechnology Ltd	Sc-364462	5	10
CXD101	SGC, Oxford	N/A	5	10
GSK2801	SGC, Oxford	N/A	2.5	10
GSK484	SGC, Oxford	N/A	2.5	10
GSKJ4	SGC, Oxford	N/A	2.5	10
GSKLSD1	SGC, Oxford	N/A	0.25	1
ICBP112	SGC, Oxford	N/A	2.5	10
IOX1	SGC, Oxford	N/A	100	1000
IOX2	SGC, Oxford	N/A	100	1000
JQ1	SGC, Oxford	N/A	0.5	1
LAQ824	SGC, Oxford	N/A	0.5	1
LLY-507	SGC, Oxford	N/A	2.5	10
LP99	SGC, Oxford	N/A	2.5	10
NI-57	SGC, Oxford	N/A	2.5	10
OICR-9429	SGC, Oxford	N/A	2.5	5
Olaparib	SGC, Oxford	N/A	5	10
OF-1	SGC, Oxford	N/A	2.5	5
Panobinostat	Cayman Chemicals	13280-5MG	0.1	0.5
PFI-1	SGC, Oxford	N/A	2.5	10
PFI-2	SGC, Oxford	N/A	2.5	10
PFI-3	SGC, Oxford	N/A	5	20
PFI-4	SGC, Oxford	N/A	2.5	10

PXD101	Cambridge Bioscience	2480-5	5	10
Romidepsin	Cambridge Bioscience	17130-500 µg-CAY	0.0025	0.005
SAHA	Sigma-Aldrich	SML0061-5MG	5	10
SGC0946	SGC, Oxford	N/A	2.5	10
SGC707	SGC, Oxford	N/A	2.5	10
SGC-CBP30	SGC, Oxford	N/A	0.5	3
Trichostatin A	Sigma-Aldrich	T8552-1MG	0.01	0.1
UNC1999	SGC, Oxford	N/A	2.5	5
UNC0638	SGC, Oxford	N/A	2.5	5
UNC0642	SGC, Oxford	N/A	2.5	5
UNC1215	SGC, Oxford	N/A	2.5	5

Table 8: List of HDACi concentrations used in this study. For supplier information see Tables 6 and 7. Details about biochemical inhibition of HDAC1-9 by HDACis (Ki) can be found in Appendix Table 2.

Name	Concentration 'low' (µM)	Concentration 'medium' (µM)	Concentration 'high' (µM)
CI-994	2.5	5	10
Chidamide	2.5	5	10
CXD101	2.5	5	10
Dinaline	2.5	5	10
Entinostat (MS-275)	2.5	5	10
LAQ824	0.25	0.5	1
Mocetinostat (MGCD0103)	2.5	5	10
Panobinostat	0.1	0.25	0.5
PXD101	2.5	5	10
Romidepsin	0.001	0.0025	0.005
SAHA	2.5	5	10
Trichostatin A	0.01	0.05	0.1

Table 9: List of topoisomerase inhibitors and their concentrations used in this study.

Name	Supplier	Catalogue number	Concentration (µM)
Amonafide	Stratech Scientific Ltd	S1367-SEL-10MG	7.5
Camptothecin	Sigma-Aldrich	C9911-100MG	1
Colchicine	Sigma-Aldrich	C9754-100MG	3
Daunorubicin hydrochloride	Sigma-Aldrich	D8809-1MG	0.1
Doxorubicin hydrochloride	Sigma-Aldrich	D1515-10MG	1
Epirubicin hydrochloride	Sigma-Aldrich	E9406-10MG	1
Idarubicin hydrochloride	Stratech Scientific Ltd	S1228-SEL-10MG	0.1
Mitoxantrone	Sigma-Aldrich	M6545-10MG	1
Teniposide	Sigma-Aldrich	SML0609-1MG	7.5
Topotecan	Cambridge Bioscience	14129-25MG-CAY	1

Cell passaging components

Cells were expanded by trypsinising an attached confluent sheet of cells using 0.05% trypsin-ethylenediaminetetraacetic acid (w/v) (EDTA) (Gibco, Cat. No. 25300-054) and splitting them at an appropriate dilution.

DharmaFECT® transfection reagent I

DharmaFECT® transfection reagent I was used for the transfection of small interfering RNAs (siRNAs) into cells (Cat. No. T-2001). A 25-nM final siRNA concentration, with 2.5 µL of transfection reagent in 1 mL, was the optimal condition for reverse transfection in a 24-well plate (for further details see *Methods*). Cell numbers varied depending on the cell line used for the experiment (see Table 18).

Freezing media for cell storage

Cells were trypsinised and detached using 0.05% Trypsin-EDTA. Subsequently, cells were spun down and resuspended in the freezing medium described below.

10% (v/v) dimethyl sulfoxide (DMSO) (Sigma-Aldrich, Cat. No. D8418)

90% (v/v) FBS (Biosera)

Freezing media for T-cell storage

Cells were resuspended through pipetting, spun down and resuspended in the freezing medium described below.

RPMI 1640 (Thermo Fisher Scientific, Cat. No. 11875093)

20% (v/v) FBS (Biosera)

10% (v/v) DMSO (Sigma-Aldrich, Cat. No. D8418)

Isolation of peripheral blood mononuclear cells (PBMCs) from Buffy cones

Buffy cones (NHS Blood and Transplant, Oxford Blood Donor Centre)

Lymphoprep (Axis-Shield PoCAS, Cat. No. 1114544)

Leucosep tube (Greiner bio-one, Cat. No. 227290)

T-cell growth medium

Iscove's Modified Dulbecco's Medium (IMDM) (Life Technologies Ltd, Cat. No. 12440053)

2 mM L-glutamine (Thermo Fisher Scientific, Cat. No. 25030)

100 units/mL penicillin and 100 µg/mL streptomycin (Thermo Fisher Scientific, Cat. No. 15140122)

10% human serum (Sigma-Aldrich, Cat. No. H3667-100ML)

100 U/mL human IL-2 (PeproTech EC Ltd, Cat. No. 200-02 50 ug)

2.1.2. Materials for cell-based assays

4',6-diamidino-2-phenylindole dihydrochloride

4',6-Diamidino-2-phenylindole dihydrochloride (DAPI) (Sigma-Aldrich, Cat. No. D8417-5MG), diluted 1 mg/mL in DEPC-treated water.

Enzyme-linked immunosorbent assay (ELISA)

For standard: Human IFN-γ carrier-free recombinant protein, eBioscience™ (Thermo Fisher Scientific, Cat. No. 34-8319-82)

3,3',5'5-tetramethylbenzamide liquid substrate (MP Biomedicals, Cat. No. 0215234691)

Anti-human IFN-γ monoclonal antibody (mAb) 1-D1K, purified (Mabtech, Cat. No. 3420-3-250)

Anti-human IFN-γ mAb 7-B6-1, biotinylated (Mabtech, Cat. No. 3420-6-250)

Nunc™ MaxiSorp™ ELISA plates (BioLegend, Cat. No. 423501)

Streptavidin-horseradish peroxidase (HRP) (Mabtech, Cat. No. 3310-9)

ELISA incubation buffer

Phosphate-buffered saline (PBS) containing 0.05% Tween 20 and 1% bovine serum albumin (BSA)

ELISA wash buffer

PBS containing 0.05% Tween 20

Flow cytometry

AbC™ Anti-mouse Bead Kit (Thermo Fisher Scientific, Cat. No. A10344)

ArC™ Amine Reactive Compensation Bead Kit (Thermo Fisher Scientific, Cat. No. A10346)

Fixation/Permeabilization Solution Kit (BD Biosciences, Cat. No. 554714)

LIVE/DEAD™ Fixable Aqua Dead Cell Stain Kit (Thermo Fisher Scientific, Cat. No. L34965)

Pierce 16% formaldehyde (w/v), methanol-free (Life Technologies Ltd, Cat. No. 28908)

Immunofluorescence on coverslips

Antibody Diluent, Background Reducing (Dako, Cat. No. S302283-2)

Antibody Diluent (Dako, Cat. No. S080983-2)

Cover slips, round 13 mm no.1 (VWR, Cat. No. 631-0149)

Image-iT™ FX Signal Enhancer (Thermo Fisher Scientific, Cat. No. I36933)

Pierce 16% formaldehyde (w/v), methanol-free (Life Technologies Ltd, Cat. No. 28908)

Polysine™ Microscope Adhesion Slides (Thermo Fisher Scientific, Cat. No. P4981)

ProLong Gold Antifade Mountant (Life Technologies Ltd, Cat. No. P36930)

Immunofluorescence of screening experiments

BSA (Sigma-Aldrich, Cat. No. A9418-50G)

Columbus software (PerkinElmer)

FlexDrop PLUS (PerkinElmer)

IN Cell Analyzer 6000 (GE Healthcare Life Sciences)

Flexible JANUS® G3 Automated Workstation (PerkinElmer)

Microplate Washer EL x 405 Select CW (BioTek)

Pierce 16% formaldehyde (w/v), methanol-free (Life Technologies Ltd, Cat. No. 28908)

Pharmakon 1600 library (MicroSource Discovery Systems)

PBS (1×, pH 7.0)

5 mM NaCl

1 mM NaH_2PO_2

1.6 mM Na_2HPO_4

PBS-Tween solution (PBS-T, 1×)

Dissolve 2 mL Tween 20 in 1 L PBS.

2.1.3. Reagents for DNA- and RNA-based techniques

Agarose gels for DNA electrophoresis

Agarose (Thermo Fisher Scientific, Cat. No. BP1356) was dissolved at a concentration of 0.8% (w/v) in 1× Tris-acetate-EDTA (TAE) buffer and was used to separate DNA fragments by electrophoresis. Next, 0.4 µg/mL ethidium bromide (Sigma-Aldrich, Cat. No. E1510) was added to the agarose and DNA was visualised using an ultraviolet (UV) transilluminator (BioDoc-It System, UVP).

TAE (50×)

242 g Tris base

57.1 mL glacial acetic acid

100 mL 0.5 M EDTA

Bring volume to 1 L with H_2O. Working solution was 1×.

DNA primers

Unless otherwise stated, Eurofins MWG Operon synthesised the primers. The lyophilised primers were dissolved in water at a concentration of 100 µM.

Table 10: List of DNA primers used in this study. b2m – beta-2-microglobin; EBV – Epstein-Barr virus; GAPDH – glyceraldehyde 3-phosphate dehydrogenase.

Name	Host	Forward sequence	Reverse sequence
b2m	Human	5′-GGAATTGATTTGGGAGAGCATC-3′	5′-CAGGTCCTGGCTCTACAATTTACTAA-3′
BALF5	EBV	5′-CTTTGGCGCGGATCCTC-3′	5′-AGTCCTTCTTGGCTAGTCTGTTGAC-3′
BBLF4	EBV	5′-AAGCCTGCCTCATCCTTGACC-3′	5′-GACGAGCCTCTCCTTCACGG-3′
BcLF1	EBV	5′-CCTCCCTGACCGTTCCCAG-3′	5′-GCAGTTTGAGACCGCCACATC-3′
BGLF4	EBV	5′-TCGCGTTTTCGAAAGAAGGC-3′	5′-TCTACGTAATGACGGACCCA-3′
BGLF5	EBV	5′-TTCGGCCGCTATTAGCTTAG-3′	5′-GACGGGGGAATAATCAACCT-3′
BLLF1	EBV	5′-GTCACCTGTGTTATATTTTCACCACTT-3′	5′-CCTACCAACCTCACCGCACC-3′
BMRF1	EBV	5′-CGTGCCAATCTTGAGGTTTT-3′	5′-CGGAGGCGTGGTTAAATAAA-3′
BRLF1	EBV	5′-CCTGTCTTGGACGAGACCAT-3′	5′-AAGGCCTCCTAAGCTCCAAG-3′
BZLF1	EBV	5′-GCACATCTGCTTCAACAGGA-3′	5′-CCAAACATAAATGCCCCATC-3′
GAPDH	Human	5′-GCCTCCTGCACCACCAACTG-3′	5′-CGACGCCTGCTTCACCACCTTCT-3′′
TP53	Human	5′-GATGGGATTGGGGTTTTCCCCT-3′	5′-AATGCACTCTGTGAGGTAGGTG-3′

Real-time quantitative polymerase chain reaction (RT-qPCR)

cDNA levels were quantified using the QuantiTect SYBR Green PCR kit (QIAGEN, Cat. No. 204143).

RNA isolation

Isolation of RNA from cells was performed using the RNeasy Mini Kit (QIAGEN, Cat. No. 74106) including on-column DNA digestion with the RNase-Free DNase Set (QIAGEN, Cat. No. 79254).

RNA to cDNA conversion

cDNA was prepared from RNA using the SuperScript™ Reverse Transcriptase III (Invitrogen, Cat. No. 18080093). Additionally, components included: Oligo$(dT)_{12\text{-}18}$ Primer (Invitrogen, Cat. No. 18418-012), 10 mM deoxyribonucleotide triphosphate (dNTP) mix (Invitrogen, Cat. No. 18427-013) and RNAseOUT™ Recombinant Ribonuclease Inhibitor (Invitrogen, Cat. No. 10777-019).

Sequencing of the *TP53* gene

dNTP mix (Invitrogen, Cat. No. 18427-013)

Phusion® High-Fidelity DNA Polymerase (New England Biolabs, Cat. No. M0530S)

QIAquick Gel Extraction Kit (QIAGEN, Cat. No. 28704)

siRNA-induced gene silencing

siRNAs were dissolved and stored in 1× siRNA buffer (Dharmacon, Cat. No. B-002000-UB-100). For transfection, oligos as well as DharmaFECT I transfection reagent were dissolved in Opti-MEM reduced serum medium (Thermo Fisher Scientific, Cat. No. 31985062).

Table 11: List of siRNA oligos used in this study.

Name	Catalogue number	Company
Set of 4: ON-TARGET plus TP53 siRNA	LQ-003329-00-0005	GE Healthcare
Set of 4: Sp1 siGENOME siRNA set	MQ-026959-00-0002	GE Healthcare

Quantitative PCR for EBV genome load

Isolation of DNA from cells was performed using the DNeasy Blood & Tissue Kit (QIAGEN, Cat. No. 69506). PCRs were performed using the Taqman™ Universal PCR Master mix (Thermo Fisher Scientific, Cat. No. 4304437) with probes synthesised by Eurofins MWG Operon. The lyophilised probes were dissolved in water to a concentration of 100 µM.

Table 12: List of Taqman™ probes used for quantification of the EBV load per cell. b2m – beta-2-microglobin; EBV – Epstein-Barr virus.

Name	Host	Sequence	5' label	3' label
b2m	Human	5′-CATCAAGAAGCTGCTGGCGGCC-3′	FAM	BHQ1
BALF5	EBV	5′-AGTGTGACTGGGCAGATCATCCACCTTC-3′	YY	BHQ1

2.1.4. Reagents for protein-based techniques

Antibodies

Table 13: List of primary antibodies used in this study. FITC – fluorescein isothiocyanate; Flow – flow cytometry; HDAC – histone deacetylase; HLA – human leukocyte antigen; IF – immunofluorescence; m – mouse; mAb – monoclonal antibody; pAb – polyclonal antibody; panH3ac – acetylated histone H3; rb – rabbit; VCA – viral capsid antigen; WB – western blot.

Primary antibodies				
Antigen	**Antibody clone**	**Host/type**	**Source/product code**	**Applications**
beta-actin	C4	m mAb	sc-47778, Santa Cruz	WB (1:2000)
Ea-D	8.F.92	m mAb	ab30541, Abcam	WB (1:1000)
HDAC1	10E2	m mAb	sc-81598, Santa Cruz	WB (1:1000)
HDAC2	3F3	m mAb	sc-81599, Santa Cruz	WB (1:1000)
HDAC3	40	m mAb	sc-136290, Santa Cruz	WB (1:1000)
HLA-A,B,C PE	W6/32	m mAb	311406, BioLegend	Flow (1:50)
panH3ac	-	rb pAb	39139, Active Motif	WB (1:1000)
p53	DO-I	m mAb	sc-126, Santa Cruz	WB (1:2000)
VCA	2E08	m mAb	ab48414, Abcam	IF (1:100)
Zebra FITC	BZ1	m mAb	sc-53904, Santa Cruz	Flow (1:200)
Zebra	BZ1	m mAb	sc-53904, Santa Cruz	WB (1:1000); IF (1:100); screening (1:1000)

Table 14: List of secondary antibodies used in this study. HRP – horseradish peroxidase; IF – immunofluorescence; WB – western blot.

Secondary antibodies			
Antibody name	**Host**	**Source/product code**	**Applications**
Alexa Fluor 546® anti-mouse Immunoglobulin G (heavy+light)	Goat	A-11030, Invitrogen	IF (1:250); screening (1:500)
Anti-mouse immunoglobulins/HRP	Rabbit	PO161, Dako	WB (1:2000)
Anti-rabbit immunoglobulins/HRP	Swine	PO217, Dako	WB (1:2000)

Ammonium persulfate solution (10%)

10% (w/v) stock solution was prepared in water and used within 4 weeks of preparation. The ammonium persulfate solution used was purchased from Sigma-Aldrich (Cat. No. A3678-25G).

Blocking solution

5% (w/v) skimmed milk powder (Marvel) in Tris-buffered saline-Tween (TBS-T) was used for blocking of protein membranes.

Mass spectrometry of p53 interactors

500 cm^2 square tissue culture-treated dishes (Corning, Cat. No. 431110)

Agarose-coupled p53 (DO-1) antibody (Santa Cruz, Cat. No. Sc-126-Ac)

Disuccinimidyl sulfoxide (Cambridge Bioscience, Cat. No. 9002863)

Mass spectrometry lysis buffer

50 mM Tris-HCl pH 7.6

120 mM NaCl

1% NP40

1 mM EDTA

COmplete™ protease (Cat. No. 5056489001) and PhosSTOP phosphatase inhibitor cocktails (Cat. No. 04906837001) from Roche were added to the buffer before use.

Polyacrylamide gel preparation

Table 15: Recipe for the preparation of stacking and resolving SDS-polyacrylamide gels. APS – ammonium persulphate solution; SDS – sodium dodecyl sulfate; TEMED – N,N,N',N-tetramethyl-ethylenediamine.

Stacking gel		**Resolving gels**				
4	**Acrylamide %**	6	8	10	12	15
1.3 mL	**30% Acrylamide/Bis**	2 mL	2.7 mL	3.3 mL	4.0 mL	5.0 mL
--	**1.5 M Tris-HCl pH 8.8**	2.5 mL	2.5 mL	2.5 mL	2.5 mL	2.5 mL
2.5 mL	**1.0 M Tris-HCl pH 6.8**	--	--	--	--	--
100 µL	**10% SDS**	100 µL	100 µL	100 µL	100 µL	100 µL
100 µL	**10% APS**	100 µL	100 µL	100 µL	100 µL	100 µL
10 µL	**TEMED**	10 µL	8 µL	5 µL	5 µL	5 µL
6.1 mL	**Distilled water**	5.3 mL	4.6 mL	4.0 mL	3.3 mL	2.3 mL
10 mL	**Total volume**	10 mL	10 mL	10 mL	10 mL	10 mL

Ponceau S staining solution

Ponceau solution was obtained from Sigma-Aldrich (Cat. No. P7170).

Protein molecular weight markers

A New England Biolabs pre-stained protein marker (Cat. No. P7706) was used as a size standard for sodium dodecyl sulfate (SDS)-polyacrylamide gel electrophoresis.

SDS solution (10%)

Dissolve 10 g SDS (Sigma-Aldrich, Cat. No. 71725-50G) in 100 mL water and use within 6 months of preparation.

SDS sample buffer (5×)

0.3 M Tris-HCl pH 6.8

50% (v/v) glycerol

10% (w/v) SDS

0.05% (w/v) bromophenol blue in double-distilled H_20

25% (v/v) β-mercaptoethanol

Tris-HCl, 1.5 M, pH 8.8

To prepare a 1.5 M solution, dissolve 181.65 g of Tris-base in 0.7 L of water, adjust the pH to 8.8 and bring volume to 1 L with water. Autoclave the solution before use.

Tris-HCl, 1.0 M, pH 6.8

To prepare a 1 M solution, dissolve 121.1 g of Tris-base in 0.7 L of water, adjust the pH to 6.8 and bring volume to 1 L with water. Autoclave the solution before use.

TBS buffer (20×)

121 g Tris-Cl

175.2 g NaCl

Adjust pH to 7.5 with 1 M HCl and bring volume to 1 L with H_2O.

TBS-T buffer (1×)

50 mL 20× TBS

1 mL Tween 20

Solubilised in 1 L of water.

Urea buffer

8 M Urea

1M Thiourea

0.5% (w/v) CHAPS

50 mM dithiothreitol

24 mM spermine

2.2 Methods

2.2.1. Cell culture methods

Automated cell counting

Cells were washed with PBS and then incubated with 0.2% (w/v) trypan blue solution diluted with PBS for 1 min. After removing the solution, the cells were immediately fixed with 4% paraformaldehyde in PBS for 10 min. Fixed cells were washed three times with PBS before being stained for 10 min with DAPI diluted 1:1,500 in PBS for a final concentration of 0.5 μg/mL. Cells were washed again with PBS and stored at 4 °C until imaging.

Cells were visualised using a Zeiss LSM 710 laser scanning confocal microscope equipped with the following lasers: argon 458/488, HeNe 543 and HeNe 633. The images were acquired using Zeiss LSM 710 software supplied with the microscope.

The percentage of live cells was determined by an ImageJ macro written specifically for this purpose by Mark Shipman (University of Oxford). In brief, this macro identified nuclei and measured the total nuclear area. The macro then identified a nuclear threshold on the image of each well, measured the signal in the second channel (representing the autofluorescence of trypan blue) and created an overlay image. The threshold of the second channel was set manually for each experiment based on the signal in the control sample.

Cell passaging and freezing

Cells reaching around 90% confluence were washed with 1x PBS and incubated with 0.05% trypsin-EDTA at 37 °C until cells detached from the surface of the dish. Next, trypsin was inhibited by the addition of growth medium. The cells were subsequently pelleted for 5 min at 500 × g. Cells were either resuspended in growth medium and plated at the desired density, or 5×10^6 cells resuspended in 0.75 mL freezing medium and added to cryovials (Corning, Cat. No. 377267). Cryovials were placed in Nalgen Cryo containers in a −80 °C freezer for at least 24 h, before being transferred to a liquid nitrogen tank for long-term storage.

Cell treatment

For treatment with different compounds, cells were plated at appropriate densities in growth medium. After 24 h, growth medium was removed and replaced with growth medium containing the stated concentrations of compound. Control samples were treated with matching amounts of solvent, DMSO if not stated otherwise. Cells were treated for 48 h if not stated otherwise, before being collected in an appropriate manner for downstream analysis (see details below).

Isolation of PBMCs from Buffy cones

Buffy cones were emptied into 50 mL tubes and PBS added to dilute the solution to a volume of 60 mL. Next, 25–30 mL of this mixture was carefully added to 50 mL Leucosep tubes containing 15 mL Lymphoprep. After centrifugation for 20 min at 600 × g without acceleration and brake, the interphase containing mononuclear cells was collected and added into a new 50 mL tube. The cells were diluted to 50 mL with cold RPMI and then centrifuged for 7 min at 300 × g at 4 °C. This washing step was repeated once before the cells were counted. Cells were then frozen in normal freezing medium until needed or added into a 24-well plate for irradiation.

T-cell culture

T-cell clones were culture in 24-well plates with stimulator cells in 1 mL T-cell culture medium. Next, 2×10^6 PBMCs and 2×10^5 PLPH EBV cells were irradiated at 30 Gy before 1×10^6 T-cells (DIPE clone) were added to the wells.

2.2.2. Cell-based assays

ELISA

ELISA plates were coated overnight with 50 µL/well mAb 1-D1K 1:500 diluted in PBS at 4 °C. After removing the coating solution, plates were blocked by incubation for 1 h with 200 µL/well ELISA incubation buffer. During this time, an IFN-γ 1:1 serial dilution was prepared in RPMI medium starting from 2 ng/mL with seven subsequent dilutions. After washing the plate six times with ELISA wash buffer, 50 µL of standard dilution or sample supernatant was added per well and incubated for 2 h at room temperature. After six washes with ELISA wash buffer, 50 µL/well of mAB 7-B6-1-Biotin diluted 1:1,000 in ELISA incubation buffer was added to the wells for 1 h. Following six washes in ELISA wash buffer, 50 µL of streptavidin-HRP diluted at 1:1,000 in ELISA incubation buffer was added per well and

incubated for 30 min. After this step, the plate was washed eight times with ELISA wash buffer, before 100 µL/well substrate solution, 3,3',5'5-tetramethylbenzamide liquid substrate, was added to the plate. When the standard became visible, the reaction was stopped by adding 100 µL/well 1 M HCl. The plate was read in a spectrophotometer (Anthus Labtech Instrument, using Magellan software) at an absorbance of 450 nm and the concentration of IFN-γ in sample supernatants determined based on the standard curve.

Flow cytometry

Cells were washed once with PBS before being scraped off and counted using trypan blue. First, 5×10^5 cells were collected in a 200 µL PBS within a V-bottom 96-well plate. After washing with 200 µL PBS, cells were spun down at 500 × g for 3 min. Cells were then resuspended in 20 µL LD Aqua live/dead stain diluted 1:200 in PBS and incubated for 10 min at room temperature in the dark. After washing and spinning the cells as before, cells were fixed with 100 µL BD CytoFix for 15 min at room temperature in the dark. Cells were washed twice with 100 µL BD Permwash and spun down as before. Cells were then stained intracellularly for 15 min at room temperature in the dark with the appropriate amounts of antibody diluted in BD Permwash. Afterwards, cells were washed twice with 100 µL Permwash and spun down before being resuspended in 200 µL 4% paraformaldehyde. Cells can be stored in this state at 4 °C until being analysed by flow cytometry.

Flow cytometry analysis was performed using CyAN ADP (Dako Cytomation) and the results examined using FlowJo V10.

Immunofluorescence (on coverslips)

The following is the standard staining protocol used for all immunofluorescence staining. Changes in buffers and machines used for liquid handling for screening experiments will be discusses separately.

All steps of immunofluorescene staining protocol were performed at room temperature. After washing with PBS, cells were fixed by the addition of 4% formaldehyde in PBS for 10 min, washed three times with PBS and incubated with 0.1% Triton X-100 for 20 min. After three more washes, coverslips were incubated with Signal Enhancer for 30 min. Following one wash, cells were incubated with the primary antibody diluted in antibody diluent with background reducing agent for 90 min. After washing three times, coverslips were incubated with secondary antibody solution containing DAPI diluted in antibody diluent for 1 h in the dark. Coverslips were washed three times with PBS and once in purified water before coverslips were mounted on Polysine™ Microscope Adhesion slides with ProLong Gold Antifade Mountant.

Cells affixed on slides were visualised using a Zeiss LSM 710 laser scanning confocal microscope equipped with the following lasers: argon 458/488, HeNe 543 and HeNe 633. The images were acquired using Zeiss LSM 710 software supplied with the microscope. Adjustments to acquired images were limited to contrast enhancement, cropping and merging channels of different fluorophores. Cell counting of immunofluorescence staining was performed from at least five different fields of view per sample. Those fields were chosen based on the DAPI signal, not considering the staining of interest.

Immunofluorescence for screening experiments

The protocol used for the staining of cell culture dishes was the same as stated above in *Immunofluorescence (on coverslips)*, and only differences between the two will be mentioned here.

Cells were fixed in cell culture dishes after washing once with PBS. After permeabilisation with Triton X-100, the samples were incubated with 3% BSA in 0.1% PBS-T for 1 h. Next, 1% BSA in PBS-T was used as the diluent for the primary antibody, and PBS-T for the secondary antibody and DAPI. After finishing the staining procedure, wells were filled with PBS and stored at 4 °C until imaging.

Imaging of the plates was performed as stated for 'Immunofluorescence on coverslips'. The percentage of Zebra-positive cells was determined by an ImageJ macro written specifically for this purpose by Mark Shipman (University of Oxford). In brief, this macro identified nuclei and measured the total nuclear area. The macro then identified a nuclear threshold on the image of each well, measured the signal in the second channel and created an overlay image. The threshold of the second channel was set manually for each experiment based on the signal in the control sample. All compounds inducing Zebra expression in more than 5% of cells were considered as hits, but compounds that decreased cell numbers to less than 25% compared to controls were excluded.

Immunofluorescence for the high-throughput screening experiment

The protocol used for staining of cell culture dishes was the same as stated above in *Immunofluorescence for screening experiments*, and only differences between the two will be mentioned here.

All screening plates for high-throughput screening experiments were run in duplicate. Liquid handling for cell plating, drug treatment and cell fixation was performed using a JANUS PerkinElmer Automated Workstation. All washing steps of the staining procedure were performed with a BioTek Microplate Washer EL x 405 Select CV. All other staining steps were performed with a FlexDrop PLUS (PerkinElmer). Cells were visualised using a GE IN Cell Analyzer 6000 with a 10× objective. Percentages of Zebra-positive cells within the wells were assessed with a protocol established within the Columbus software. Z-scores were calculated by the TDI Cellular High Throughput Screening Facility, Oxford. Compounds fulfilling the following criteria were considered as potential hits: a Z-score ≥ 1.96, Zebra expression levels ≥ 5% and wells containing more than 1,000 cells after treatment.

2.2.3. DNA- and RNA-based methods

RNA extraction and reverse transcription

RNA was extracted from cells using the QIAGEN RNeasy Mini Kit, following the manufacturer's instructions. Possible contamination with genomic DNA was removed by treatment with DNase I as suggested by the manufacturer. Then, 1 µg was used to generate cDNA using the SuperScript™ Reverse Transcriptase III System following the manufacturer's instructions.

RT-qPCR

The QuantiTect SYBR Green PCR kit was used to perform RT-qPCR using the StepOnePlus real-time PCR system (Applied Biosystem). Reactions were performed in duplicate and in a final volume of 20 µL. Reaction constituents are shown in Table 16.

Table 16: Composition of RT-qPCR reactions.

Reagent	Per reaction (µL)
2× SYBR Green reagent	10
Forward/reverse primer mix (10 µM)	0.5
RNAse-free water	7.5
cDNA (~20 ng/µL)	2

The following cycle conditions were used for all samples:

95 °C	15 min	
95 °C	15 s	Cycles were repeated 40×
55 °C	30 s	
72 °C	1 min	

Relative mRNA abundances were normalised to endogenous glyceraldehyde 3-phosphate dehydrogenase (GAPDH) mRNA levels. Shown qPCR results were analysed by the $\Delta\Delta C_t$-method as previously described, with the threshold cycles being determined by the Applied Biosystems software (Schmittgen & Livak, 2008).

Sequencing of the *TP53* gene

RNA extraction and reverse transcription were performed as stated above. The Phusion polymerase was used to perform PCR using the ProFlex PCR system (Applied Biosystems). Reactions were performed in a final volume of 50 µL. Reaction constituents were:

Table 17: Composition of the PCR reaction for the amplification of *TP53* cDNA.

Reagent	Per reaction (µL)
Phusion polymerase GC buffer (5×)	10
TP53 forward primer (10 µM)	2.5
TP53 reverse primer (10 µM)	2.5
dNTP mix (10 mM)	1
Phusion polymerase (2 U/µL)	0.5
RNAse-free water	26
cDNA (~20 ng/µL)	7.5

The following cycle conditions were used for all samples:

98 °C	30 min	
98 °C	10 s	Cycles were repeated 35×
65 °C	30 s	
72 °C	75 s	
72 °C	10 min	

PCR products were analysed on 0.8% agarose gels and the DNA of the right sized band isolated using the QIAquick Gel Extraction Kit following the manufacturer's instructions. Isolated *TP53* cDNA was sequenced by Eurofins MWG Operon using the *TP53* forward primer. *TP53* status was determined by comparing the generated sequences to National Center for Biotechnology Information reference sequence NM_000546.5.

siRNA-induced gene silencing

siRNA oligos purchased from Dharmacon (Table 11) were used to silence the expression of specific genes of interest. Cells were transiently transfected with DharmaFECT I transfection reagent by reverse transfection with the cell number stated in Table 18. In brief, 25 nM of siRNA were added to a total of 100 µL Opti-MEM, and 2.5 µL DharmaFECT to 100 µL Opti-MEM, in separate tubes. After incubation for 5 min, the contents of the two tubes were combined and incubated for 20 min. The appropriate amount of cells in antibiotic-free growth medium was added to the transfection mixture, brought to a 1 mL total volume and added to a 24-well plate.

Table 18: Cell numbers used for reverse transfection in 24-well plates.

Cell line	Cell number/well
AGS rEBV-GFP	1.2×10^5
C666.1	3.5×10^5
SNU-NCC-24	3.0×10^5
YCCEL1	3.5×10^5

Quantitative PCR for EBV genome load

Cells were washed once with ice-cold PBS before being scraped off the dish in PBS. Subsequently, the DNA was isolated using the QIAGEN DNeasy Blood & Tissue Kit following the manufacturer's instructions. The TaqMan™ Universal PCR Master Mix was used to perform RT-qPCR using the

StepOnePlus real-time PCR system (Applied Biosystem). DNA from Namalwa cells, containing two integrated EBV genomes per cell, was used as the standard to prepare a calibration curve (Hui & Chiang, 2010). Reactions were performed in duplicate and in a final volume of 20 µL. Composition of the reactions as well as the used cycle conditions are stated in the following.

Table 19: Composition of qPCR reactions for the quantification of the EBV genome load per cell.

Reagent	Per reaction (µL)
2× TaqMan™ Universal PCR Master Mix	10
BALF5 forward primer (10 µM stock)	0.4
BALF5 reverse primer (10 µM stock)	0.4
BALF5 probe (10 µM stock)	0.4
b2m forward primer (6 µM stock)	0.2
b2m reverse primer (8 µM stock)	0.2
b2m probe (5 µM stock)	0.4
RNAse-free water	4
DNA (~5 ng/µL)	4

The following cycle conditions were used for all samples:

50 °C	2 min	
95 °C	10 min	
95 °C	15 s	Cycles were repeated
60 °C	1 min	40×

2.2.4. Protein-based methods

Mass spectrometry of p53 interactors

YCCEL1 cells were treated for 24 h with different compound combinations. For collection, cells were washed twice with ice-cold PBS before being scraped off the dish in mass spectrometry (MS) lysis buffer and lysed for 30 min at 4 °C during constant rotation. Lysates were cleared by centrifugation at 2500 × g for 15 min at 4 °C and their protein content subsequently quantified by Bradford assay. Part of the lysate was kept as an input control and the rest was incubated with pre-coupled agarose beads for 4 h at 4 °C with constant rotation. Beads were then washed two times with MS lysis buffer, with the suspension spun down for every wash at 2500 x g for 2 min at 4 °C. This was followed by two washes with PBS before all liquid was removed from the beads. A final concentration of 5 mM Disuccinimidyl Sulfoxide in PBS was then added to the beads and incubated for 30 min on ice. To stop the reaction, lysis buffer was added to a 20 mM final concentration of Tris and the samples incubated for 15 min on ice. Finally, excess crosslinker was removed from the beads and the beads washed twice with PBS. The dry beads were then stored at –80 °C until analysis by MS through the Advanced Proteomics Facility of the TDI, Oxford by Dr Roman Fischer and Georgina Berridge. Subsequent data analysis was performed by Dr Thomas Leissing, University of Oxford.

Western blotting

Cells were washed once with ice-cold PBS before being scraped off the dish in PBS. The cells were pelleted at 2500 × g for 5 min at 4 °C and lysed with urea buffer on ice for 30 min. Lysates were cleared by centrifugation at 2500 × g for 20 min at 4 °C. Protein concentration was determined by Bradford assay. Samples were boiled in 1× SDS sample buffer for 5 min and subsequently separated on manually casted SDS-acrylamide gels with a pre-stained protein marker as a molecular weight standard. Proteins were transferred on a nitrocellulose membrane (GE Healthcare), blocked with 5% dried skimmed milk

in TBS-T for 1 h and incubated with the primary antibody (Table 13) diluted in 1% milk in TBS-T overnight at 4 °C. After washing, membranes were incubated with the appropriate HRP-conjugated secondary antibody (1:2,000; Dako) in TBS-T for 1 h at room temperature before visualising with an enzymatic chemiluminescence detection system (GE Healthcare).

Scanned autoradiographs from western blots were only modified for size, brightness and contrast. No signal was otherwise modified in relation to the raw image.

Protein concentration determination

Bio-Rad Protein Assay Dye Reagent Concentrate (Bio-Rad, Cat. No. 5000006) was used to determine protein concentrations of cell lysates. Six dilutions of 2 mg/mL BSA were used as a standard curve. Dilutions of BSA or 1 µL of cell lysate were pipetted into a 96-well plate and mixed with 200 µL of 1x Bio-Rad assay reagent. The plate was read in a spectrophotometer (Anthus Labtech Instrument, using Magellan software) at an absorbance of 595 nm and the concentration of the cell lysate determined based on the standard curve.

Chapter 3: Inhibition of HDACs by benzamides induces Zebra expression in epithelial cells

3.1 Introduction

Through alterations in DNA accessibility and chromatin structure the epigenome regulates cellular gene expression. The epigenome encompasses heritable chemical modifications of histones and DNA sequences that are established by chromatin-associated proteins. While several factors can induce changes in the chromatin structure, covalent modifications of histones and DNA are the most decisive elements coordinating this process (reviewed in Segal & Widom, 2009). By changing the interaction between the DNA sequence and histones, chromatin modifications modify the accessibility of specific loci and thereby their gene expression.

Different DNA and histone modifications such as phosphorylation, acetylation and methylation have been shown to define the epigenetic code, the map of covalent modifications on DNA and histones (reviewed in Falkenberg & Johnstone, 2014). The proteins related to those post-translational modifications (PTMs) are chromatin-interacting proteins that are classified based on their property of adding, recognising or removing specific PTMs (Figure 13). Epigenetic writers such as histone methyltransferases or HATs add chemical modifications to histones, while epigenetic erasers such as histone demethylases and HDACs remove those modifications. Proteins encompassing domains that recognise particular histone modifications are classified as epigenetic readers. Examples of this group are bromodomain or tudor domain containing proteins such as CREBBP, BRD4 and 53BP1.

The reversibility of epigenetic modifications compared to the irreversibility of genomic mutations allows for correction of aberrant epigenetic profiles and therefore makes them a potential therapeutic target. Several epigenetic therapies (such as 5-Aza) inhibiting DNA methyltransferases and different compounds inhibiting HDACs have been approved by the US Food and Drug Administration (FDA) for

the treatment of myelodysplastic syndrome, different cancer types and hypertension (reviewed in Simõ-Riudalbas & Esteller, 2015).

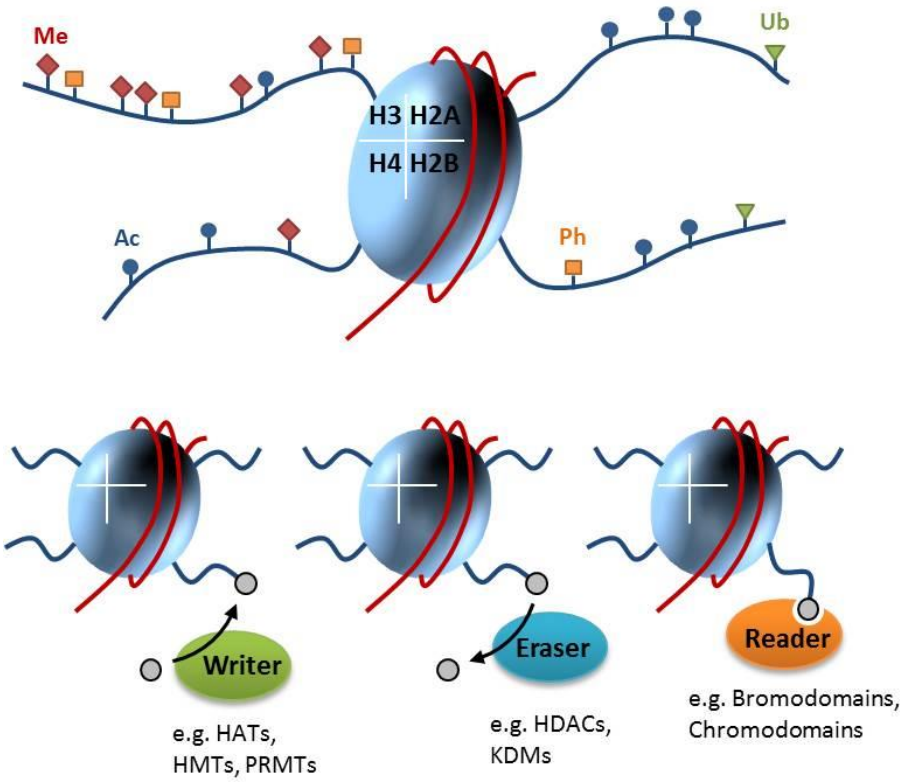


Figure 13: Overview of histone modifications and epigenetic readers, writers and erasers. The nucleosome is the basic functional unit of chromatin and consists of DNA wrapped around histones (H2A, H2B, H3 and H4). Post-translational modifications such as methylation, acetylation, phosphorylation and ubiquitination can be placed on the core histone tails protruding from the nucleosomes. The main regulators of epigenetic marks can be categorised into writers, readers and erasers of post-translational modifications (based on Simõ-Riudalbas & Esteller, 2015). Ac – acetylation; HAT – histone acetyltransferase; HDAC – histone deacetylase; HMT – histone methyltransferases; KDM – histone lysine demethylase; Me – methylation; Ph – phosphorylation; PRMT – protein arginine methyltransferases; Ub – ubiquitination

HDACs are a class of enzyme that remove acetylation marks on lysine residues that have been transferred there by HATs. In humans, there are four different classes of HDACs, defined based on their function and DNA sequence similarity, with 18 members in total (Table 20) (reviewed in Seto & Yoshida, 2014).

Table 20: Classification of HDAC members into four classes. Adapted from (Seto & Yoshida, 2014). HDAC – histone deacetylase; SIRT – sirtuin.

HDAC class	HDAC class members
Class I	HDAC1, HDAC2, HDAC3, HDAC8
Class II	HDAC4, HDAC5, HDAC6, HDAC7, HDAC9 HDAC10
Class III	SIRT1-7
Class IV	HDAC11

Class I, II and IV HDACs belong to the arginase/deacteylase superfamily of proteins, while class III HDACs belong to the deoxyhypusine synthase-like nicotinamide adenine dinucleotide (NAD)/flavin adenine dinucleotide (FAD)-binding domain superfamily. Class III HDACs, the so called sirtuins, are NAD^+-dependent enzymes, whereas the 'classical' HDAC family of enzymes (classes I, II and IV) share a common catalytic mechanism that requires a zinc ion. Therefore, most HDACis are designed to chelate metal ions, more specifically zinc (reviewed in Falkenberg & Johnstone, 2014). The first group of HDACis use hydroxamic acid as the zinc-interacting group. Hydroxamate-based HDACis such as trichostatin A (TSA) and SAHA inhibit a broad range of HDACs (Falkenberg & Johnstone, 2014). Other zinc-binding groups have been introduced to increase specificity, the most common of which are benzamide derivatives. Those benzamide-based HDACis, like CI-994 and mocetinostat, are generally more restricted to inhibiting class I HDACs (Beckers *et al.*, 2007).

Epigenetic modifications are not just important for the regulation of cellular gene expression, but also for the control of the life cycle of EBV. Upon infection, EBV induces DNA methylation of its own as well as of the cellular genome, and thereby establishes and maintains the viral latent state (Bergbauer *et al.,* 2010; Zhao *et al.,* 2013; Matsusaka *et al.,* 2017). Accordingly, repressive histone marks such as H3K27me3 and H4K20me3 are introduced to lytic promoters such as Zp (Murata *et al.,* 2012). Changes in histone marks such as increased histone acetylation in IE and E lytic promoter regions have been

shown to be associated with lytic cycle induction (Jenkins *et al.*, 2000; Countryman *et al.*, 2008; Mansouri *et al.*, 2013). Therefore, it is not surprising that perturbing the epigenetic landscape of the cell through demethylating agents or HDACis is sufficient to induce lytic cycle expression in EBV-positive cells (Feng *et al.*, 2004a; Stoker *et al.*, 2015; Hui *et al.*, 2016).

The aim of this study was to identify novel epigenetic inhibitors that are able to reactivate EBV in epithelial cells in an unbiased manner.

3.2 Results

3.2.1 Only HDACis induce Zebra expression in a panel of epigenetic inhibitors

In order to characterise the ability of epigenetic inhibitors to reactivate EBV in epithelial cells, a Zebra-based screening system was established using Zebra as a marker for lytic cycle induction. To establish the screening protocol, standard immunofluorescence protocols were adapted for use in multiwell dishes and antibody concentrations titrated to a minimum to reduce the cost of the screening procedure.

YCCEL1 cells were plated in multiwell dishes and treated with a library of different epigenetic compounds. Cells were fixed and stained for Zebra within the dish and imaged using fluorescence microscopy 48 h after treatment. This method has been developed using YCCEL1 cells, a gastric cancer cell line derived from an EBV-positive tumour, but other cell lines have also been successfully used with this protocol (Figure 14).

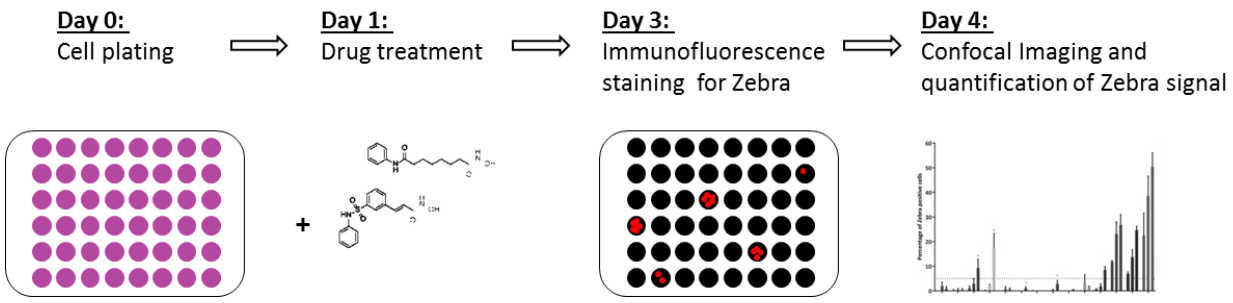


Figure 14: Zebra-based screening method for EBV reactivation in epithelial cells. Cells were plated in multiwell dishes before treatment with different compounds for 48 h. At the endpoint, cells were fixed, stained and imaged using fluorescence microscopy. Analysis was performed with an ImageJ macro kindly provided by Mark Shipman (University of Oxford).

Image analysis by a macro, kindly provided by Mark Shipman (University of Oxford), allowed fast and unbiased analysis of the reactivating abilities of different compounds. This macro identified nuclei based on the DAPI signal within a specified size range, excluding small debris as well as large objects, and then measured the Zebra signal within the generated nuclear mask (Figure 15). For each

experiment, a manual threshold for the Zebra signal was set based on the background in control samples, thereby controlling for variation between experiments. Compounds that induced Zebra expression in more than 5% of cells were considered as potential hits.

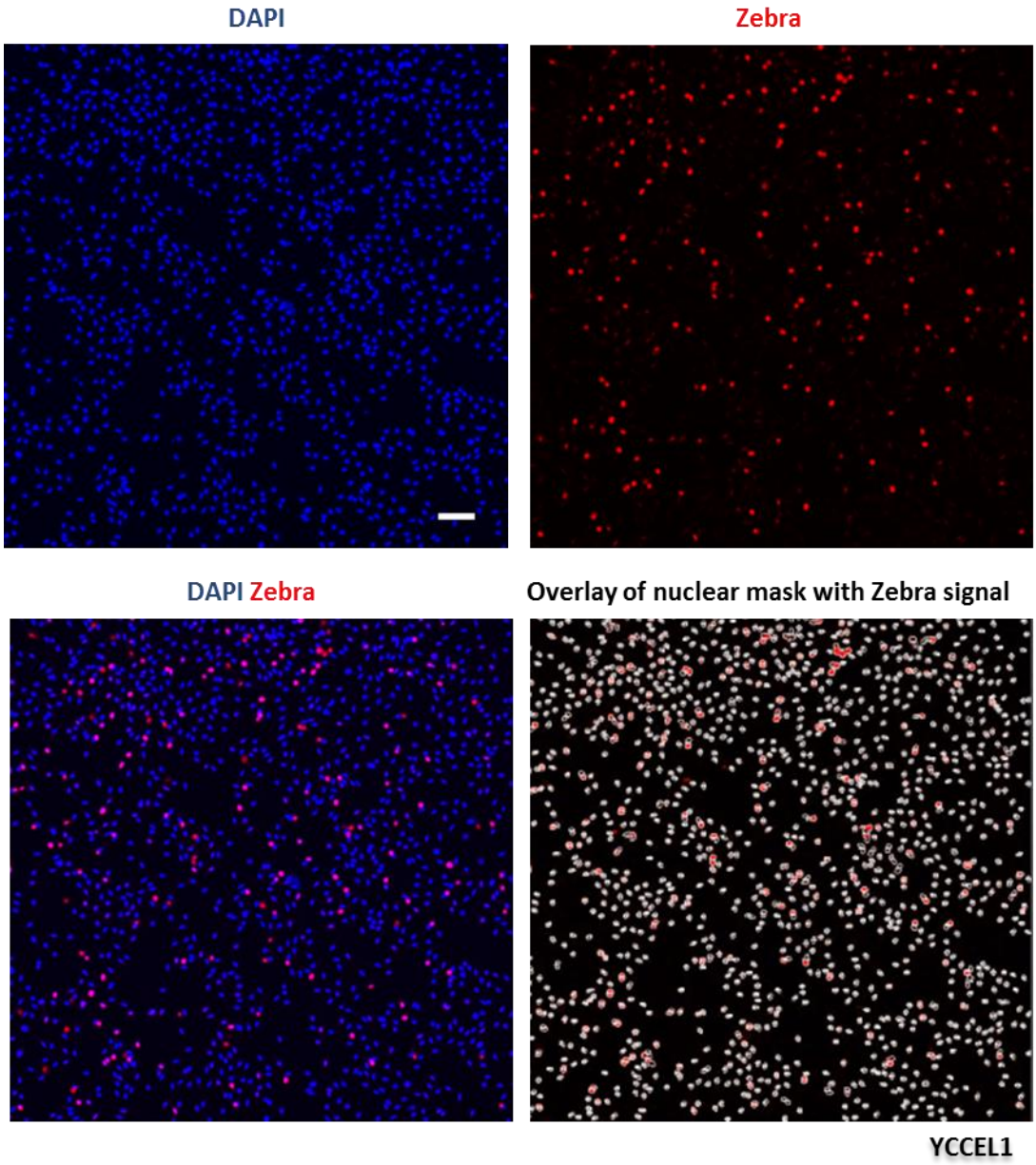


Figure 15: Example of nuclear identification by an ImageJ macro used for the analysis of immunofluorescence images. A nuclear mask was generated based on the DAPI signal within a set size range (white). The Zebra signal (red) was then determined within the nuclear mask (overlay image). The threshold for the discrimination of positive Zebra staining from the background was set based on control samples. The scale bar represents 100 µm. Analysis was performed with an ImageJ macro kindly provided by Mark Shipman (University of Oxford). DAPI – 4',6-diamidino-2-phenylindole dihydrochloride.

To identify epigenetic inhibitors that induce Zebra expression in YCCEL1 cells, a screening experiment was performed using an extended epigenetic inhibitor library. This library was kindly provided by the Structural Genomics Consortium (SGC), Oxford (Chapter 2.1.1, Table 7) and targeted a broad panel of epigenetic readers, writers and erasers such as bromodomain and extra-terminal (BET) proteins, HDACs and histone methyltransferases (for extended compound information see Appendix Table 1). All compounds were tested at two different concentrations based on publicly available compound information (Chapter 2.1.1, Table 7).

Most of the tested compounds did not induce any detectable Zebra expression (Figure 16). The HDACis chidamide and CXD101 were the only compounds that induced Zebra expression in over 5% of cells at both tested concentrations. Panobinostat, an HDACi, was able to induce Zebra expression in around 7% of cells at the higher concentration tested, but at this concentration less than 25% of the seeded cells were still alive. Compounds that decreased cell numbers to less than 25% of controls were excluded as potential hits. Two other HDACis, PXD101 and romidepsin, induced Zebra expression in less than 2% of cells. CI-994, also an HDACi, induced Zebra expression in ~2.5% of the cells at both tested concentrations. Overall, it seems that only compounds with HDACi activity were able to induce Zebra expression reproducibly in this screen.

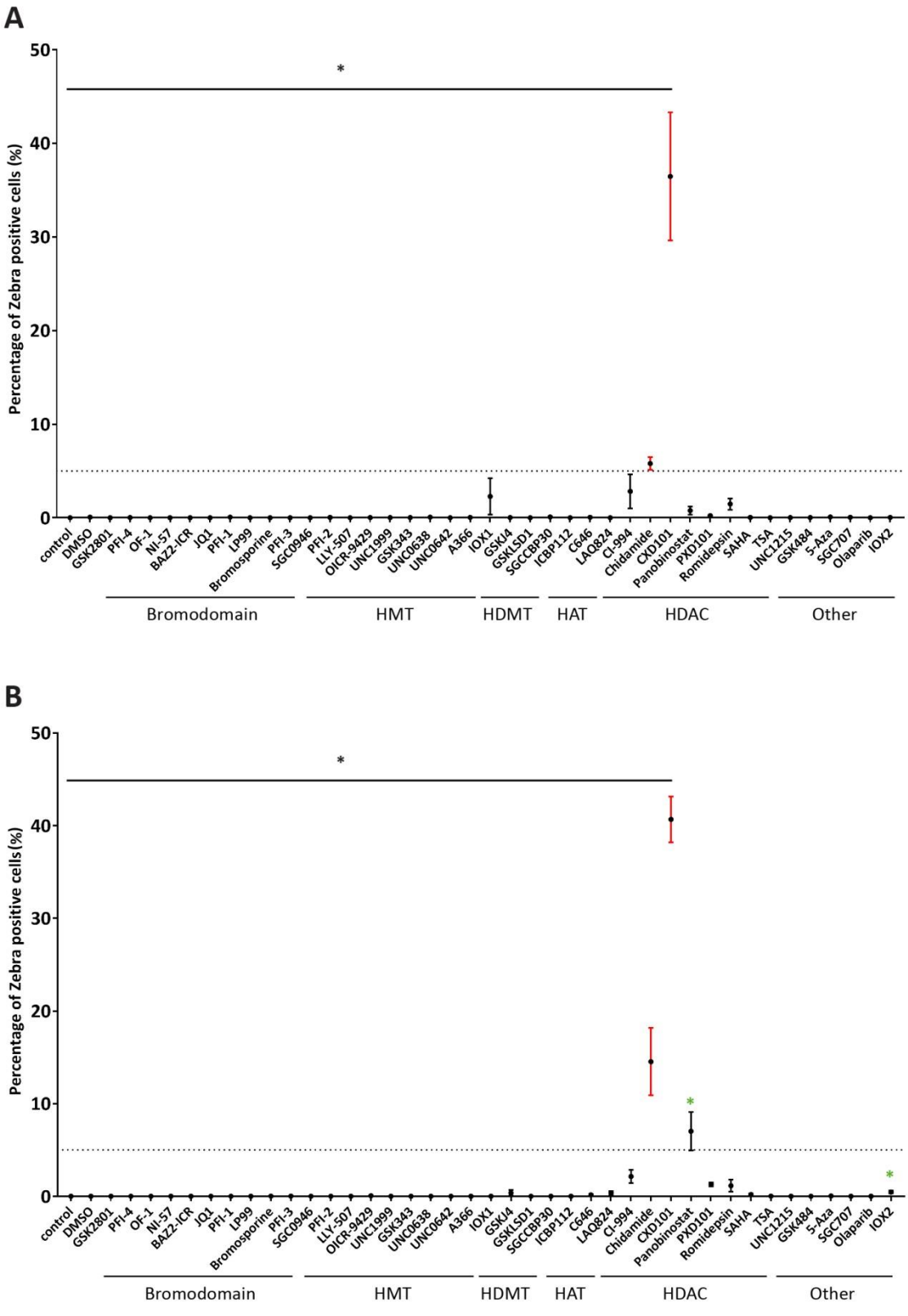


Figure 16: Epigenetic inhibitor screening for EBV reactivation in YCCEL1 cells. YCCEL1 cells were treated for 48 h with the indicated compounds at two different concentrations (for detailed concentrations see Table 7). Screening results for the low concentrations (A) and the high

concentrations (B) are shown. Compounds were grouped based on their target activity. Control samples were treated with DMSO. All measured percentages have been normalised to control cells. The green asterisks indicate cell survival of less than 25%. The dotted line represents Zebra expression in 5% of cells, which was defined as the cut-off definition for hits. Bars represent the average of three independently performed experiments. n = 3, error bars ± SEM. $P^* \leq 0.05$; $P^{**} \leq 0.01$; $P^{***} \leq 0.005$. Significances were calculated using Dunnett's multiple comparison test relative to control cells. Bromodomain – bromodomain-containing protein; DMSO – dimethyl sulfoxide; HAT – histone acetyltransferase; HDAC – histone deacetylase; HDMT – histone demethylase; HMT – histone methyltransferase.

To validate the screening results and to exclude the possibility that the observed effects were an artefact of the novel imaging-based screening method (Figure 14), western blot analysis was performed with a subset of epigenetic compounds included in the extended SGC epigenetic inhibitor library (for extended compound information see Appendix Table 1). Similarly to the screen, western blot analysis showed that most of the tested compounds did not induce any Zebra expression after 48 h of treatment (Figure 17). CI-994 induced Zebra expression at a low level, while chidamide and CXD101 induced significantly higher levels. The western blot further confirmed that CXD101 induced the highest levels of Zebra expression of those three compounds. Panobinostat induced Zebra expression levels similar to CXD101 treatment (Figure 17).

Overall, this suggests that, of the panel of tested epigenetic inhibitors, HDACis are the most efficient compound class in inducing Zebra expression.

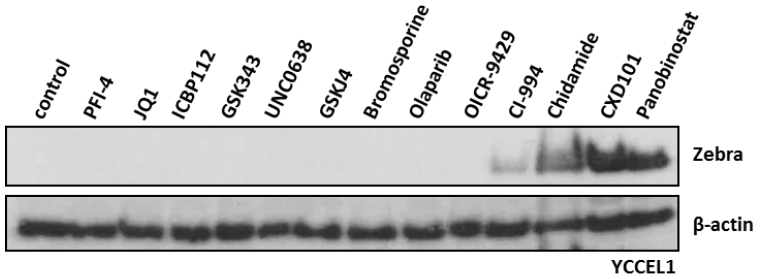


Figure 17: Zebra expression induced by epigenetic inhibitor treatment in YCCEL1 cells analysed by western blot. YCCEL1 cells were treated for 48 h with the indicated compounds at the high concentrations stated in Table 7 before being lysed for protein isolation. The results shown are representative for three independent repeats of this experiment.

3.2.2 Benzamide HDACis are more potent in inducing Zebra expression than other HDACi classes

The results in Chapter 3.2.1 indicated that HDACis are the most potent group of epigenetic inhibitors in inducing the viral reactivation of EBV. In addition, the results suggested that CI-994, chidamide and CXD101 are more potent in inducing reactivation than other HDACis in YCCEL1 cells. A structural comparison of those three compounds with other HDACi compounds included in the screen identified structural differences between those groups of HDACis (Figure 18). SAHA, PXD101, panobinostat, TSA and LAQ824 are all hydroxamate-based HDACis. In contrast, CI-994, chidamide and CXD101 are benzamide-based HDACis. Romidepsin, another HDACi included in the screen, was excluded from this analysis because it belongs to the smaller group of cyclic peptides.

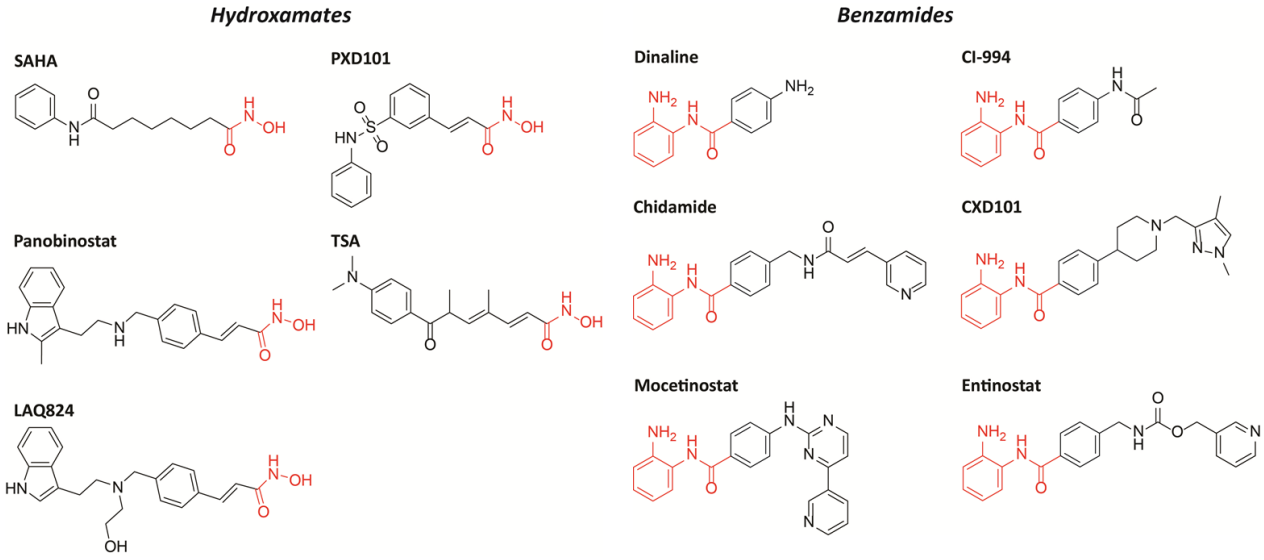


Figure 18: **Structural comparison of HDACi classes.** Hydroxamates and benzamide HDACis significantly differ in their zinc-binding group highlighted in red. HDACi – histone deacetylase inhibitor; TSA – Trichostatin A.

Comparison of the induced Zebra expression suggested that benzamide HDACis are potentially more potent in inducing EBV reactivation than hydroxamate HDACis (Figure 16). In order to test this

hypothesis, the panel of benzamide HDACis was extended to include dinaline, mocetinostat and entinostat.

To examine whether benzamide HDACis are more potent in inducing Zebra expression in YCCEL1 cells, a screening experiment with all HDACis included in the structural analysis was performed (Figure 19). To reduce the potential of artefacts based on a chosen concentration, all HDACis were used at three different concentrations that were chosen based on publicly available compound information (concentrations stated in Table 8). The screening showed that control treatment with DMSO induced Zebra expression in less than 2% of cells, representing the low level of background in this experimental set-up. As in the initial screen, panobinostat led to Zebra expression in an increased number of cells, ~18%, at the highest concentration used. This was also linked to decreased cell survival, reducing cell numbers to less than 25% compared to control cells (Table 21). The same was observed with LAQ824, but this compound only led to the induction of Zebra expression in ~9% of cells. The other hydroxamate HDACis as well as romidepsin, which was included as a control, induced Zebra expression in less than 2.5% of cells. The HDACi dinaline, the deacetylated derivate of CI-994, did not induce Zebra expression, while CI-994 induced Zebra expression in less than 5% of cells. Chidamide, CXD101, entinostat and mocetinostat showed strong dose responses. Increased concentrations of compounds led to a significant increase in the percentage of Zebra-positive cells.

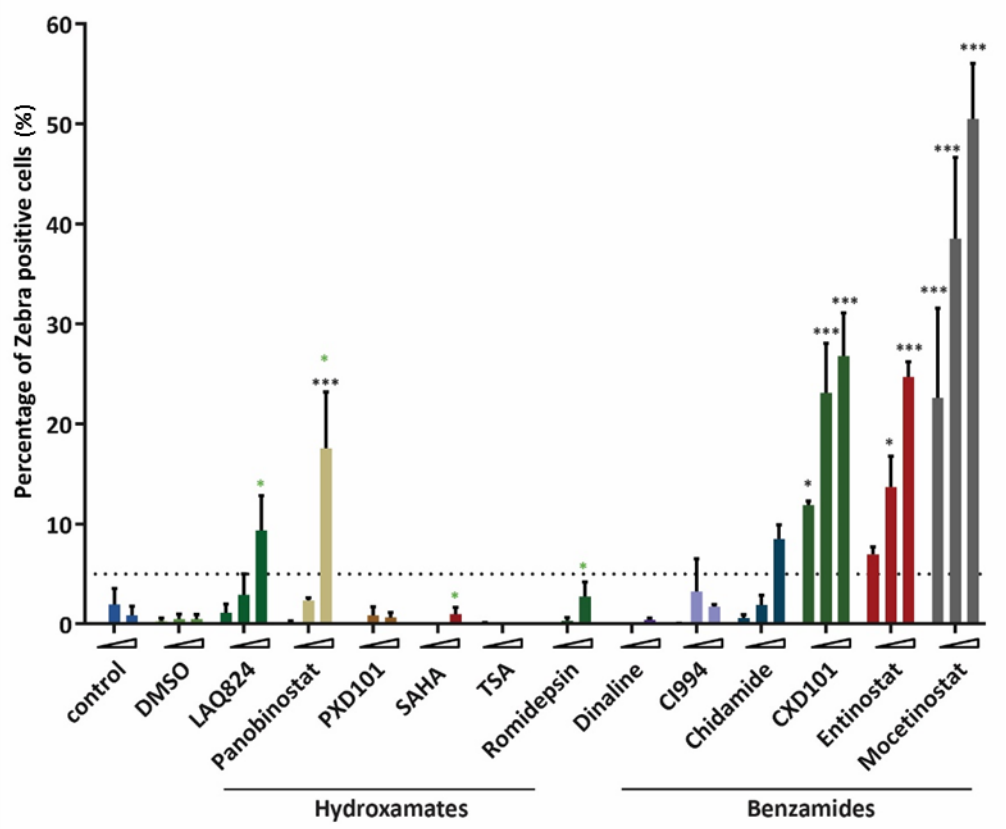


Figure 19: Comparison of the EBV reactivation potential of hydroxamates and benzamide HDACi. YCCEL1 cells were treated for 48 h with the stated compounds. Each compound was used at three different concentrations as indicated by the triangle (concentrations stated in Table 8). DMSO samples were treated with increasing concentrations of DMSO. The green asterisks indicate cell survival of less than 25% in comparison to control samples. Bars represent the average of three independently performed experiments. *n* = 3, error bars ± SEM. *P** ≤ 0.05; *P*** ≤ 0.01; *P**** ≤ 0.005. Significances were calculated using Dunnett's multiple comparison test relative to control cells. DMSO – dimethyl sulfoxide; EBV – Epstein-Barr virus; SAHA – suberoylanilide hydroxamic acid; TSA – Trichostatin A.

In addition to differences in Zebra expression levels, differences in compound toxicity were observed in the HDACi comparison. After 48 h of treatment, hydroxamate HDACis showed 17–100% of the amount of cells compared to control samples, while benzamide HDACis showed 49–212% (Table 21). Notably, none of the benzamide HDACis were considered toxic, which was defined as containing less than 25% of cells compared to the control, but three out of five hydroxamate HDACis were considered toxic.

The comparison of HDACis by an imaging-based screen indicated that mocetinostat is the most potent reactivating agent in this study, inducing Zebra expression in ~50% of cells at the highest concentration

used (10 μM). Overall, the results suggested that benzamide HDACis are more potent at inducing Zebra expression, while also being less toxic than hydroxamate HDACis.

Table 21: Table summarising the Zebra expression and cellular toxicities of a panel of HDACis in YCCEL1 cells. YCCEL1 cells were treated for 48 h with the indicated compounds at the highest concentration stated in Table 8. Zebra expression and cell numbers were determined using an ImageJ macro kindly provided by Mark Shipman (University of Oxford). Compound specificities were provided by the suppliers. TSA – Trichostatin A.

Compound	HDAC specificity	Average percentage of Zebra expressing cells (%)	Average percentage of cells relative to DMSO control samples (%)
LAQ824	Class I and II	9.37	20.07
Panobinostat	Class I, II and IV	17.58	22.10
PXD101	Class I, II and IV	0.64	46.23
SAHA	Class I and II	0.97	17.23
TSA	Class I and II	0.00	101.90
Romidepsin	HDAC1, 2 and 3	4.79	18.33
CI994	Class I	1.73	212.93
Dinaline	Class I	0.42	141.30
Chidamide	HDAC1, 2, 3 and 10	8.50	153.73
CXD101	Class I and HDAC4, 5 and 9	26.79	129.50
Entinostat	Class I	24.69	49.37
Mocetinostat	Class I and IV	50.49	56.20

To confirm the results of the HDACi comparison by immunofluorescence (Figure 19), Zebra expression upon HDACi treatment was analysed in YCCEL1 and SNU719 cells by western blot (Figure 20). Both cell lines are gastric carcinoma cell lines derived from EBV-positive tumours. As with the screening results,

only a limited number of HDACis were able to induce Zebra expression. The hydroxamate-based HDACis LAQ824 and panobinostat, as well as the benzamide-based HDACis chidamide, CXD101, entinostat and mocetinostat induced Zebra expression in SNU719 and YCCEL1 cells (Figure 20). Mocetinostat induced the highest levels of Zebra expression in both cell lines. The Zebra expression levels of the different benzamide-based HDACis mirrored the screening results, in which the percentage of Zebra-positive cells increased from chidamide to mocetinostat (Figure 19).

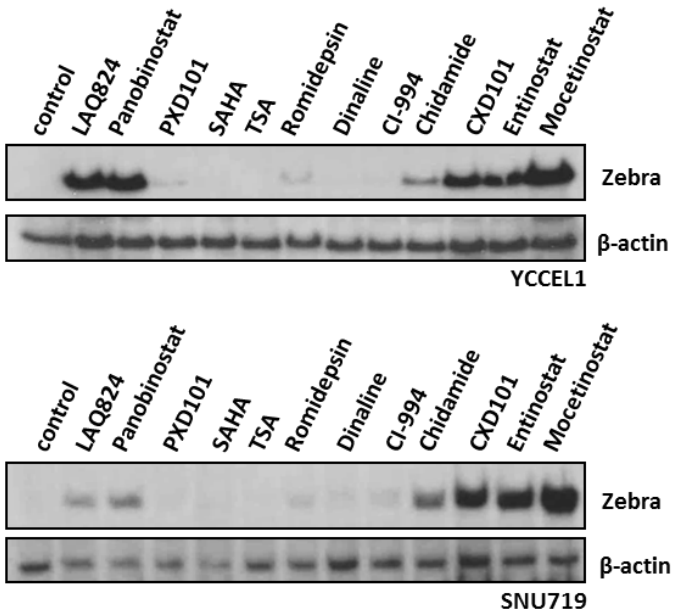


Figure 20: Comparison of Zebra expression levels upon HDACi treatment by western blot. YCCEL1 cells (top) and SNU719 cells (bottom) were treated for 48 h with compounds at the medium concentrations stated in Table 8. Control samples were treated with dimethylsulfoxide. Results shown are representative examples of three independent repeats of this experiment. SAHA – suberoylanilide hydroxamic acid; TSA – Trichostatin A.

In summary, this shows that benzamide-based HDACis are overall more potent in inducing Zebra expression than hydroxamate-based HDACis in EBV-positive epithelial cell lines. While panobinostat and LAQ824 also induced Zebra expression, this was generally associated with increased toxicity.

3.2.3 The differences between groups of HDACis are not caused by differential histone H3 acetylation or HDAC expression

Increased histone acetylation is a marker for the ability of a HDACi to inhibit HDAC activity. To exclude the possibility that the observed effect of benzamide HDACis on EBV is caused by a higher efficacy of those HDACis to inhibit HDAC function in comparison to hydroxamates, histone acetylation levels upon HDACi treatment were assessed by western blotting in different cell lines (Figure 21).

The levels of global histone H3 acetylation were consistent between different hydroxamate HDACis in both YCCEL1 and SNU719 cells (Figure 21.A and B). TSA induced lower levels of histone acetylation in YCCEL1 cells than the other HDACis, but in SNU719 cells its effect was comparable to other hydroxamate HDACis. Dinaline and CI-994 showed slightly lower levels of histone acetylation than other benzamide HDACis. Overall, there was no significant difference in histone acetylation between benzamide and hydroxamate HDACis.

In order to further elucidate whether the effect is dependent on global histone acetylation, SNU719 cells were treated with increasing concentrations of SAHA, chidamide or CXD101 (Figure 21.C). The results showed that even with an increased HDACi concentration, the levels of histone acetylation stayed at a comparable level. In contrast, Zebra levels increased in a concentration-dependent manner in chidamide- and CXD101-treated cells independently of histone acetylation levels.

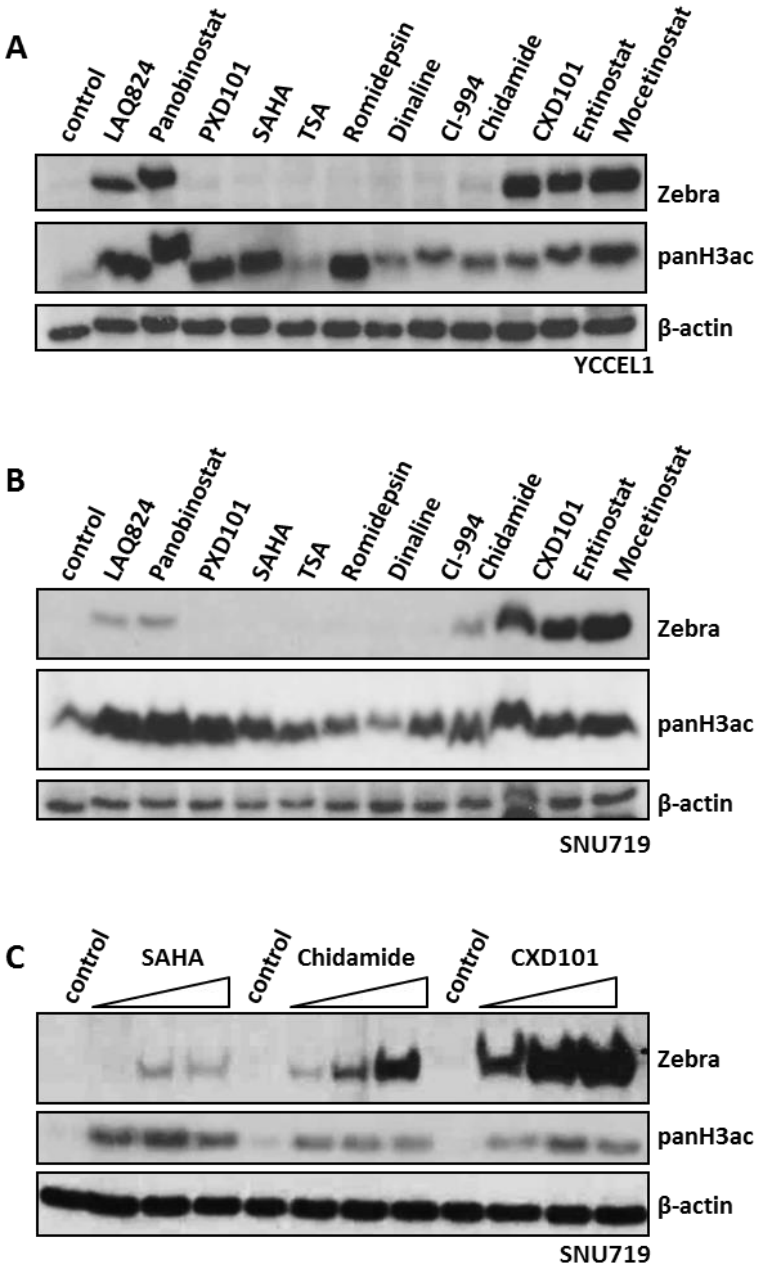


Figure 21: Comparison of histone H3 acetylation upon HDACi treatment. YCCEL1 (A) and SNU719 (B) cells were treated for 48 h with the mentioned compounds at the medium concentrations stated in Table 8. Control samples were treated with DMSO. Results shown are representative examples of three independent repeats of this experiment. C) SNU719 cells were treated for 48 h with SAHA, chidamide and CXD101 at concentrations of either 0.5, 2.5 or 5 µM (triangle represents increasing concentrations). The results shown are representative for two independent experiments performed in four different cell lines. DMSO – dimethyl sulfoxide; panH3ac – acetylated histone H3; SAHA – suberoylanilide hydroxamic acid; TSA – Trichostatin A.

Benzamide-based HDACis are more specific to class I HDACs such as HDAC1, HDAC2 and HDAC3 than hydroxamate-based HDACis, which inhibit a broader range of HDACs (reviewed in Falkenberg & Johnstone, 2014). Therefore, whether benzamide HDACi treatment affects class I HDAC levels and thereby causes EBV reactivation was examined. In both cell lines (YCCEL1 and SNU719) the levels of HDAC1, HDAC2 and HDAC3 did not change significantly independently of the HDACi used for treatment (Figure 22).

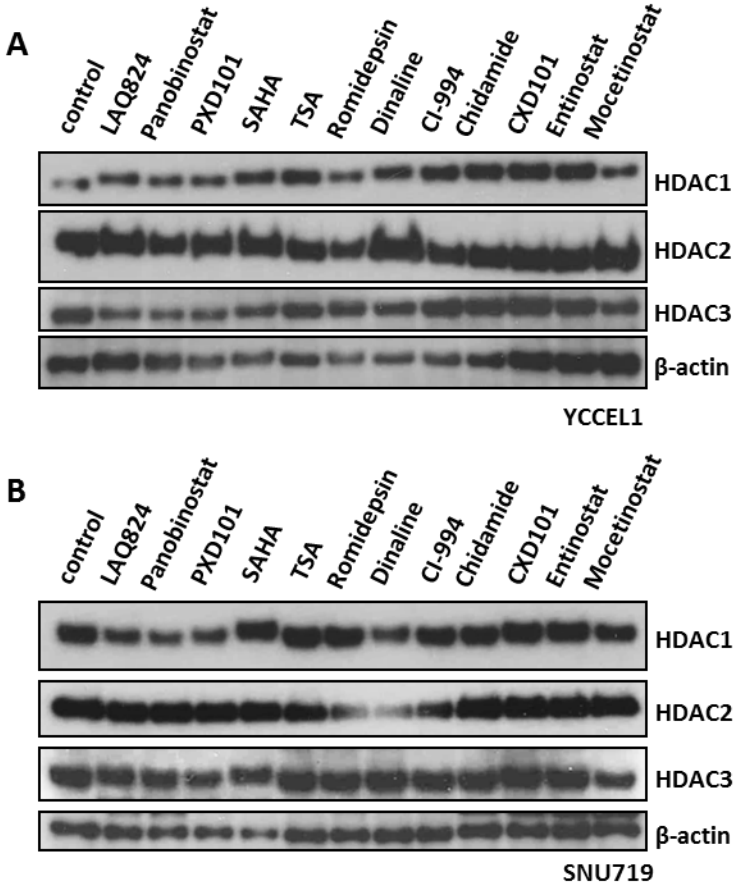


Figure 22: Western blot comparison of HDAC class I expression levels upon HDACi treatment. YCCEL1 (A) and SNU719 (B) cells were treated for 48 hours with the mentioned compounds at the medium concentrations stated in Table 8. Control samples were treated with DMSO. Results shown are representative examples of three independent repeats of this experiment. DMSO – dimethyl sulfoxide; TSA – Trichostatin A.

3.2.4 Benzamide-containing HDACis, but not all benzamides, induce Zebra expression

In order to identify more compounds that induce reactivation of EBV, we performed a high-throughput screen based on the screening method described in Chapter 3.2.1 with a library of around 1600 structurally diverse and medicinally active FDA-approved compounds (library information in Chapter 2.1.2). The four benzamide HDACis chidamide, CXD101, entinostat and mocetinostat were used as positive controls for this experiment. Potential hits were identified based on the Z-score, Zebra expression levels as well as cell survival. The Z-score defines the effect of one compound normalised to the mean and standard deviation of the whole plate (according to Guyon *et al.*, 2015). Thereby, the Z-score allows comparisons of scores among plates. For this study, compounds were considered as hits if they had a Z-score ≥ 1.96 and Zebra expression levels ≥ 5%. In addition, cell numbers were considered as a measure of cell survival and only compounds with > 1,000 cells per well after treatment were considered as hits.

Based on those criteria, nine compounds were identified as potential hits (Table 22). The number of Zebra-expressing cells induced by those compounds varied between 5–12.5%. Notably, the level of Zebra expression was significantly higher in the positive controls, with expression levels varying between 10–50% depending on the HDACi. In contrast, DMSO-negative controls induced Zebra expression in ~2.3% of cells.

Table 22: Hits of FDA-approved compound screen. The screening experiment was performed in YCCEL1 cells and each plate was performed in duplicate. Treatment was performed for 48 h with all compounds at a concentration of 3 μM. This list contains all compounds classified as hits based on Zebra expression ≥5%, Z-score ≥1.96 and cell number higher than 1,000 per well.

Compound	Average Zebra expression (%)	Z-score of average Zebra expression	Average cell count
Daunorubicin	12.47	3.81	5,991
Doxorubicin	11.37	2.88	5,798
Adapalene	11.80	7.83	3,315
Piroctone olamine	10.48	2.74	3,486
Actinomycin D	9.47	3.98	2,300
Teniposide	6.36	6.05	2,826
Ancitabine hydrochloride	5.89	4.89	15,506
Mitomycin C	5.69	5.92	1,686
Chlorhexidine dihydrochloride	5.06	5.20	1,955

To validate the hits of the high-throughput screen, SNU719 and YCCEL1 were treated with the compounds mentioned in Table 22 and Zebra expression was analysed by western blot. Chidamide was added to this experiment as a positive control (Figure 23). The results showed that the efficacy of those compounds to induce Zebra expression differed significantly between cell lines, while the chidamide-positive control showed strong Zebra expression in both cell lines. Adapalene and mitomyin C induced strong levels of Zebra expression in YCCEL1 cells (Figure 23.A). In the same cell background, ancitabine hydrochloride, piroctone olamine and teniposide induced low levels of Zebra expression while the other compounds induced no Zebra expression. In SNU719 cells, piroctone olamine and teniposide induced high and low levels of Zebra expression, respectively (Figure 23.B). All other compounds did

not induce Zebra expression in this cell line. Thus, piroctone olamine and teniposide were the only two compounds inducing Zebra expression in both cell lines.

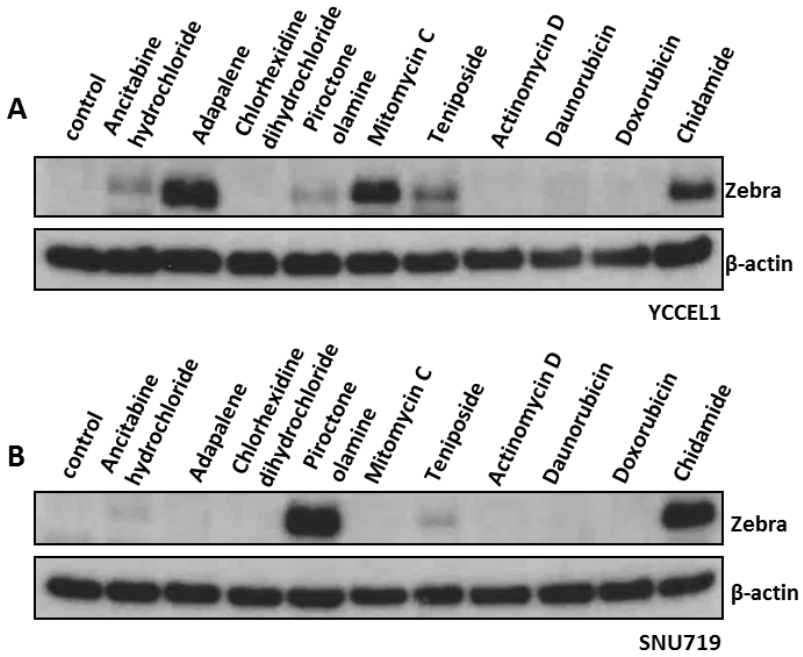


Figure 23: Western blot validation of hits identified in the high-throughput screen. YCCEL1 (A) and SNU719 (B) cells were treated for 48 h with the stated compounds at a final concentration of 5 µM. Control samples were treated with DMSO. Results shown are representative examples of three independent repeats of this experiment. DMSO – dimethyl sulfoxide.

In cooperation with Dr Felix Zhou (University of Oxford), the data from the high-throughput screen were used to examine whether all benzamide-based compounds are able to induce Zebra expression or the characteristic is specific to benzamide-based HDACis. For this analysis, all benzamide-based compounds in the library were identified based on their PubChem database entries (based on Kim *et al.*, 2016b). This identified 37 compounds out of the 1600 compounds of the library as benzamides (Table 23), none of which were shown to induce Zebra expression (Table 22).

Table 23: Benzamide compounds contained in the FDA-approved library. Benzamides were classified based on the information contained in their PubChem database entry (based on Kim *et al.*, 2016b). Analysis courtesy of Dr Felix Zhou (University of Oxford).

Benzamide-containing compounds in the FDA-approved library		
Acecainide hydrochloride	Glyburide	Pentamidine isethionate
Aklomide	Imatinib	Phenoxybenzamine hydrochloride
Benurestat	Indapamide	Procainamide hydrochloride
Bromopride	Itopride hydrochloride	Procarbazine hydrochloride
Cosantel	Labetalol hydrochloride	Saccharin
Diethyltoluamide	Lufenuron	Salicylamide
Dinitolmide	Metoclopramide hydrochloride	Salyclanilide
Eprobemide	Niclosamide	Sulfabenzamide
Ethamivan	Nifuroxazide	Tiarpride hydrochloride
Ethenzamide	Nifursol	Trimethobenzamide hydrochloride
Eticlopride hydrochloride	Nitazoxanide	Sulpiride
Etosalamide	Nitromide	
Exalamide	Oxyclozanide	

Comparison of the average Zebra expression of the hits to the negative control showed an increase in Zebra expression in the hit samples from ~2.3 to ~6.4% (Figure 24). The 37 benzamide-type compounds on the other hand only induced Zebra expression in ~0.24% of cells. In comparison, the average Zebra expression levels of the four benzamide HDACi-positive controls (chidamide, CXD101, entinostat and mocetinostat) over all screening plates showed high Zebra expression levels with CXD101 inducing ~45% and mocetinostat ~50% Zebra-positive cells.

This suggests that benzamide groups themselves are not sufficient to induce Zebra expression, but that this effect is specific to benzamide-containing HDACis.

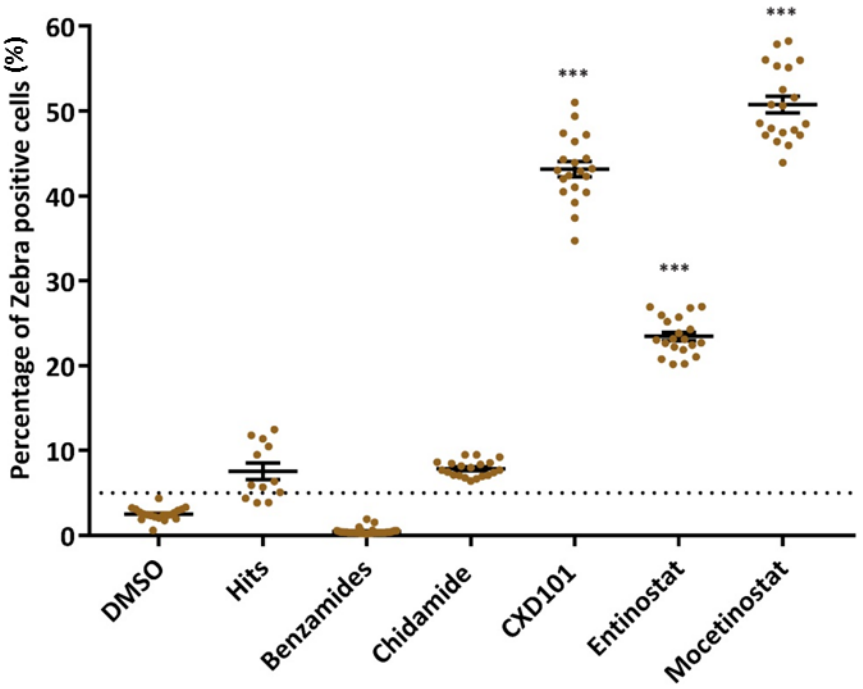


Figure 24: Comparison of potential hits with benzamide HDACi controls as well as benzamide-based compounds included in the FDA-approved library screen. All benzamides identified in the library can be found in Table 23 and all hits in Table 22. Every dot represents the average of two technical replicates performed in this screening experiment. Significance has been calculated relative to control samples by Dunnett's multiple comparison test. $P^* \leq 0.05$; $P^{**} \leq 0.01$; $P^{***} \leq 0.005$. DMSO – dimethyl sulfoxide.

3.3 Summary and brief discussion

The development of a screening method based on the lytic cycle regulator Zebra allows the high-throughput screening of compounds and analysis of their effects on the lytic cycle of EBV. In Chapter 3.2, it was shown that from a panel of epigenetic inhibitors, only HDACis were able to induce Zebra expression. Further experiments focussing on HDACi classes suggested that this effect was specific to benzamide-based HDACis and not hydroxamate-based HDACis. Similar levels of global histone H3 acetylation, as well as class I HDAC expression, upon treatment indicated that the differences in the reactivation potentials were not caused by differential acetylation capabilities or class I HDAC degradation through compound treatment. A high-throughput screen with 1600 FDA-approved compounds did not identify new classes of reactivating agents that worked in multiple cell lines, but showed that other benzamide-based compounds do not induce viral reactivation. Therefore, the overall conclusion was that only benzamides with HDACi functions induce Zebra expression in EBV-positive epithelial cells.

High-throughput screening methods for the identification of lytic cycle-inducing agents have been established in previous studies. Those screening methods were dependent on either cells infected with GFP-labelled EBV or on stable reporter cell lines for lytic promoters such as Zp as markers for lytic cycle induction (Tikhmyanova *et al.*, 2014; Choi *et al.*, 2015). The screening method described in Chapter 3.2.1 has the advantage that it can be performed with any epithelial cell line infected with EBV and therefore allows the identification of reactivating compounds in patient-derived cell lines.

Recently, HDACis have been studied for their effect on the life cycle of different viruses. In a study in KSHV-related PEL cells, HDACis of all classes were shown to induce apoptosis in a large proportion of cells while only inducing lytic cycle expression in a small proportion of cells (Niedermeier *et al*., 2006). However, a study of latency-reversing agents in HIV-positive T-cells showed that while all HDACis induce the lytic cycle, benzamide HDACis are less toxic in this setting (Kobayashi *et al.*, 2017). This is in

accordance with the results of Chapter 3.2.2 in EBV-positive epithelial cells. Those results showed that three out of five hydroxamate HDACis were considered to be toxic while none of the benzamide HDACis fulfilled those criteria (Table 21). In addition, our results showed not just a difference in toxicity but also in the level of lytic cycle induction, with benzamides being the most potent group of reactivating agents (Figure 19 and Figure 20).

In EBV-positive lymphoma cell lines, large panels of HDACis, spanning both benzamides and hydroxamates, have been shown to induce viral reactivation with subsequent sensitisation to GCV treatment (Daigle *et al.*, 2011; Ghosh *et al.*, 2012a). Studies in EBV-positive epithelial cells have shown that not all HDACis induce reactivation in epithelial cells, with only SAHA and romidepsin identified as reactivating HDACis (Hui & Chiang, 2010; Hui *et al.,* 2016). SAHA was not confirmed as a reactivating agent in Chapter 3.2, but romidpesin induced low levels of Zebra expression (Figure 19). This is not surprising considering that the study examining SAHA's effect on the reactivation of EBV relied exclusively on *in vitro*-infected cell lines and, as shown in Chapter 4.2, those cell lines commonly behave differently from cell lines derived from EBV-positive tumours (Figure 25) (Hui & Chiang, 2010). In contrast, romidepsin was studied in a broader set of cell lines and thus the chosen cell lines do not explain the observed differences in reactivation potential (Hui *et al.,* 2016). The observed weaker expression of Zebra could thus be due to minor differences in the experimental set-up, such as the amount of loaded protein for the western blot.

The identification of benzamide HDACis as the most potent group of reactivating agents from a panel of epigenetic inhibitors is in accordance with the recent finding that the inhibition of class I HDACs was sufficient to induce the lytic cycle in EBV-positive epithelial cells (Hui *et al.,* 2016). Nevertheless, this is the first large-scale study comparing HDACis in EBV-positive epithelial cells, which supports further research efforts into the benzamide-type HDACis and their potential applications for targeted cell killing of EBV-related cancer cells.

Chapter 4: Characterisation of two novel HDACis and their potential to reactivate EBV

4.1 Introduction

HDACs have been shown to be involved in cancer through a multitude of biological processes such as the reversal of chromatin acetylation, alteration of transcription of oncogenes and tumour suppressor genes, and the deacetylation of numerous non-histone substrates (reviewed in Li & Seto, 2016).

Thus, it is not surprising that the inhibition of HDACs in cancer cells through HDACi treatment has been shown to induce strong antitumour effects *in vitro* as well as in patients (reviewed in Li & Seto, 2016). TSA has been shown to induce apoptosis in glioblastoma cells and enhance antitumour immunity (Höring *et al*., 2013). In bladder cancer cells, romidepsin, TSA and SAHA induce cell death and inhibit proliferation (Li *et al.*, 2016). Additionally, SAHA has been shown to induce tumour-specific apoptotic transcription and autophagic cell death in several cell lines (Shao *et al.*, 2004; Bolden *et al.*, 2013). SAHA has further been shown to induce a tumour response in patients with different lymphomas as well as to selectively kill lymphoma cells in a B-cell lymphoma model in humanised mice (Lindemann *et al.,* 2007; Kirschbaum *et al.*, 2011). It is therefore not surprising that SAHA was the first HDACi approved for clinical use by the US FDA in 2006 (Mann *et al.*, 2007). Since then, romidepsin, PXD101 and panobinostat have been approved for clinical use by the US FDA and chidamide by the Chinese FDA (Table 24). Notably, all HDACis approved for clinical use are approved for the treatment of haematological malignancies.

Table 24: HDACis approved for clinical use. CTCL – cutaneous T-cell lymphoma; FDA – Food and Drug Administration; PTCL – peripheral T-cell lymphoma; SAHA – suberoylanilide hydroxamic acid.

Name of HDACi	Approved treatment for the following diseases	Board of approval	Year of approval	Reference
SAHA (Vorinostat, Zolinza)	CTCL	US FDA	2006	(Mann *et al.*, 2007)
Romidepsin (Istodax)	CTCL, PTCL	US FDA	2009	(Jain & Zain, 2011; Iyer & Foss, 2015;)
PXD101 (Belinostat, Beleodaq)	PTCL	US FDA	2014	(Lee *et al.,* 2015)
Chidamide (Epidaza)	PTCL	Chinese FDA	2014	(Lu *et al.*, 2016)
Panobinostat (Farydak)	Multiple myeloma	US FDA	2015	(Garnock-Jones, 2015)

Even though HDACis have been mostly used for the treatment of haematological malignancies, some successes in solid cancers have been reported (reviewed in Halsall & Turner, 2016). For example, SAHA in combination with different chemotherapeutic agents has been shown to lead to pathological complete responses in certain subtypes of locally advanced breast cancer (Tu *et al.,* 2014). Accordingly, novel HDACis such as mocetinostat, and also already approved HDACis such as SAHA, are currently undergoing clinical trials in a broad spectrum of malignancies (Luu *et al.*, 2008; Traynor *et al.,* 2009; Halsall & Turner, 2016). CXD101 is an example of a novel HDACi that is currently undergoing phase I clinical trials in advanced cancer patients to assess its safety and pharmacokinetics (Eyre *et al.*, 2016).

In addition to being used for cancer treatment, a multitude of HDACis are in clinical trials either alone or in combination with antiretroviral compounds for the treatment of infectious diseases such as HIV infection. At the moment, this focusses mainly on hydroxamate-type HDACis such as SAHA and

panobinostat, but romidepsin is also being tested in several clinical trials in HIV-positive patients (reviewed in Delagreverie *et al.*, 2016). Interestingly, chidamide in combination with antiretroviral agents is currently in phase II/III clinical trials in HIV patients with current antiretroviral therapy (Bethesda: National Library of Medicine (US), 2000).

In order to induce cell death in virus-infected cells by combining HDACis with antiviral agents, it is crucial to induce the expression of viral proteins that activate antiviral agents. Therefore, the aim of this study was to assess the ability of two novel reactivating agents, chidamide and CXD101, to activate the whole lytic cascade in EBV-positive epithelial cancer cells. Mocetinostat, which induced higher Zebra expression levels in direct comparison, was not chosen for this study as it induced significant toxicity and adverse effects in clinical trials (Younes *et al.*, 2011). To examine the potential of chidamide and CXD101 for use in lytic induction therapy, additional focus was set on cell killing in combination with antiviral compounds, as well as their effect on antigen presentation and recognition by CTLs.

4.2 Results

4.2.1 Chidamide and CXD101 induce Zebra expression in a panel of epithelial cell lines

To examine the reactivation potential of chidamide and CXD101 shown in Chapter 3.2.1 in more detail, Zebra expression upon chidamide or CXD101 treatment was compared with the FDA-approved HDACis SAHA, romidepsin and PXD101 in a broader panel of epithelial cell lines. Western blot analysis showed that EBV-negative cell lines such as AGS and OE19 show no Zebra expression (Figure 25.A and B). Dr Christopher Dawson (University of Birmingham) kindly provided us with EBV-infected counterparts of those cell lines, AGS rEBV-GFP (AGS EBV) and OE19 rEBV-GFP (OE19 EBV). Treatment with all tested HDACis induced Zebra expression in those cell lines (Figure 25.C and D). Notably, AGS EBV already expressed low levels of Zebra in control cells treated with DMSO. In cell lines derived from patients with EBV-positive stomach cancer, such as SNU719 and YCCEL1, only chidamide and CXD101 treatment induced high levels of Zebra expression (Figure 25.E and F). Treatment with romidepsin induced low levels of Zebra expression in both cell lines, while SAHA and PXD101 did not induce any Zebra expression.

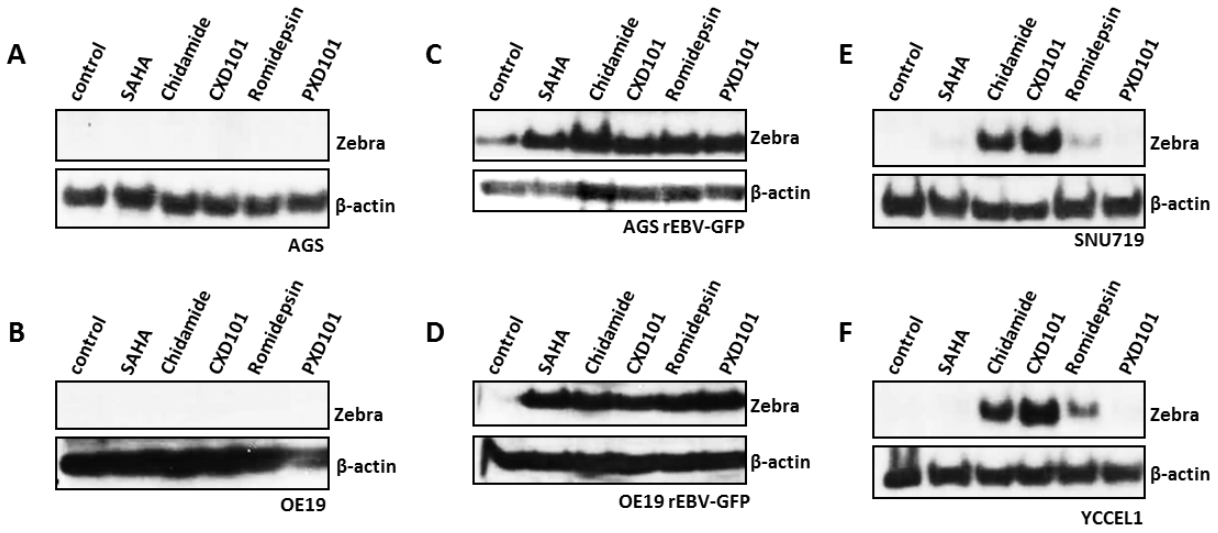


Figure 25: Western blot analysis of Zebra expression upon HDACi treatment in a panel of epithelial cell lines. All cell lines were treated for 48 h with DMSO, 5 µM SAHA, 5 µM chidamide, 2.5 µM CXD101, 2.5 nM romidepsin or 5 µM PXD101. Cell lines used were A) AGS, B) OE19, C) AGS rEBV-GFP,

D) OE19 rEBV-GFP, E) SNU719 and F) YCCEL1. Results are representative examples of three independent repeats of this experiment. DMSO – dimethyl sulfoxide; GFP – green fluorescent protein; SAHA – suberoylanilide hydroxamic acid.

To assess the proportion of cells reactivated by HDACi treatment, immunofluorescence staining with subsequent quantification of Zebra-positive cells was performed (staining examples in Figure 26.A).

Quantification of the percentage of Zebra-expressing cells in different cell lines showed that in AGS EBV and OE19 EBV cells, all HDACis induced similar proportions of Zebra expression. The overall proportion of reactivated cells was higher in AGS EBV (~40-50%) compared to OE19 EBV cells (~10-25%) (Figure 26.B). In OE19 EBV cells, SAHA induced Zebra expression in the highest proportion of cells (~28%) compared to chidamide and CXD101, which induced Zebra expression in less than 20% of cells. In AGS EBV and OE19 EBV cells, ~1–5% of cells expressed Zebra in the DMSO-treated control samples. In contrast, less than 0.4% of SNU719 and YCCEL1 cells expressed Zebra in control samples and SAHA treatment only increased the proportion to less than ~1%. In those two cell lines, chidamide increased the number of reactivated cells significantly compared with control cells to ~10% in SNU719 cells and ~20% in YCCEL1 cells. In CXD101-treated samples, ~30% of SNU719 cells and ~50% of YCCEL1 cells showed Zebra expression.

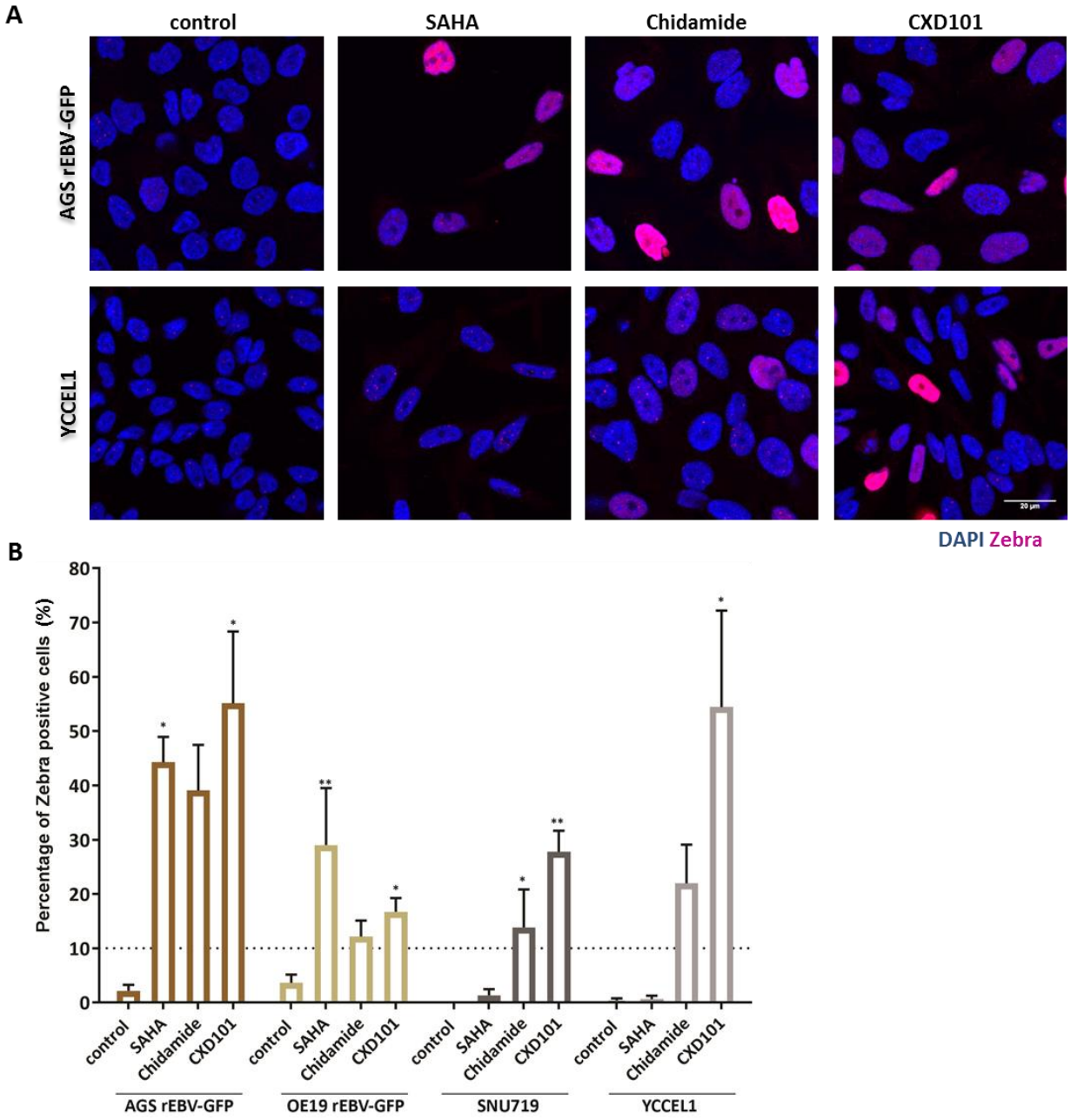


Figure 26: Quantification of Zebra expressing cells upon HDACi treatment in different cell lines by immunofluorescence. Cells were treated for 48 h with 5 µM SAHA, 5 µM chidamide or 2.5 µM CXD101. DMSO treatment was used as a control. A) Immunofluorescence images of AGS rEBV-GFP (top) and YCCEL1 (bottom) cells. Images are representative examples of three independent replicates of this experiment with at least five images taken per sample. B) Quantification of Zebra-positive cells based on immunofluorescence images acquired as stated for part A). Bars represent the average of three independently performed experiments. *n* = 3, error bars ± SEM. *P** ≤ 0.05; *P*** ≤ 0.01; *P**** ≤ 0.005. Significance was calculated using Dunnett's multiple comparison test relative to control cells. DAPI – 4',6-diamidino-2-phenylindole dihydrochloride; DMSO – dimethyl sulfoxide; GFP – green fluorescent protein; SAHA – suberoylanilide hydroxamic acid.

As mentioned in Chapter 1.4, EBV can be found in the B-lymphocytes of more than 90% of adults worldwide (Young & Rickinson, 2004; Young *et al.*, 2016). Therefore, the potential of chidamide and CXD101 to reactivate EBV in different B-cell lines was examined. Namalwa, Akakta and Raji cells are cell lines derived from Burkitt's lymphoma patients, which did not express Zebra in DMSO- or HDACi-treated samples (Figure 27.A–C). In two lymphoblastoid cell lines (LCLs), PD LCL and PLPH LCL, generated by infecting peripheral blood lymphocytes with EBV, Zebra expression was detected in DMSO-treated control samples (Figure 27.D and E). Upon HDACi treatment, the levels of Zebra expression in those cell lines stayed consistent or decreased compared to DMSO controls, rather than increased as observed in epithelial cell lines.

In all five B-cell lines, an increase in histone H3 acetylation upon HDACi treatment was observed compared to control samples, with acetylation levels varying depending on the treated cell line.

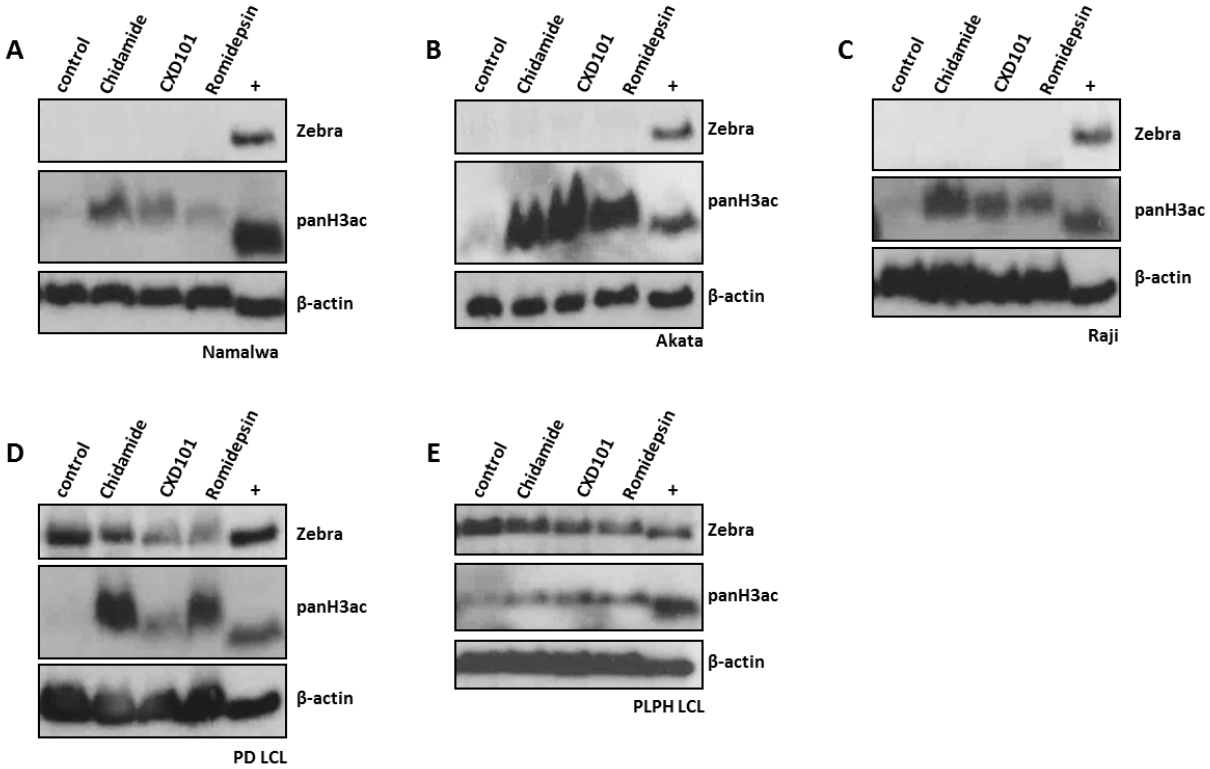


Figure 27: Western blot analysis of Zebra expression upon HDACi treatment in a panel of B-cell lines. Cells were treated with either DMSO, 5 µM chidamide, 2.5 µM CXD101 or 2.5 nM romidepsin for 48 h. DMSO treatment was used as a control. YCCEL1 cells treated with 5 µM chidamide were used as a

positive control (+). Cell lines used were A) Namalwa, B) Akata, C) Raji, D) PD LCL and E) PLPH LCL. Results shown are representative examples of three independent repeats of this experiment. DMSO – dimethyl sulfoxide; LCL –lymphoblastoid cell line; panH3ac – acetylated histone H3.

Overall, this showed that chidamide and CXD101 treatment is more potent in inducing Zebra expression in EBV-positive epithelial cells than in EBV-positive B-cell lines. Those results are important for the potential use of those compounds as treatment for EBV-associated epithelial malignancies as 95% of the adult population worldwide carries EBV within their B-cell population. Treatment with an agent that reactivates EBV in both B-cells and epithelial cells could lead to a drastic increase in the EBV titre in the blood and thereby induce severe adverse effects for the patient (Kim *et al.*, 2016). Therefore, treatment with a compound that only reactivates EBV in epithelial cells would be advantageous.

4.2.2 Expression of the whole lytic cascade is induced by HDAC inhibition

In order for HDACis to be used as lytic induction therapy for EBV-positive malignancies, it is crucial that they induce the expression of E lytic genes such as *BGLF4*. Thus, lytic gene expression of a panel of IE, E and L genes upon HDACi treatment was analysed by qPCR.

AGS EBV cells showed induction of IE and E gene expression upon SAHA, chidamide and CXD101 treatment (Figure 28.A). In contrast, none of the three treatments induced significant L gene expression in these cell lines. In OE19 EBV cells, SAHA induced higher expression levels of IE, E and L genes than chidamide and CXD101, which only induced low levels of lytic cycle gene expression (Figure 28.B). SNU719 and YCCEL1 cells showed similar expression patterns. In both cell lines, only chidamide and CXD101 treatment induced high levels of IE, E and L gene expression (Figure 28.C and D).

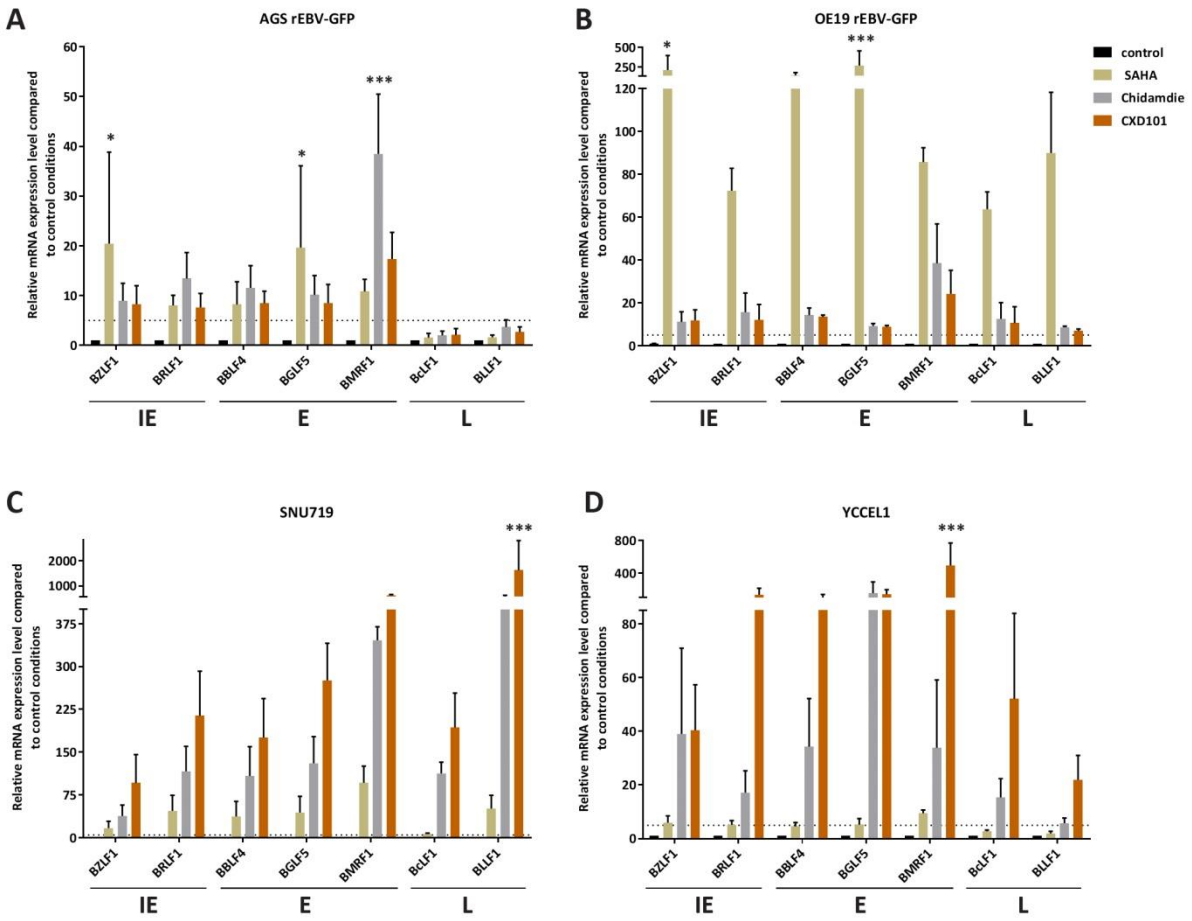


Figure 28: Comparison of lytic RNA expression levels upon HDACi treatment in different cell lines. Cells were treated for 48 h with 5 µM SAHA, 5 µM chidamide or 2.5 µM CXD101. DMSO treatment was used as a control. Cell lines used were A) AGS rEBV-GFP, B) OE19 rEBV-GFP, C) SNU719 and D) YCCEL1. Results represent $\Delta\Delta C_t$-values normalised to GAPDH levels within the same samples as well as to control samples of each primer. Bars represent the average of three independently performed experiments. *n* = 3, error bars ± SEM. *P** ≤ 0.05; *P*** ≤ 0.01; *P**** ≤ 0.005. Significance was calculated using Dunnett's multiple comparison test relative to control cells. DMSO – dimethyl sulfoxide; E – early genes; GAPDH – glyceraldehyde 3-phosphate dehydrogenase; GFP – green fluorescent protein; IE – immediate early genes; L – late genes; SAHA – suberoylanilide hydroxamic acid.

To confirm that the changes in RNA levels detected by qPCR correspond with the changes at the protein level, the percentage of cells expressing the L viral capsid antigen (VCA) gene was quantified by immunofluorescence staining (Figure 29). In AGS EBV cells, low numbers of VCA-expressing cells (~2%) were detected in control samples (Figure 29.B, left panel). Treatment with any of the three HDACis (SAHA, chidamide or CXD101) increased the proportion of VCA-expressing cells to ~6–9%. In YCCEL1 cells, no VCA expression was detected in control samples (Figure 29.B, right panel). SAHA

treatment induced the expression of VCA in less than 0.5% of the cells. In contrast, chidamide and CXD101 treatment induced VCA expression in ~5 and ~7% of cells, respectively.

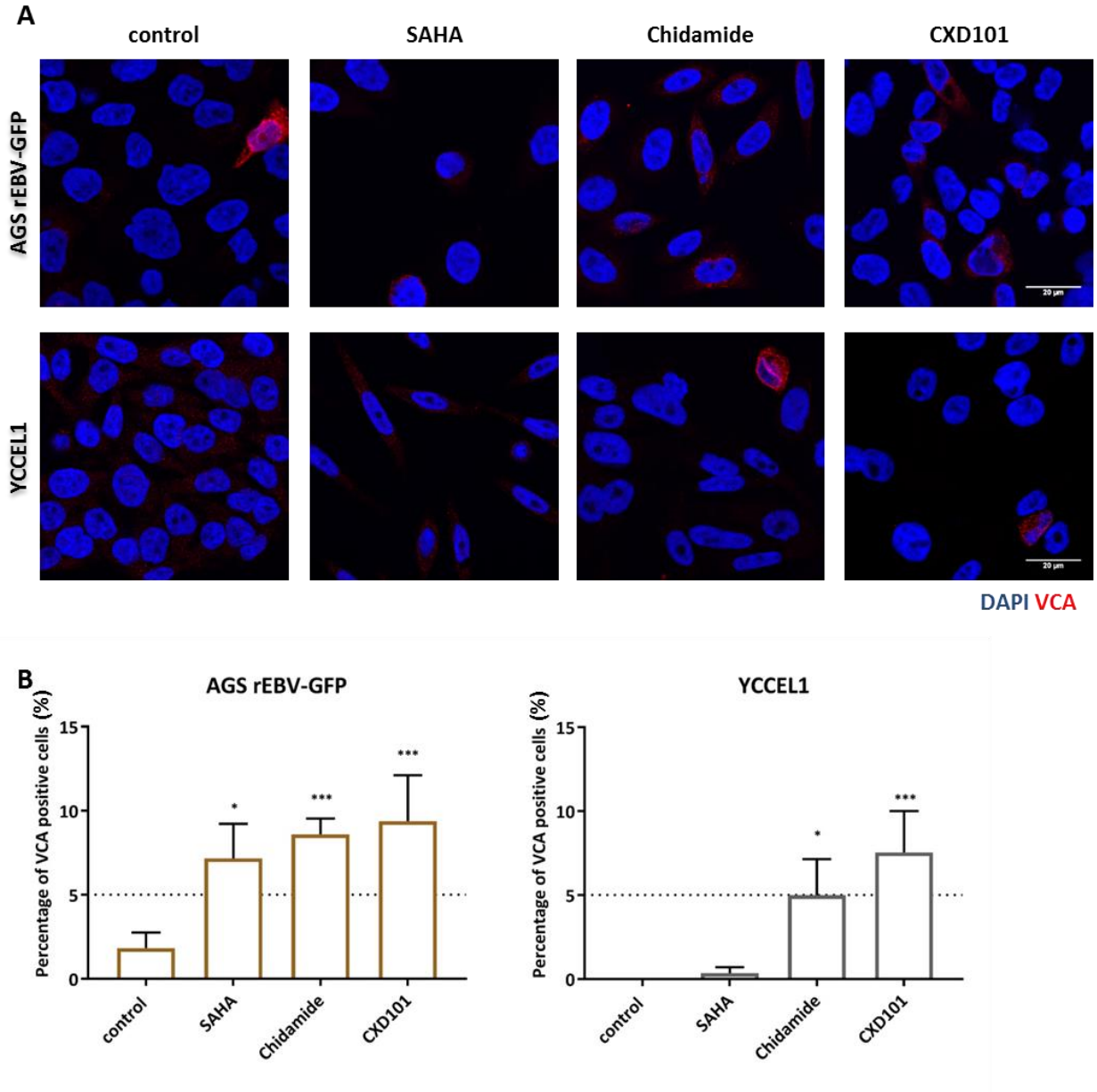


Figure 29: Quantification of VCA expression levels in different cell lines by immunofluorescence. Cells were treated for 48 h with 5 µM SAHA, 5 µM chidamide or 2.5 µM CXD101. DMSO treatment was used as a control. A) Immunofluorescence images of AGS rEBV-GFP (top) and YCCEL1 cells (bottom) are shown. Images are representative examples of three independent replicates of this experiment with at least five images taken per sample. B) Quantification of VCA-positive cells based on immunofluorescence images acquired as described for figure A). Bars represent the average of three independently performed experiments. n = 3, error bars ± SEM. $P^* \leq 0.05$; $P^{**} \leq 0.01$; $P^{***} \leq 0.005$. Significance was calculated using Dunnett's multiple comparison test relative to control cells. DAPI –

4',6-diamidino-2-phenylindole dihydrochloride; DMSO – dimethyl sulfoxide; GFP – green fluorescent protein; SAHA – suberoylanilide hydroxamic acid; VCA – viral capsid antigen.

In summary, this showed that chidamide and CXD101 treatment is sufficient to induce the expression of the full lytic cycle in different EBV-positive epithelial cell lines. Interestingly, the levels of lytic cycle expression seem to be higher in cell lines derived from EBV-positive tumours compared to *in vitro*-infected cell lines.

4.2.3 The combination of HDACi treatment with antiviral compounds leads to increased cell death

Expression of the viral protein kinase (EBV-PK), the product of the *BGLF4* gene, is crucial for the activation of antiviral compounds such as GCV *in vivo* (Meng *et al.,* 2010). Therefore, the expression of this kinase following HDACi treatment was assessed by qPCR (Figure 30.A). In AGS EBV cells, all HDACis induced *BGLF4* expression ~5-fold in comparison to DMSO-treated cells, with chidamide leading to the strongest induction (~8-fold). In contrast, in OE19 EBV cell treatment with SAHA increased *BGLF4* expression ~75-fold compared to DMSO treatment, while chidamide and CXD101 treatment increased expression less than 15-fold. SAHA treatment induced *BGLF4* expression ~25-fold in SNU719 cells, but in this cell line chidamide and CXD101 induced higher levels of *BGLF4* with ~100-fold and ~200-fold induction of expression, respectively. In YCCEL1 cells, SAHA treatment induced *BGLF4* expression less than 5-fold while chidamide treatment induced a ~20-fold increase in expression. CXD101 treatment increased BGLF4 levels ~200-fold in YCCEL1 cells. In a cell line derived from an EBV-infected NPC patient, C666.1, SAHA treatment did not induce *BGLF4* expression. Chidamide and CXD101 treatment increased expression levels around 10-fold compared to control samples in this NPC cell line.

Based on the *BGLF4* expression data, it was tested whether chidamide and CXD101 could be used for targeted cell killing in combination with antiviral treatment. In order to address this question, an EBV-negative cell line and its EBV-positive counterpart, AGS and AGS EBV, as well as one cell line derived from an EBV-positive tumour, YCCEL1, were treated with either HDACis, antivirals or both, and the percentage of live cells measured subsequently (Figure 30.B and C). The antivirals used in this study are the guanine nucleoside analogues GCV and ACV.

In AGS cells, the amount of live cells in HDACi-treated samples was not reduced compared to the DMSO-treated control sample, independently of the antiviral compound added (Figure 30.B). In AGS EBV cells, the combination of DMSO or CXD101 with antivirals did not induce any changes in cell viability (Figure 30.B). In AGS EBV cells treated with chidamide without subsequent antiviral treatment, the percentage of live cells was reduced to ~60% compared to the control. The addition of ACV did not induce any further changes to the amount of live cells, but adding GCV decreased the number of live cells to ~30%. In YCCEL1 cells, the addition of antivirals to DMSO-treated cells did not change cell viability (Figure 30.C). In contrast, in samples treated with only GCV, the number of live cells increased to ~160% compared to DMSO controls. In YCCEL1 cells, HDACi treatment alone was sufficient to decrease cell survival to ~50%. As observed in AGS EBV cells, ACV treatment did not lead to any further decrease in cell numbers. However, the addition of GCV decreased the percentage of live cells to ~10% in combination with chidamide and to ~20% in combination with CXD101 treatment.

Overall, the combination of chidamide and CXD101 with GCV led to increased cell killing in EBV-positive cell lines compared to HDACi treatment alone. Notably, this effect was only achieved with GCV and not with ACV treatment.

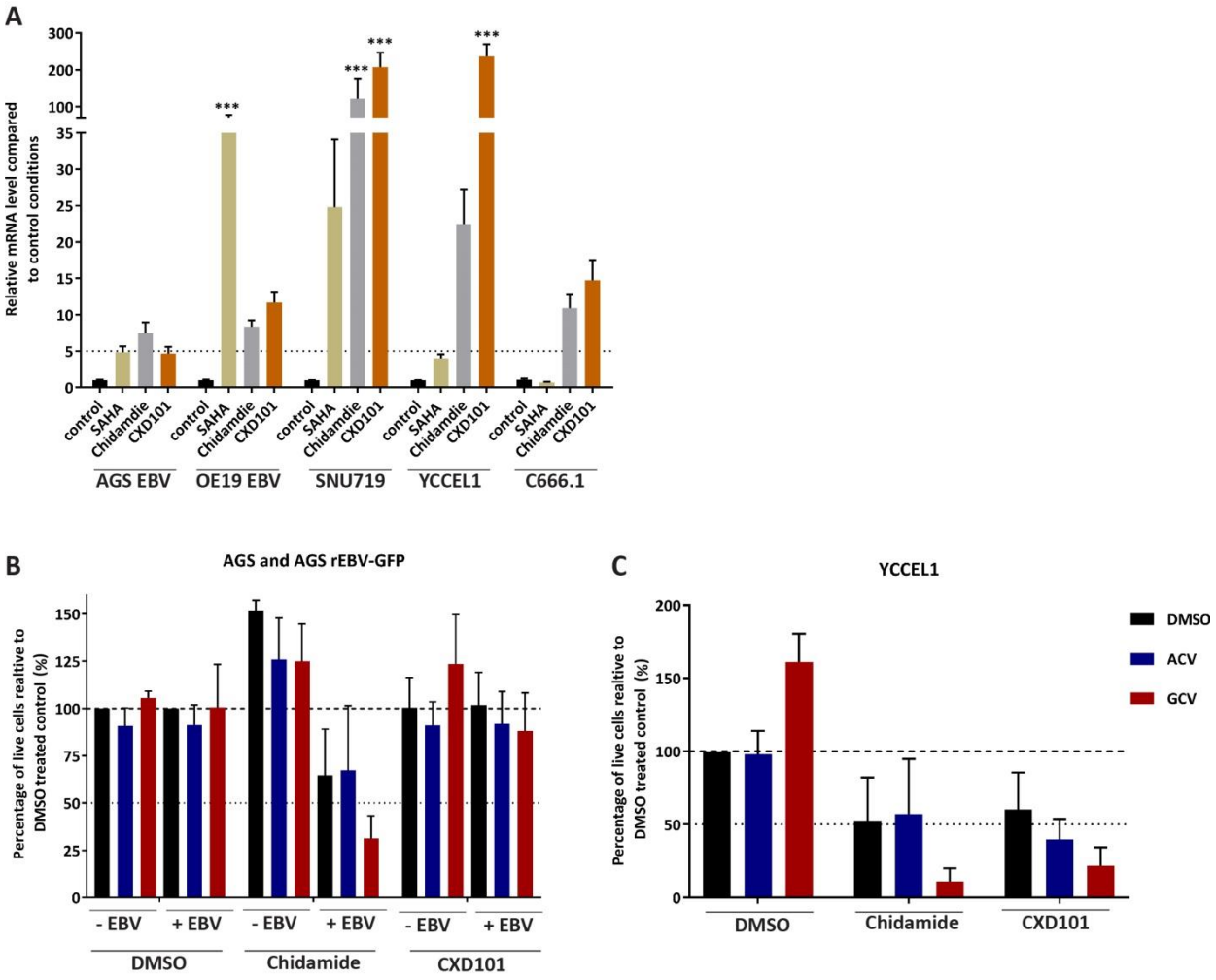


Figure 30: BGLF4 expression and cell killing by antiviral compounds in HDACi-treated cells. A) BGLF4 expression in different cell lines evaluated by qPCR. Cells were treated for 48 h with 5 µM SAHA, 5 µM chidamide or 2.5 µM CXD101. DMSO treatment was used as a control. The results represent $\Delta\Delta C_t$-values normalised to GAPDH levels within the same samples as well as the control samples for each primer. B+C) Percentage of live cells upon antiviral treatment relative to DMSO controls. AGS, AGS rEBV-GFP or YCCEL1 were treated for 72 h with either DMSO, 5 µM chidamide or 2.5 µM CXD101. Afterwards the medium was replaced with medium containing either DMSO, 10 µg/µL ACV or 20 µg/µL GCV before collection for cell viability assessment after 6 days. Bars represent the average of three independently performed experiments. *n* = 3, error bars ± SEM. *P** ≤ 0.05; *P*** ≤ 0.01; *P**** ≤ 0.005. Significances were calculated using Dunnett's multiple comparison test relative to control cells. ACV – Acyclovir; AGS EBV – AGS rEBV-GFP; DMSO – dimethyl sulfoxide; GAPDH – glyceraldehyde 3-phosphate dehydrogenase; GCV – Ganciclovir; OE19 EBV – OE19 rEBV-GFP; GFP – green fluorescent protein; SAHA – suberoylanilide hydroxamic acid.

4.2.4 Reactivation by HDACi treatment downregulates HLA class I expression

HLA I is a key sensor for aberrations in intrinsic cellular processes including viral infections. Through recognition by CTLs, this allows the clearance of affected cells (reviewed in Blackwell *et al*., 2009). It has been suggested that HDACis can lead to differential gene expression of up to 20% of genes, including important genes for immune regulation and recognition (reviewed in Minucci & Pelicci, 2006). Thus, whether treatment with chidamide and CXD101 impairs the expression of HLA class I molecules that are important for presenting epitopes for T-cell recognition was investigated. In collaboration with Dr Thomas Partridge (University of Oxford), this was examined by flow cytometry after compound treatment.

In EBV-negative AGS and YCCEL1 cells, HDACi treatment did not significantly change HLA I expression compared to DMSO-treated cells (Figure 31.A and D). Similar results were observed in the EBV-positive NPC cell line C666.1. Notably, in CXD101-treated C666.1 cells, a separate population expressing low levels of HLA I was detected in addition to the main population (Figure 31.B). In SNU719 cells, treatment with HDACis increased the level of HLA I expression compared to the DMSO-treated samples (Figure 31.C).

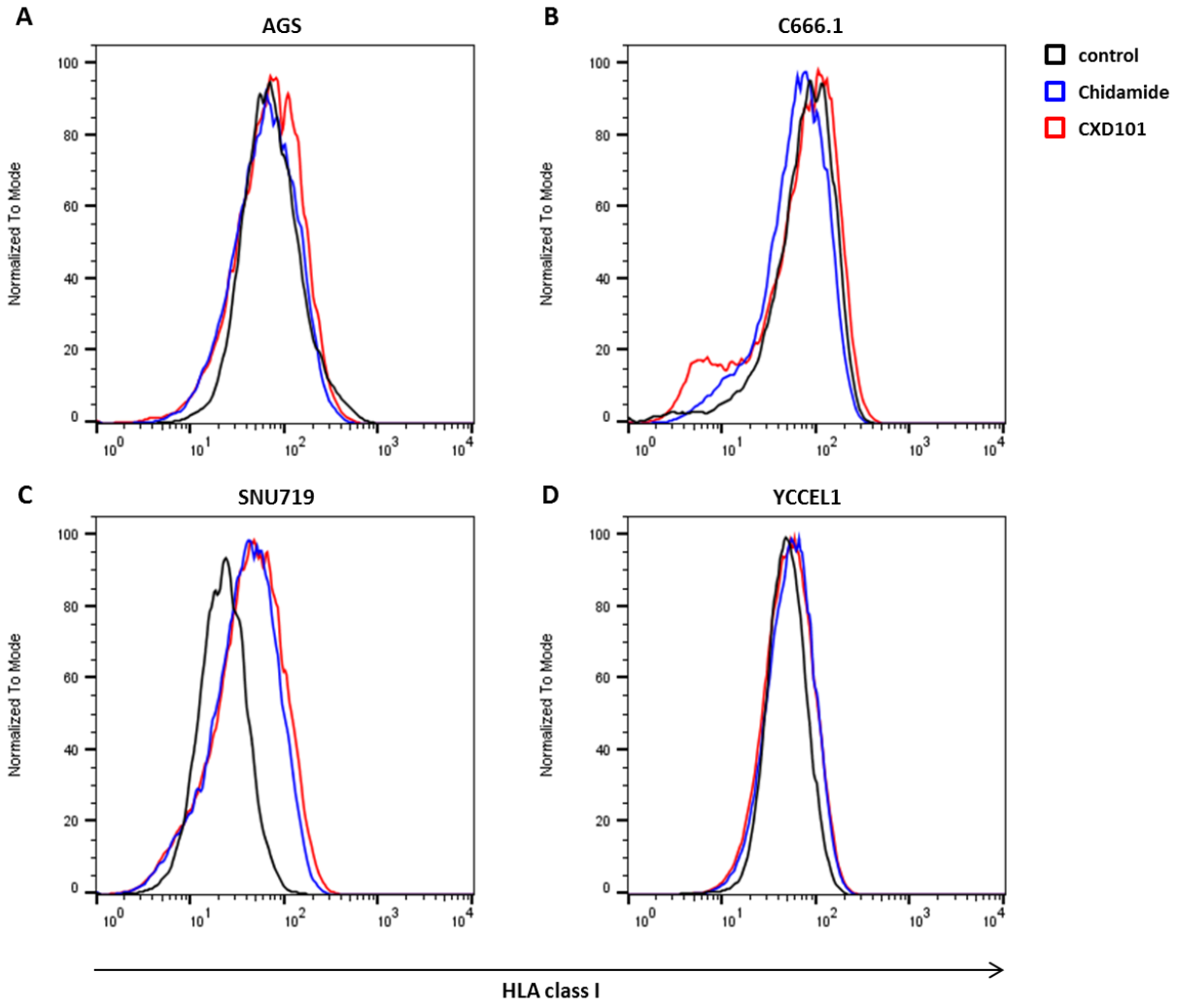


Figure 31: HLA class I expression levels upon HDACi treatment in epithelial cell lines analysed by flow cytometry. Cells were treated for 48 h with either DMSO as a control, 5 µM chidamide or 2.5 µM CXD101, before being dissociated for flow cytometric analysis. Results are representative examples of two independent replicates of this experiment performed in collaboration with Dr Thomas Partridge, University of Oxford. DMSO – dimethyl sulfoxide; HLA – human leukocyte antigen.

It has been previously reported that the reactivation of EBV can lead to the downregulation of important molecules for antigen processing and presentation, such as HLA I molecules (Ressing *et al.,* 2005; Croft *et al.,* 2009; Horst *et al.*, 2009). Therefore, HLA I expression in reactivated and non-reactivated cells was examined. EBV-negative AGS cells were used as a control for this experiment. As expected, AGS cells did not show any Zebra expression or change in HLA I expression upon HDACi treatment (Figure 32.A). In SNU719 cells, the levels of HLA I expression in Zebra-negative, so not

reactivated cells, increased upon HDACi treatment (Figure 32.B). In chidamide- and CXD101-treated samples, ~4% of cells expressed Zebra. Those cells showed lower HLA I expression levels compared to the non-reactivated population. In YCCEL1 cells, less than 1% and ~4% in chidamide- and CXD101-treated samples were positive for Zebra expression (Figure 32.C). The non-reactivated cells showed an increase in HLA I expression upon HDACi treatment, as observed in SNU719 cells, while the reactivated cells expressed slightly lower levels of HLA I.

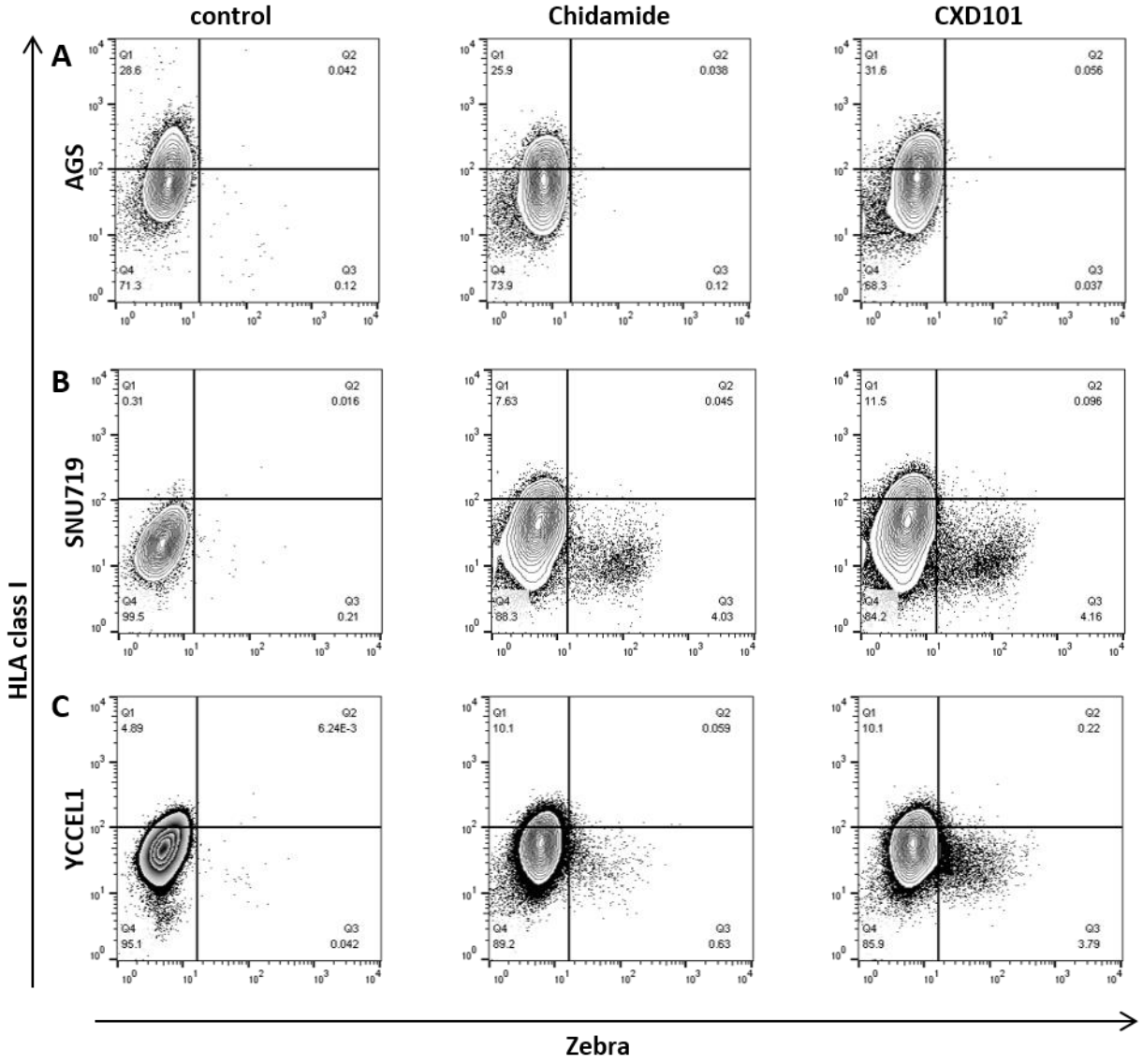


Figure 32: Changes in HLA class I expression levels relative to Zebra levels upon HDACi treatment in different cell lines analysed by flow cytometry. Cells were treated for 48 h with either DMSO as a control, 5 µM chidamide or 2.5 µM CXD101 before being dissociated for flow cytometric analysis. This

experiment was performed in A) AGS, B) SNU719 and C) YCCEL1 cells. Results are representative examples of two independent replicates of this experiment performed in collaboration with Dr Thomas Partridge, University of Oxford. DMSO – dimethyl sulfoxide; HLA – human leukocyte antigen.

Overall, this showed that while HDACi treatment alone does not negatively influence HLA class I expression on the cell surface, HLA I is specifically downregulated in the Zebra-expressing cell population.

4.2.5 Reactivation through HDACi treatment is sufficient to activate cytotoxic T-cells

Although only minimal effects of HDACi treatment on HLA I expression were observed, the potential of reactivated epithelial cells to activate cytotoxic $CD8^+$ T-lymphocytes was examined. For this, a T-cell clone (GLC) specific to an epitope on the EBV early lytic protein BMLF1 was used. In collaboration with Dr Carol Leung (University of Oxford), this HLA-A2-restricted T-cell clone was co-cultured with HLA-A2-positive AGS cells and T-cell activation was indicated by subsequent IFNγ secretion, which was measured by ELISA (Figure 33).

EBV-negative AGS cells were included as a control in the T-cell assay to show that the recognition was specific to the EBV antigen. Co-culture between those two cell types induced only very low levels of detectable IFNγ in the supernatant (less than 50 pg/mL), independent of the HDACi treatment or T-cell number used in the assay. DMSO-treated AGS EBV cells induced a modest response of the T-cell clone (~175 pg/mL IFNγ), whereas both chidamide- and CXD101-treated AGS EBV cells stimulated higher responses (270–950 pg/mL IFNγ), which increased with increasing numbers of T-cells. This trend was observed for different T-cell numbers used in the co-culture experiment. Notably, AGS or AGS EBV cells cultured alone only induced minimal levels of detectable IFNγ in the supernatant (~15 pg/mL IFNγ, data not shown).

Overall, this showed that reactivation of AGS EBV cells through HDACi treatment is sufficient to induce activation of EBV-specific $CD8^+$ T-cells.

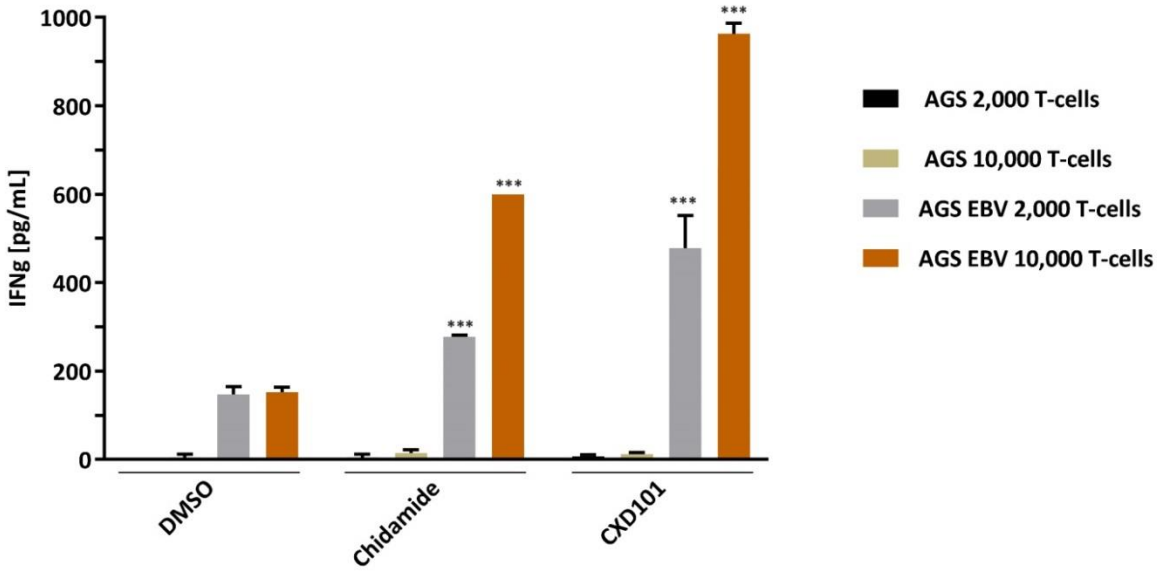


Figure 33: Measurement of INF-γ secretion by ELISA in co-cultures of HDACi-treated epithelial cells with a T-cell clone specific to the lytic protein BMLF1. AGS and AGS EBV cells were treated with either DMSO as a control, 5 µM chidamide or 2.5 µM CXD101 for 48 h. Afterwards, cells were detached, plated in 96-well plates, and either 2,000 or 10,000 T-cells (clone GLC, BMLF1) added per well. After 16 h, supernatants were collected and used for subsequent analysis by ELISA. Results are representative of three independent repeats of this experiment performed in duplicate in collaboration with Dr Carol Leung, University of Oxford. Bars represent the average of the performed duplicates. $n = 3$, error bars ± SD. $P^* \leq 0.05$; $P^{**} \leq 0.01$; $P^{***} \leq 0.005$. Significance was calculated using Dunnett's multiple comparison test relative to control cells. DMSO – dimethyl sulfoxide; EBV – Epstein-Barr virus; IFNγ – Interferon γ.

4.3 Summary and brief discussion

Chidamide and CXD101 induced efficient reactivation of EBV in epithelial cell lines, as shown by the expression of IE, E and L lytic genes (Chapter 4.2). In contrast, EBV-positive B-cell lines were not reactivated by treatment with those two HDACis. Induction of the lytic cycle by chidamide and CXD101 treatment was sufficient to induce targeted cell killing in combination with GCV, with chidamide being more potent than CXD101. This effect was EBV-specific and was not achieved by the alternative antiviral agent ACV. Treatment with either chidamide or CXD101 did not significantly decrease the expression of HLA I molecules on the cell surface, but in some cell lines even increased its expression. Even though Zebra-expressing cells were shown to downregulate HLA I expression, reactivated cells were able to stimulate CTLs specific to the EBV lytic protein BMLF1.

Due to the importance of histone acetylation for the regulation of EBV's life cycle, different HDACis have been tested in EBV-positive cell lines. The effects of HDACis on EBV-positive cell lines have been shown to be independent of the efficacy of the HDACi to induce histone acetylation, and instead seem to depend on the cell type and the viral latency stage of EBV (Countryman *et al.*, 2008; Hui & Chiang, 2010). An example of this is SAHA, which has been shown to only reactivate EBV in latency II-infected epithelial cells, but not latency II-infected cells of other cellular origins (Hui & Chiang, 2010). Thus, it is not surprising that chidamide and CXD101 treatment induce EBV reactivation in epithelial cells only, and not in B-cell lines (Chapter 4.2.1).

The different patterns of viral reactivation observed between *in vitro*- and *in vivo*-infected EBV cell lines could potentially be explained by the different routes of infection (Figure 25). The *in vitro*-infected cell lines, AGS EBV and OE19 EBV, were both infected with the B95-8 strain of EBV, which was isolated from a patient with infectious mononucleosis (Fischer *et al.,* 1981). This strain has been shown to differ from strains found in epithelial cells (Tsai *et al.,* 2013; Kanda *et al.*, 2016). In addition, those cells were cultured under constant selection pressure in order to maintain the EBV genome within the cell

population. This suggests that the viral episome is not stabilised and silenced in the same way that it would be during *in vivo* infection. The fact that those cell lines can be easily reactivated by a broad range of different epigenetic modulators supports this hypothesis. In contrast, cell lines derived from EBV-positive tumours, SNU719 and YCCEL1, are infected with strains that are more similar to the two NPC strains GD1 and M81, and more distinct from the wild-type EBV strain B95-8 (Kanda *et al.,* 2016). Chapters 3.2 and 4.2 have shown that only very few compounds are able to induce reactivation in those cell lines, suggesting that EBV is more effectively silenced and therefore only specific stimuli are able to induce reactivation. An additional cause for the differences in reactivation might be the distinct mutational signature of EBVaGC in comparison to non-EBV associated GC cases, which might influence the response of those different sets of cell lines to compound treatment (Cancer Genome Atlas Research, 2014). Since SNU719 and YCCEL1 cells were derived from EBV-positive tumours and thus are infected with strains more commonly found in epithelial cancers and contain mutations commonly found in EBVaGC, compounds identified to reactivate this set of cell lines are potentially more relevant for further study and evaluation for use in the clinic.

Even though both chidamide and CXD101 were able to induce expression of the full lytic cascade at the RNA level, there was a significant difference between the proportion of cells expressing IE and L proteins. For example, in YCCEL1 cells, 20–50% of cells expressed Zebra depending on the HDACi treatment, but only ~5% of cells expressed the L marker VCA (Figure 26 and Figure 29). This discrepancy could be an artefact of the experimental design, since both IE and L gene expression were examined after 48 h of HDACi treatment. This time point was chosen as it represented the earliest time point of strong Zebra expression. Therefore, it is possible that the actual proportion of VCA-expressing cells reaches its maximum at a later time point when the lytic cycle has progressed further. Alternatively, it has been suggested that following completion of the lytic cycle, cell death is induced and virions released (Kawanishi, 1993a; Hong *et al.*, 2005). Therefore, it is possible that cells that have progressed

to the L stage of the lytic cycle have started to die, and that the measured amount of L gene-expressing cells is therefore lower than the actual number of L gene-expressing cells. Lastly, it could be that chidamide and CXD101 only induce the expression of the full lytic cycle in a subset of reactivated cells. In the majority of Zebra-expressing cells, the pattern of lytic cycle expression could be abortive, meaning that only IE and E genes are highly expressed and the progression to L gene expression does not occur in all cells. This pattern of abortive lytic cycle expression has been previously reported in humanised mouse models and infectious mononucleosis patients (Ma *et al.*, 2012; Lerner *et al.*, 2012).

Targeted cell killing of EBV-positive cells that were first reactivated with HDACis and then treated with antiviral compounds such as GCV has been shown in both B-cells and epithelial cells (Hui & Chiang, 2010; Ghosh *et al.*, 2012a; Hui *et al.*, 2016). In our study, both AGS EBV and YCCEL1 cells showed increased levels of cell death when treated with chidamide and GCV (Figure 30.B and C). The same was true for the combination of CXD101 with GCV, but only in YCCEL1 cells. The differences in the efficacy of cell death induction between chidamide and CXD101 in AGS EBV cells could potentially be explained by the slightly lower expression levels of BGLF4 in CXD101-treated cells compared to chidamide-treated cells (Figure 30.A). The observation that GCV is more potent in inducing cell killing than ACV fits with results of previous studies in HSV-infected cells, which showed that ACV induces cell cycle arrest while GCV induces apoptosis (Thust *et al.*, 2000; Shaw *et al.,* 2001). This effect was linked to the chain-terminating properties of ACV in comparison to GCV, which becomes internally incorporated before leading to the termination of strand synthesis. This strand incorporation may activate excision repair and thus ultimately lead to apoptosis, thereby explaining the increased cell death in GCV-treated cells compared to ACV-treated cells.

HDACis have been shown to drastically change cellular gene expression, including important genes for immune regulation and recognition such as HLA I and II (Khan *et al.,* 2008; Cycon *et al.*, 2013). Even though certain studies have observed increases in HLA I expression upon HDACi treatment, this does

not necessarily lead to more potent antigen presentation, as it has been found that antigen presentation might be impaired by the same treatment (Pellicciotta *et al.,* 2008). Examination of the effects of chidamide and CXD101 on HLA I expression has shown that they do not induce any significant changes in the expression of HLA I (Figure 31).

Another factor potentially influencing HLA expression is Zebra expression and subsequent reactivation. Zebra has been shown to be involved in multiple mechanisms to avoid immune recognition, such as influencing IFN expression, downregulating the receptors for TNFα and IFNγ, and specifically HLA I presentation (see Chapter 1.7.2) (Keating *et al.,* 2002; Morrison *et al.,* 2004; Hahn *et al*., 2005). Therefore, it is not surprising that the population of Zebra-expressing cells showed downregulation of HLA I expression levels (Figure 32). Since HDACi treatment alone does not seem to influence HLA I expression levels, it can be concluded that the decrease of HLA I expression is a result of Zebra expression and viral reactivation, and not HDACi treatment.

Since both HDACi treatment and EBV infection have been shown to not just interfere with HLA I expression but also affect antigen processing pathways, a functional T-cell assay was performed to investigate if antigen processing and presentation is impaired. T-cell activity was monitored by the secretion of IFNγ, a marker for antigen-activated $CD8^+$ T-lymphocytes (Ghanekar *et al.*, 2001). In reactivated cells, even though Zebra-expressing cells downregulate HLA I expression, the viral antigen BMLF1 is still presented sufficiently to induce T-cell activation (Figure 33). The low levels of IFNγ detected in CTLs co-cultured with DMSO-treated AGS EBV cells agrees with previous results showing that AGS EBV cells express low levels of Zebra in untreated controls (~2.5% of cells, Figure 26). This suggests that a low percentage of cells could present the antigen to CTLs in DMSO treated samples and thereby induce IFNγ secretion.

In conclusion, this chapter showed that chidamide and CXD101 can be used as reactivating agents for lytic induction therapy in EBV-positive epithelial cells. This treatment does not seem to inhibit a potent

immune response against reactivated cells, which could be advantageous for potential treatment in patients by maximising the cell killing of reactivated cells. Thus, this study showed for the first time that HDACi treatment of EBV-positive epithelial cancer cells is not only an efficient method to kill cells through antiviral compounds, but also through T-cell immune control against EBV lytic antigens. This supports further exploration to assess the exact mechanisms of reactivation in more detail, including the potential interplay with the immune system, which would be crucial for the potential progression of those compounds to the clinic as specific treatments for EBV-associated epithelial cancers.

Chapter 5: The role of p53 in the induction of Zebra expression

5.1 Introduction

Different chemotherapeutic agents, as well as radiation, have been shown to induce reactivation of EBV in both B-cells and epithelial cells (Westphal *et al.*, 2000; Feng *et al.,* 2002; Nandakumar *et al.*, 2017). Those studies showed that, in different EBV-related tumour models, the combination of chemotherapeutics and radiation with antiviral agents led to more effective cell killing than either treatment alone (Westphal *et al.,* 2000; Feng *et al.,* 2002). These data suggest that antiviral agents such as GCV enhance the efficacy of conventional cancer treatments for EBV-positive tumours. Notably, this effect was not confirmed for all chemotherapeutic agents. In EBV-transformed B-cells, gemcitabine and doxorubicin induced lytic cycle expression, but cisplatin and 5-FU did not (Feng *et al.*, 2004a). In contrast, cisplatin and 5-FU have been shown to induce reactivation and increased cell killing in combination with GCV in different epithelial cancer models (Feng *et al.,* 2002).

Synergistic effects on the reactivation of EBV and targeted killing have also been reported for different HDACis. In NPC cells and mouse models, the HDACis 12-O-tetradecanoylphorbol-13-acetate and SB induced increased reactivation of EBV in combination with N-methyl-N'-nitro-N-nitrosoguanidine, a carcinogenic agent found in cigarette smoke and different foods (Huang *et al.*, 2010a; Fang *et al.*, 2012). The protease inhibitor bortezomib has been shown to induce reactivation and cell killing in combination with SAHA in EBV-positive NPC and B-cell lines (Hui *et al.*, 2013; Hui *et al.*, 2014). In addition, the HDACi VPA has shown synergistic antitumour effects in combination with the chemotherapeutic agent gemcitabine in NPC cells and patients (Wildeman *et al.,* 2012; Hsu *et al.*, 2015; Stoker *et al.*, 2015; Novalić *et al.,* 2017).

Based on emerging evidence regarding the synergistic effects of HDACis with other compounds on EBV reactivation, the aim of this chapter was to identify potential classes of compounds that can synergise

with HDACis in inducing viral reactivation. In order to address this aim, a high-throughput screen was performed with an extended FDA-approved library using either the library alone or in combination with the HDACi chidamide.

5.2 Results

5.2.1 Topoisomerase inhibitors increase Zebra expression in combination with chidamide

A high-throughput screen with an extended FDA-approved library was performed to identify compounds that could synergise with the HDACi chidamide in inducing Zebra expression. Chidamide at a concentration of 2.5 μM was chosen for this experiment as it induced Zebra expression in less than 1% of cells when treated alone (Figure 19, left bar). This should enable the identification of potential synergistic compounds without increased background through reactivation by HDACi treatment alone. The extended FDA-approved library used for this screen contains 1800 compounds that are structurally diverse and medicinally active (see Chapter 2.1.2 and Appendix Table 3). In comparison to the compound library used in Chapter 3.2.4, an expanded oncology drug set containing both experimental and approved oncology-specific compounds was added (Appendix Table 3).

The screening method for this experiment was based on immunofluorescence staining for Zebra, which was established in Chapter 3.2. YCCEL1 cells were treated either with the library alone or in combination with chidamide. DMSO treatment was included as the negative control and treatment with mocetinostat, another HDACi shown to induce strong Zebra expression (see Chapter 3.2), was used as the positive control for this experiment. Chidamide was included as a control on every screening plate to identify the background Zebra expression for treatment with this compound alone.

Compounds fulfilling the following criteria were considered as potential hits: a Z-score ≥ 1.96, Zebra expression levels ≥ 5% and wells containing more than 1,000 cells after treatment. Based on those criteria, 30 hits were identified for the library alone and 21 for the library in combination with chidamide (see Appendix Table 4 for complete list). To detect potential classes of compounds that were potent in inducing Zebra expression, the compounds contained in the library as well as the identified hits were grouped based on their target activity (Figure 34.A-C). Those compound classifications were

determined based on the information contained in their PubChem database entries in collaboration with Dr Felix Zhou (University of Oxford), according to (Kim *et al.*, 2016b).

The extended FDA-approved library contained a broad spectrum of compound classifications (Figure 34.A). The most enriched compound classifications for library treatment alone compared to the composition of the library were antiparasitic agents (~17-fold) and in combination with chidamide tubulin modulators (~11-fold) (Figure 34.D and E). The only classifications found in both the hits for library treatment alone and in combination with chidamide were antifungal agents and topoisomerase II inhibitors (Figure 34.B and C). Additionally, topoisomerase II inhibitors were the second most enriched class of compound in both screening conditions with 6-fold and 8.5-fold enrichment.

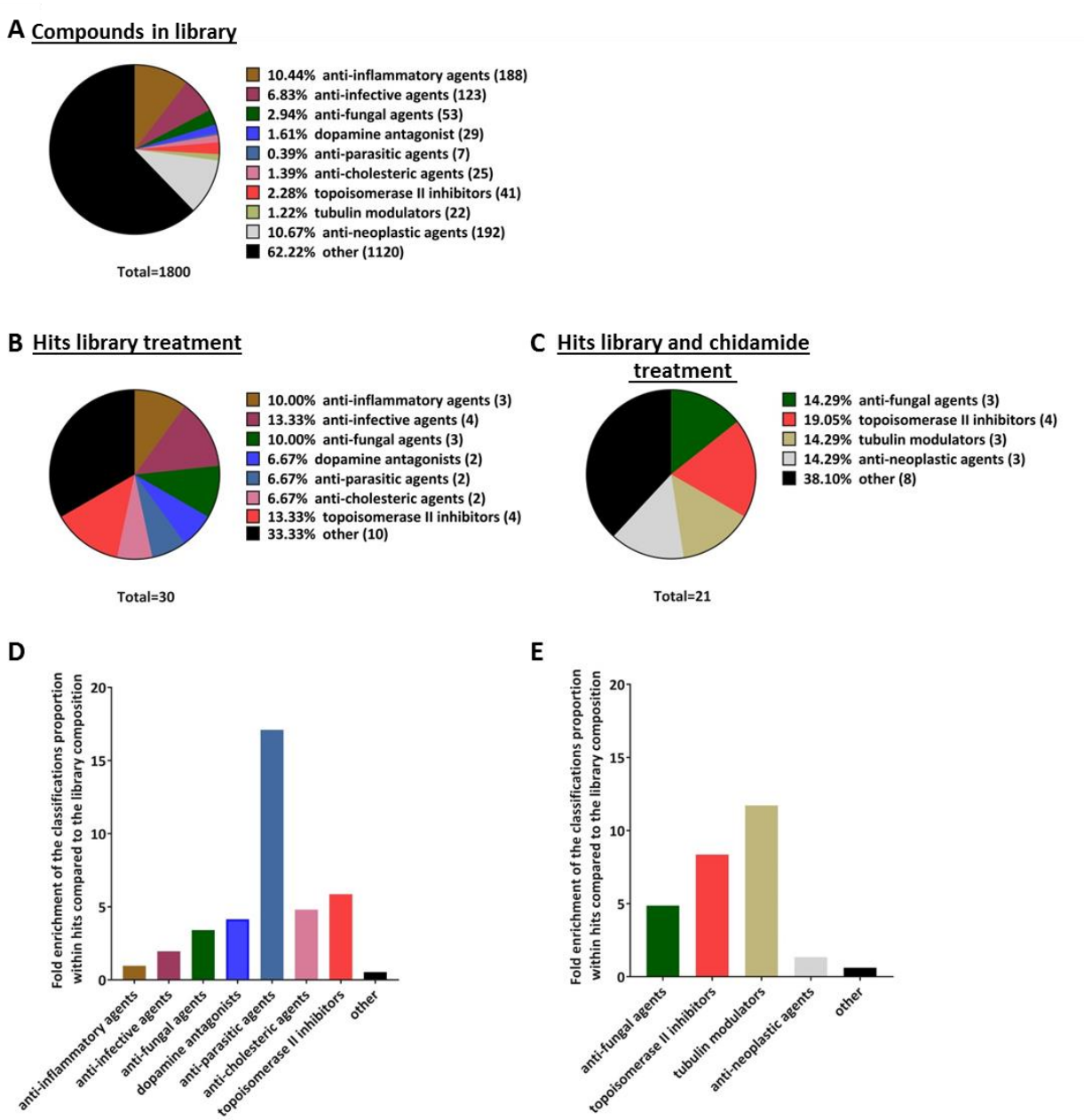


Figure 34: Distribution of compound classifications in the extended FDA library and in the identified hits. Compounds included in the extended US FDA library can be found in Chapter 2.1.2 and Appendix Table 3, and a list of all compounds classified as hits in Appendix Table 4. Compound classifications were determined based on the information contained in their PubChem database entries according to (Kim *et al.*, 2016b). Analysis courtesy of Dr Felix Zhou (University of Oxford). A–C) Proportion of different compound classifications in either the library used for treatment or the identified hits. The numbers in brackets represents the absolute number of compounds within the classification. D–E) Fold enrichment of different compound classifications identified in the hits compared to their proportion within the compound library. D) Enrichment of the hits identified for the library alone and E) for the library together with chidamide. FDA - Food and Drug Administration.

Additionally, the compound activities of the top 10 identified hits in either treatment with the library alone or in combination with chidamide, based on the induced percentage of Zebra-expressing cells, were analysed in more detail (Table 25). Analysis of the compound classifications showed that for treatment with the library alone, 2 of the top 10 hits were classified as topoisomerase II inhibitors and one as a topoisomerase I inhibitor. In combination with chidamide, 4 out of 10 compounds were classified as topoisomerase II inhibitors and one as a topoisomerase I inhibitor. Thus, 5 out of 10 hits with chidamide treatment belonged to the class of topoisomerase inhibitors. This suggests that in addition to being one of the most enriched classifications among hits, topoisomerase inhibitors are among the most potent compound classes inducing Zebra expression in combination with chidamide. Therefore, topoisomerase inhibitors were chosen for further in-depth examination.

Table 25: Top 10 hits identified in a high-throughput screen of an extended FDA library with or without the addition of chidamide in YCCEL1 cells. The order of hits is based on their Zebra expression levels. Compound classifications were determined based on the information contained in their PubChem database entry according to (Kim *et al.*, 2016b). Analysis was courtesy of Dr Felix Zhou (University of Oxford). FDA - Food and Drug Administration ; HDAC – histone deacetylase; PI3K – phosphoinositide-3-kinase; Topo inhibitor – Topoisomerase inhibitor.

Top 10 hits (without chidamide treatment)			**Top 10 hits (with chidamide treatment)**		
Name of compound	**Classification of compound**	**Average Zebra expression (%)**	**Name of compound**	**Classification of compound**	**Average Zebra expression (%)**
Pyrvinium pamoate	Anti-parasitic agent	52.71	Daunorubicin	Topo II inhibitor	49.68
Acrisorcin	Other	47.33	Decitabine	Anti-neoplastic agent	31.80
Daunorubicin	Topo II inhibitor	45.39	Quinacrine HCl	Anti-asthmatic agent	30.83
Entinostat	HDAC inhibitor	44.65	Mitoxantrone	Topo II inhibitor	28.14
PIK-75 HCl	PI3K inhibitor	43.76	Teniposide	Topo II inhibitor	26.43
Topotecan	Topo I inhibitor	31.93	Epirubicin	Topo II inhibitor	25.70
Nonoxynol-9	Spermatocidal agent	30.83	Mycophenolate mofetil	Anti-neoplastic agent	23.23
Acriflavine	Anti-infective agent	24.37	Topotecan	Topo I inhibitor	13.16
Teniposide	Topo II inhibitor	23.18	Thiram	Anti-fungal agent	12.03
Dichlorophen	Anti-fungal agent	20.96	Podofilox	Tubulin modulator	11.95

The extended FDA-approved library used for this screening experiment contained 45 topoisomerase inhibitors (Appendix Table 5). For further examination of those topoisomerase inhibitors, the top 10 topoisomerase inhibitors in combination with chidamide were identified based on their Zebra expression levels (Table 26). Those were also the only topoisomerase inhibitors contained in the compound library that induced Zebra expression in more than 5% of cells when treated together with chidamide. Most of the topoisomerase inhibitors were class II inhibitors, except camptothecin and topotecan, which inhibit class I topoisomerases (reviewed in Kathiravan *et al.*, 2013). While Zebra expression induced by those 10 topoisomerase inhibitors was high enough for them to be classified as hits, some of them had to be excluded based on their Z-score or toxicity levels (Table 26). For example, idarubicin and camptothecin decreased cell numbers to less than 1,000 per well, and thereby had to be excluded with and without chidamide treatment. Doxorubicin treatment only led to increased cell killing in combination with chidamide and not as a single treatment. Other compounds, such as amonafide and epirubicin, were excluded as hits because their Z-score was lower than 1.96. Only daunorubicin, mitoxantrone, teniposide and topotecan fulfilled all necessary criteria for hits, either in library treatment alone or in combination with chidamide.

Table 26: Top 10 topoisomerase inhibitors included in the extended FDA library based on their Zebra expression in combination with chidamide treatment. The Z-score was calculated as stated in (Guyon *et al.*, 2015), allowing the comparison of scores among plates. Compounds were considered as hits with a Z-score ≥ 1.96, Zebra expression levels ≥ 5% and more than 1000 cells per well after treatment. All values represent the average of the two duplicates performed per compound. Values highlighted in red did not fulfil the criteria for a hit and therefore led to exclusion of the compound. CH – Chidamide.

	Average percentage of Zebra expressing cells (%)		Z-score		Average cell number per well	
Compound name	**- CH**	**+ CH**	**- CH**	**+ CH**	**- CH**	**+CH**
Amonafide	8.92	56.21	0.11	5.63	1,628.5	384
Daunorubicin	45.39	49.68	4.80	8.51	2,786	2,929.5
Idarubicin	30.00	39.27	1.11	2.58	4.5	349
Doxorubicin	36.98	38.21	8.74	7.34	1,349.5	735.5
Camptothecin	46.10	35.82	2.12	2.29	321	532.5
Mitoxantrone	18.21	28.14	3.16	7.73	1,319.5	2,248
Teniposide	23.18	26.43	2.71	7.50	1,274	2,961
Epirubicin	5.53	25.70	1.03	4.80	3,050.5	1,865.5
Topotecan	31.93	13.16	3.90	3.34	2,157	3,294.5
Colchicine	7.56	10.27	0.47	1.42	4,877.5	5,419.5

In order to differentiate the potential of topoisomerase inhibitors to induce Zebra expression from compound toxicity, those 10 topoisomerase inhibitors were examined at different concentrations. The optimal concentration for each compound in combination with chidamide was determined based on maximum Zebra expression and minimal effect on cell survival, using the screening method described in

Chapter 3.2.1. All topoisomerase inhibitors were used at their optimal concentrations, as identified by this titration experiment (Appendix Figure 1, for concentrations see Table 9).

Chidamide alone induced Zebra expression in less than 1% of cells (Figure 35.A). Analysis of the number of Zebra-expressing cells for all 10 topoisomerase inhibitors together with chidamide showed that doxorubicin and epirubicin induced Zebra expression in the highest proportion of cells (~35%) (Figure 35.A). Overall, most topoisomerase inhibitors induced Zebra expression in an increased number of cells when chidamide was added. In contrast, Camptothecin and colchicine showed Zebra expression in ~5% of cells with single treatment, but the percentage of Zebra expression did not increase upon the addition of chidamide. The other eight topoisomerase inhibitors led to Zebra expression in less than 10% of cells when treated alone, and this increased to 15–35% in combination with chidamide (Figure 35.A). Similar trends of Zebra expression were observed by western blot analysis (Figure 35.B). Notably, while camptothecin treatment showed Zebra expression in ~5% of cells by immunofluorescence staining (Figure 35.A), western blot analysis did not detect Zebra expression (Figure 35.B, right blot).

In summary, the FDA compound screen together with chidamide identified several classes of compound with potential synergy on Zebra expression. Topoisomerase inhibitors were one of the most significant compound classes to induce this effect.

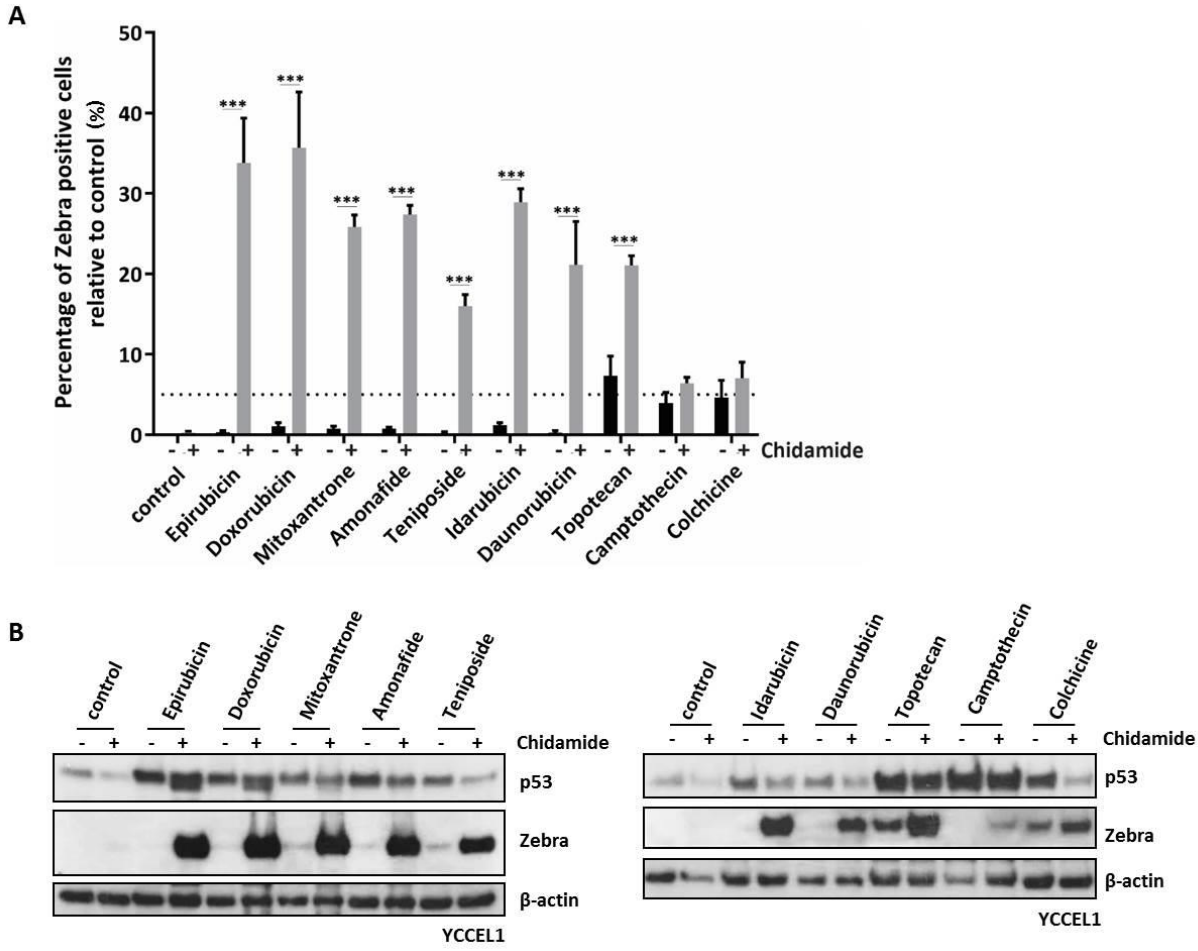


Figure 35: Induction of Zebra expression by topoisomerase inhibitors treatment alone or in combination with chidamide in YCCEL1 cells. Cells were treated for 48 h with either DMSO or 2.5 μM chidamide in combination with the stated topoisomerase inhibitors (for concentrations see Table 9). A) Immunofluorescence imaging and analysis via an ImageJ macro (provided by Mark Shipman, University of Oxford) was used to identify the percentage of Zebra-expressing cells. Dotted line represents the 5% cut-off line for compounds characterised as hits. Bars represent the average of three independently performed experiments. *n* = 3, error bars ± SEM. *P** ≤ 0.05; *P*** ≤ 0.01; *P**** ≤ 0.005. Significance was calculated using Sidak's multiple comparison test. B) Western blot analysis of cell lysates after 48 h of treatment. Results are representative of three independent repeats of this experiment. DMSO – Dimethyl sulfoxide.

5.2.2 Not all chemotherapeutic agents induce Zebra expression together with chidamide

Topoisomerase inhibitors such as epirubicin and doxorubicin are used as chemotherapeutic agents for different cancer types (reviewed in Larsen *et al.*, 2003). Gastric cancer in the UK is commonly treated with different combinations of chemotherapeutic agents such as epirubicin, cisplatin, 5-FU or etoposide (Orditura *et al.*, 2014). In order to determine if chemotherapeutic agents used for the treatment of gastric cancer are able to induce viral reactivation, their ability to induce Zebra expression alone or in combination with chidamide was examined by immunofluorescence staining and western blot (Figure 36). Since many chemotherapeutic compounds have been shown to induce DNA damage and p53 stabilisation (Woods & Turchi, 2013), treatment with Nutlin-3a was included as a control for this experiment. Nutlin-3a is a compound that specifically inhibits the interaction of p53 with its negative regulator mouse double minute 2 homolog (MDM2) and thereby leads to stabilisation of p53 at the protein level (Vassilev *et al.,* 2004).

All chemotherapeutic agents tested were able to induce p53 levels (Figure 36.B). Those levels decreased for most chemotherapeutic agents when cells were treated simultaneously with chidamide. This effect was not observed for treatment with Nutlin-3a, epirubicin and doxorubicin in combination with chidamide in both YCCEL1 and C666.1 cells.

Total acetylation of histone H3 was examined as a marker for increased histone acetylation through chidamide treatment. In both YCCEL1 and C666.1 cells, an increase of acetylated histone H3 (panH3ac) levels was detected with the addition of chidamide compared to treatment with chemotherapeutic agents alone. Interestingly, all chemotherapeutic treatments alone induced an increase in panH3ac levels compared to DMSO controls in C666.1 cells (Figure 36.B, bottom panel). The same was observed for YCCEL1 cells except for Nutlin-3a treatment, which was the only treatment that did not induce H3 acetylation in single treatment (Figure 36.B, top panel).

In YCCEL1 and C666.1 cells, treatment with chemotherapeutic agents alone induced no Zebra expression, while double treatment with chidamide induced Zebra expression with certain compounds (Figure 36.B). Notably, chidamide treatment alone did not induce Zebra expression in either cell line. When treated together with chidamide, epirubicin and doxorubicin induced Zebra expression in ~45% of YCCEL1 cells (Figure 36.A). The combination of chidamide with epirubicin or doxorubicin also showed the strongest Zebra expression levels in YCCEL1 and C666.1 cells by western blot analysis (Figure 36.B). Nutlin-3a treatment with chidamide increased the percentage of Zebra-expressing cells to ~15%, while etoposide and cisplatin together with chidamide induced expression in ~8% of cells (Figure 36.A). In contrast, 5-FU induced Zebra expression in less than 2% of YCCEL1 cells in combination with chidamide and no Zebra expression was detected by western blot for C666.1 cells. The comparison of Zebra expression in both cell lines showed that epirubicin, doxorubicin, etoposide and Nutlin-3a induced Zebra expression with chidamide, while Cisplatin and 5-FU were much less effective in C666.1 and YCCEL1 cells.

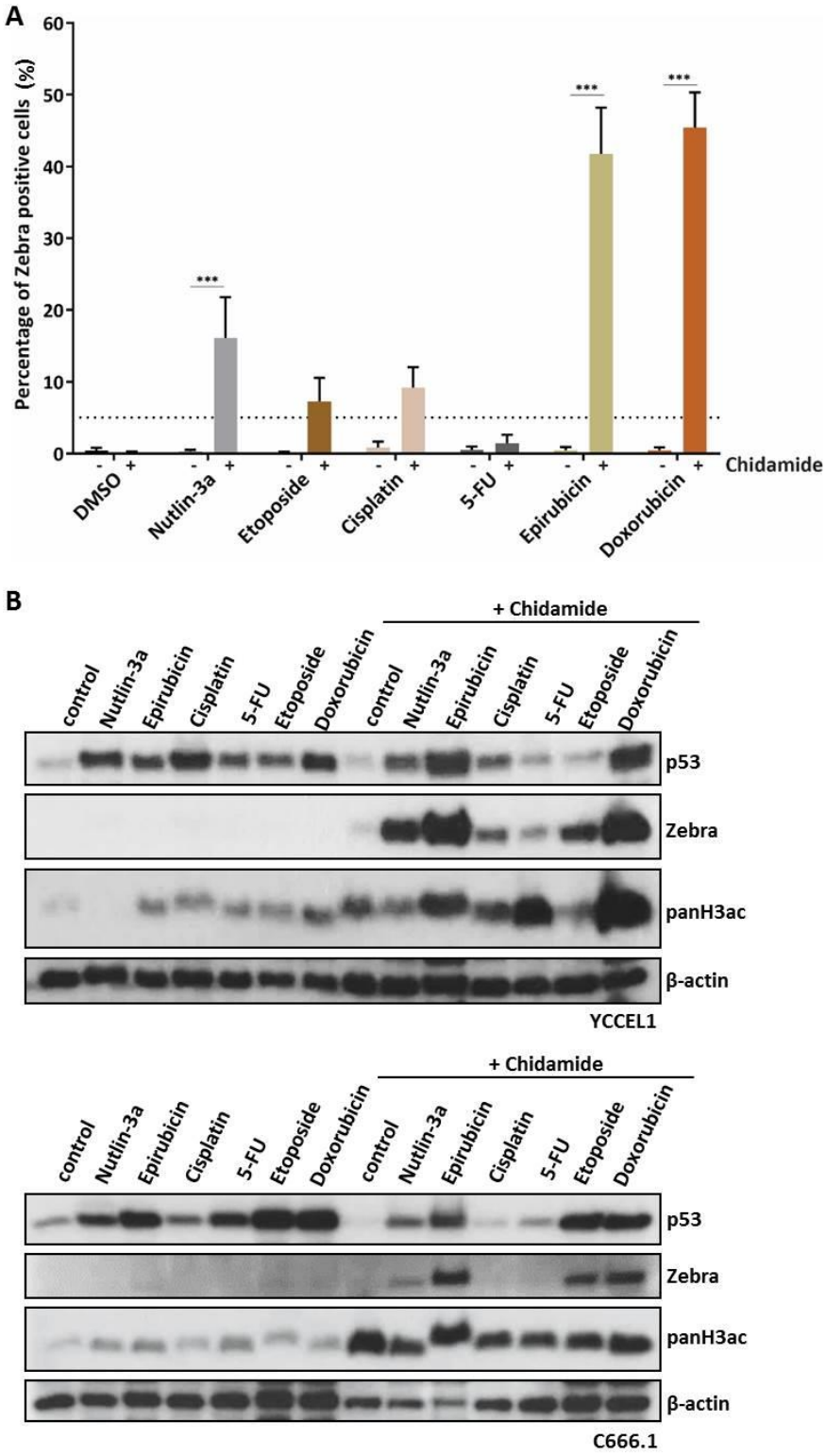


Figure 36: Zebra expression induced by chemotherapeutic treatment in combination with chidamide. Cells were treated for 48 h with either DMSO or 2.5 µM chidamide in combination with 2.5 µM Nutlin-3a, 1 µM epirubicin, 25 µM cisplatin, 1 µM 5-FU, 10 µM etoposide or 1 µM doxorubicin. Cellular expression was analysed subsequently by either immunofluorescence staining or western blot. A) Quantification of Zebra-expressing cells based on immunofluorescence staining in YCCEL1 cells. Bars

represent the average of three independently performed experiments. *n* = 3, error bars ± SEM. *P** ≤ 0.05; *P*** ≤ 0.01; *P**** ≤ 0.005. Significances were calculated using Sidak's multiple comparison test. B) Western blot analysis of Zebra expression in YCCEL1 (top) and C666.1 (bottom) cells. Results are representative of three independent repeats of this experiment. 5-FU – 5-fluorouracil; DMSO – dimethyl sulfoxide; panH3ac – acetylated Histone H3.

5.2.3 Induction of p53 increases the level of Zebra expression induced by HDACi treatment

All chemotherapeutic compound treatments in combination with chidamide have been shown to increase p53 protein levels compared to chidamide treatment alone, which correlated with increased Zebra expression in combination with chidamide (Figure 36.B). Therefore, it was tested whether p53 induction was sufficient for increased HDACi-induced EBV lytic cycle induction. This was achieved by treating different cell lines with Nutlin-3a, either alone or in combination with different HDACis (Figure 37).

In AGS EBV cells, HDACi treatment induced Zebra expression and the addition of Nutlin-3a increased Zebra expression levels further compared to HDACi treatment alone (Figure 37.A). Notably, Nutlin-3a treatment alone was able to induce Zebra expression in AGS EBV cells, but not in any of the other three tested cell lines (SNU719, YCCEL1 and C666.1). In SNU719 cells, romidepsin, chidamide and CXD101 induced Zebra expression, with chidamide and CXD101 leading to the highest levels of Zebra expression (Figure 37.B). Treatment with Nutlin-3a and chidamide or CXD101 in SNU719 cells induced Zebra expression, but the levels were lower than in samples treated with those HDACis alone (Figure 37.B). In YCCEL1 cells, chidamide and CXD101 induced Zebra expression when treated alone, but levels increased through the addition of Nutlin-3a (Figure 37.C). Romidepsin treatment only induced high levels of Zebra expression in combination with Nutlin-3a, but none of the other samples showed significant Zebra expression in YCCEL1 cells. In C666.1 cells, no Zebra expression was detected with HDACi treatment alone, but in combination with Nutlin-3a, chidamide and CXD101 induced Zebra expression (Figure 37.D).

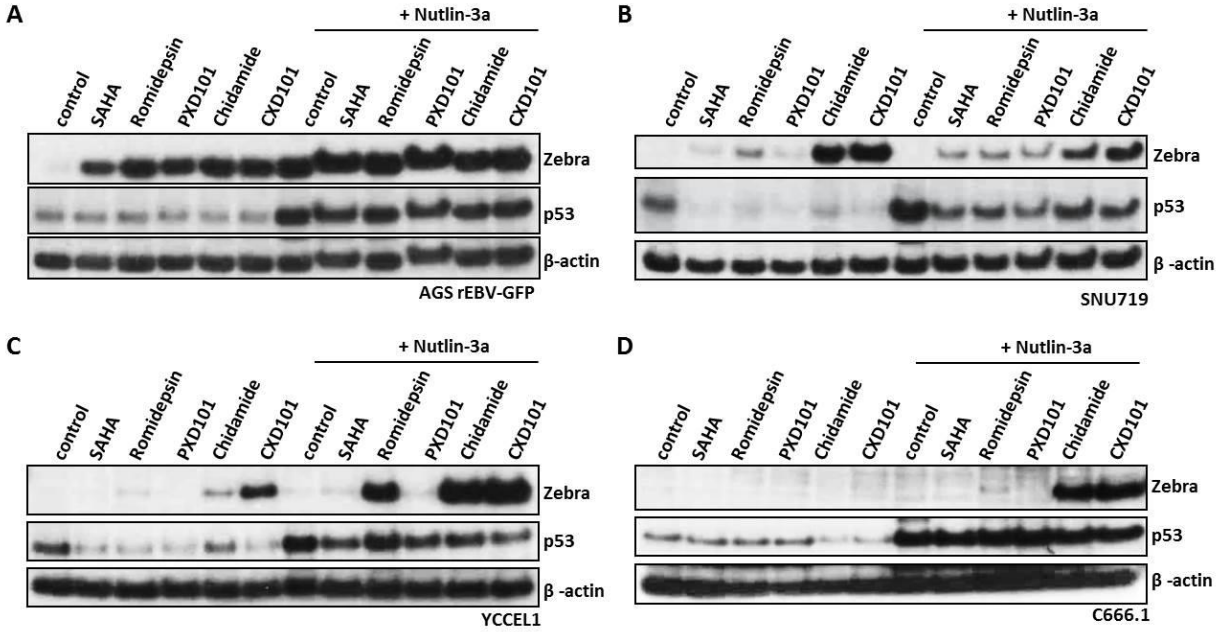


Figure 37: Zebra expression levels upon HDACi treatment in combination with Nutlin-3a assessed by western blot in a panel of EBV-positive epithelial cell lines. Cells were treated for 48 h with either DMSO or 10 µM Nutlin-3a in combination with 5 µM SAHA, 2.5 nM romidepsin, 2.5 µM PXD101, 5 µM chidamide or 2.5 µM CXD101, and then analysed by western blot. Results are representative of two independent repeats of this experiment. DMSO – dimethyl sulfoxide; GFP – green fluorescent protein; SAHA – suberoylanilide hydroxamic acid.

To determine the percentage of Zebra-expressing cells in samples treated with HDACis and Nutlin-3a, immunofluorescence staining with subsequent quantification of Zebra-positive cells was performed (Figure 38). In AGS EBV cells, Nutlin-3a treatment induced Zebra expression in ~20% of cells, while DMSO-treated control cells expressed Zebra in less than 1% of cells (Figure 38.A). Chidamide and CXD101 treatment alone induced Zebra expression in 10–20% of AGS EBV cells, and co-treatment with Nutlin-3a increased the percentage of Zebra-expressing cells to ~50% (Figure 38.A). In YCCEL1 cells, chidamide and CXD101 alone induced Zebra expression in 10–15% of cells (Figure 38.B). The addition of Nutlin-3a increased this percentage to 35% with chidamide and 60% with CXD101 in YCCEL1 cells. Nutlin-3a alone induced Zebra expression in less than 5% of cells in YCCEL1 cells. In both YCCEL1 and C666.1 cells, no Zebra expression was detected in DMSO-treated control cells (Figure 38.B and C). In the NPC cell line C666.1, chidamide, CXD101 and Nutlin-3a treatment induced Zebra expression in less than

5% of cells (Figure 38.C). The addition of Nutlin-3a to HDACi-treated cells increased the percentage of Zebra-expressing cells to ~20% in C666.1 cells.

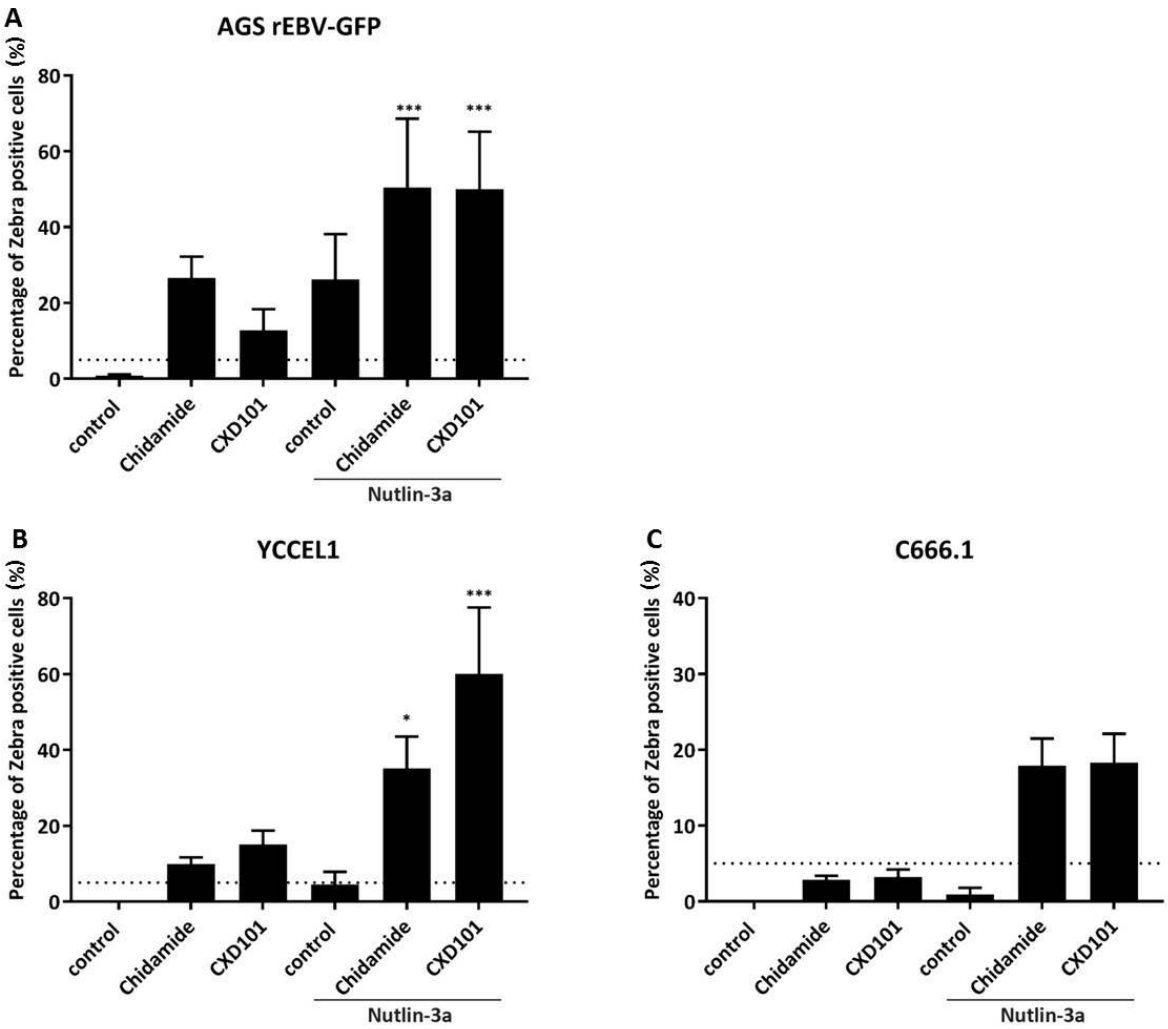


Figure 38: Quantification of Zebra-expressing cells in different epithelial cell lines treated with chidamide and CXD101 alone or in combination with Nutlin-3a. AGS rEBV-GFP, YCCEL1 or C666.1 cells were treated for 48 h with either 5 µM chidamide or 2.5 µM CXD101 in combination with DMSO or 5 µM Nutlin-3a, and then examined by immunofluorescence staining. The dotted lines represent Zebra expression in 5% of cells. Bars represent the average of three independently performed experiments with five random images taken per experiment. n = 3, error bars ± SEM. $P^* \leq 0.05$; $P^{**} \leq 0.01$; $P^{***} \leq 0.005$. Significances were calculated using Dunnett's multiple comparison test relative to control cells. DMSO – dimethyl sulfoxide; GFP – green fluorescent protein.

In YCCEL1 cells, analysis of the immunofluorescence images showed that DMSO and Nutlin-3a treatment induced no Zebra expression, and that the addition of Nutlin-3a to HDACi-treated cells led to

an increased number of Zebra-expressing cells (Figure 39). In addition, the expression levels were significantly higher than in just chidamide- or CXD101-treated samples. Thus, CXD101- and Nutlin-3a-treated samples did not only express Zebra in the highest percentage of cells, but also showed the highest levels of Zebra expression per cell.

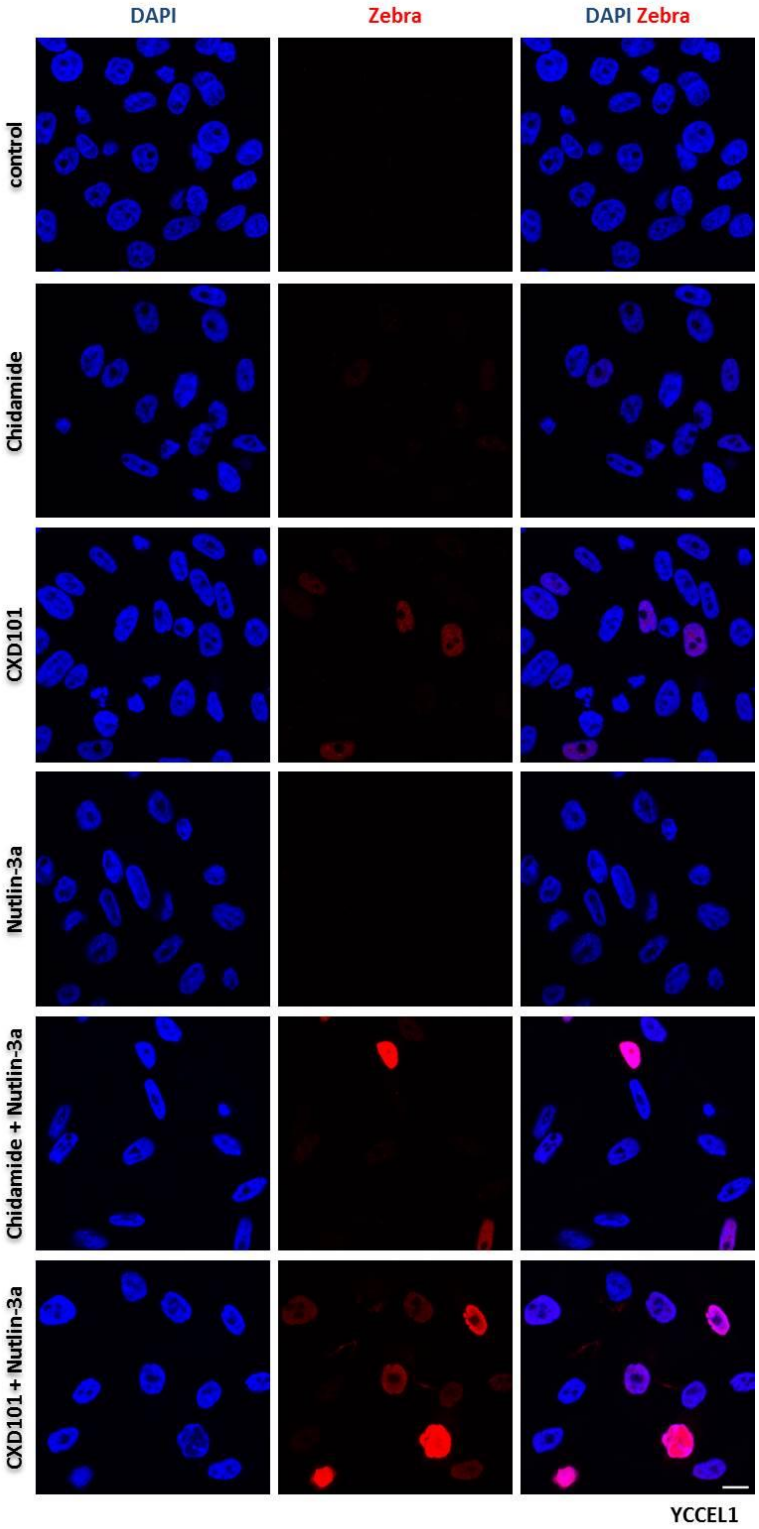


Figure 39: Zebra expression levels upon HDACi treatment in combination with Nutlin-3a treatment assessed by immunofluorescence staining in YCCEL1 cells. Cells were treated for 48 h with either 5 µM chidamide or 2.5 µM CXD101 in combination with DMSO or 5 µM Nutlin-3a, and then analysed by immunofluorescence staining. The scale bar represents 10 µm. Results are representative of three

independent repeats of this experiment with five random images taken per experiment. DAPI – 4',6-diamidino-2-phenylindole dihydrochloride; DMSO – dimethyl sulfoxide.

To see how Nutlin-3a influences the percentage of Zebra-expressing cells together with a broader range of HDACis, Nutlin-3a was added to the panel of HDACis described in Chapter 3.2.2 and the percentage of Zebra-expressing cells determined using the immunofluorescence-based screening method described in Chapter 3.2.1 (Figure 40). In YCCEL1 cells, DMSO control treatment with and without Nutlin-3a induced Zebra expression in less than 2.5% of cells. In combination with the HDACis LAQ824, panobinostat, romidepsin and SAHA, Nutlin-3a led to a small increase in the percentage of Zebra-expressing cells from ~2.5% to a maximum of ~15%. But the combination of those compounds with Nutlin-3a also led to increased toxicity, reducing cell numbers to less than 25% of the DMSO controls. Dinaline and CI994 treatment induced Zebra expression in less than 3% of cells, but adding Nutlin-3a increased the percentage to ~5 and ~10%, respectively. Chidamide treatment in combination with Nutlin-3a increased the percentage of Zebra-expressing cells from ~2.5 to ~25%. CXD101 treatment alone induced Zebra expression in ~20% of cells, but Nutlin-3a increased it to ~55%. In entinostat-treated cells, the percentage increased from ~15 to ~35% with Nutlin-3a, and in mocetinostat-treated cells from ~40 to ~50%.

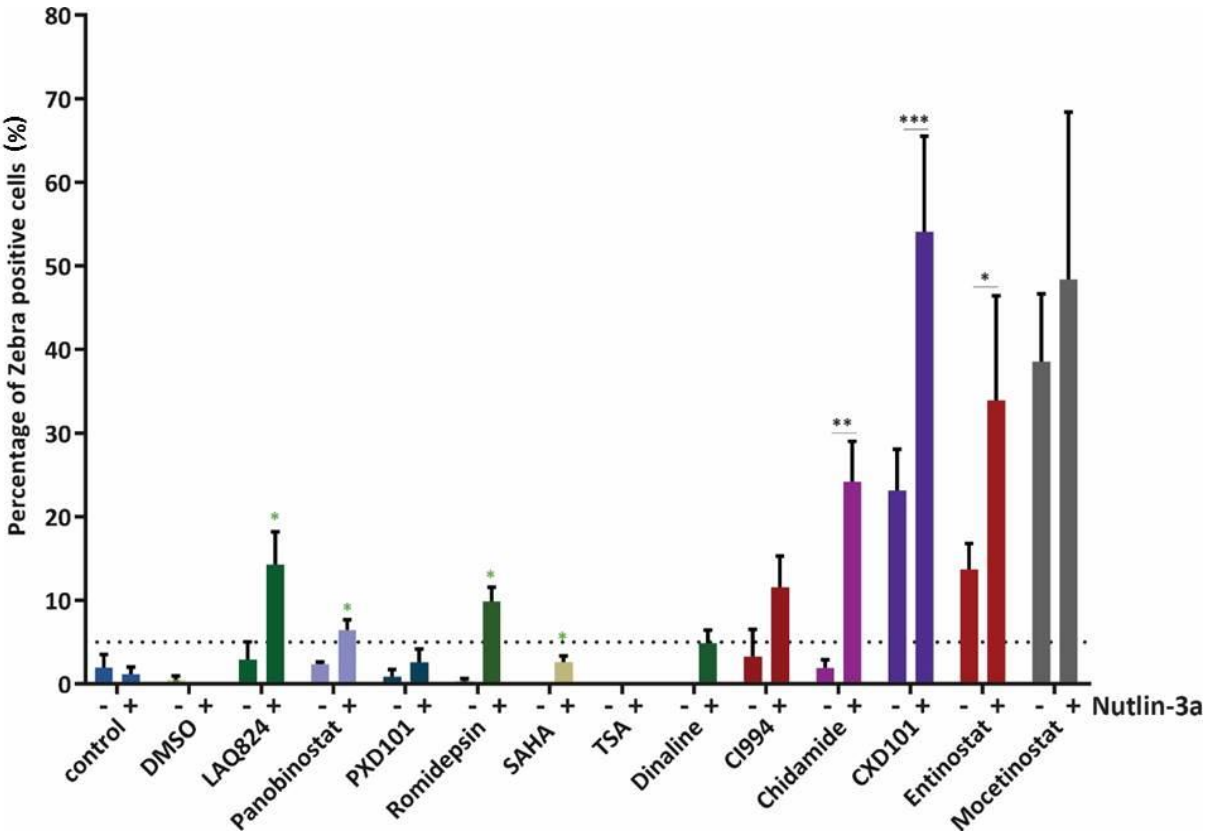


Figure 40: Percentage of Zebra-expressing cells in YCCEL1 cells upon treatment with a panel of HDACis with or without Nutlin-3a. YCCEL1 cells were treated for 48 h with the indicated HDACis (medium concentration as stated in Table 8) alone or with 2.5 µM Nutlin-3a. Control samples were treated with DMSO. The green asterisks indicate cell survival of less than 25%. Significance has been calculated by Sidak's multiple comparison test relative to HDACi treatment alone. *n* = 3, error bars ± SEM. *P** ≤ 0.05; *P*** ≤ 0.01; *P**** ≤ 0.005. DMSO – dimethyl sulfoxide; SAHA – suberoylanilide hydroxamic acid; TSA – trichostatin A.

Next, it was examined whether the combination of HDACi treatment with p53-inducing agents was sufficient to induce Zebra expression in different cellular backgrounds such as B-lymphocytes. In order to examine this, the B-cell line PD LCL was compared to the epithelial cell line YCCEL1 treated with HDACis in combination with either Nutlin-3a or epirubicin by western blot analysis (Figure 41).

As observed in previous experiments, chidamide and CXD101 treatment in combination with Nutlin-3a or epirubicin led to strong Zebra expression in YCCEL1 cells. PD LCL cells already expressed low levels of Zebra in control conditions, which increased upon the addition of Nutlin-3a or epirubicin to PD LCL cells. In contrast, neither chidamide nor CXD101 treatment alone induced more Zebra expression in PD LCL

cells. Interestingly, the combination of Nutlin-3a with any of the two HDACis did not increase the level of Zebra expression in PD LCL cells. However, Zebra levels in HDACi- and epirubicin-treated cells were higher than in combination with Nutlin-3a.

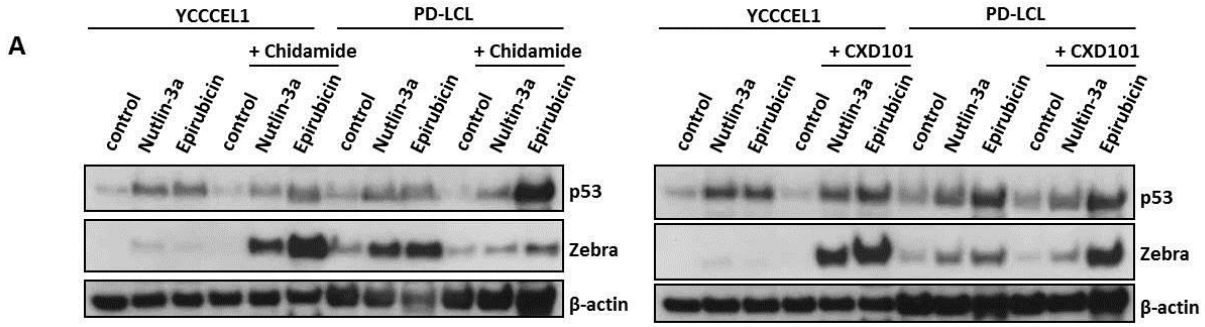


Figure 41: Comparison of Zebra expression levels upon HDACi treatment in combination with Nutlin-3a and epirubicin in epithelial and B-cell lines. YCCEL1 and PD LCL cells were treated for 48 h with either 2.5 µM Nutlin-3a or 1 µM epirubicin in combination with DMSO, 2.5 µM chidamide or 1 µM CXD101, and then analysed by western blot. Results are representative of three independent repeats of this experiment. DMSO - dimethyl sulfoxide.

Overall, the results in this chapter showed that Nutlin-3a treatment was sufficient to induce increased Zebra expression in combination with benzamide-based HDACis in EBV-positive epithelial cells. In contrast, Nutlin-3a was more efficient in inducing Zebra expression in B-cell lines than the combination of HDACis with p53-inducing agents.

5.2.4 Knockdown of p53 abolishes the reactivation potential of HDACis

To examine the importance of p53 for Zebra expression, p53 was knocked down in different epithelial cell lines by siRNA transfection before treatment with HDACis and Nutlin-3a (Figure 42). In AGS EBV cells, reduction of p53 protein levels led to a significant reduction of Zebra expression (Figure 42, top panel). Chidamide-treated AGS EBV cells, either alone or with Nutlin-3a, were the only sip53-transfected samples in which Zebra was detected, but those levels were lower than in the same samples transfected with scrambled control siRNAs. In YCCEL1 and C666.1 cells, the p53 knockdown

was successful and abolished Zebra expression, even when Nutlin-3a treatment was combined with HDACis (Figure 42, second and fourth panels).

NCC-24 cells are a cell line derived from an EBV-positive gastric tumour that contained a DNA-binding mutation within the *TP53* gene (Ku *et al.,* 2012). NCC-24 cells did not express Zebra under any of the tested treatment conditions, which was not altered by p53 knockdown (Figure 42, third panel). Notably, this cell line already expressed high p53 levels before Nutlin-3a treatment, so Nutlin-3a did not induce an increase in p53 protein levels.

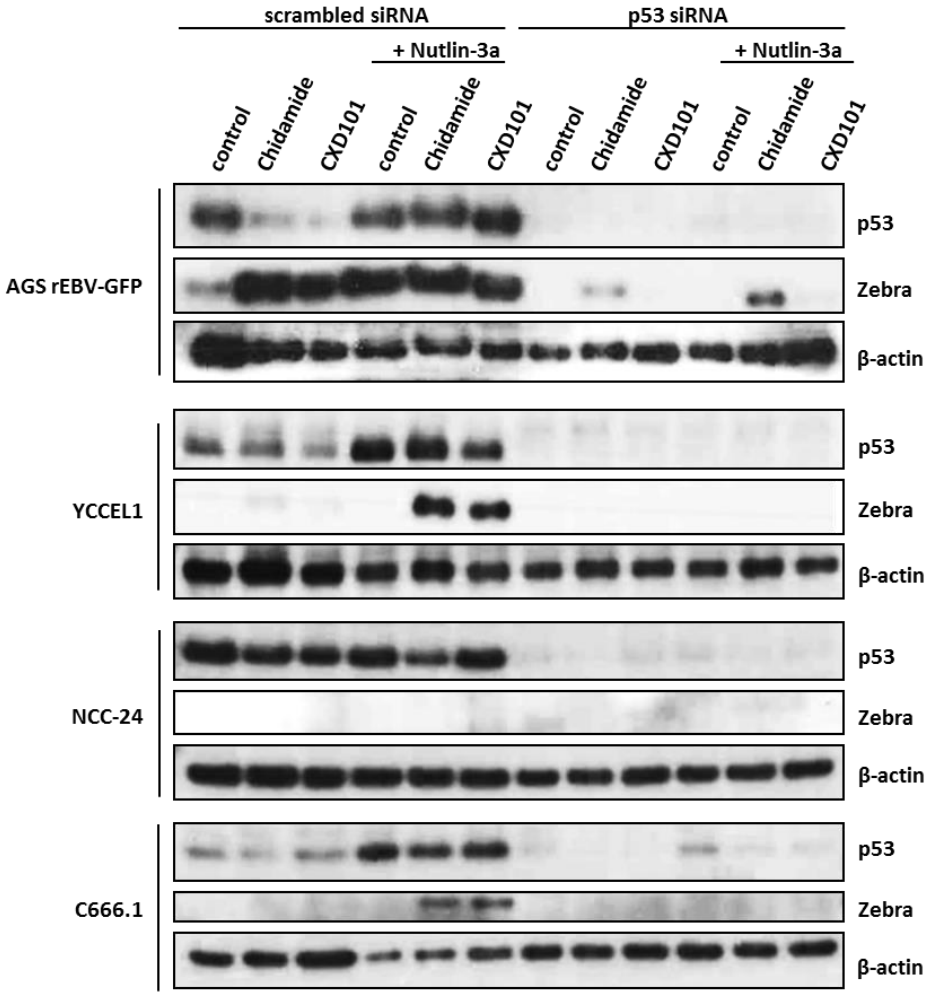


Figure 42: Zebra expression after p53 knockdown in a panel of epithelial cells treated with either chidamide or CXD101 with Nutlin-3a. Cells were treated for 48 h with either 5 µM chidamide or 2.5 µM CXD101 in combination with DMSO or 5 µM Nutlin-3a 48 h after transfection with siRNAs, and then analysed by western blot. Results are representative of two independent repeats of this experiment for

each cell line. DMSO - dimethyl sulfoxide; GFP – green fluorescent protein; siRNA – small interfering RNA.

To test whether the reduction of p53 levels is sufficient to abolish Zebra expression in combination with other p53-inducing agents, the p53 knockdown experiment was repeated with YCCEL1 cells treated with chidamide in combination with epirubicin or doxorubicin (Figure 43). As seen before, the p53 knockdown completely abolished Zebra expression in YCCEL1 cells independently of the treatment used.

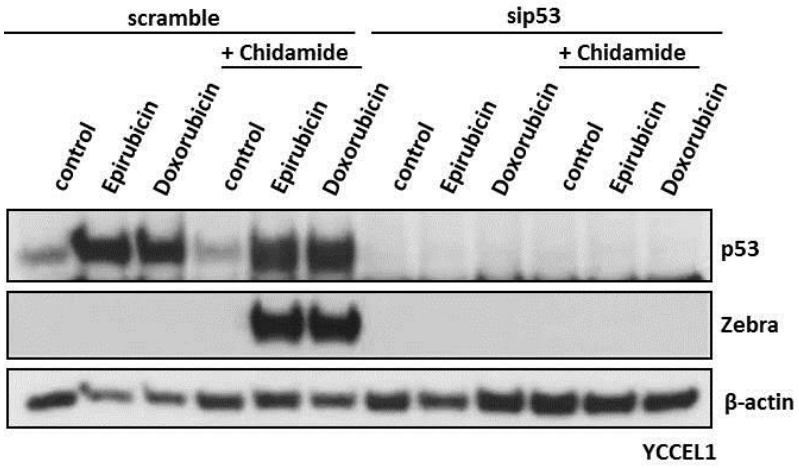


Figure 43: Zebra expression after p53 knockdown in YCCEL1 cells treated with doxorubicin or epirubicin in combination with chidamide. Cells were treated for 48 h with either 1 µM epirubicin or 1 µM doxorubicin in combination with DMSO or 2.5 µM chidamide 48 h after transfection with siRNAs, and then analysed by western blot. Results are representative of two independent repeats of this experiment. DMSO – dimethyl sulfoxide; siRNA – small interfering RNA.

Overall, this showed that the knockdown of p53 is sufficient to abolish Zebra expression induced by different treatment combinations.

5.2.5 Protein levels of p53 and Sp1 influence the level of Zebra expression

To induce the expression of its target genes, p53 commonly binds to the promoters of those genes at consensus p53-binding sites (Kruse & Gu, 2009). Although p53 has been shown to bind to the Zp

promoter, no consensus p53-binding site has been identified within the Zp promoter in previous studies In an attempt to understand how this is facilitated, previous studies have underlined the importance of Sp1 for p53's binding to the Zp promoter. It was suggested that Sp1 mediates the effect of p53 on Zebra expression, meaning that Sp1 binds to Zp and that p53 then forms a complex with Sp1 (Chua *et al.*, 2012). In order to examine this mechanism in the identified treatment combinations, the effect of Sp1 knockdown on Zebra expression levels in cells was analysed (Figure 44).

Reduction of Sp1 levels by siRNA transfection led to a decrease in Zebra expression in all treated YCCEL1 samples. More specifically, Zebra expression was completely abolished when Sp1 knockdown cells were treated with HDACis, and significantly reduced when those treatments were combined with Nutlin-3a (Figure 44.A). Notably, the levels of p53 were reduced in samples treated with HDACis and Nutlin-3a, and not detectable in HDACi-treated samples. This was also observed in an experiment directly comparing Sp1 knockdown to p53 knockdown cells (Figure 44.B). This experiment further showed that a knockdown of p53 increased Sp1 levels. In both sip53- and sip53/Sp1-transfected samples, Zebra expression was abolished. The transfection of Sp1 siRNA reduced Zebra levels significantly compared to scrambled controls, with no Zebra expression detectable in chidamide-treated samples and reduced levels in chidamide- and Nutlin-3a-treated samples (Figure 44.B).

Overall, those results suggested that Sp1 and p53 influence each other's expression as well as the expression of Zebra.

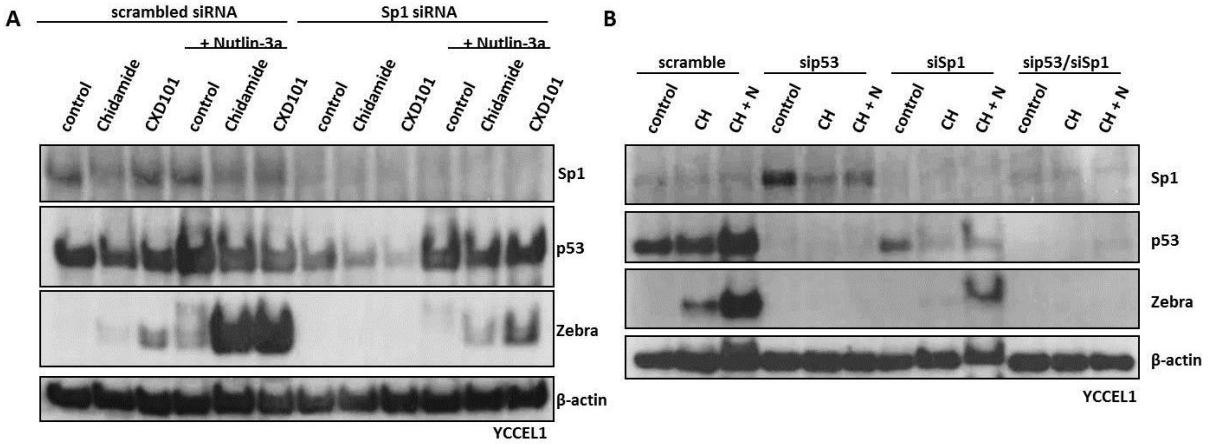


Figure 44: Influence of Sp1 and p53 levels on Zebra expression in YCCEL1 cells treated with different HDACis and Nutlin-3a. A) 48 h after transfection with siRNAs, YCCEL1 cells were treated for 48 h with either DMSO, 5 µM chidamide or 2.5 µM CXD101 in combination with 5 µM Nutlin-3a, and then analysed by western blot. Results are representative of three independent repeats of this experiment for each cell line. B) YCCEL1 cells were treated for 48 h with either DMSO, 5 µM chidamide or chidamide in combination with 5 µM Nutlin-3a 48 h after transfection with siRNAs, and then analysed by western blot. CH – Chidamide; DMSO – dimethyl sulfoxide; N – Nutlin-3a; siRNA – small interfering RNA.

5.2.6 Identification of novel interactions between p53 and lytic EBV proteins

Results from Chapters 5.2.3 and 5.2.4 suggested a crucial role of p53 in the induction of the lytic cycle of EBV in epithelial cells. While Sp1 has been previously shown to facilitate p53 binding to the Zp promoter (Chua *et al.*, 2012), the results from Chapter 5.2.5 indicate that additional mechanisms might be important for the p53-mediated effect on Zebra expression and lytic cycle expression. To identify additional p53 interactors with a potential role in the life cycle of EBV in an unbiased manner, interactors of p53 were analysed by MS. For this experiment, YCCEL1 cells were treated for 24 h with either 5-FU, epirubicin or Nutlin-3a alone or in combination with chidamide. Three independent experiments were performed to allow more accurate downstream analysis of the MS data. After treatment, p53 was immunoprecipitated and potential binding partners of p53 identified by MS. This experiment was performed in collaboration with Dr Thomas Leissing (University of Oxford). MS analysis

was performed at the Advanced Proteomics Facility of the TDI, Oxford by Dr Roman Fischer and Georgina Berridge.

Western blot analysis of samples generated for the p53 interactome experiment showed that p53 levels were successfully induced in samples treated with Nutlin-3a, epirubicin and 5-FU (Figure 45). As previously observed (Figure 36.B), the levels of p53 in chidamide, as well as in 5-FU- and chidamide-treated samples, were lower than for other treatment combinations. Following the immunoprecipitation of p53, p53 levels were similarly enriched in all samples according to western blot analysis. HDAC1 is a protein that is known to bind to p53 (Ito *et al.*, 2002). HDAC1 levels were similar in all input and immunoprecipitated samples, but lower HDAC1 levels were detected in epirubicin-treated samples after the immunoprecipitation.

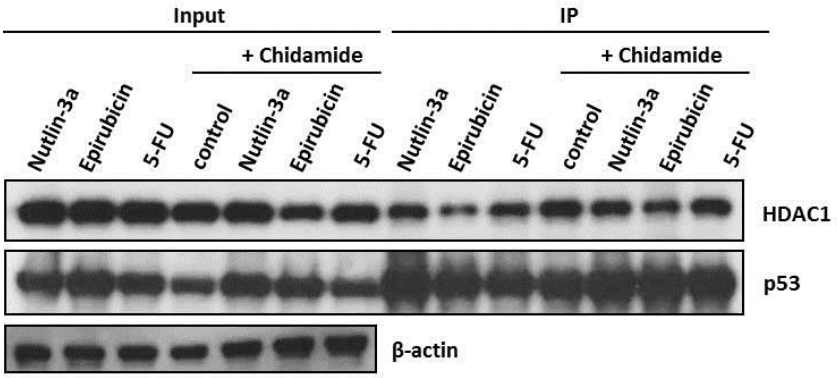


Figure 45: Western blot analysis of p53 interactome samples used for MS analysis. YCCEL1 cells were treated for 24 h with either 2.5 µM Nutlin-3a, 1 µM epirubicin or 1 µM 5-FU alone or in combination with 2.5 µM chidamide. Subsequently, cells were lysed (Input samples) and p53 immunoprecipitation performed (IP samples). Results are representative of three replicates performed for this experiment. 5-FU – 5-fluorouracil; HDAC – histone deacetylase; IP – immunoprecipitation.

In total, 1801 proteins were identified in the MS of the p53 immunoprecipitation (Figure 46.A). The abundance of detected p53 protein after MS was examined for all treatments to get an insight into the quality of the immunoprecipitation experiment (Figure 46.C, top left panel). Chidamide treatment showed the lowest p53 levels, which was expected as those samples did not include treatment with a p53-inducing agent. In contrast, 5-FU and 5-FU samples with chidamide showed reduced p53 levels

compared to the rest of the samples. Notably, the levels of p53 in Nutlin-3a and epirubicin treated samples were similar.

To examine whether the performed MS analysis of p53 interactors in differently treated YCCEL1 cells was successful in identifying known p53 interactors described in the UniProt entry for p53 (UniProt Consortium, 2018), the overlap between those two datasets was compared (Figure 46.A). This showed that of the 1801 observed interactors, 39 proteins were previously described p53 interactors including proteins such as Sp1, HDAC1 and EP300 (Figure 46.B). The detected abundance of HDAC1 bound to p53 did not change between the different treatments, but both Sp1 and EP300 were detected at lower abundance in chidamide and epirubicin samples (Figure 46.C). The identification of known p53-binding proteins by MS underlined the success of the p53 immunoprecipitation.

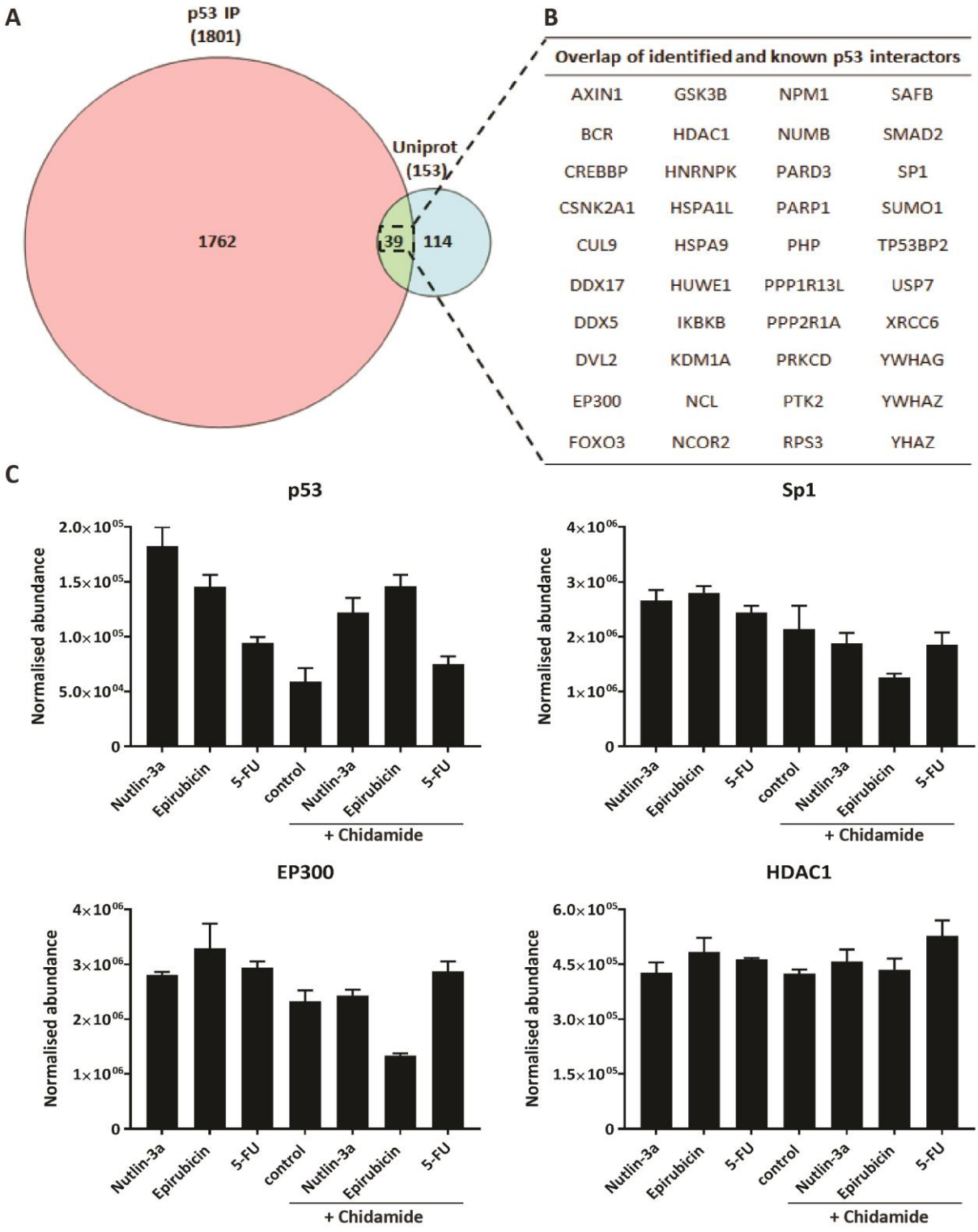


Figure 46: Comparison of identified and previously reported p53 interactors and examples of their detected abundance. A) Venn diagram of all identified p53 interactors by MS of a p53 IP experiment in differently treated YCCEL1 cells and the binary p53 interactors described in the p53 UniProt entry (UniProt Consortium, 2018). B) Proteins identified with PEAKS8.5 using the human and EBV database, and quantification was performed with Progenesis using label-free quantification of all identified

proteins with the top three peptides of each identified protein. Bars represent the average of three independently performed experiments. Figures courtesy of Dr Thomas Leissing (University of Oxford). *n* = 3, error bars ± SEM. 5-FU – 5-fluorouracil; EBV – Epstein-Barr virus; HDAC – histone deacetylase; IP – immunoprecipitation.

Four different EBV lytic proteins have been identified as potential interactors with p53 by MS (Figure 47). SM, the gene product of *BMFL1*, was detected in all samples with the highest levels measured in chidamide and epirubicin, and the lowest levels in 5-FU-treated samples (Figure 47.C). Low levels of the EBV thymidine kinase were detected in chidamide- and epirubicin-treated samples, and high levels upon chidamide and Nutlin-3a treatment (Figure 47.D).

Notably, two of those four proteins, early antigen diffuse component (Ea-D) and major DNA binding protein (mDBP), are members of the viral DNA replication complex (Zeng *et al.*, 1997) and have been shown to differently bind to p53 depending on the treatment (Figure 47.A and B). The highest levels of Ea-D were identified in chidamide- and epirubicin-treated samples, while Ea-D was detected at a lower level in cells treated with chidamide and Nutlin-3a. In contrast, mDBP was only detected in chidamide- and Nutlin-3a-treated samples, and not for any other treatment condition.

Validation of the identified interactions between EBV lytic proteins and p53 is currently ongoing, but an additional MS experiment identified the same EBV proteins as p53 interactors, increasing confidence in the detected interaction between EBV and different lytic E proteins (Appendix Figure 3). While the MS experiment did not identify any novel cellular p53 binding proteins with a potential role in EBV reactivation, this is the first time that potential binding of p53 to Ea-D and mDBP was described.

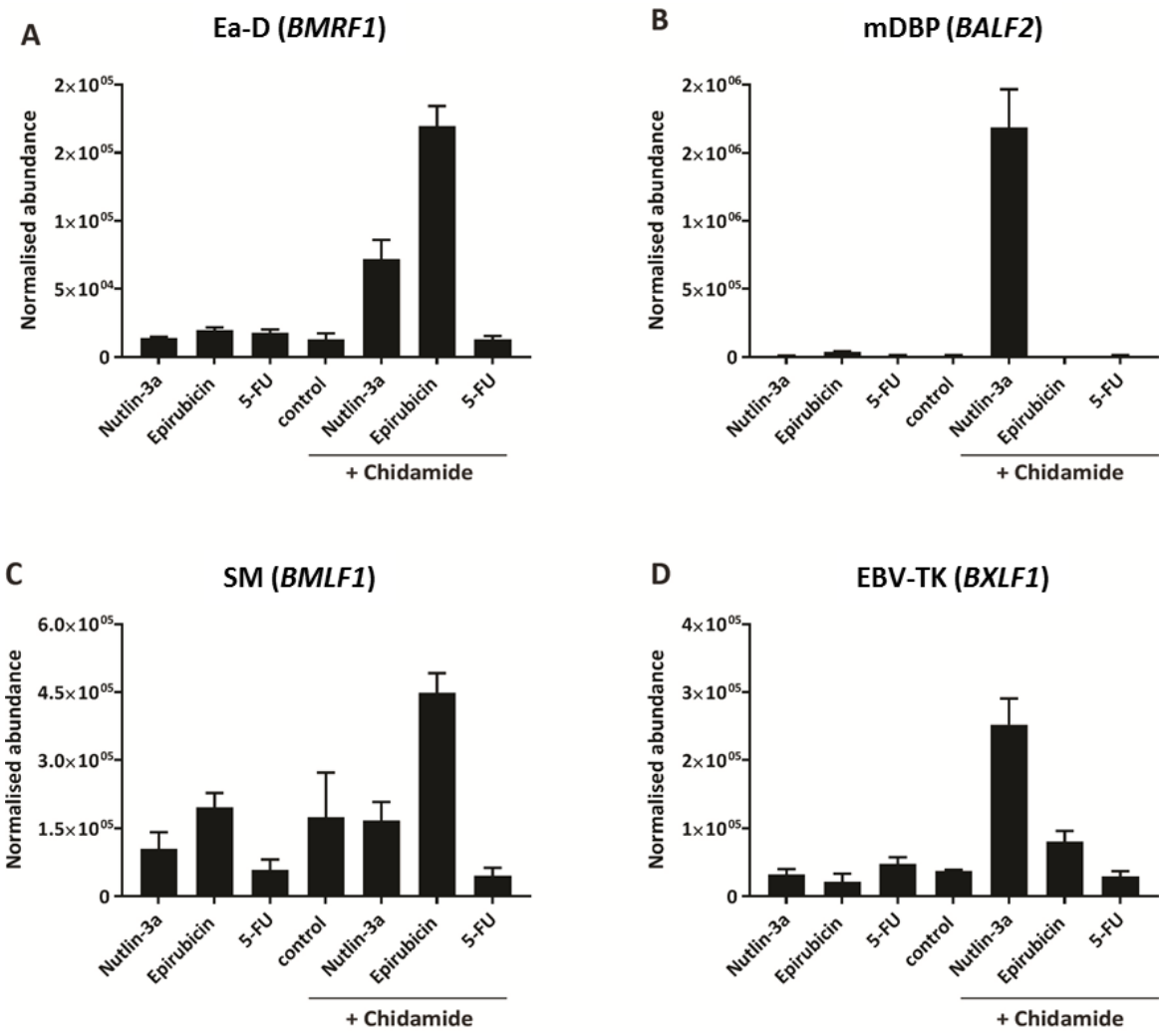


Figure 47: EBV proteins identified to bind p53 after 24 h of compound treatment and their normalised abundance. Proteins identified with PEAKS8.5 using the human and EBV database, and quantification was performed with Progenesis using label-free quantification of all identified proteins with the top three peptides of each identified protein. Bars represent the average of three independently performed experiments and the names in brackets the gene names of the identified proteins. Figures courtesy of Dr Thomas Leissing (University of Oxford). *n* = 3, error bars ± SEM. Ea-D – early antigen diffuse component; EBV-TK – Epstein-Barr virus thymidine kinase; mDBP – major DNA-binding protein.

5.2.7 Differential effect of combinatorial treatment on cell viability in gastric cancer cells

Since chemotherapeutic agents have been previously reported to lead to increased cell killing in epithelial cells either alone or in combination with VPA (Feng *et al.,* 2002; Wildeman *et al.,* 2012; Stoker *et al.,* 2015), it was examined whether this is also the case for chidamide. The expression of the *BGLF4*

gene, encoding the viral protein kinase that activates antiviral agents, was examined by qPCR in YCCEL1 cells treated for 48 h with epirubicin or Nutlin-3a either alone or in combination with chidamide.

BGLF4 was induced less than 5-fold in control cells or in cells treated with epirubicin or Nutlin-3a (Figure 48.A). Treatment with chidamide induced *BGLF4* gene expression ~17-fold, while in combination with epirubicin it only increased expression ~24-fold compared to control cells. In contrast, cells treated with chidamide and Nutlin-3a showed strong expression of *BGLF4* with ~250-fold induction.

To assess if the *BGLF4* expression levels are sufficient to induce targeted cell killing, AGS, AGS EBV and YCCEL1 cells were treated with chidamide, epirubicin or Nutlin-3a alone or in combination before the antiviral agents ACV and GCV were added to the cells (Figure 48.B–D). The impact on cell viability was measured by trypan blue staining as described in Chapter 2.2.1.

Treatment with DMSO either alone or with an antiviral agent did not induce significant toxicity in any of the examined cell lines, and the same was true for chidamide treatment alone or with ACV in AGS and AGS EBV cells (Figure 48.D). The addition of GCV reduced the cell number to ~65% compared to the DMSO control in AGS EBV cells (Figure 48.C). In YCCEL1 cells, cell numbers for chidamide-treated samples with or without ACV remained between 75–100% relative to control cell numbers, but the addition of GCV reduced cell numbers to less than 25% (Figure 48.B). In contrast, epirubicin treatment led to a significant reduction in cell numbers in all cell lines independently of the presence of antiviral agents, reducing cell numbers to less than 5%. This was independent of the addition of chidamide to the initial treatment. Nutlin-3a treatment alone did not induce any significant toxicity in any of the three cell lines tested independently of the antiviral agents added, except for YCCEL1 cells in combination with GCV (Figure 48.B). In AGS cells, combination treatment of chidamide and Nutlin-3a reduced cell numbers to ~50% and the addition of antiviral agents did not significantly change that (Figure 48.D). In AGS EBV cells, chidamide and Nutlin-3a led to cell numbers between 2–10% depending on the treatment, with GCV treatment reducing the cell numbers to ~2% (Figure 48.C). In YCCEL1 cells,

this combination of treatment either alone or with ACV decreased cell numbers to ~30%, and the addition of GCV reduced cell numbers further to less than 3% relative to DMSO-treated samples (Figure 48.B).

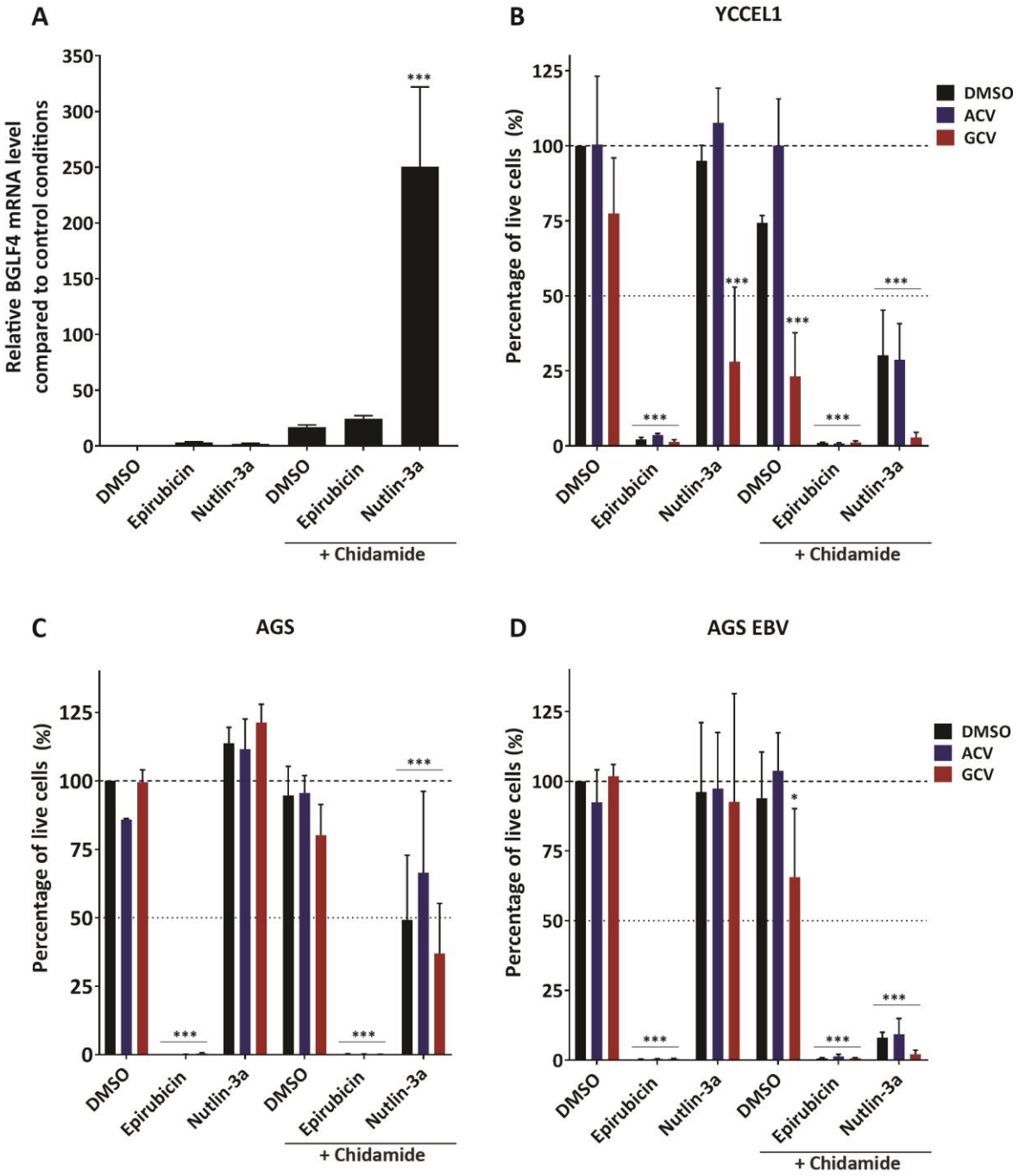


Figure 48: BGLF4 expression and cell killing in combination therapy together with antiviral agents. A) BGLF4 expression in different cell lines was evaluated by qPCR. YCCEL1 cells were treated for 48 h with 2.5 µM Nutlin-3a or 1 µM epirubicin in combination with DMSO or 2.5 µM chidamide. The results represent $\Delta\Delta C_t$-values normalised to GAPDH levels within the same samples as well as the control

samples for the BGLF4 primer. B+C) Percentage of live cells upon antiviral treatment relative to DMSO controls. AGS, AGS rEBV-GFP or YCCEL1 were treated for 48 h with either DMSO, 2.5 µM chidamide, 2.5 µM Nutlin-3a or 1 µM epirubicin, or a combination of those compounds. Afterwards, the medium was replaced with medium containing either DMSO, 10 µg/µL ACV or 20 µg/µL GCV, and treated for 5 days before collection for cell viability assessment. Bars represent the average of three independently performed experiments. n = 3, error bars ± SEM. $P^* \leq 0.05$; $P^{**} \leq 0.01$; $P^{***} \leq 0.005$. Significance was calculated using Dunnett's multiple comparison test relative to control cells. ACV – Acyclovir; AGS EBV – AGS rEBV-GFP; DMSO – dimethyl sulfoxide; GAPDH – glyceraldehyde 3-phosphate dehydrogenase; GCV – Ganciclovir, OE19 EBV – OE19 rEBV-GFP; qPCR - quantitative polymerase chain reaction.

Overall, those results indicated that while epirubicin treatment is toxic for all cell lines independently of their EBV status, Nutlin-3a treatment with chidamide leads to increased toxicity specifically in EBV-positive cell lines.

5.3 Summary and brief discussion

Chapter 5.2 has shown that topoisomerase inhibitors in combination with chidamide treatment have a synergistic effect on Zebra expression. This property was shared by other chemotherapeutic agents such as cisplatin, but not by 5-FU. Through Nutlin-3a treatment, which inhibits p53 degradation by MDM2 and thereby stabilises p53 levels, it was suggested that p53 levels are crucial for this synergistic effect. p53 knockdown experiments further showed that without p53 induction, the synergistic effect on Zebra expression levels by HDACis and p53-inducing treatments is abolished. A comparison of the synergy between p53-inducing agents and HDACis in different cellular backgrounds suggested that this effect is specific to epithelial cells and not shared by B-cell lines. In the literature, Sp1 has been suggested as the protein mediating the effect of p53 on Zebra expression. Knockdown experiments of Sp1 and p53 suggested that those two proteins regulate each other's expression as well as the expression of Zebra. Since these data did not fully explain the role of p53 in the regulation of Zebra expression, potential novel p53 interactors were examined in chidamide treatment in combination with different p53-inducing agents. This MS experiment indicated that p53 binds the E lytic protein Ea-D in both chidamide with Nutlin-3a- and chidamide with epirubicin-treated samples, while the other E lytic protein mDBP was only found to interact with p53 in chidamide and Nutlin-3a treatment. Finally, it was shown that epirubicin treatment alone or in combination with chidamide led to cell killing independently of the presence of EBV. Although the combination of chidamide and Nutlin-3a treatment decreased cell numbers in EBV-negative cells, cell killing in EBV-positive cells was significantly higher.

Previous studies on EBV and topoisomerase inhibitors suggest that treatment with topoisomerase inhibitors impairs lytic cycle gene expression of EBV (Kawanishi, 1993b; Wang *et al.*, 2009; Wu et al., 2014). Thus, it was surprising to identify topoisomerase inhibitors as a compound class that induces strong Zebra expression in combination with HDACi treatment.

Camptothecin and etoposide have been shown to inhibit EBV transcription as well as DNA replication (Wang *et al.,* 2009). The suggested cause for this effect is the disruption of Zebra binding to topoisomerase I, which abolishes its subsequent recruitment to the oriLyt where the complex usually induces viral DNA replication. Another study identified topoisomerase II inhibitors as a class of compounds with strong antiviral properties that inhibit viral DNA replication (Wu *et al.*, 2014). Notably, all topoisomerase inhibitors used in this study belong to the group of catalytic inhibitors of topoisomerases, while all topoisomerase inhibitors used in Chapter 5.2.1 belong to the group of topoisomerase poisons. Topoisomerase poisons are compounds that stabilise covalent DNA–topoisomerase complexes (Wilstermann *et al.,* 2007; Wu *et al.,* 2011). In contrast, catalytic topoisomerase inhibitors are a more heterogeneous class of compounds that can interfere with topoisomerase function through several mechanisms, such as interfering with DNA binding by topoisomerases or the inhibition of ATP binding to the enzyme (reviewed in Larsen *et al.*, 2003). Thus, the difference between the literature and the results in Chapter 5.2.1 could be explained by the different mechanisms exploited by the two groups of topoisomerase inhibitors, and point towards a potential role of covalent DNA–topoisomerase complexes in viral reactivation.

Another explanation for the discrepancy between the past studies and the results of the screening experiment described in Chapter 5.2.1 could be the focus on Zebra expression rather than the whole lytic cascade in the current study. Therefore, it cannot be excluded that topoisomerase inhibitors induce an abortive lytic cycle rather than full lytic cycle progression. Analysis of E and L gene product expression, as well as measurement of viral DNA replication upon treatment, should be performed in order to answer those questions.

A previous study reported that cisplatin and 5-FU induce lytic expression in epithelial cancer cells and that this can be exploited for target cell killing by GCV (Feng *et al.,* 2002). This stands in contrast to the results in Chapter 5.2.2, which show that cisplatin and 5-FU only induce low levels of Zebra expression

when combined with chidamide treatment. This difference between studies can potentially be explained by the cell lines used for the experiments. Feng *et al*. focussed their work on the AGS EBV cell lines, while the results presented in the current study have been generated in YCCEL1 and C666.1 cells. As shown in Figure 25 and Figure 37, AGS EBV cells seem to be more easily reactivated than YCCEL1 cells.

The results in Chapter 5.2.3 suggested that treatment with p53-inducing agents together with HDACis associates with increased Zebra expression levels. The importance of p53 has been further underlined by the elimination of Zebra expression in cells with p53 knockdown. Nevertheless, the fact that HDACi treatment is necessary to induce Zebra expression with those synergistic compounds, and that 5-FU treatment induces p53 protein levels but does not induce Zebra expression in combination with chidamide, showed that p53 induction alone is not sufficient to induce Zebra expression. This suggests that p53 might need to obtain certain PTMs or activate specific downstream targets to activate Zebra expression.

The results obtained in NCC-24 cells, which did not show any Zebra expression independently of the drug treatment, underlined the importance of p53 in reactivation. This cell line is the only one in the panel of cell lines used, which contains a mutation within the DNA-binding domain of p53 (Appendix Table 6) (Ku *et al.,* 2012). In addition, it has been found that even though p53 is commonly mutated in gastric cancer cases, p53 is more commonly found in its wild-type conformation in EBVaGC (Cancer Genome Atlas Research, 2014). The ability of the virus to reactivate might depend on wild-type p53, so that the virus has a potential exit strategy in case of cellular stress. This suggests that wild-type p53 is of importance for the life cycle of the virus and is thus selected for by the virus.

The difference in the efficacy of induction of Zebra expression by different treatments between YCCEL1 and PD LCL cells could be an artefact of the chosen cell lines (Figure 41), but could also be caused by differences in the cellular backgrounds, their mutational spectra and the viral strains in those cell lines.

A recent study has shown that the viral strains contained in SNU719 and YCCEL1 cells are closer to NPC strains such as GD1 and M81 than to B-cell strains such as B95.8 (Kanda *et al.*, 2016). The fact that the synergy between p53-inducing compounds and HDACis was not observed in the EBVaGC cell line SNU719 suggests that differences in the viral strain are less likely to be the cause of the differences in reactivation potential. Thus, this suggests that the cellular backgrounds and the mutational spectra of the cells are crucial for the efficacy of compound treatments, which is in agreement with the patterns of Zebra expression upon compound treatment observed in Chapter 3.2 and previously published studies (Hui & Chiang, 2010).

Western blot analyses of p53 protein levels indicated that the addition of Chidamide to treatment with chemotherapeutic agents reduced p53 levels compared to treatment with chemotherapeutic agents alone (Figure 36). This effect varied between chemotherapeutic agents, with 5-FU showing a strong decrease of p53 levels upon the addition of chidamide and no alteration in p53 levels in epirubicin- and doxorubicin-treated samples together with chidamide. These data suggest that the effect on p53 levels is caused by the combination of chidamide with certain compounds. While it has been suggested in the literature that Zebra induces p53 degradation by a ubiquitin ligase complex (Sato *et al.*, 2009a), this seems to be less a likely explanation because 5-FU samples did not show Zebra expression but strongly reduced p53 levels, while epirubicin samples showed strong Zebra expression and unchanged p53 levels.

Finally, no canonical p53-binding site has been identified in Zp. Different studies have shown that p53 cannot bind the Zp promoter directly but rather binds to Sp1, which is bound to the promoter (Chua *et al.,* 2012). p53 and Sp1 regulate several downstream targets such as DNMT1 synergistically (Im *et al.*, 2002; Lin *et al.*, 2010). The ratio of the two proteins to each other often regulates if the promoter is repressed or activated. Therefore, it is not surprising that p53 and Sp1 levels influence each other and thus potentially Zebra expression. The fact that a p53 mutant cell line cannot be reactivated might

underline this interplay, as it has been shown that p53 needs to be in its wild-type conformation to bind Sp1 (Chua *et al.,* 2012). Thus, Sp1 binding is important to facilitate the role of p53 in Zebra expression, but it seems that this is not the only way by which p53 influences Zebra expression and the lytic cycle.

Analysis of the p53 interactome upon reactivation showed that no significant differences were observed in the binding of cellular proteins to p53 in different treatment conditions (Figure 46). Interestingly, four viral proteins were found to bind p53 (Figure 47). Of those, Ea-D and DNBI were identified as binding partners in specific treatment conditions and were also independently identified in a previously performed p53 interactome experiment (Appendix Figure 3). Even though Ea-D and mDBP were identified in two separate MS experiments, it is crucial to validate the suggested interactions through other experimental methods before continuing with further examination of the importance of possible binding. Nevertheless, potential mechanisms behind the importance of the p53 interaction with Ea-D and mDBP will be discussed in the following paragraph. While Ea-D and mDBP have not been previously identified as p53-binding proteins, it has been shown that Ea-D and Zebra synergise to activate the BHLF1 promoter, and it has been suggested that this might be mediated by a cellular transcription factor (Yang *et al.*, 2008). Additionally, Ea-D and mDBP have been shown to interact with each other as part of the viral replication complex (Zeng *et al.,* 1997). This suggests that p53 might interact with those two proteins as part of the viral replication complex and thereby support viral lytic replication.

mDBP and p53 binding was only observed in chidamide- and Nutlin-3a-treated samples, and not in chidamide- and epirubicin-treated samples. Since the expression levels of mDBP have not been examined in this study, this might be caused by a lack of expression of mDBP upon chidamide and epirubicin treatment. Assuming that mDBP is expressed in chidamide- and epirubicin-treated samples, this would suggest that mDBP/p53 binding is disrupted by PTMs on either mDBP or p53 that do not occur upon chidamide and Nutlin-3a treatment. Therefore, after validation of the interaction and

protein expression levels, in-depth examination of potential PTMs of both proteins should be performed to identify key residues and modifications that mediate their interaction.

The analysis of cell killing in different treatment conditions showed increased toxicity of epirubicin treatment, either alone or in combination with chidamide, independently of the EBV status of the cell line (Figure 48). The long-term of toxicity of those treatments, even after removal of the compound, can be explained by severe DNA damage through double-strand breaks (DSBs) caused by epirubicin treatment (Yang *et al.*, 2015). While Nutlin-3a has also been shown to inhibit proliferation and induce apoptosis, lytic EBV gene expression has been shown to protect cells from cell death (Inman *et al.*, 2001; Oussaief *et al.*, 2009a; Wang *et al.*, 2012). Together, this suggests that while EBV is able to protect cells from apoptosis, lytic gene expression might not be sufficient to overcome the effects of the severe DNA damage caused by epirubicin treatment and to rescue the cells.

In conclusion, this chapter showed that topoisomerase inhibitors, as well as other p53-inducing agents, are able to induce increased Zebra expression in EBV-positive gastric cancer cell lines in combination with HDACi treatment. While p53 expression is necessary but not sufficient for the successful induction of Zebra expression, no binding site for p53 on Zp is known. The role of Sp1, the suggested mediator of p53's influence on Zp, could not be fully resolved as both transcription factors influenced the expression of Zebra as well as of each other. Thus, the identified interaction of p53 with Ea-D and mDBP could help to further explain the importance of the presence of p53 for lytic cycle expression. For this, it would be crucial to validate those proteins as binding partners and further elucidate the importance of this interaction for the progression of the lytic cycle.

Chapter 6: Different patterns of viral lytic gene expression upon drug treatment

6.1 Introduction

The results described in Chapter 5 identified topoisomerase inhibitors as efficient inducers of Zebra expression in combination with chidamide. This stands in contrast to previous studies, which suggest that treatment with topoisomerase inhibitors impairs the lytic cycle expression of EBV as well as lytic viral DNA replication (Kawanishi, 1993b; Wang *et al.*, 2009; Wu *et al.*, 2014). Those discrepancies could be explained by differences in the experimental set-up, such as the analysed viral transcripts and the fact that topoisomerase inhibitors were combined with chidamide in our study. To better understand lytic cycle induction through topoisomerase inhibitor treatment, in this chapter, viral lytic cycle gene expression in chidamide- and topoisomerase inhibitor-treated cells was examined. This will enable us to understand how topoisomerase inhibitors in combination with chidamide influence the viral lytic cycle in EBVaGC cells.

6.2 Results

6.2.1 Combination of chidamide with epirubicin treatment induces abortive lytic cycle expression

To analyse the potential differences in lytic cycle progression between samples treated with chidamide with epirubicin and chidamide with Nutlin-3a, the RNA levels of a panel of EBV lytic genes were examined by qPCR in YCCEL1 cells (Figure 49). This experiment was performed for three different treatment times (24, 48 and 72 h), to exclude the possibility that observed differences in lytic cycle progression were an artefact of a chosen time point.

Epirubicin or Nutlin-3a treatment in combination with chidamide induced upregulation of the EBV IE genes *BRLF1* and *BZLF1* (Figure 49). In particular, we observed up to ~400-fold and ~140-fold increased levels of *BRLF1* when cells were treated with epirubicin with chidamide or Nutlin-3a with chidamide, respectively (Figure 49, middle panel). Single treatment with any of the tested compounds did not induce any significant change in the expression of EBV IE genes.

Chidamide and Nutlin-3a treatment induced high expression of all three examined E genes (*BGLF5*, *BMRF1* and *BHLF1*), while most single treatments did not induce more than 10-fold induction (Figure 49, middle panel). The combination of chidamide with epirubicin induced expression of *BMRF1* (330–750-fold), with 48 h showing the highest expression levels. Expression levels of *BGLF5* and *BHLF1* were significantly lower in those samples and reached their highest values after 72 h of treatment (9–47-fold; Figure 49, bottom panel).

BcLF1 and *BLLF1* gene expression was examined as examples of L gene expression. Nutlin-3a treatment promoted a mild but consistent upregulation of *BcLF1* (~32-fold) and *BLLF1* (~16-fold) after 72 h of treatment (Figure 49, bottom panel). The other single treatment conditions did not induce any significant expression of those transcripts. *BLLF1* expression was induced in samples treated with

chidamide with epirubicin and chidamide with Nutlin-3a (75–125-fold; Figure 49, bottom panel). In contrast, *BcLF1* was only significantly expressed in chidamide- and Nutlin-3a-treated samples (~155-fold; Figure 49, middle panel).

In summary, the results of the qPCR analysis showed that the pattern of viral lytic gene expression was consistent throughout the three examined time points and that only the levels of the transcripts varied. The lytic gene expression observed in samples treated with only one of the compounds was generally negligible. While chidamide- and Nutlin-3a-treated samples showed expression of all examined transcripts, chidamide- and epirubicin-treated samples expressed high levels of IE genes, but only specific E and L genes were expressed.

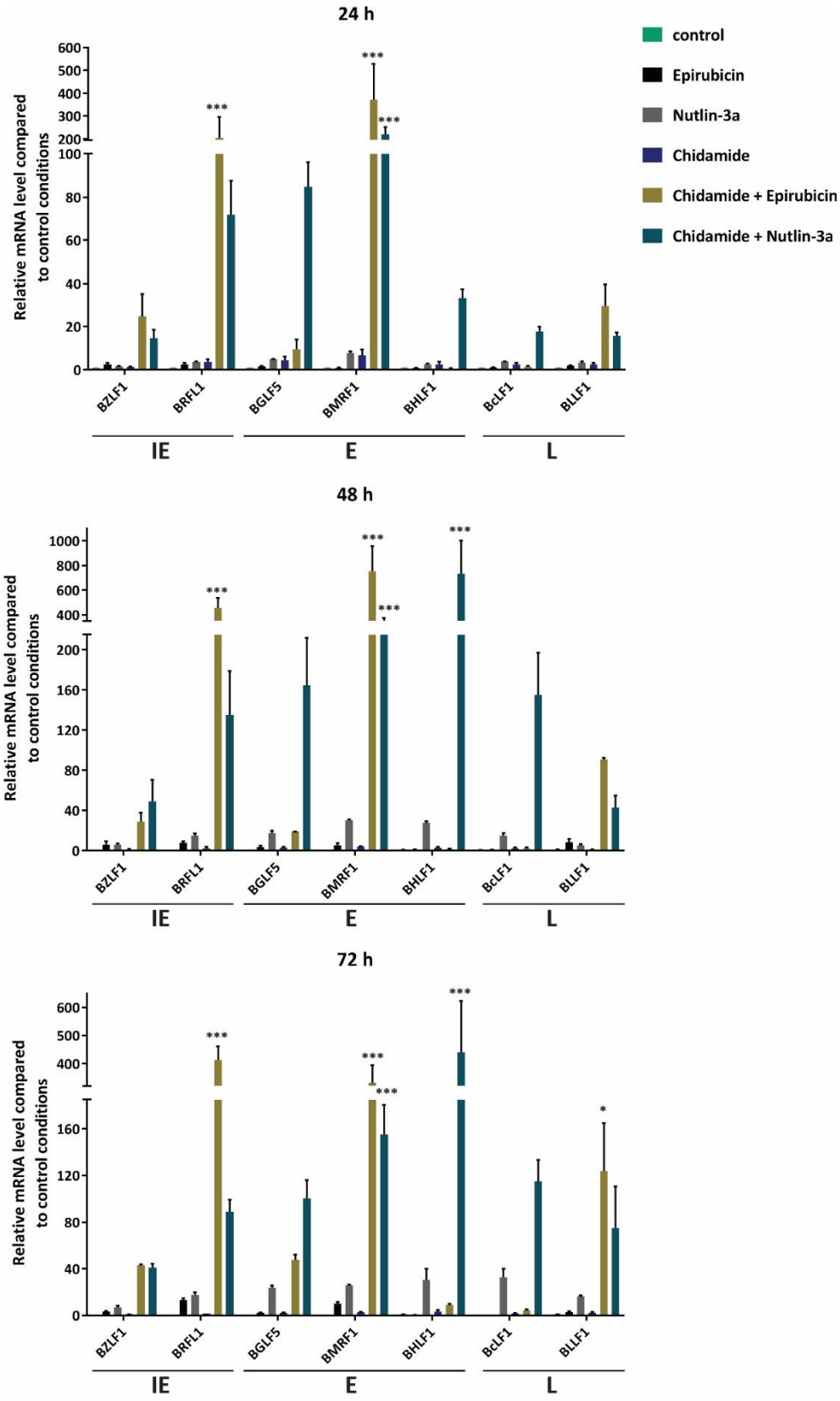


Figure 49: EBV lytic gene expression upon different combinatorial treatments with chidamide assessed by qPCR. Cells were treated for 24, 48 or 72 h with 2.5 µM chidamide, 2.5 µM Nutlin-3a, 1 µM epirubicin or a combination of those compounds. DMSO treatment was used as a control. Lytic gene

expression was evaluated by qPCR. The results represent $\Delta\Delta C_t$-values normalised to GAPDH levels within the same samples as well as the control samples for the same primer. Bars represent the average of three independent replicates of this experiment. n = 3, error bars ± SEM. $P^* \leq 0.05$; $P^{**} \leq 0.01$; $P^{***} \leq 0.005$. Significance was calculated using Dunnett's multiple comparison test relative to DMSO controls. DMSO – dimethyl sulfoxide; E – early genes; GAPDH – glyceraldehyde 3-phosphate dehydrogenase; IE – Immediate early genes; L – late genes; qPCR – quantitative polymerase chain reaction.

To examine whether the difference in E gene expression observed at the RNA level also reflected the differences at the protein level, Ea-D gene expression was analysed in a panel of different treatments (Figure 50). While none of the chemotherapeutic agents or chidamide alone induced Zebra expression, Zebra expression was observed for all compounds in combination with chidamide except 5-FU. The pattern of Ea-D expression mirrored the one described for Zebra. Ea-D antibodies have been shown to recognise two or three bands between 49–55 kDa based on the phosphorylation status of the Ea-D protein (Daibata & Sairenji, 1993; Tsurumi, 1993). Notably, two bands were observed for Ea-D and most samples showed similar strengths of both bands. However, cisplatin- and chidamide-treated samples showed a stronger upper than lower band for Ea-D.

These data showed that while both Zebra and Ea-D are expressed at the protein level in different treatment conditions, the RNA expression of lytic cycle genes differs between treatments. Chidamide and Nutlin-3a treatment induced the expression of all examined IE, E and L lytic cycle genes, while chidamide and epirubicin treatment only induced the expression of a subset of genes.

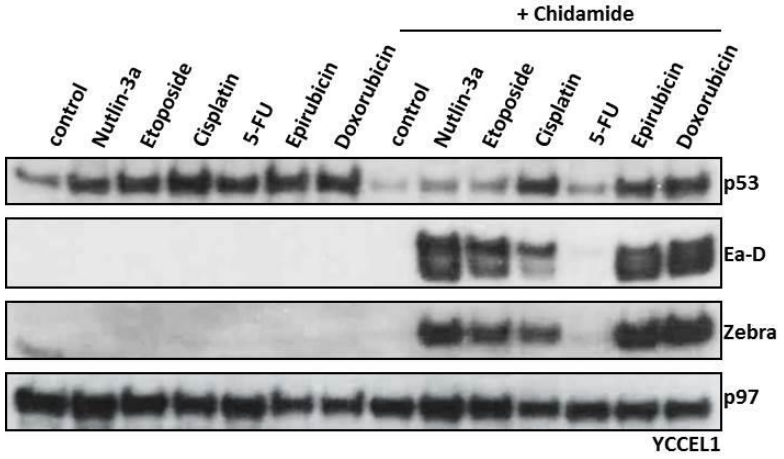


Figure 50: Zebra and Ea-D expression induced by chemotherapeutic treatment in combination with chidamide. Cells were treated for 48 h with either DMSO or 2.5 µM chidamide in combination with 2.5 µM Nutlin-3a, 1 µM epirubicin, 25 µM cisplatin, 1 µM 5-FU, 10 µM etoposide or 1 µM doxorubicin. Cellular expression was subsequently analysed by western blot. Results are representative of three independent repeats of this experiment. 5-FU – 5-fluorouracil; DMSO – dimethyl sulfoxide; Ea-D – early antigen diffuse component

6.2.2 Effects of topoisomerase inhibitors on viral DNA replication

To examine the influence of topoisomerase inhibitor treatment on viral lytic DNA replication, EBV copy number per cell was measured after compound treatment (Figure 51). For quantification of the EBV copy number per cell, qPCR was performed on cellular DNA with a probe for the cellular genome, beta-2-microglobulin, and one for the viral genome, BALF5. As previously reported, normalisation was conducted using a standard curve from Namalwa cells, a cell line that contains two integrated EBV copies per cell, and the ratio of EBV genomes to cellular genomes calculated (Hui & Chiang, 2010).

No significant differences in the EBV copy number were observed in single treatment with DMSO, Nutlin-3a, chidamide or epirubicin, nor for double treatment with chidamide and epirubicin. In contrast, chidamide- and Nutlin-3a-treated samples showed a ~25-fold increase in the EBV copy number per cell compared to control cells, leading to the highest EBV copy number measured in all samples.

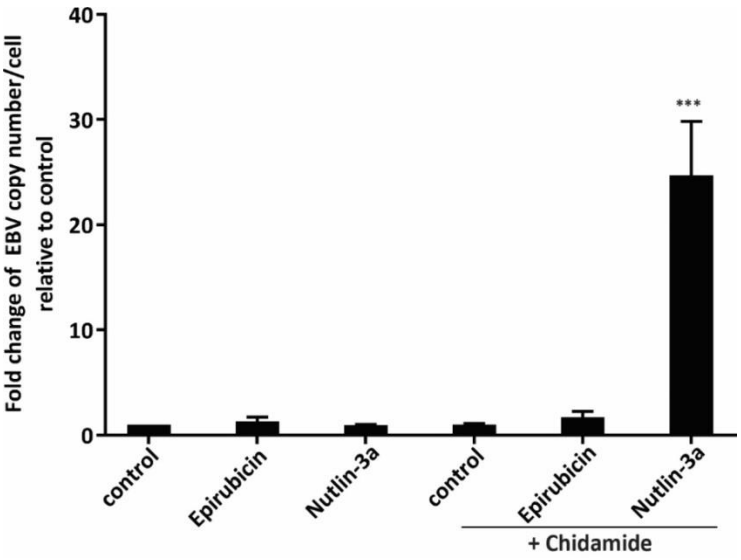


Figure 51: Examination of viral DNA amplification upon treatment with epirubicin and Nutlin-3a alone or in combination with chidamide. Cells were treated for 48 h with either 1 µM epirubicin or 2.5 µM Nutlin-3a alone or in combination with 2.5 µM chidamide before DNA isolation. DNA was used for qPCR using a probe for the cellular b2m gene as well as the viral BGLF5 gene, which allowed the calculation of EBV load per cell. The EBV load was normalised to the EBV load contained in Namalwa control cells. Bars represent the average of three independently performed experiments. *n* = 3, error bars ± SEM. *P** ≤ 0.05; *P*** ≤ 0.01; *P**** ≤ 0.005. Significance was calculated using Dunnett's multiple comparison test relative to control cells. b2m – beta-2-microglobin; EBV – Epstein-Barr virus; qPCR – quantitative PCR.

To examine whether the observed difference between epirubicin- and Nutlin-3a-treated samples was specific to epirubicin or shared by all topoisomerase inhibitors, viral DNA copy numbers were compared for a broader spectrum of topoisomerase inhibitors (Figure 52). Compared to DMSO-treated samples, the addition of chidamide, epirubicin or both compounds together did not induce a significant increase in the EBV copy number. The other four topoisomerase inhibitors (doxorubicin, mitoxantrone, amonafide and teniposide) induced an increase of the EBV copy number from 2.5–4-fold when treated alone and 7–11-fold when treated together with chidamide. Nutlin-3a treatment, which was included as a control, induced only a minimal increase in the EBV copy number (~1.5-fold), but with chidamide it increased the EBV copy number significantly (~30-fold).

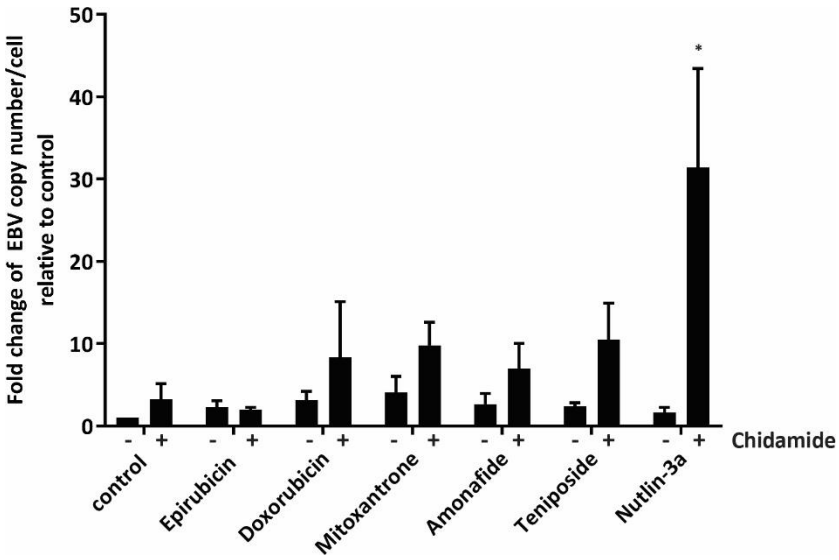


Figure 52: Examination of viral DNA amplification upon treatment with different topoisomerase inhibitors and Nutlin-3a alone or in combination with chidamide. YCCEL1 cells were treated for 48 h with either DMSO or 2.5 µM chidamide in combination with the stated topoisomerase inhibitors (for concentrations see Table 9) or 2.5 µM Nutlin-3a. DNA was used for qPCR using a probe for the cellular b2m gene as well as the viral BGLF5 gene, which allowed calculation of EBV load per cell. The EBV load was normalised to the EBV load contained in Namalwa control cells. Bars represent the average of three independently performed experiments. n = 3, error bars ± SEM. $P^* \leq 0.05$; $P^{**} \leq 0.01$; $P^{***} \leq 0.005$. Significance was calculated using Dunnett's multiple comparison test relative to control cells. b2m – beta-2-microglobin; DMSO – dimethyl sulfoxide; EBV – Epstein-Barr virus; qPCR – quantitative polymerase chain reaction.

Overall, this experiment showed that topoisomerase inhibitors can be classified in two groups based on their viral replication levels with chidamide. Compounds such as epirubicin or doxorubicin only induced minimal viral replication when treated alone, and this was not significantly changed through the addition of chidamide. On the other hand, compounds such as amonafide and teniposide induced low levels of viral replication via single treatment, but through the addition of chidamide reached less than half the level of viral DNA replication observed in chidamide- and Nutlin-3a-treated samples. Notably, no combination of chidamide and topoisomerase inhibitors was able to induce viral DNA replication to the same level as chidamide and Nutlin-3a treatment.

6.2.3 Epirubicin and chidamide treatment together increases the occurrence of modified Zebra

Zebra has been reported to carry different PTMs, such as phosphorylation or sumoylation (El-Guindy & Miller, 2004; El-Guindy, *et al.*, 2006; Hagemeier *et al.*, 2010; Murata *et al.,* 2010). Those modifications have been shown to interfere with the ability of Zebra to act as a transcriptional activator (El-Guindy & Miller, 2004; Hagemeier *et al.,* 2010; Murata *et al.,* 2010). Sumoylated Zebra has been suggested to preferentially bind to HDACs and thereby regulate the transcriptional activity of Zebra (Murata *et al.,* 2010). Therefore, the potential sumoylation of Zebra was examined to better understand the differences between lytic cycle induction upon drug treatment.

Small ubiquitin-like modifier (SUMO), which is covalently placed onto lysine residues of target proteins, is an 11-kDa protein that is related to ubiquitin (reviewed in Park-Sarge & Sarge, 2008). Through the addition of SUMO to the target protein, the size at which the protein migrates on a protein gel differs from the unmodified protein. Based on the size of the Zebra protein, unmodified Zebra is expected to migrate at ~35 kDa, while sumoylated Zebra is expected to migrate at a higher molecular weight based on the number of SUMO molecules added to the protein. Therefore, western blot analysis of Zebra expression was performed for different treatments in YCCEL1 cells, with particular focus on potential shifts in the migration pattern.

As described in Chapter 5.2.1, all tested topoisomerase inhibitors and Nutlin-3a induced Zebra expression in combination with chidamide (Figure 53). Without chidamide treatment, no significant Zebra expression was detected. Epirubicin and doxorubicin treatment together with chidamide showed a strong band at ~46 kDa, in addition to the unmodified Zebra band observed at ~32 kDa (Figure 53, lanes 4 and 6). In addition, another weaker band was observed at ~58 kDa. Chidamide treatment with mitoxantrone, amonafide, teniposide and Nutlin-3a showed strong expression of unmodified Zebra

at ~32 kDa, but only a weak band at ~46 kDa. None of those treatments showed expression of the band at ~58 kDa.

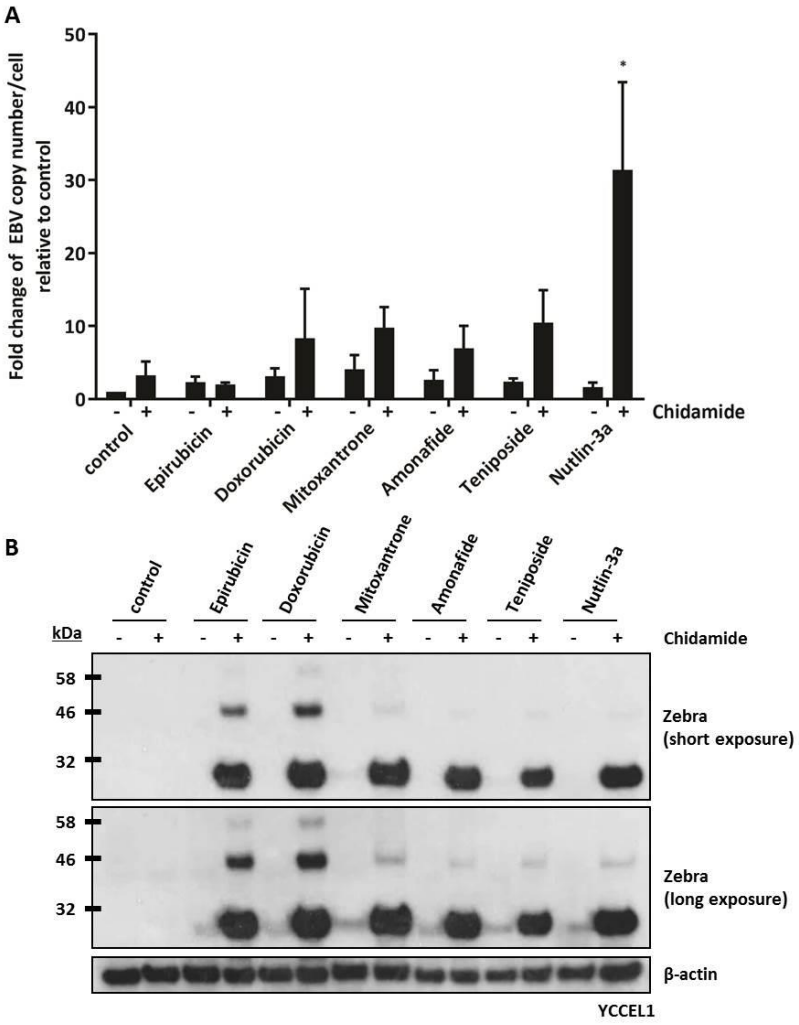


Figure 53: Modifications of Zebra detected by western blot in YCCEL1 cells treated with topoisomerase inhibitors in combination with chidamide. YCCEL1 cells were treated for 48 h with either DMSO or 2.5 µM chidamide in combination with the stated topoisomerase inhibitors (for concentrations see Table 9) and 2.5 µM Nutlin-3a. A) Figure 52 was duplicated to underline the potential correlation between DNA replication and Zebra modifications. DNA was used for qPCR using a probe for the cellular b2m gene as well as the viral BGLF5 gene, which allowed calculation of the EBV load per cell. The EBV load was normalised to the EBV load contained in Namalwa control cells. Bars represent the average of three independently performed experiments. *n* = 3, error bars ± SEM. *P** ≤ 0.05; *P*** ≤ 0.01; *P**** ≤ 0.005. Significance was calculated using Dunnett's multiple comparison test relative to control cells. B) Cellular expression was analysed by western blot. Results are representative of three independent repeats of this experiment. b2m – beta-2-microglobin; DMSO – dimethyl sulfoxide; EBV – Epstein-Barr virus; qPCR – quantitative polymerase chain reaction.

To see whether the additional band observed at ~46 kDa for certain topoisomerase inhibitor treatments together with chidamide could also be observed for other compound combinations, the migration pattern of Zebra was compared for chemotherapeutic agent treatment with different HDACis in YCCEL1 cells (Figure 54). While none of the chemotherapeutic agents or HDACis induced Zebra expression when treated alone, any HDACi in combination with epirubicin, doxorubicin, Nutlin-3a or cisplatin induced Zebra expression at ~32 kDa at different levels. An additional band at ~46 kDa was only observed for samples treated with epirubicin or doxorubicin in combination with an HDACi (Figure 54). Interestingly, those were also the samples that consistently showed the strongest Zebra band at ~32 kDa.

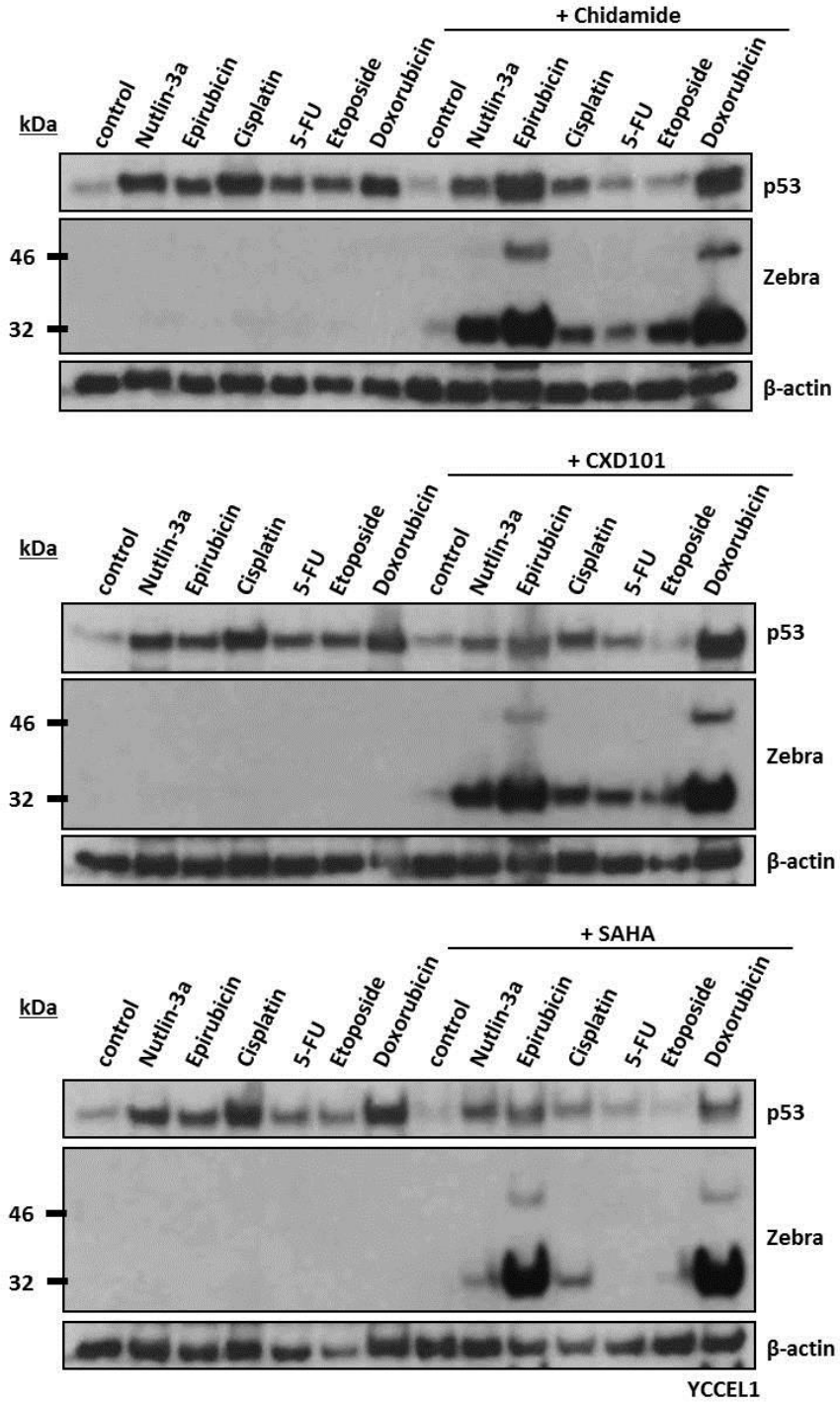


Figure 54: Modifications of Zebra detected by western blot in YCCEL1 cells treated with chemotherapeutic agents in combination with different HDACis. Cells were treated for 48 h with either DMSO, 2.5 µM chidamide, 1 µM CXD101 or 2.5 µM SAHA in combination with 2.5 µM Nutlin-3a, 1 µM epirubicin, 25 µM cisplatin, 1 µM 5-FU, 10 µM etoposide or 1 µM doxorubicin. Subsequently cellular expression was analysed by western blot. Results are representative of three independent repeats of this experiment. 5-FU – 5-fluorouracil; DMSO – dimethyl sulfoxide; SAHA – suberoylanilide hydroxamic acid.

It has been suggested that the occurrence of sumoylated Zebra increases throughout lytic cycle progression (Murata *et al.*, 2010). Thus, Zebra expression and potential modifications were examined after 24, 48 or 72 h of treatment in YCCEL1 cells (Figure 55). Strong Zebra expression was detected for all analysed time points in epirubicin- or Nutlin-3a-treated samples in combination with chidamide. While the occurrence and strength of the bands at ~46 and ~58 kDa differed over time for epirubicin with chidamide-treated samples, only the band ~32 kDa was detected in chidamide- and Nutlin-3a-treated samples. In epirubicin and chidamide-treated samples, the Zebra band at ~46 kDa increased in strength from 24 to 72 h of treatment. The band at ~58 kDa was only detected for longer treatment periods, in this case 72 h.

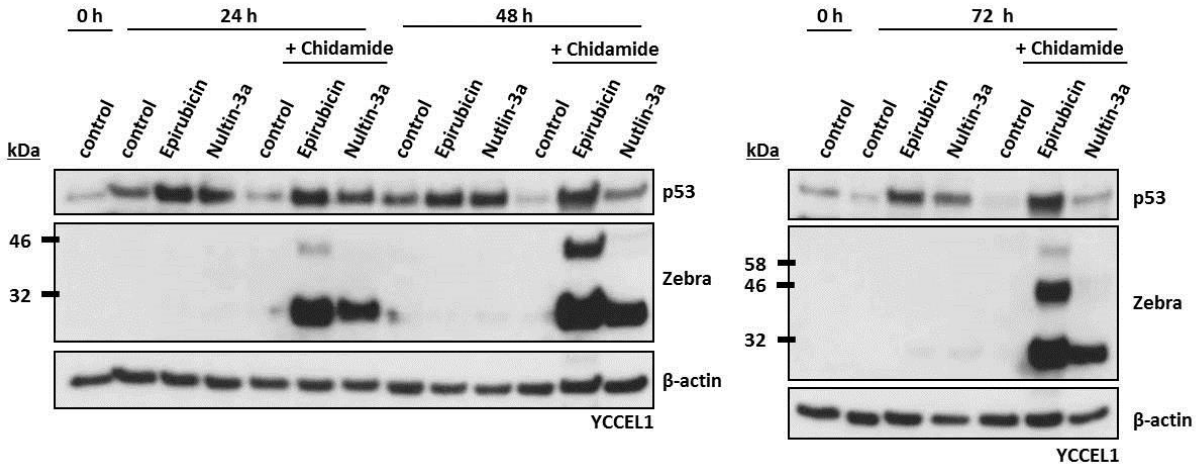


Figure 55: Time course of the occurrence of Zebra modifications by western blot in YCCEL1 cells treated with epirubicin or Nutlin-3a in combination with chidamide. YCCEL1 cells were treated with either 2.5 µM Nutlin-3a or 1 µM epirubicin in combination with DMSO or 2.5 µM chidamide. Cells were collected after the indicated treatment time and cellular expression was analysed by western blot. Results are representative of two independent repeats of this experiment. DMSO – dimethyl sulfoxide.

Together, this showed that the occurrence of potentially sumoylated Zebra does not solely depend on lytic cycle progression, but rather seems to only occur for specific treatments, in this case chidamide and epirubicin treatment.

6.3 Summary and brief discussion

The aim of this chapter was to examine the details of the observed lytic cycle induction by topoisomerase inhibitor treatment in combination with chidamide. Differences in lytic viral replication have been observed between chidamide with Nutlin-3a- and chidamide with topoisomerase inhibitor-treated YCCEL1 cells. While treatment with chidamide and Nutlin-3a induced a strong increase in the viral copy number per cell, the combination of chidamide with topoisomerase inhibitors induced less viral replication. Nevertheless, some diversity was observed between the levels of viral replication upon topoisomerase inhibitor treatment. Epirubicin and doxorubicin induced only minimal viral replication, while mitoxantrone, amonafide and teniposide induced intermediate levels of viral replication, reaching less than half the levels of chidamide and Nutlin-3a-treated cells. The differences in viral DNA replication translated to differences in lytic gene expression. While all samples expressed *BZLF1* at the RNA and protein levels, only chidamide- and Nutlin-3a-treated samples induced expression of all examined lytic cycle genes. In contrast, chidamide and epirubicin samples expressed high levels of *BRLF1, BMRF1* and *BLLF1*, but not *BHLF1* and *BcLF1*. To understand those different patterns of lytic cycle expression, Zebra modifications in different treatments have been examined, more specifically potential sumoylation. In doxorubicin- and epirubicin-treated samples together with different HDACis strong additional Zebra bands at ~46 kDa, and to a lesser degree at ~58 kDa. The topoisomerase inhibitors mitoxantrone, amonafide, teniposide and Nutlin-3a together with chidamide only showed weak bands for the Zebra band detected at ~46 kDa and no ~58 kDa band. While this effect was independent from the time of treatment, the ~58 kDa band appeared only for longer times of treatment.

Different studies have identified topoisomerase inhibitors as agents that inhibit the DNA replication of EBV as well as lytic EBV transcription (Wang *et al.*, 2009; Wu *et al.*, 2014). The same effect was not observed for the combination of chidamide with topoisomerase inhibitor treatment. While all

topoisomerase inhibitor treatments with chidamide showed reduced lytic DNA replication compared to chidamide and Nutlin-3a treatment, overall induction of viral gene expression and lytic DNA replication was observed in comparison to control cells (Chapters 6.2.1 and 6.2.2). In addition, these data suggest that the effect on lytic DNA replication differs between different topoisomerase inhibitor treatments. While epirubicin and doxorubicin treatment in combination with chidamide induced nearly no viral DNA replication, other topoisomerase inhibitors such as amonafide and mitoxantrone still significantly increased viral copy numbers in combination with chidamide. The differences between topoisomerase inhibitors and their effect on lytic DNA replication could be explained by differences in the chemical structures of those compounds. While epirubicin and doxorubicin belong to the group of anthracyclines, teniposide is a podophyllotoxin derivate and amonafide is a napthalimide (Clark, 1992; Kaklamani & Gradishar, 2003; Zhu *et al.,* 2007). Interestingly, while mitoxantrone is an anthracycline derivate, it has been shown to have a different mechanism of action than other anthracyclines, including being less toxic (Wadler *et al.*, 1986). Therefore, a more detailed structural comparison of a larger panel of topoisomerase inhibitors and analysis of their effect on lytic viral replication might be able to identify the necessary structure for the inhibition of lytic replication.

While strong Zebra and Ea-D protein expression was observed for the combination of topoisomerase inhibitors with chidamide, the profile of lytic RNA expression was less consistent (Figure 49). Neither *BHLF1* nor *BcLF1* were expressed by epirubicin and chidamide treatment, while high levels of those gene products were achieved in combination with Nutlin-3a. *BcLF1* is a late gene whose transcription depends on Zebra and Rta binding to its promoter (Serio *et al.*, 1997; Chang *et al.*, 1998; Chua *et al.*, 2007). The expression of *BcLF1* has been shown to drastically increase in the presence of lytic DNA replication (Djavadian *et al.*, 2016). Since chidamide- and epirubicin-treated samples showed significantly less lytic DNA replication than those subjected to chidamide and Nutlin-3a treatment, it is consistent with the literature that *BcLF1* levels were also significantly lower in those samples.

BHLF1 is an early gene that is transcribed from the oriLyt and whose transcription can be initiated by both Zebra and Rta (Schepers *et al.*, 1996; Zhang *et al.*, 1996). Reduced *BHLF1* transcription in epirubicin- and chidamide-treated samples can be explained with the reported reduction in viral lytic DNA replication upon topoisomerase inhibition (Kawanishi, 1993b). It has been shown that topoisomerase inhibitor treatment decreases the association of Zebra with the oriLyt (Wang *et al.,* 2009). By reducing Zebra binding to the oriLyt topoisomerase inhibitor treatment could potentially reduce *BHLF1* transcription.

The differences in lytic gene expression levels for genes such as *BHLF1* between chidamide and epirubicin-treated and chidamide and Nutlin-3a-treated samples were in contrast to the high levels of Zebra and Rta expression that have been observed in both samples (Figure 49). One potential explanation for this discrepancy is that while these regulators of the lytic cycle are expressed, their activity might be altered by PTMs such as sumoylation and phosphorylation. Examination of Zebra PTMs was prioritised as they have been shown to modify the transactivation potential of Zebra as well as the binding of Zebra to HDACs, and might thus play a role in the synergistic effects observed with HDACi treatment (Adamson, 2005; Murata *et al.,* 2010). While Rta has also been shown to be sumoylated, this was not further examined since no change in Rta transactivation has been observed for sumoylated Rta, and it was therefore assumed that the observed differences in lytic gene expression are less likely to be caused by Rta modifications (Chang *et al.,* 2004; Adamson, 2005).

In epirubicin and doxorubicin samples with chidamide, a shift in Zebra protein migration was detected from ~32 to ~46 kDa and ~58 kDa (Figure 54). Based on its size, sumoylation is expected to shift the migration of a protein of a protein by ~11 kDa. This suggests that the additional bands detected in chidamide- and epirubicin-treated samples could indeed be sumoylated Zebra, which would be further supported by the migration patterns observed in previous studies (Adamson, 2005). In order to conclusively prove this hypothesis, further experiments would be necessary, which could include the

immunoprecipitation of Zebra and detection of sumoylation as done by Murata and colleagues (Murata *et al.,* 2010), or the inhibition of sumoylation through drug treatments and targeted knockdown.

In addition, the patterns of lytic cycle expression observed for chidamide and epirubicin treatment match the one expected for sumoylated Zebra based on the literature. While sumoylation of Zebra has been shown to reduce binding of Zebra to the *BMRF1* promoter and thus abrogate transcription, the addition of Rta has been shown to abolish this effect and allow effective *BMRF1* transcription (Adamson, 2005; Murata *et al.,* 2010). Therefore, the expression of *BMRF1* at the RNA and protein levels does not contradict the possibility of sumoylated Zebra, since high BRLF1 RNA expression was detected simultaneously. *BLLF1* is an L lytic gene whose expression is regulated by Rta alone and not by Zebra (El-Guindy & Miller, 2004). Therefore, the high expression levels of *BLLF1* RNA in chidamide- and epirubicin-treated samples are consistent with the high Rta levels in those samples.

A recent study has identified EBV-encoded SUMO-modifying proteins (De La Cruz-Herrera *et al.*, 2018). This showed that Rta induces the overall loss of SUMOylated proteins, in a proteasome-dependent manner, and that SM, the gene product of *BMLF1*, has E3 SUMO ligase activity. While the RNA expression levels of Rta were high for both chidamide with epirubicin and chidamide with Nutlin-3a treatment (Figure 49), the expression levels of SM have not been examined. Therefore, examination of SM expression levels in different treatment conditions as well as its potential implications for Zebra sumoylation should be performed in the future.

Notably, only a small percentage of the detected Zebra seems to be modified, but differences in viral lytic gene expression were observed nonetheless (Chapters 6.2.1 and 6.2.3). This is in accordance with a previous study that showed that sumoylated Zebra has a dominant negative effect on the transactivation abilities of unmodified Zebra (Murata *et al.*, 2010). Therefore, a small proportion of sumoylated Zebra is sufficient to modify the transactivation properties of unmodified Zebra.

Murata and colleagues suggested that sumoylation of Zebra occurs mainly to control Zebra's function during the lytic cycle, and thus only occurs at later time points during the lytic cycle (Murata *et al.,* 2010). The time course experiment performed in Chapter 6.2.3 showed that while sumoylation increases during the time of treatment with chidamide and epirubicin, and leads to the addition of an additional band at ~58 kDa, it does not induce sumoylation in chidamide and Nutlin-3a samples (Figure 55). This suggests that rather than being a conserved mechanism to control Zebra's functions, Zebra sumoylation is specific to treatment conditions. Therefore, it would be interesting to further examine how the combination of topoisomerase inhibitor treatment with chidamide could be involved in Zebra sumoylation.

In summary, this chapter showed that certain topoisomerase inhibitors such as epirubicin inhibit lytic DNA replication, while others such as amonafide induce it in combination with chidamide. Interestingly, a link between epirubicin and doxorubicin treatment and PTMs of Zebra has been suggested, which seems to be important for the altered lytic cycle expression in those samples. Further analysis is needed to prove that the observed shift in protein migration is caused by sumoylation and to show how topoisomerase inhibition may potentially result in the sumoylation of Zebra. Additionally, the same phenomenon needs to be examined in a larger panel of cell lines, as all experiments in Chapter 6.2 were performed in YCCEL1 cells.

Chapter 7: Final discussion and perspectives

7.1 Overview

The aim of this research project was to identify compounds for efficient lytic induction therapy for EBVaGC and use them as a tool to determine important molecules and pathways for EBV reactivation.

HDACis were identified as potent inducers of Zebra expression in a comparison of the reactivation potential of epigenetic inhibitors (Figure 16). It was further shown that benzamide-based HDACis were more potent in inducing this effect than hydroxamate-based HDACis (Figure 19). Benzamide-based HDACis were shown to be efficient in inducing targeted cell killing in combination with antiviral compounds, making them a good candidate for potential lytic induction therapy. Simultaneously, benzamide HDACis did not impair HLA class I expression and T-cell recognition of reactivated epithelial cells, suggesting that the immune system would be able to assist targeted cell killing *in vivo*.

In an attempt to identify drug combinations that are able to synergise with chidamide in the induction of Zebra expression, a high-throughput screen identified topoisomerase inhibitors as a class of compounds with potential synergistic effects on Zebra expression together with chidamide (Figure 34). Together with an identified synergy with chemotherapeutic agents, this showed that induction of p53 was able to induce higher Zebra expression levels. In addition, knockdown of p53 abolished all Zebra expression (Figure 42 and Figure 43), underlining the importance of p53 for Zebra expression. The literature suggests that the effect of p53 on Zebra expression is mediated by the ubiquitous transcription factor Sp1 (Chua *et al.*, 2012). Due to the effect of Sp1 on Zebra and p53 expression levels, it was not possible to infer the importance of Sp1 on the p53-mediated effect on Zebra expression. In an attempt to characterise additional p53 binding partners that could be involved in its synergistic effect on Zebra expression, the E proteins Ea-D and mDBP were identified as a potential novel binding partners, and thereby additional players in p53-dependent lytic cycle regulation (Figure 47).

The combinations of chidamide with epirubicin and chidamide with Nutlin-3a treatment have been shown to result in high levels of Zebra expression, but surprisingly the expression levels of other lytic cycle genes varied drastically between those treatments (Figure 49). Those differences could be linked to potential PTMs of Zebra influencing Zebra's transactivation abilities. Differences in viral lytic DNA replication could be explained by the inhibition of topoisomerases that play an important role in viral lytic DNA replication by epirubicin treatment. Additional differences between those two treatment combinations were observed in the cell killing abilities. In contrast to chidamide and Nutlin-3a treatment, which induced stronger cell death in EBV-positive cells, epirubicin led to cell death independently of the EBV-status of the cell line (Figure 48).

The findings in this study showed that HDACis either alone or in combination with p53-inducing agents are efficient in inducing viral Zebra expression. The positive effect of compound treatment on the immune response towards reactivated cells, as well as the identified effect on cancer cell killing, provide useful insights for the potential translation of those compounds into the clinic.

7.2 Role of class I HDACs and histone acetylation in EBV reactivation

The identification of HDACis as the most potent group of EBV lytic induction agents is in accordance with the literature, which describes the reactivation potential of various HDACis in different cellular backgrounds (Luka *et al.*, 1979; Countryman *et al.*, 2008; Hui & Chiang, 2010; Wildeman *et al.*, 2012; Hui *et al.*, 2016). Nevertheless, this was the first study identifying the reactivation potential of benzamide HDACis through a large-scale comparison of HDACis in EBV-positive epithelial cells.

Benzamide-based HDACis have been shown to specifically inhibit class I HDACs (Falkenberg & Johnstone, 2014). This is in agreement with a previous study that suggested that inhibition of class I HDACs was sufficient to induce lytic cycle expression in EBV-positive epithelial cells

(Hui *et al.,* 2016). This was underlined by the expression of Zebra following the knockdown of HDAC1, 2 or 3. Since a reduction in the protein levels of those HDACs was linked to Zebra expression, the potential degradation of those HDACs upon HDACi treatment was examined in different EBVaGC cell lines. The results in Chapter 3.2 suggest that the differences between HDACis are not caused by the degradation of HDAC1, 2 or 3. However, this does not exclude the possibility that the difference between HDACi treatments is caused by differential inhibition of HDAC activity. In order to assess this possibility, the HDAC activity in treated cells should be examined with an HDAC activity assay. This could help to decipher which HDAC is the most important target for lytic cycle induction.

To further examine the importance of different HDACs for the maintenance of viral latency and subsequent reactivation, the knockdown experiment performed by Hui and colleagues in *in vitro*-infected NPC cells should be repeated in a broader set of cell lines (Hui *et al.,* 2016). As observed in Chapter 4.2, *in vitro*-infected cell lines seem to be more easily reactivated than *in vivo*-infected cell lines. Therefore, the repetition of this experiment in *in vivo*-infected cell lines would be important to clarify the importance of those HDACs for reactivation.

While global histone H3 acetylation did not differ between treatment with hydroxamate and benzamide HDACis, and was therefore less likely to be the cause of differential Zebra expression, it cannot be excluded that specific histone marks were differently altered through HDACi treatment. Therefore, it would be necessary to specifically examine the pattern of histone modifications in treated cells by MS of histone proteins. Another possibility is that even though specific modifications do not change globally, they do so specifically at EBV lytic promoters. A chromatin immunoprecipitation-PCR experiment specifically focussing on different histone modifications at those promoters would be able to examine this possibility.

As an alternative, the effect of HDACis could be independent of histone acetylation and instead be caused by non-histone acetylation, which occurs at high levels upon HDACi treatment (reviewed in

Ocker, 2010). Thus, reducing the potential effect of HDACi treatment on histone acetylation might not be sufficient to fully explain their role in EBV reactivation. Immunoprecipitation with subsequent detection of acetylated lysine residues would help to examine the protein acetylation of certain proteins of interest.

Overall, HDACi treatment induces complex epigenetic and transcriptional changes, which complicates the clear identification of their critical target for EBV reactivation. Therefore, more in-depth work on histone modification and potential off-target effects would be necessary to elucidate their effect on EBV reactivation. Nevertheless, this study provides the most comprehensive comparison of HDACi efficacy in EBV-positive epithelial cancers for potential lytic induction therapy to date.

7.3 Mechanisms of drug-induced reactivation

7.3.1 The involvement of p53 in Zebra induction

The identified link between the levels of p53 and the Zebra expression levels induced through different compound treatments suggested an important role of p53 levels in the regulation of Zebra expression. However, the potential effect of p53 on Zebra expression seems to be more complex than suggested by the current literature. The Zp promoter does not contain a canonical p53 binding site, though it has been suggested that the effect of p53 on Zebra expression is mediated through binding to Sp1, which in turn binds to Zp (Chua *et al.,* 2012). While the results in Chapter 5.2.5 support this model, they further indicate that Sp1 and p53 influence each other's expression. This complicates the separate examination of the importance of those two transcription factors for Zebra expression. Nevertheless, 5-FU-treated samples, which show increased p53 levels but no reactivation in combination with chidamide, suggest that activation of p53 is not sufficient to induce Zebra expression. This indicates that potential PTMs of

p53 or the expression of certain p53 downstream targets might be crucial for the p53-mediated effect on lytic cycle expression.

As many as 50 individual PTMs including phosphorylation and acetylation have been shown on the p53 protein (Meek & Anderson, 2009). Since HDACis do not just induce histone acetylation but also protein acetylation, it is possible that the addition of low levels of chidamide induce the acetylation of p53 at key residues. p53 contains several acetylation sites, but specifically lysines 381 and 382 have been shown to be acetylated upon HDACi treatment and to restore its induction of p21 gene expression in different cancer settings (Zhao *et al.,* 2006; Condorelli *et al.*, 2008). Additionally, different chemotherapeutic agents have been shown to induce the phosphorylation of p53. Phosphorylation at serine 46, which can be induced by high levels of chemotherapeutic treatment, has been shown to influence the promoter selectivity of p53 (Mayo *et al.,* 2005). By modifying the protein binding abilities and thus expression of p53 downstream targets, PTMs could help to induce the necessary cellular environment for efficient viral reactivation. Examples of potential downstream pathways and their importance for lytic cycle progression will be discussed in more detail later in the chapter.

The treatment combinations identified in this study should be sufficient to enable the identification of p53 modifications that are necessary or sufficient to induce Zebra and full lytic cycle expression by either western blot or MS analysis.

7.3.2 Potential role of the cell cycle state in EBV reactivation

p53 regulates a diverse set of downstream targets that are important for the cellular response to processes such DNA damage, nutrient depletion and heat shock (Hunziker *et al.*, 2010). The expression of those genes affects the cell fate by influencing DNA repair, apoptosis, cell cycle progression and senescence. The potential role of p53 downstream targets for EBV lytic cycle induction could be further

examined by different unbiased methods such as siRNA screens or RNA sequencing. Ideally, RNA sequencing should be performed in a single-cell manner to allow the discrimination of non-reactivated cells from reactivated cells. Those experiments should indicate which set of p53 target genes are more likely to be responsible for lytic cycle induction, which could subsequently be examined in more detail.

Several studies have indicated the importance of the cell cycle, including p53 and its downstream target p21, for the reactivation of EBV in different cellular backgrounds.

In EBV-infected B-cells and keratinocytes, it has been shown that an S-phase-like environment is advantageous for the viral lytic replication of EBV (Mauser *et al.*, 2002; Kudoh *et al.*, 2003a). This is underlined by a knock-down of S-phase cyclin-dependent kinase activity, which abolishes lytic cycle expression. The S-phase-like environment during lytic replication of EBV is characterised by elevated cyclin E/A levels, the accumulation of hyperphosphorylated Rb protein and blocking of cellular DNA replication (Kudoh *et al.*, 2003b). In contrast, in EBV-positive epithelial cell lines, treatment with SAHA was suggested to induce lytic cycle expression predominantly in cells arrested in G2/M (Hui & Chiang, 2010). Interestingly, a comparison of different lytic cycle-inducing agents in a panel of cell lines has shown that while G1 growth arrest was observed in most systems before Zebra expression, this was not true for all lytic cycle-inducing agents (Rodriguez *et al.*, 2001). This suggests that the effect on the cell cycle and reactivation is specific to the treatment as well as the cell line used. Therefore, it would be important to assess the influence of the compounds used in the current study on the cell cycle state.

Different cell cycle stages could be examined by flow cytometry using propidium iodide DNA staining. In addition, the cell cycle state of the cell population before treatment could be synchronised and its influence on Zebra expression and viral replication analysed. To achieve cell synchronisation, cells could be either treated with thymidine, which inhibits DNA synthesis and leads to G1/S arrest, or a microtubule inhibitor such as nocodazole, which prevents mitosis and therefore induces G2/M arrest (Ma & Poon, 2011).

7.3.3 Potential role of the DNA damage response in EBV reactivation

The chemotherapeutic agents used in this study induce DNA damage, but they differ in the type of DNA damage as well as the repair pathways that they induce (Table 27). Since p53 has been shown to influence the cell's reaction to DNA-damaging agents (Zhang *et al.*, 2011), this has been examined in more detail. Topoisomerase inhibitors have been shown to induce DSBs, but the induced DNA repair pathways differ between topoisomerase I and II inhibitors (reviewed in Brown *et al.*, 2017). DNA DSBs induced by topoisomerase I inhibitors such as etoposide are mainly repaired by homologous recombination. This repair pathway functions only in the S- and G2-phases of the cell cycle using homologous chromatids. In contrast, DSBs induced by topoisomerase II inhibitors such as epirubicin are more commonly repaired by non-homologous end joining, which functions throughout the cell cycle and does not require the presence of a homologous counterpart. This suggests that the DNA damage response and cell cycle state might be linked through the induction of DNA damage and p53 downstream targets.

Table 27: Overview of different types of DNA damage and the DNA repair pathways they induce. Adapted from O'Connor, 2015 and Brown *et al.*, 2017. ATM – ataxia-telangiectasia mutated protein; ATR – ataxia-telangiectasia and Rad3-related protein; APE1 – Apurinic/apyrimidinic endonuclease 1; DNA-PK – DNA-dependent protein kinase; ERCC1 – Excision repair cross-complementation group 1; MLH1 – MutL homolog1; MSH – MutS protein homolog; MTH1 – MutT homologue 1; PARP – Poly (ADP-ribose) polymerase; Topo – topoisomerase; XP proteins – Xeroderma pigmentosum protein.

Type of damage	Repair targets	Repair pathway	Damaging agent(s)	Example(s)
Single-strand breaks	APE1 PARP	**B**ase **E**xcision **R**epair	Alkylating agents	Methyl methanesulfonate
Double-strand breaks	ATR ATM	**H**omologous **R**ecombination Repair	Topo I inhibitors Nucleoside analogue	Etoposide Irinotecan
	ATM DNA-PK	**N**on-**H**omologous **E**nd **J**oining	Topo II inhibitors	Doxorubicin Epirubicin
Bulky adducts	ERCC1 XP proteins	**N**ucleotide **E**xcision **R**epair and **T**rans**L**esion **S**ynthesis	UV light Platinum agents	Cisplatin Carboplatin
Mismatch	MLH1, MSH, MTH1	**M**is**M**atch **R**epair	Replication errors Alkylating agents	Hydroxyurea

The DNA damage response has also been implicated in viral lytic cycle progression. Induction of lytic EBV replication has been shown to trigger a strong DNA damage response mediated by ataxia-telangiectasia mutated protein (ATM), which localises at the viral replication compartment. ATM-mediated phosphorylation of p53 at serine 15 has been shown to induce binding of p53 to Zebra and its

localisation in the replication compartment (Kudoh *et al.,* 2005). While phosphorylated p53 was shown to be important for the early stages of the viral lytic cycle, it was degraded during later stages of lytic reactivation through a Zebra-directed ubiquitin ligase complex (Chang *et al.*, 2008; Sato *et al.*, 2009a, 2009b, 2010; Chua *et al.*, 2012). The degradation of p53 was suggested to promote an S-phase-like environment for more efficient viral replication.

Additionally, it has been shown that activation of ATM can be induced by Zebra expression independently of lytic DNA replication (Wang'Ondu *et al.*, 2015). The importance of ATM was further underlined by the loss of replication compartments through ATM inhibition or knockdown of ATM despite abundant expression of viral lytic proteins (Hau *et al.,* 2015). This suggests that inducing ATM might be important for efficient Zebra expression by topoisomerase inhibitor treatment.

In contrast to ATM, little is known about the role of ataxia-telangiectasia and Rad3-related protein or DNA-dependent protein kinase (DNA-PK) in lytic cycle induction of EBV. In KSHV-positive cells, DNA-PK has been identified as an oriLyt binding protein (Wang *et al.,* 2008). This suggests a potential role of DNA-PK in lytic DNA replication of KSHV, which might be shared by its close relative EBV.

Overall, the data presented in Chapter 5.2 suggest a model in which HDACi treatment and DNA-damaging agents such as topoisomerase inhibitors work together to induce efficient viral lytic DNA replication and lytic cycle progression (Figure 56). Treatment with DNA-damaging agents alone is not sufficient to induce Zebra expression, which suggests that DNA damage alone is not sufficient to open the viral chromatin at important lytic cycle promoters such as Zp. Chidamide on the other hand is able to open the chromatin of the cellular and viral genome, including at Zp. This induces the expression of low levels of Zebra, which has been shown to induce γH2AX as well as ATM activation, either directly or by inducing the expression of the E gene *BGLF4* (Tarakanova *et al.,* 2007). The treatment with DNA-damaging agents could synergise with chidamide treatment by inducing the host cell DNA damage response, thereby inducing further ATM activation (Ismail *et al.*, 2005). ATM is then able to increase the

ability of Zebra to induce its own expression, leading to an increase in the levels of Zebra expression and an acceleration of lytic cycle progression (Wang'Ondu *et al.,* 2015). EBV-PK, the gene product of BGLF4, phosphorylates minichromosome maintenance complex 4 as well as p27 and thereby helps to block chromosomal DNA replication while maintaining an S-phase-like environment (Kudoh *et al.*, 2003b, 2006; Iwahori *et al.*, 2009). This is aided by phosphorylated p53, which is induced by ATM. Efficient lytic DNA replication is ensured by the activation of ATM and DNA-PK through the host DNA damage response as well as lytic cycle gene expression (Kudoh *et al.,* 2009).

The importance of ATM and DNA-PK for this model of potential lytic cycle regulation upon DNA damage assumes that only DNA-damaging agents, which induce those repair targets, are able to induce the reactivation of EBV in epithelial cells. Notably, compounds like cisplatin that induce bulky adducts have been observed to induce lower levels of synergy on Zebra expression with different HDACis (Figure 54). This suggests that while the described model focusses on the strong effects of topoisomerase inhibitors on Zebra expression, it is possible that other DNA repair pathways and their targets could also help to activate lytic cycle expression to a lesser extent.

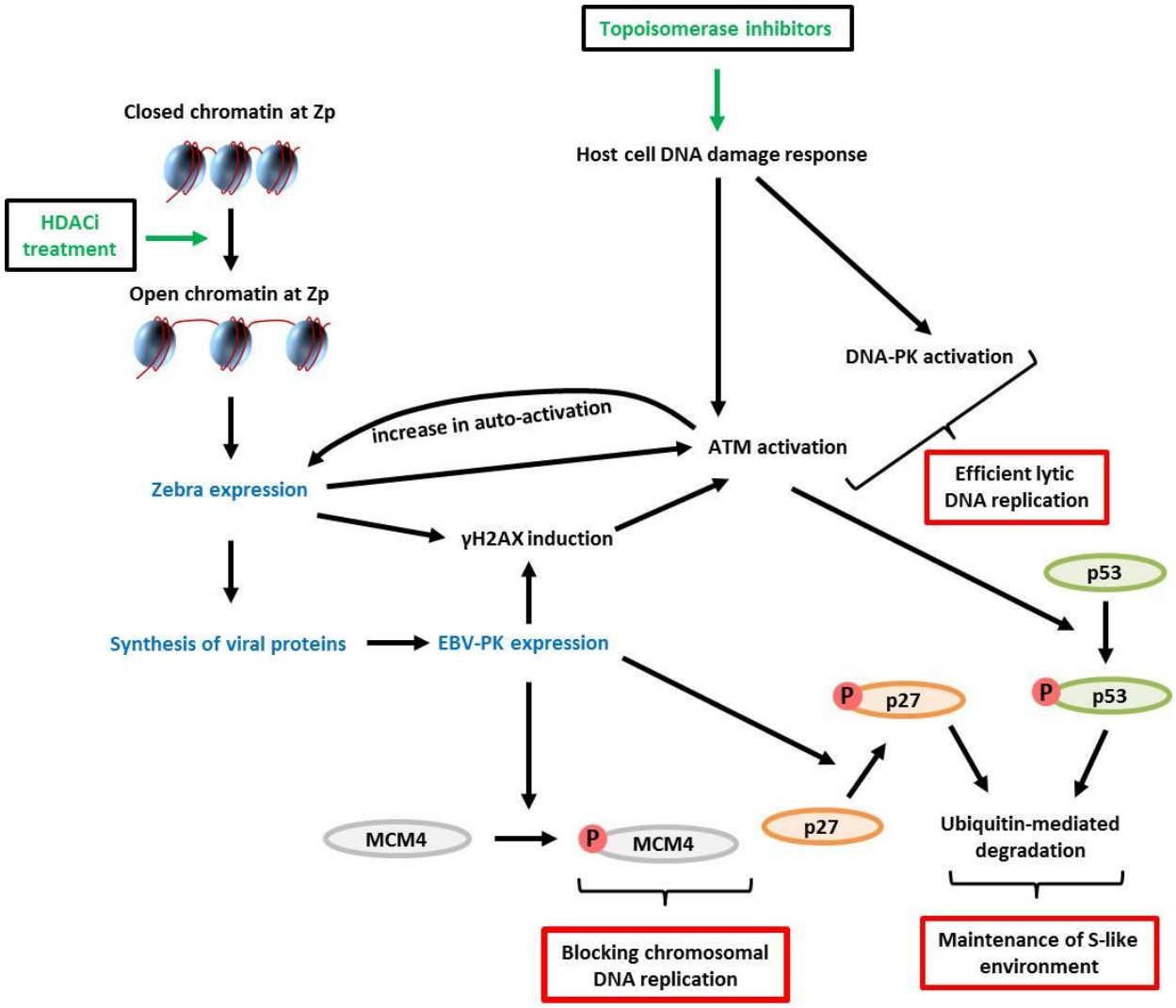


Figure 56: Model of the synergistic effect of HDACi and topoisomerase inhibitor treatment on EBV lytic cycle induction. The cellular as well as the viral chromatin is opened through HDACi treatment. The change in chromatin structure at Zp is sufficient to induce low levels of Zebra expression, which subsequently induces γH2AX induction and ATM activation. ATM increases Zebra's ability to activate its own expression and thus leads to higher Zebra levels and overall lytic gene expression. Treatment with topoisomerase inhibitors could further enhance ATM activation by activating the host cell DNA damage response. Overall, those changes in the cellular environment block chromosomal DNA replication while enhancing an S-like environment that is favourable to efficient lytic DNA replication. Viral proteins are highlighted in blue and cellular proteins are marked in black. The points of influence of HDACi and topoisomerase inhibitor treatments are highlighted in green (based on Sato & Tsurumi, 2010 and Wang'Ondu *et al.*, 2015). ATM – ataxia-telangiectasia mutated protein; DNA-PK – DNA-dependent protein kinase; EBV-PK – EBV-protein kinase; HDACi – histone deacetylase inhibitor; MCM4 – minichromosome maintenance complex 4; p27 – cyclin-dependent kinase inhibitor 1B; p53 – cellular tumour antigen p53; Zp – Zebra promoter.

7.3.4 Effect of posttranslational Zebra modifications on EBV reactivation

Differences in viral lytic cycle expression were observed between chidamide with Nutlin-3a- and chidamide with epirubicin-treated samples (Chapter 6.2.1). Analysis of potential Zebra modifications in those samples suggested that in chidamide with epirubicin-treated cells, Zebra protein occurs in differently sumoylated forms (Chapter 6.2.3). Those modifications were not observed in chidamide- and Nutlin-3a-treated samples. The fact that topoisomerase inhibitor treatment has been connected with increased sumoylation of topoisomerase I and II suggests that topoisomerase inhibitor treatment might induce increased overall sumoylation of cellular as well as viral proteins (Mao *et al.*, 2000a, 2000b). The sumoylation of topoisomerases has been shown to induce the degradation of topoisomerase IIβ, delocalise topoisomerase I from the nucleus into the cytoplasm and decrease the catalytic function of topoisomerase I (Mo *et al.*, 2002; Isik *et al.*, 2003; Zhou *et al.*, 2011).

Before examining this possibility, it is crucial to first show that the observed shift in migration for Zebra in chidamide with epirubicin-treated samples is linked to sumoylation, following which it would be interesting to assess the overall protein sumoylation in different treatment combinations to compare the effect of different topoisomerase inhibitor treatments on sumoylation. It would further be crucial to add chidamide treatment to see whether chidamide induces additional sumoylation or if the overall effect on sumoylation is independent of chidamide.

Together, these data support a model in which p53 and Sp1 cooperate to induce Zebra expression, but the subsequent progression of lytic cycle gene expression is regulated by PTMs of viral and cellular genes (Figure 57). During latency, no lytic genes are expressed, even though Sp1/3 is bound at the Zp promoter (Chua *et al.,* 2012). Treatment with chidamide and Nutlin-3a or chidamide and epirubicin induces binding of p53 to Sp1/3 at Zp and thereby induces the expression of Zebra. In chidamide and Nutlin-3a-treated samples, Zebra is not modified and can therefore induce the expression of E genes and lytic DNA replication by binding to the oriLyt together with the EBV replication complex and

topoisomerases (Kawanishi, 1993b; Wang *et al.,* 2009). In contrast, chidamide and epirubicin treatment might induce sumoylation of Zebra. The sumoylated form of Zebra recruits HDACs to early gene promoters and the oriLyt and thereby silences their gene expression as well as lytic DNA replication (Murata *et al.,* 2010). The inhibition of topoisomerases by epirubicin further supports this effect by blocking the Zebra-induced recruitment of topoisomerases to the oriLyt, which usually promotes the assembly of the replication complex (Kawanishi, 1993b; Wang *et al.,* 2009).

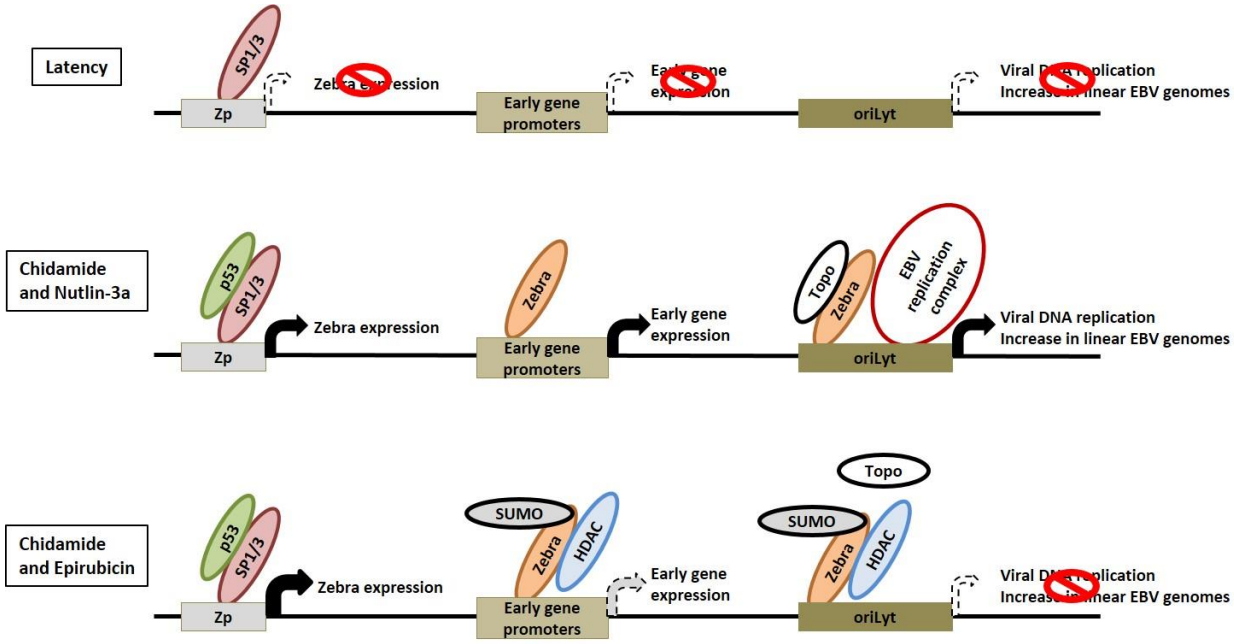


Figure 57: Model of the role of Zebra modifications in EBV lytic cycle induction by treatment with different compounds. During EBV latency in epithelial cells, all lytic promoters are inactive and no lytic transcripts are expressed, even though Sp1/3 is already bound to the Zp promoter at this stage. The addition of chidamide and Nutlin-3a induces p53 binding of Sp1/3 at the Zp site and thereby induces Zebra expression. Subsequently, early lytic genes are expressed and viral lytic DNA replication is induced through a complex of cellular and viral proteins. While chidamide and epirubicin treatment induces Zebra expression in a similar way, sumoylation of Zebra leads to the recruitment of HDACs to early gene promoters as well as the oriLyt and thereby represses their activity (based on Murata *et al.*, 2010 and Chua *et al.*, 2012). EBV – Epstein-Barr virus; HDAC – histone deacetylase; oriLyt – origin of lytic replication; SP1/3 – specificity protein 1/3; topo – topisomerase; Zp – Zebra promoter.

7.3.5 A potential role of p53 in the lytic replication of EBV

The identification of Ea-D and mDBP as potential binding partners of p53 by MS could further underline the importance of p53 in viral lytic cycle expression as well as DNA replication. Interaction of p53 with Ea-D was observed in both chidamide and Nutlin-3a- and chidamide and epirubicin-treated samples. In contrast, the interaction of mDBP with p53 was only detected in chidamide and Nutlin-3a-treated cells. Both Ea-D and mDBP have been shown to be part of the viral replication complex of EBV, in which those two proteins interact (Zeng *et al.,* 1997). Serine 15-phosphorylated p53, but not unphosphorylated p53, has been previously shown to co-localise with Ea-D in the viral replication compartment (Kudoh *et al.*, 2005). This suggests that epirubicin and nutlin-3a treatment might induce p53 phosphorylation at serine 15, thereby inducing p53 localisation within the viral replication compartment, where p53 could bind to Ea-D (Figure 58). The chidamide- and nutlin-3a-treatment data from Chapter 5.2.6 further suggest that this might also be sufficient to induce binding of p53 to mDBP.

The transcription factor Sp1, which has already been implicated as mediating the effect of p53 on the Zp promoter, has also been shown to bind to the oriLyt as well as to promote the assembly of the EBV replication complex when phosphorylated by ATM (Gruffat *et al.*, 1995; Chua *et al.,* 2012; Hau *et al.*, 2015). Therefore, Sp1 might play an important role in not just assembling the EBV replication complex but also in recruiting p53 to it.

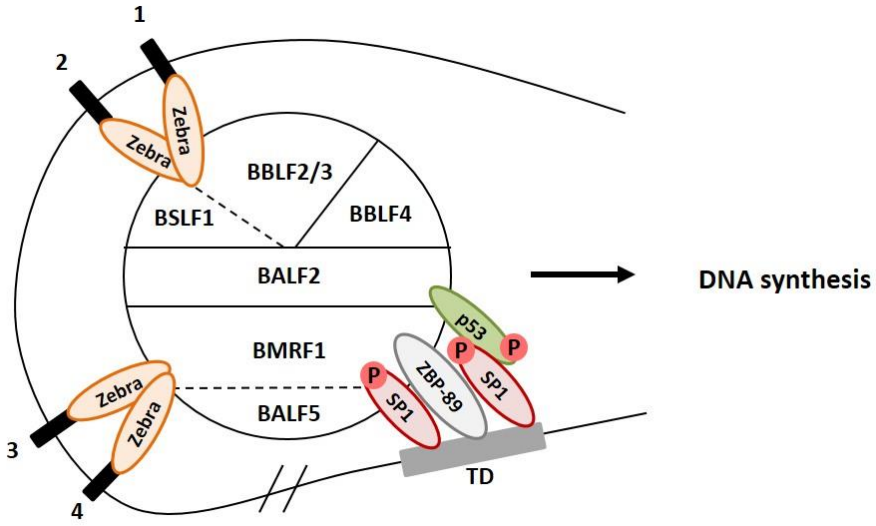


Figure 58: Model of the role of p53 in lytic DNA replication of EBV. SP1 and ZBP-89 have been shown to bind to the TD element during the latent and lytic state, but phosphorylated Sp1 has been shown to be important for the assembly of the viral replication complex. Sp1 might further recruit serine 15-phosphorylated p53 towards the replication complex where it binds to Ea-D (*BMRF1*) and mDBP (*BALF2*), thereby enabling viral replication (based on Baumann *et al.*, 1999 and Hau *et al.*, 2015). EBV – Epstein-Barr virus; oriLyt – origin of lytic replication; Sp1 - Specificity protein 1; ZBP-89 - Zinc-finger DNA-binding protein 89; ZRE – Zebra-response element.

Upon chidamide and epirubicin treatment, p53 was only observed to bind to Ea-D but not to mDBP, which might be caused by PTMs on either protein. It has been previously suggested that Ea-D can be sumoylated, even though it was not conclusively shown that the observed modification is SUMO (Adamson, 2005). This could hint towards potential sumoylation of Ea-D upon chidamide and epirubicin treatment leading to impaired recruitment of mDBP to the EBV replication complex, and thus abolishing the p53/mDBP interaction. Alternatively, the differential binding of p53 to mDBP might be linked to changed behaviour of topoisomerases upon epirubicin treatment. Topoisomerase I has been shown to recruit the cellular protein RecQL1 to the oriLyt for efficient viral replication (Wang *et al.*, 2009). It cannot be excluded that topoisomerases have a similar effect on viral lytic proteins. Therefore, it could be possible that the inhibition of topoisomerases through epirubicin treatment interferes with mDBP recruitment to the oriLyt, and therefore abolishes its binding to p53 and subsequent viral DNA replication.

Further work is necessary to establish the exact mechanisms underlying the model proposed in this chapter. Firstly, the observed interaction of p53 with Ea-D and mDBP would need to be confirmed by alternative methods such as immunoprecipitation. Secondly, expression levels of mDBP upon chidamide and epirubicin treatment need to be examined to exclude the possibility that the differences in binding are caused by differential expression. Thirdly, it would be important to assess whether the binding of p53 to E lytic proteins depends on its phosphorylation, as proposed in the current model. Finally, the role of topoisomerases for the assembly of the viral replication complex should be examined in more detail in the established experimental system. Nonetheless, the potential binding of p53 to Ea-D and mDBP has not been previously reported, and could therefore help to understand the mechanisms of lytic DNA replication of EBV in more detail.

7.3.6 Alternative compound classes with an effect on EBV reactivation

In Chapter 5.2.1, the validation of the identified hits of the screening experiment was focussed on topoisomerase inhibitors. Nevertheless, the list of potential hits also contained other compounds that should be examined in more detail.

The HDACi entinostat was identified as one of the top hits in YCCEL1 cells treated with the library alone. This underlines the results of Chapter 3.2 in which entinostat was independently described as a strong reactivating agent in different EBVaGC cell lines.

Tubulin modulators were the second most enriched group of compounds in the identified hits for library treatment together with chidamide. One member of this compound class, paclitaxel (Taxol), has been shown to induce the lytic cycle in different EBV-positive B-cell models, but this has not yet been examined in an epithelial cell setting (Feng *et al.,* 2002; Hagemeier *et al.*, 2012). The results of the screening experiment in YCCEL1 cells showed that treatment with this compound class induced Zebra

expression in ~4–9% of cells, which did not change significantly when chidamide was added (~6–11%) (Table 25). This could suggest that there is no synergistic effect of tubulin modulators and chidamide, but it could also be an artefact of the compound concentrations used for this experiment. Therefore, it would be interesting to characterise those compounds at different concentrations to examine whether or not they are able to show synergy with chidamide. Exploring this in different EBV-positive epithelial cell lines would also give an insight into the ability of this compound class to reactivate EBV in epithelial cells.

Decitabine is a demethylating agent and therefore a treatment influencing the epigenetic state of the cell. The identification of decitabine as a potential reactivating agent is not surprising as it has been previously shown to induce Zebra expression in SNU719 cells (Nakamura *et al.,* 2016). In the current study, it was only identified as a hit in combination with chidamide, inducing Zebra expression in ~31% of cells (Table 25). Notably, it did induce Zebra expression in ~12% of cells when treated alone, but had to be excluded as a hit based on its low Z-score. A similar trend in the amount of Zebra-expressing cells has been shown in an initial titration experiment of this compound alone and in combination with chidamide (Appendix Figure 4). This shows that decitabine itself induces low levels of Zebra expression while the addition of chidamide leads to a further increase in Zebra expression, suggesting that DNA demethylation is less potent in inducing Zebra expression than an increase in histone and protein acetylation through HDACi treatment.

The PI3K inhibitor PIK75 HCl (PIK75) is an interesting hit as the *PIK3CA* gene has been shown to be commonly mutated in EBVaGC (Fang *et al.*, 2016). While this gene is mutated in 3–42% of other gastric cancer groups, mutations were found in ~80% of EBVaGC cases (Cancer Genome Atlas Research, 2014). The importance of PI3K alterations are further supported by two human immunodeficiency disorders with mutations in the *PIK3* gene that have been shown to be predisposed for severe herpesvirus infections and virus-associated malignancies (Angulo *et al.,* 2013; Lucas *et al.*, 2014). Different latent

EBV genes such as LMP1 and LMP2A have been shown to induce PI3K/AKT signalling, supporting a role of this pathway in transformation and the establishment of viral latency (Fukuda & Longnecker, 2007; Yang *et al.,* 2013). Interestingly, in different Burkitt's lymphoma cell lines it has been shown that PI3K inhibition reduces reactivation through either the activation of BCR signalling or TGFβ stimulation (Iwakiri & Takada, 2004; Oussaief *et al.*, 2009b; Goswami *et al.*, 2012). This stands in contrast to the high percentage of Zebra-expressing cells upon PIK75 treatment-detected cells in the screening experiment in YCCEL1 (~43%, Table 25). Since the viral latency of EBV differs between B-cells and epithelial cells, and the efficacy of reactivating agents has been shown to differ in previous studies, it is possible that this could be explained by genetic differences between cell lines and virus strains. Therefore, in addition to the validation of PIK75 as a hit, it would be crucial to sequence the *PIK3* gene in the panel of cell lines used in this study. Those insights could be used to further progress our understanding of the role of PI3K in herpesvirus latency and reactivation.

Overall, a diverse set of hits with possible impacts on the reactivation of EBV in epithelial cells has been identified. The validation of those compounds in different cell lines and models of reactivation will be important to give insights into the potential mechanisms underlying EBV reactivation in epithelial cells. In addition, this could help to advance potential therapeutic strategies for EBV-associated epithelial malignancies as all compounds identified in this screen have been approved for use in the clinic by the US FDA.

7.4 Potential lytic induction therapy for EBV-associated epithelial malignancies

Current clinical trials of lytic induction therapy are mainly focussed on the treatment of HIV infection. Those clinical trials include a broad panel of HDACis such as SAHA, panobinostat, romidepsin and chidamide. Interestingly, while most trials are focussed on hydroxamate HDACis, the only benzamide

HDACi currently in clinical trials is chidamide. This is not surprising, as most HDACis currently approved for the use in the clinic are hydroxamate HDACis (Falkenberg & Johnstone, 2014).

For viral lytic induction therapy to be successful, it is important that the inducing agent does not inhibit a functional immune response towards presented viral epitopes and that the lytic cycle expression is sufficient to induce targeted cell killing by antiviral treatment.

7.4.1 Potential novel treatment combinations for the treatment of EBV-related epithelial cancers

While epirubicin and chidamide treatment induced significant cell death independently of the EBV status of the cell line, chidamide and Nutlin-3a treatment decreased cell numbers more specifically in EBV-positive cell lines (Figure 48).

The increased toxicity of chidamide and Nutlin-3a treatment in EBV-positive cell lines suggests that the use of similar compound combinations for the therapy of EBV-related cancers might be possible without depending on the use of an antiviral agent. Unfortunately, Nutlin-3a is not approved for use in the clinic and its high level of clinical adverse events, such as haematological toxicity, have led to the development of more potent MDM2 inhibitors for use in the clinic instead (Ray-Coquard *et al.,* 2012; Patnaik *et al.,* 2015). Those second-generation MDM2 inhibitors, such as idasanutlin and HDM201, are currently undergoing phase I–III clinical trials for the treatment of different cancer types (Tisato *et al.*, 2017). For the future, it would be important to see if those compounds have the same effect on EBV reactivation as Nutlin-3a and could therefore be potentially translated into the clinic as treatments for EBV-related epithelial malignancies in combination with an HDACi.

7.4.2 The role of the immune system in lytic induction therapy

The results in Chapter 5.2 suggest that chidamide and CXD101 have no negative influence on HLA class I expression and subsequent T-cell recognition, and could even enhance those parameters in certain cell lines.

The results of the T-cell assay (Figure 33) suggest that HDACi-treated epithelial cells do not just maintain HLA expression, but that presentation of lytic EBV epitopes is sufficient to activate CTLs. To further strengthen this data, it would be necessary to perform similar T-cell assays with different EBV-positive cell lines and T-cell clones. However, this is challenging considering that HLA-matched T-cell clones and cancer cell lines are required for this experiment. One possibility to overcome this limitation would be to induce HLA-A2 overexpression in EBV-positive epithelial cell lines and thereby overcome the HLA restriction with the already tested GLC T-cell clone. This would enable testing of this T-cell clone in combination with a broader panel of EBV-positive epithelial cell lines. As an alternative approach, already described T-cell clones could be collected, but depending on the HLA restriction of those clones they might not be compatible with the available EBV-positive epithelial cell lines.

A potential lack of T-cell activation in further assays could either be caused by impaired HLA presentation in the epithelial cell lines through inhibition by EBV or HDACi treatment, or by a lack of presentation of the specific EBV antigen recognised by the T-cell clone. To fully understand which EBV epitopes are presented in reactivated epithelial cells, an HLA class I-associated immunopeptidome could be generated for differently treated cell lines. This experimental approach is based on immunoprecipitation of HLA class I molecules from cell lysates with subsequent MS analysis of bound peptides (Ternette *et al.,* 2016). The identification of presented EBV peptides on reactivated epithelial cells would further have the advantage that it would allow the generation of T-cell clones that are specific to the presented peptides, and thus improve the examination of CTL activation by reactivated epithelial cells.

One concern of HDACi treatment *in vivo* is that compounds are immunotoxic and therefore inhibit any potential immune response towards the reactivated cells. Impaired function of CTLs against HIV infection, as well as impaired NK function after treatment with HDACis, has been observed in different studies (Ogbomo *et al.*, 2007; Jones *et al.*, 2014). Contradicting studies on the effect of HDACis on cancer immunity suggest that they promote an antitumour immune response (Murakami *et al.,* 2008; Cao *et al.,* 2015). Therefore, it is necessary to perform further experiments to assess HDACi toxicity on T-cells in our model of HDACi-mediated EBV reactivation for a better understanding of potential *in vivo* effects. To achieve this, it would be crucial to include HDACi-treated T-cells as controls for further T-cell assays.

Overall, this is the first study to examine the effect of HDACi treatment on the antigen presentation of EBV-positive epithelial cells and their ability to activate CTLs. Further experiments are needed to fully characterise the interaction of HDACi treatment, viral reactivation and immune cell activation in this setting.

7.4.3 Implications of the latent EBV pool in B-cells for lytic induction therapy

For lytic induction therapy of EBV-positive epithelial cancers, it is important to consider that ~90% of adults carry latent EBV within their B-cell population. Therefore, it is important to not just assess the effect of potential therapies on EBV reactivation in epithelial cells, but also the effect that those treatments have on B-cells. Otherwise, the potential reactivation of the EBV pool within B-cells or within the tumour by HDACi treatment could lead to a rapid increase of the virus titre in the blood and thereby induce adverse health effects for patients (Kim *et al.*, 2016a).

Even though strong Zebra expression was observed with HDACi treatment either alone or with chemotherapeutics in epithelial cancer cells, the same was not observed in B-cells (Chapters 4.2.1

and 5.2.3). In B-cells, no increase in Zebra expression was observed upon treatment. Since the reactivation potential of those treatment combinations was only examined in a small number of B-cell lines, this result needs to be replicated in a broader set of cell lines to underline its physiological relevance. Nevertheless, those results are promising for the potential use of those treatment combinations in the clinic.

For the future, it would be important to elucidate the effect of different treatments on EBV latency in B-cells. Apart from the replication of the results in different cell lines, it would be interesting to examine blood samples of cancer patients treated with either HDACis or both chemotherapeutics and HDACis independently of their cancer type. This would give crucial insights into the effect of those treatment combinations on the EBV reservoir within the B-cells and address safety concerns for a potential clinical trial.

7.5 Final remarks

While most studies on the life cycle of EBV to date have focussed on either B-cell lines or *in vitro*-infected epithelial cell lines, this thesis has examined the effects of compound treatment on a broad panel of EBV-positive epithelial cell lines. Through the novel screening method developed in this study, it was possible to perform large-scale screens on EBV-positive epithelial cell lines to identify EBV-reactivating agents. This novel method now allows examination of the effect of compound treatment on cell lines derived from patients without further modifications. This will help to progress the identification of suitable lytic induction therapies for EBV-related epithelial malignancies. Lastly, the synergistic effects observed with different p53-inducing agents, and the potential interaction of p53 with Ea-D and mDBP, extend the current view on the involvement of p53 in lytic cycle induction of EBV and might lead to a better mechanistic understanding of the processes underlying reactivation.

Bibliography

Adachi, Y., Yasuda, K., Inomata, M., Sato, K., Shiraishi, N., & Kitano, S. (2000). Pathology and prognosis of gastric carcinoma: Well versus poorly differentiated type. *Cancer*, *89*(7), 1418–1424. https://doi.org/10.1002/1097-0142(20001001)89:7<1418::AID-CNCR2>3.0.CO;2-A

Adamson, A. L. (2005). Effects of SUMO-1 upon Epstein-Barr virus BZLF1 function and BMRF1 expression. *Biochemical and Biophysical Research Communications*. https://doi.org/10.1016/j.bbrc.2005.08.036

Adamson, A. L., Darr, D., Holley-Guthrie, E., Johnson, R. A., Mauser, A., Swenson, J., & Kenney, S. (2000). Epstein-Barr virus immediate-early proteins BZLF1 and BRLF1 activate the ATF2 transcription factor by increasing the levels of phosphorylated p38 and c-Jun N-terminal kinases. *Journal of Virology*. https://doi.org/10.1128/JVI.74.3.1224-1233.2000

Adamson, A. L., & Kenney, S. (1999). The Epstein-Barr Virus BZLF1 Protein Interacts Physically and Functionally with the Histone Acetylase CREB-Binding Protein. *Journal of Virology*.

Adamson, A. L., & Kenney, S. C. (1998). Rescue of the Epstein-Barr virus BZLF1 mutant, Z(S186A), early gene activation defect by the BRLF1 gene product. *Virology*. https://doi.org/10.1006/viro.1998.9396

Adldinger, H. K., Delius, H., Freese, U. K., Clarke, J., & Bornkamm, G. W. (1985). A putative transforming gene of jijoye virus differs from that of Epstein-Barr virus prototypes. *Virology*. https://doi.org/10.1016/0042-6822(85)90253-3

Ahlquist, P. (2006). Parallels among positive-strand RNA viruses, reverse-transcribing viruses and double-stranded RNA viruses. *Nature Reviews Microbiology*. https://doi.org/10.1038/nrmicro1389

Ahmed, W., Philip, P. S., Tariq, S., & Khan, G. (2014). Epstein-Barr virus-encoded small RNAs (EBERs) are present in fractions related to exosomes released by EBV-transformed cells. *PLoS ONE*. https://doi.org/10.1371/journal.pone.0099163

Alibek, K., Bekmurzayeva, A., Mussabekova, A., & Sultankulov, B. (2012). Using antimicrobial adjuvant therapy in cancer treatment: a review. *Infectious Agents and Cancer*, *7*, 33. https://doi.org/10.1186/1750-9378-7-33

Altmann, M., & Hammerschmidt, W. (2005). Epstein-barr virus provides a new paradigm: A requirement for the immediate inhibition of apoptosis. *PLoS Biology*. https://doi.org/10.1371/journal.pbio.0030404

Amon, W., & Farrell, P. J. (2005). Reactivation of Epstein-Barr virus from latency. *Rev Med Virol*, *15*, 149–156. https://doi.org/10.1002/rmv.456

Angulo, I., Vadas, O., Garçon, F., Banham-Hall, E., Plagnol, V., Leahy, T. R., … Nejentsev, S. (2013). Phosphoinositide 3-kinase δ gene mutation predisposes to respiratory infection and airway damage. *Science*. https://doi.org/10.1126/science.1243292

Araujo, I., Foss, H. D., Bittencourt, a, Hummel, M., Demel, G., Mendonca, N., … Stein, H. (1996). Expression of Epstein-Barr virus-gene products in Burkitt's lymphoma in Northeast Brazil. *Blood*.

Babcock, G. J., Decker, L. L., Volk, M., & Thorley-Lawson, D. A. (1998). EBV persistence in memory B cells in vivo. *Immunity*. https://doi.org/10.1016/S1074-7613(00)80622-6

Baltimore, D. (1971). Expression of animal virus genomes. *Bacteriological Reviews*.

Baryawno, N., Rahbar, A., Wolmer-solberg, N., Taher, C., Odeberg, J., Darabi, A., … Söderberg-nauclér, C. (2011). Detection of human cytomegalovirus in medulloblastomas reveals a potential therapeutic target. *J Clin Invest*. https://doi.org/10.1172/JCI57147.colon

Baumann, M., Feederle, R., Kremmer, E., & Hammerschmidt, W. (1999). Cellular transcription factors recruit viral replication proteins to activate the Epstein-Barr virus origin of lytic DNA replication, oriLyt. *EMBO Journal*. https://doi.org/10.1093/emboj/18.21.6095

Beasley, R. P., Lin, C.-C., Hwang, L.-Y., & Chien, C.-S. (1981). HEPATOCELLULAR CARCINOMA AND HEPATITIS B VIRUS: A Prospective Study of 22 707 Men in Taiwan. *The Lancet*. https://doi.org/10.1016/S0140-6736(81)90585-7

Beckers, T., Burkhardt, C., Wieland, H., Gimmnich, P., Ciossek, T., Maier, T., & Sanders, K. (2007). Distinct pharmacological properties of second generation HDAC inhibitors with the benzamide or hydroxamate head group. *International Journal of Cancer*. https://doi.org/10.1002/ijc.22751

Bejarano, M. T., & Masucci, M. G. (1998). Interleukin-10 abrogates the inhibition of Epstein-Barr virus-induced B-cell transformation by memory T-cell responses. *Blood*.

Bellows, D. S., Howell, M., Pearson, C., Hazlewood, S. a, & Hardwick, J. M. (2002). Epstein-Barr virus BALF1 is a BCL-2-like antagonist of the herpesvirus antiapoptotic BCL-2 proteins. *Journal of Virology*. https://doi.org/10.1128/jvi.76.5.2469-2479.2002

Bergbauer, M., Kalla, M., Schmeinck, A., Göbel, C., Rothbauer, U., Eck, S., … Hammerschmidt, W. (2010). CpG-methylation regulates a class of Epstein-Barr virus promoters. *PLoS Pathogens*. https://doi.org/10.1371/journal.ppat.1001114

Bethesda: National Library of Medicine (US). (2000). Identifier: NCT02902185. Retrieved April 18, 2018, from https://clinicaltrials.gov/ct2/show/NCT02902185

Bhende, P. M., Dickerson, S. J., Sun, X., Feng, W.-H., & Kenney, S. C. (2007). X-box-binding protein 1 activates lytic Epstein-Barr virus gene expression in combination with protein kinase D. *Journal of Virology*. https://doi.org/10.1128/JVI.00154-07

Bhende, P. M., Seaman, W. T., Delecluse, H.-J., & Kenney, S. C. (2004). The EBV lytic switch protein, Z, preferentially binds to and activates the methylated viral genome. *Nature Genetics*. https://doi.org/10.1038/ng1424

Blackadar, C. B., Brian, C., Clarke, B., Blackadar, B., Blackadar, C. B., Researcher, V., … Researcher, V. (2016). Historical review of the causes of cancer. *World J Clin Oncol World J Clin Oncol February*. https://doi.org/10.5306/wjco.v7.i1.54

Blackwell, J. M., Jamieson, S. E., & Burgner, D. (2009). HLA and infectious diseases. *Clinical Microbiology Reviews*. https://doi.org/10.1128/CMR.00048-08

Bolden, J. E., Shi, W., Jankowski, K., Kan, C. Y., Cluse, L., Martin, B. P., … Johnstone, R. W. (2013). HDAC inhibitors induce tumor-cell-selective pro-apoptotic transcriptional responses. *Cell Death and Disease*. https://doi.org/10.1038/cddis.2013.9

Bouvard, V., Baan, R., Straif, K., Grosse, Y., Secretan, B., El Ghissassi, F., … Ghissassi, F. El. (2009). A review of human carcinogens--Part B: biological agents. *Lancet Oncology*. https://doi.org/10.1016/S1470-2045(09)70096-8

Boyle, P., & Levin, B. (2014). World Cancer Report 2014. In *World Cancer Report 2014*.

Braciale, T. J., & Hahn, Y. S. (2013). Immunity to viruses. *Immunological Reviews*. https://doi.org/10.1111/imr.12109

Bradner, J. E., West, N., Grachan, M. L., Greenberg, E. F., Haggarty, S. J., Warnow, T., & Mazitschek, R. (2010). Chemical phylogenetics of histone deacetylases. *Nature Chemical Biology*. https://doi.org/10.1038/nchembio.313

Bristol, J. a, Robinson, A. R., Barlow, E. a, & Kenney, S. C. (2010). The Epstein-Barr virus BZLF1 protein inhibits tumor necrosis factor receptor 1 expression through effects on cellular C/EBP proteins. *Journal of Virology*. https://doi.org/10.1128/JVI.00712-10

Brown, J. S., O'Carrigan, B., Jackson, S. P., & Yap, T. A. (2017). Targeting DNA repair in cancer: Beyond PARP inhibitors. *Cancer Discovery*. https://doi.org/10.1158/2159-8290.CD-16-0860

Bryant, H., & Farrell, P. J. (2002). Signal Transduction and Transcription Factor Modification during Reactivation of Epstein-Barr Virus from Latency. *Journal of Virology*. https://doi.org/10.1128/JVI.76.20.10290-10298.2002

Buisson, M., Géoui, T., Flot, D., Tarbouriech, N., Ressing, M. E., Wiertz, E. J., & Burmeister, W. P. (2009). A Bridge Crosses the Active-Site Canyon of the Epstein-Barr Virus Nuclease with DNase and RNase Activities. *Journal of Molecular Biology*. https://doi.org/10.1016/j.jmb.2009.06.034

Cancer Genome Atlas Research, N. (2014). Comprehensive molecular characterization of gastric adenocarcinoma. *Nature*, *513*, 202–209. https://doi.org/10.1038/nature13480

Cancer Research UK. (2018). http://www.cancerresearchuk.org/health-professional/cancer-statistics/incidence/common-cancers-compared. Retrieved from http://www.cancerresearchuk.org/health-professional/cancer-statistics/incidence/common-cancers-compared

Cancian, L., Bosshard, R., Lucchesi, W., Karstegl, C. E., & Farrell, P. J. (2011). C-terminal region of ebna-2 determines the superior transforming ability of type 1 epstein-barr virus by enhanced gene regulation of LMP-1 and CXCR7. *PLoS Pathogens*. https://doi.org/10.1371/journal.ppat.1002164

Cao, K., Wang, G., Li, W., Zhang, L., Wang, R., Huang, Y., … Shi, Y. (2015). Histone deacetylase inhibitors prevent activation-induced cell death and promote anti-tumor immunity. *Oncogene*. https://doi.org/10.1038/onc.2015.46

Chan, A. T., Teo, P. M., & Huang, D. P. (2004). Pathogenesis and treatment of nasopharyngeal carcinoma. *Seminars in Oncology*. https://doi.org/S0093775404004051 [pii]

Chang, A. H., & Parsonnet, J. (2010). Role of bacteria in oncogenesis. *Clinical Microbiology Reviews*. https://doi.org/10.1128/CMR.00012-10

Chang, L. K., Lee, Y. H., Cheng, T. S., Hong, Y. R., Lu, P. J., Wang, J. J., … Liu, S. T. (2004). Post-translational modification of Rta of Epstein-Barr virus by SUMO-1. *Journal of Biological Chemistry*. https://doi.org/10.1074/jbc.M405470200

Chang, M. S., Uozaki, H., Chong, J. M., Ushiku, T., Sakuma, K., Ishikawa, S., … Fukayama, M. (2006). CpG island methylation status in gastric carcinoma with and without infection of Epstein-Barr virus. *Clin Cancer Res*, *12*, 2995–3002. https://doi.org/10.1158/1078-0432.CCR-05-1601

Chang, P. J., Liu, S. T., & Chang, Y. S. (1998). Characterization of the BcLF1 promoter in Epstein-Barr virus. *Journal of General Virology*, *79*(8), 2003–2006. https://doi.org/10.1099/0022-1317-79-8-2003

Chang, S. S., Lo, Y. C., Chua, H. H., Chiu, H. Y., Tsai, S. C., Chen, J. Y., … Tsai, C. H. (2008). Critical role of p53 in histone deacetylase inhibitor-induced Epstein-Barr virus Zta expression. *J Virol*, *82*, 7745–7751. https://doi.org/10.1128/JVI.02717-07

Chen, C. J., Deng, Z., Kim, A. Y., Blobel, G. A., & Lieberman, P. M. (2001). Stimulation of CREB binding protein nucleosomal histone acetyltransferase activity by a class of transcriptional activators. *Molecular and Cellular Biology*. https://doi.org/10.1128/mcb.21.2.476-487.2001

Chen, J., Sathiyamoorthy, K., Zhang, X., Schaller, S., Perez White, B. E., Jardetzky, T. S., & Longnecker, R. (2018). Ephrin receptor A2 is a functional entry receptor for Epstein-Barr virus. *Nature Microbiology*, *3*(2), 172–180. https://doi.org/10.1038/s41564-017-0081-7

Chen, M., Cai, L., Kato, T., & Kato, Y. (2016). *Ectopic expression of Human Herpesvirus 1 Thymidine Kinase induces male infertility, Herpesviridae*. (Dr. Joseph Ongradi, Ed.). InTech. https://doi.org/10.5772/64390

Chen, T., & Hudnall, S. D. (2006). Anatomical mapping of human herpesvirus reservoirs of infection. *Modern Pathology*. https://doi.org/10.1038/modpathol.3800584

Chen, Y., Williams, V., Filippova, M., Filippov, V., & Duerksen-Hughes, P. (2014). Viral carcinogenesis: Factors inducing DNA damage and virus integration. *Cancers*. https://doi.org/10.3390/cancers6042155

Chen, J., Fu, L., Zhang, L. Y., Kwong, D. L., Yan, L., & Guan, X. Y. (2012a). Tumor suppressor genes on frequently deleted chromosome 3p in nasopharyngeal carcinoma. *Chinese Journal of Cancer*. https://doi.org/10.5732/cjc.011.10364

Chen, J.N., He, D., Tang, F., & Shao, C. K. (2012b). Epstein-Barr virus-associated gastric carcinoma: a newly defined entity. *J Clin Gastroenterol*, *46*, 262–271. https://doi.org/10.1097/MCG.0b013e318249c4b8

Chen, J., Rowe, C. L., Jardetzky, T. S., & Longnecker, R. (2012c). The KGD motif of Epstein-Barr virus gH/gL is bifunctional, orchestrating infection of B cells and epithelial cells. *mBio*, *3*(1), 1–9. https://doi.org/10.1128/mBio.00290-11

Chesnokova, L. S., Nishimura, S. L., & Hutt-Fletcher, L. M. (2009). Fusion of epithelial cells by Epstein-Barr virus proteins is triggered by binding of viral glycoproteins gHgL to integrins alphavbeta6 or alphavbeta8. *Proceedings of the National Academy of Sciences of the United States of America*. https://doi.org/10.1073/pnas.0907508106

Chesnokova, L. S. & Hutt-Fletcher, L. M. (2011). Fusion of Epstein-Barr Virus with Epithelial Cells Can Be Triggered by alphavbeta5 in Addition to alphavbeta 6 and alphavbeta 8, and Integrin Binding Triggers a Conformational Change in Glycoproteins gHgL. *Journal of Virology*. https://doi.org/10.1128/JVI.05580-11

Cho, K. R., & Vogelstein, B. (1992). Genetic alterations in the adenoma–carcinoma sequence. *Cancer*. https://doi.org/10.1002/1097-0142(19920915)70:4+<1727::AID-CNCR2820701613>3.0.CO;2-P

Choi, C. K., Ho, D. N., Hui, K. F., Kao, R. Y., & Chiang, A. K. S. (2015). Identification of novel small organic compounds with diverse structures for the induction of Epstein-Barr Virus (EBV) lytic cycle in EBV-positive epithelial malignancies. *PLoS ONE*. https://doi.org/10.1371/journal.pone.0145994

Chua, H.-H., Lee, H.-H., Chang, S.-S., Lu, C.-C., Yeh, T.-H., Hsu, T.-Y., … Tsai, C.-H. (2007). Role of the TSG101 gene in Epstein-Barr virus late gene transcription. *Journal of Virology*. https://doi.org/10.1128/JVI.02289-06

Chua, H. H., Chiu, H. Y., Lin, S. J., Weng, P. L., Lin, J. H., Wu, S. W., … Tsai, C. H. (2012). p53 and Sp1 cooperate to regulate the expression of Epstein-Barr viral Zta protein. *J Med Virol*, *84*, 1279–1288. https://doi.org/10.1002/jmv.23316

Clark, P. I. (1992). Clinical pharmacology and schedule dependency of the podophyllotoxin derivatives. *Seminars in Oncology*.

Clarke, P. A., Schwemmle, M., Schickinger, J., Hilse, K., & Clemens, M. J. (1991). Binding of epstein-barr virus small RNA EBER-1 to the double-stranded RNA-activated protein kinase DAI. *Nucleic Acids Research*. https://doi.org/10.1093/nar/19.2.243

Cohen, J. I., Fauci, A. S., Varmus, H., & Nabel, G. J. (2011). Epstein-Barr virus: an important vaccine target for cancer prevention. *Sci Transl Med*, *3*, 107fs7. https://doi.org/10.1126/scitranslmed.3002878

Cohen, J. I., Wang, F., Mannick, J., & Kieff, E. (1989). Epstein-Barr virus nuclear protein 2 is a key determinant of lymphocyte transformation. *Proc Natl Acad Sci U S A*.

Condorelli, F., Gnemmi, I., Vallario, A., Genazzani, A. A., & Canonico, P. L. (2008). Inhibitors of histone deacetylase (HDAC) restore the p53 pathway in neuroblastoma cells. *British Journal of Pharmacology*. https://doi.org/10.1038/sj.bjp.0707608

Countryman, J. K., Gradoville, L., & Miller, G. (2008). Histone hyperacetylation occurs on promoters of lytic cycle regulatory genes in Epstein-Barr virus-infected cell lines which are refractory to disruption of latency by histone deacetylase inhibitors. *J Virol*, *82*, 4706–4719. https://doi.org/10.1128/JVI.00116-08

Croft, N. P., Shannon-Lowe, C., Bell, A. I., Horst, D., Kremmer, E., Ressing, M. E., … Hislop, A. D. (2009). Stage-specific inhibition of MHC class I presentation by the epstein-barr virus BNLF2a protein during virus lytic cycle. *PLoS Pathogens*. https://doi.org/10.1371/journal.ppat.1000490

Cycon, K. A., Mulvaney, K., Rimsza, L. M., Persky, D., & Murphy, S. P. (2013). Histone deacetylase inhibitors activate CIITA and MHC class II antigen expression in diffuse large B-cell lymphoma. *Immunology*. https://doi.org/10.1111/imm.12136

Daibata, M., & Sairenji, T. (1993). Epstein-Barr virus (EBV) replication and expressions of EA-D (BMRF1 gene product), virus-specific deoxyribonuclease, and DNA polymerase in EBV-activated Akata cells. *Virology*. https://doi.org/10.1006/viro.1993.1555

Daigle, D., Gradoville, L., Tuck, D., Schulz, V., Wang'ondu, R., Ye, J., … Miller, G. (2011). Valproic Acid Antagonizes the Capacity of Other Histone Deacetylase Inhibitors To Activate the Epstein-Barr Virus Lytic Cycle. *Journal of Virology*. https://doi.org/10.1128/JVI.02659-10

Damania, B. (2004). Oncogenic γ-herpesviruses: Comparison of viral proteins involved in tumorigenesis. *Nature Reviews Microbiology*. https://doi.org/10.1038/nrmicro958

Dambaugh, T., Beisel, C., Hummel, M., King, W., Fennewald, S., Cheung, A., … Kieff, E. (1980). Epstein-Barr virus (B95-8) DNA VII: molecular cloning and detailed mapping. *Proc Natl Acad Sci U S A*. https://doi.org/10.1073/pnas.77.5.2999

Dambaugh, T., Hennessy, K., Chamnankit, L., & Kieff, E. (1984). U2 region of Epstein-Barr virus DNA may encode Epstein-Barr nuclear antigen 2. *Proceedings of the National Academy of Sciences of the United States of America*. https://doi.org/10.1073/pnas.81.23.7632

Dantuma, N. P., Heessen, S., Lindsten, K., Jellne, M., & Masucci, M. G. (2000). Inhibition of proteasomal degradation by the Gly-Ala repeat of Epstein–Barr virus is influenced by the length of the repeat and the strength of the degradation signal. *Proceedings of the National Academy of Sciences of the United States of America*, *97*(15), 8381–8385. Retrieved from http://www.ncbi.nlm.nih.gov/pmc/articles/PMC26956/

Davies, M. L., Xu, S., Lyons-Weiler, J., Rosendorff, A., Webber, S. A., Wasil, L. R., … Rowe, D. T. (2010). Cellular factors associated with latency and spontaneous Epstein-Barr virus reactivation in B-lymphoblastoid cell lines. *Virology*. https://doi.org/10.1016/j.virol.2010.01.002

Dawson, C. W., Laverick, L., Morris, M. A., Tramoutanis, G., & Young, L. S. (2008). Epstein-Barr Virus-Encoded LMP1 Regulates Epithelial Cell Motility and Invasion via the ERK-MAPK Pathway. *Journal of Virology*, *82*(7), 3654–3664. https://doi.org/10.1128/JVI.01888-07

De La Cruz-Herrera, C. F., Shire, K., Siddiqi, U. Z., & Frappier, L. (2018). A genome-wide screen of Epstein-Barr virus proteins that modulate host SUMOylation identifies a SUMO E3 ligase conserved in herpesviruses. *PLOS Pathogens*, *14*(7), e1007176-. Retrieved from https://doi.org/10.1371/journal.ppat.1007176

de Souza, C. R. T., de Oliveira, K. S., Ferraz, J. J. S., Leal, M. F., Calcagno, D. Q., Seabra, A. D., … Burbano, R. R. (2014). Occurrence of Helicobacter pylori and Epstein-Barr virus infection in endoscopic and gastric cancer patients from Northern Brazil. *BMC Gastroenterology*. https://doi.org/10.1186/1471-230X-14-179

Delagreverie, H. M., Delaugerre, C., Lewin, S. R., Deeks, S. G., & Li, J. Z. (2016). Ongoing clinical trials of human immunodeficiency virus latency-reversing and immunomodulatory agents. *Open Forum Infectious Diseases*. https://doi.org/10.1093/ofid/ofw189

Desbien, A. L., Kappler, J. W., & Marrack, P. (2009). The Epstein-Barr virus Bcl-2 homolog, BHRF1, blocks apoptosis by binding to a limited amount of Bim. *Proceedings of the National Academy of Sciences of the United States of America*, *106*(14), 5663–5668. https://doi.org/10.1073/pnas.0901036106

Dickerson, S. J., Xing, Y., Robinson, A. R., Seaman, W. T., Gruffat, H., & Kenney, S. C. (2009). Methylation-dependent binding of the epstein-barr virus BZLF1 protein to viral promoters. *PLoS Pathogens*. https://doi.org/10.1371/journal.ppat.1000356

Djavadian, R., Chiu, Y. F., & Johannsen, E. (2016). An Epstein-Barr Virus-Encoded Protein Complex Requires an Origin of Lytic Replication In Cis to Mediate Late Gene Transcription. *PLoS Pathogens*. https://doi.org/10.1371/journal.ppat.1005718

Dominguez-Brauer, C., Thu, K. L., Mason, J. M., Blaser, H., Bray, M. R., & Mak, T. W. (2015). Targeting Mitosis in Cancer: Emerging Strategies. *Molecular Cell*. https://doi.org/10.1016/j.molcel.2015.11.006

Durst, M., Bosch, F. X., Glitz, D., Schneider, A., & zur, H. H. (1991). Inverse relationship between human papillomavirus (HPV) type 16 early gene expression and cell differentiation in nude mouse epithelial cysts and tumors induced by HPV-positive human cell lines. *J.Virol.*

Dyson, P. J., & Farrell, P. J. (1985). Chromatin structure of Epstein-Barr virus. *Journal of General Virology*. https://doi.org/10.1099/0022-1317-66-9-1931

Eddy, B. E., Borman, G. S., Grubbs, G. E., & Young, R. D. (1962). Identification of the oncogenic substance in rhesus monkey kidney cell cultures as simian virus 40. *Virology*. https://doi.org/10.1016/0042-6822(62)90082-X

Ehlin-Henriksson, B., Gordon, J., & Klein, G. (2003). B-lymphocyte subpopulations are equally susceptible to Epstein-Barr virus infection, irrespective of immunoglobulin isotype expression. *Immunology*. https://doi.org/10.1046/j.1365-2567.2003.01601.x

El-Guindy, A., Ghiassi-Nejad, M., Golden, S., Delecluse, H.-J., & Miller, G. (2013). Essential role of Rta in lytic DNA replication of Epstein-Barr virus. *Journal of Virology*. https://doi.org/10.1128/JVI.01995-12

El-Guindy, A., Heston, L., Delecluse, H. J., & Miller, G. (2007). Phosphoacceptor site S173 in the regulatory domain of Epstein-Barr Virus ZEBRA protein is required for lytic DNA replication but not for activation of viral early genes. *J Virol*, *81*, 3303–3316. https://doi.org/10.1128/JVI.02445-06

El-Guindy, A., Heston, L., & Miller, G. (2010). A subset of replication proteins enhances origin recognition and lytic replication by the epstein-barr virus ZEBRA protein. *PLoS Pathogens*. https://doi.org/10.1371/journal.ppat.1001054

El-Guindy, A. S., & Miller, G. (2004). Phosphorylation of Epstein-Barr virus ZEBRA protein at its casein kinase 2 sites mediates its ability to repress activation of a viral lytic cycle late gene by Rta. *Journal of Virology*. https://doi.org/10.1128/JVI.78.14.7634-7644.2004

El-Guindy, A. S., Paek, S. Y., Countryman, J., & Miller, G. (2006). Identification of constitutive phosphorylation sites on the Epstein-Barr virus ZEBRA protein. *J Biol Chem*, *281*, 3085–3095. https://doi.org/10.1074/jbc.M506076200

Elegheert, J., Bracke, N., Pouliot, P., Gutsche, I., Shkumatov, A. V., Tarbouriech, N., … Savvides, S. N. (2012). Allosteric competitive inactivation of hematopoietic CSF-1 signaling by the viral decoy receptor BARF1. *Nature Structural and Molecular Biology*. https://doi.org/10.1038/nsmb.2367

Ellermann, V., & Bang, O. (1908). Experimentelle leukamie bei huhnern. *Zentralblatt Für Bacteriologie, Parasitenkunde, Infektionskrankheiten Und Hygiene*, (46), 595–609.

Ellis, A. L., Wang, Z., Yu, X., & Mertz, J. E. (2010). Either ZEB1 or ZEB2/SIP1 Can Play a Central Role in Regulating the Epstein-Barr Virus Latent-Lytic Switch in a Cell-Type-Specific Manner. *Journal of Virology*. https://doi.org/10.1128/JVI.02706-09

Epstein, M. A., Achong, B. G., & Barr, Y. M. (1964). VIRUS PARTICLES IN CULTURED LYMPHOBLASTS FROM BURKITT'S LYMPHOMA. *The Lancet*. https://doi.org/10.1016/S0140-6736(64)91524-7

Eyre, T. A., Collins, G. P., Gupta, A., Sheikh, S., Woodcock, V., Whittaker, J., … Middleton, M. R. (2016). Results of a Phase I Study to Assess the Safety, Tolerability, Pharmacokinetics and Pharmacodynamics of CXD101: Preliminary Safety and Activity in Relapsed or Refractory Hodgkin and Non-Hodgkin Lymphoma Patients. *Blood*, *128*(22), 1817. Retrieved from http://www.bloodjournal.org/content/128/22/1817.abstract

Fahmi, H., Cochet, C., Hmama, Z., Opolon, P., & Joab, I. (2000). Transforming growth factor beta 1 stimulates expression of the Epstein-Barr virus BZLF1 immediate-early gene product ZEBRA by an indirect mechanism which requires the MAPK kinase pathway. *Journal of Virology*. https://doi.org/10.1128/JVI.74.13.5810-5818.2000

Falkenberg, K. J., & Johnstone, R. W. (2014). Histone deacetylases and their inhibitors in cancer, neurological diseases and immune disorders. *Nature Reviews Drug Discovery*. https://doi.org/10.1038/nrd4360

Fang, C.-Y., Huang, S.-Y., Wu, C.-C., Hsu, H.-Y., Chou, S.-P., Tsai, C.-H., … Chen, J.-Y. (2012). The Synergistic Effect of Chemical Carcinogens Enhances Epstein-Barr Virus Reactivation and Tumor Progression of Nasopharyngeal Carcinoma Cells. *PLoS ONE*. https://doi.org/10.1371/journal.pone.0044810

Fang, C. Y., Lee, C. H., Wu, C. C., Chang, Y. T., Yu, S. L., Chou, S. P., … Chen, J. Y. (2009). Recurrent chemical reactivations of EBV promotes genome instability and enhances tumor progression of nasopharyngeal carcinoma cells. *International Journal of Cancer*. https://doi.org/10.1002/ijc.24179

Fang, W.-L., Huang, K.-H., Lan, Y.-T., Lin, C.-H., Chang, S.-C., Chen, M.-H., … Shyr, Y.-M. (2016). Mutations in PI3K/AKT pathway genes and amplifications of PIK3CA are associated with patterns of recurrence in gastric cancers. *Oncotarget*, *7*(5), 6201–6220. https://doi.org/10.18632/oncotarget.6641

Fang, W., Zhang, J., Hong, S., Zhan, J., Chen, N., Qin, T., … Zhang, L. (2014). EBV-driven LMP1 and IFN-gamma up-regulate PD-L1 in nasopharyngeal carcinoma: Implications for oncotargeted therapy. *Oncotarget*. Retrieved from http://www.ncbi.nlm.nih.gov/pubmed/25361008

Farrell, P. J., Rowe, D. T., Rooney, C. M., & Kouzarides, T. (1989). Epstein-Barr virus BZLF1 trans-activator specifically binds to a consensus AP-1 site and is related to c-fos. *The EMBO Journal*.

Fearon, E. R., & Vogelstein, B. (1990). A genetic model for colorectal tumorigenesis. *Cell*. https://doi.org/10.1016/0092-8674(90)90186-I

Feederle, R., Kost, M., Baumann, M., Janz, A., Drouet, E., Hammerschmidt, W., & Delecluse, H. J. (2000). The Epstein-Barr virus lytic program is controlled by the co-operative functions of two transactivators. *EMBO J*, *19*, 3080–3089. https://doi.org/10.1093/emboj/19.12.3080

Feng, W. H., Israel, B., Raab-Traub, N., Busson, P., & Kenney, S. C. (2002). Chemotherapy induces lytic EBV replication and confers ganciclovir susceptibility to EBV-positive epithelial cell tumors. *Cancer Research*.

Feng, W. H., Cohen, J. I., Fischer, S., Li, L., Sneller, M., Goldbach-Mansky, R., … Kenney, S. C. (2004a). Reactivation of latent Epstein-Barr virus by methotrexate: A potential contributor to methotrexate-associated lymphomas. *Journal of the National Cancer Institute*. https://doi.org/10.1093/jnci/djh313

Feng, W. H., Hong, G., Delecluse, H., & Kenney, S. (2004b). Lytic induction therapy for Epstein-Barr virus-positive B-cell lymphomas. *Journal of Virology*, *78*(4), 1893–902.

Feng, H., Shuda, M., Chang, Y., & Moore, P. S. (2008). Clonal integration of a polyomavirus in human Merkel cell carcinoma. *Science*. https://doi.org/10.1126/science.1152586

Ferguson, A. R. (1911). Associated bilharziosis and primary malignant disease of the urinary bladder, with observations on a series of forty cases. *The Journal of Pathology and Bacteriology*, *16*(1), 76–94. https://doi.org/10.1002/path.1700160107

Ferlay, J., Soerjomataram, I., Ervik, M., Dikshit, R., Eser, S., Mathers, C., … Bray, F. (2013). Cancer Incidence and Mortality Worldwide: IARC CancerBase. *GLOBOCAN 2012 v1.0*, *11*. https://doi.org/http://globocan.iarc.fr/Pages/fact_sheets_cancer.aspx

Fernández-Medarde, A., & Santos, E. (2011). Ras in cancer and developmental diseases. *Genes and Cancer*. https://doi.org/10.1177/1947601911411084

Fingeroth, J. D., Weis, J. J., Tedder, T. F., Strominger, J. L., Biro, P. a, & Fearon, D. T. (1984). Epstein-Barr virus receptor of human B lymphocytes is the C3d receptor CR2. *Proceedings of the National Academy of Sciences of the United States of America*. https://doi.org/10.1073/pnas.81.14.4510

Fischer, D. K., Miller, G., Gradoville, L., Heston, L., Weststrate, M. W., Maris, W., … Summers, W. C. (1981). Genome of a mononucleosis epstein-barr virus contains DNA fragments previously regarded to be unique to Burkitt's lymphoma isolates. *Cell*. https://doi.org/10.1016/0092-8674(81)90345-7

Fixman, E. D., Hayward, G. S., & Hayward, S. D. (1995). Replication of Epstein-Barr virus oriLyt: lack of a dedicated virally encoded origin-binding protein and dependence on Zta in cotransfection assays. *J Virol*, *69*, 2998–3006. Retrieved from http://www.ncbi.nlm.nih.gov/pubmed/7707526

Flower, K., Thomas, D., Heather, J., Ramasubramanyan, S., Jones, S., & Sinclair, A. J. (2011). Epigenetic control of viral Life-Cycle by a DNA-Methylation dependent transcription factor. *PLoS ONE*. https://doi.org/10.1371/journal.pone.0025922

Frangou, P., Buettner, M., & Niedobitek, G. (2005). Epstein-Barr virus (EBV) infection in epithelial cells in vivo: rare detection of EBV replication in tongue mucosa but not in salivary glands. *The Journal of Infectious Diseases*. https://doi.org/10.1086/426823

Fujii, K., Yokoyama, N., Kiyono, T., Kuzushima, K., Homma, M., Nishiyama, Y., … Tsurumi, T. (2000). The Epstein-Barr virus pol catalytic subunit physically interacts with the BBLF4-BSLF1-BBLF2/3 complex. *Journal of Virology*. https://doi.org/10.1128/JVI.74.6.2550-2557.2000

Fujimuro, M., Inoue, H., Teishikata, Y., Ishida, Y., & Yokosawa, H. (2006). Apoptotic effect of ganciclovir on primary effusion lymphoma cells infected with Kaposi's sarcoma-associated herpesvirus. *Nucleosides, Nucleotides and Nucleic Acids*. https://doi.org/10.1080/15257770600686311

Fukuda, M., & Longnecker, R. (2007). Epstein-Barr virus latent membrane protein 2A mediates transformation through constitutive activation of the Ras/PI3-K/Akt Pathway. *Journal of Virology*. https://doi.org/10.1128/JVI.00537-07

Garnock-Jones, K. P. (2015). Cobimetinib: First Global Approval. *Drugs*. https://doi.org/10.1007/s40265-015-0477-8

Ghanekar, S. A., Nomura, L. E., Suni, M. A., Picker, L. J., Maecker, H. T., & Maino, V. C. (2001). Gamma Interferon Expression in CD8+ T Cells Is a Marker for Circulating Cytotoxic T Lymphocytes That Recognize an HLA A2-Restricted Epitope of Human Cytomegalovirus Phosphoprotein pp65. *Clinical and Vaccine Immunology*. https://doi.org/10.1128/CDLI.8.3.628-631.2001

Ghosh, S. K., Perrine, S. P., & Faller, D. V. (2012a). Advances in virus-directed therapeutics against epstein-barr virus-associated malignancies. *Advances in Virology*. https://doi.org/10.1155/2012/509296

Ghosh, S. K., Perrine, S. P., Williams, R. M., & Faller, D. V. (2012b). Histone deacetylase inhibitors are potent inducers of gene expression in latent EBV and sensitize lymphoma cells to nucleoside antiviral agents. *Blood*. https://doi.org/10.1182/blood-2011-06-362434

Girardi, A. J., Sweet, B. H., Slotnick, V. B., & Hilleman, M. R. (1962). Development of Tumors in Hamsters Inoculated in the Neonatal Period with Vacuolating Virus, SV40. *Proceedings of the Society for Experimental Biology and Medicine*, *109*(3), 649–660. https://doi.org/10.3181/00379727-109-27298

Goswami, R., Gershburg, S., Satorius, A., & Gershburg, E. (2012). Protein kinase inhibitors that inhibit induction of lytic program and replication of Epstein-Barr virus. *Antiviral Research*. https://doi.org/10.1016/j.antiviral.2012.09.021

Gradoville, L., Kwa, D., El-Guindy, A., & Miller, G. (2002). Protein Kinase C-Independent Activation of the Epstein-Barr Virus Lytic Cycle. *Journal of Virology*. https://doi.org/10.1128/JVI.76.11.5612-5626.2002

Grange, J. M., Krone, B., & Mastrangelo, G. (2011). Infection, inflammation and cancer. *International Journal of Cancer*. https://doi.org/10.1002/ijc.25533

Gruffat, H., Duran, N., Buisson, M., Wild, F., Buckland, R., & Sergeant, A. (1992). Characterization of an R-binding site mediating the R-induced activation of the Epstein-Barr virus BMLF1 promoter. *Journal of Virology*.

Gruffat, H., & Sergeant, A. (1994). Characterization of the DNA-binding site repertoire for the epstein - Barr virus transcription factor R. *Nucleic Acids Research*. https://doi.org/10.1093/nar/22.7.1172

Gruffat, H., Renner, O., Pich, D., & Hammerschmidt, W. (1995). Cellular proteins bind to the downstream component of the lytic origin of DNA replication of Epstein-Barr virus. *Journal of Virology*, *69*(3), 1878–86. Retrieved from http://www.ncbi.nlm.nih.gov/pubmed/7853529

Gruffat, H., Batisse, J., Pich, D., Neuhierl, B., Manet, E., Hammerschmidt, W., & Sergeant, A. (2002a). Epstein-Barr virus mRNA export factor EB2 is essential for production of infectious virus. *Journal of Virology*. https://doi.org/10.1128/JVI.76.19.9635-9644.2002

Gruffat, H., Manetr, E., & Sergeant, A. (2002b). MEF2-mediated recruitment of class II HDAC at the EBV immediate early gene BZLF1 links latency and chromatin remodeling. *EMBO Reports*. https://doi.org/10.1093/embo-reports/kvf031

Gulley, M. L., Pulitzer, D. R., Eagan, P. A., & Schneider, B. G. (1996). Epstein-Barr virus infection is an early event in gastric carcinogenesis and is independent of bcl-2 expression and p53 accumulation. *Hum Pathol*, *27*, 20–27. Retrieved from http://www.ncbi.nlm.nih.gov/pubmed/8543306

Guyon, L., Lajaunie, C., Fer, F., Bhajun, R., Sulpice, E., Pinna, G., … Gidrol, X. (2015). Φ-score: A cell-to-cell phenotypic scoring method for sensitive and selective hit discovery in cell-based assays. *Scientific Reports*. https://doi.org/10.1038/srep14221

Hagemeier, S. R., Barlow, E. A., Meng, Q., & Kenney, S. C. (2012). The Cellular Ataxia Telangiectasia-Mutated Kinase Promotes Epstein-Barr Virus Lytic Reactivation in Response to Multiple Different Types of Lytic Reactivation-Inducing Stimuli. *Journal of Virology*. https://doi.org/10.1128/JVI.01850-12

Hagemeier, S. R., Dickerson, S. J., Meng, Q., Yu, X., Mertz, J. E., & Kenney, S. C. (2010). Sumoylation of the Epstein-Barr virus BZLF1 protein inhibits its transcriptional activity and is regulated by the virus-encoded protein kinase. *J Virol*, *84*, 4383–4394. https://doi.org/10.1128/JVI.02369-09

Hahn, A. M., Huye, L. E., Ning, S., Webster-Cyriaque, J., & Pagano, J. S. (2005). Interferon regulatory factor 7 is negatively regulated by the Epstein-Barr virus immediate-early gene, BZLF-1. *Journal of Virology*. https://doi.org/10.1128/JVI.79.15.10040-10052.2005

Halsall, J. A., & Turner, B. M. (2016). Histone deacetylase inhibitors for cancer therapy: An evolutionarily ancient resistance response may explain their limited success. *BioEssays*. https://doi.org/10.1002/bies.201600070

Hammerschmidt, W. (2015). The epigenetic life cycle of epstein-barr virus. In *Epstein Barr Virus*. https://doi.org/10.1007/978-3-319-22822-8_6

Hammerschmidt, W., & Sugden, B. (1988). Identification and characterization of oriLyt, a lytic origin of DNA replication of Epstein-Barr virus. *Cell*, *55*, 427–433. Retrieved from http://www.ncbi.nlm.nih.gov/pubmed/2846181

Hammerschmidt, W., & Sugden, B. (2013). Replication of Epstein-Barr viral DNA. *Cold Spring Harb Perspect Biol*, *5*, a013029. https://doi.org/10.1101/cshperspect.a013029

Hanahan, D., & Weinberg, R. (2011). The Hallmarks of cancer. *Cancer Immunology, Immunotherapy*. https://doi.org/10.1007/s00262-010-0968-0

Hanahan, D., & Weinberg, R. A. (2000). The hallmarks of cancer. *Cancer Immunology, Immunotherapy*. https://doi.org/10.1007/s00262-010-0968-0

Haneklaus, M., Gerlic, M., Kurowska-Stolarska, M., Rainey, A.-A., Pich, D., McInnes, I. B., … Masters, S. L. (2012). Cutting Edge: miR-223 and EBV miR-BART15 Regulate the NLRP3 Inflammasome and IL-1 Production. *The Journal of Immunology*. https://doi.org/10.4049/jimmunol.1200312

Hau, P. M., Deng, W., Jia, L., Yang, J., Tsurumi, T., Chiang, A. K. S., … Tsao, S. W. (2015). Role of ATM in the Formation of the Replication Compartment during Lytic Replication of Epstein-Barr Virus in Nasopharyngeal Epithelial Cells. *Journal of Virology*. https://doi.org/10.1128/JVI.01437-14

Herrero, A. B., Rojas, E. A., Misiewicz-Krzeminska, I., Krzeminski, P., & Gutiérrez, N. C. (2016). Molecular mechanisms of p53 deregulation in cancer: An overview in multiple myeloma. *International Journal of Molecular Sciences*. https://doi.org/10.3390/ijms17122003

Hino, R., Uozaki, H., Murakami, N., Ushiku, T., Shinozaki, A., Ishikawa, S., … Fukayama, M. (2009). Activation of DNA methyltransferase 1 by EBV latent membrane protein 2A leads to promoter hypermethylation of PTEN gene in gastric carcinoma. *Cancer Res*, *69*, 2766–2774. https://doi.org/10.1158/0008-5472.CAN-08-3070

Hjalgrim, H., Friborg, J., & Melbye, M. (2007). The epidemiology of EBV and its association with malignant disease. In A. Arvin, G. Campadelli-Fiume, E. Mocarski, P. S. Moore, B. Roizman, R. Whitley, & K. Yamanishi (Eds.), *Human Herpesviruses: Biology, Therapy, and Immunoprophylaxis*. Cambridge. Retrieved from http://www.ncbi.nlm.nih.gov/pubmed/21348109

Ho, J. H. C., Huang, D. P., & Fong, Y. Y. (1978). SALTED FISH AND NASOPHARYNGEAL CARCINOMA IN SOUTHERN CHINESE. *The Lancet*. https://doi.org/10.1016/S0140-6736(78)92844-1

Hong, G. K., Gulley, M. L., Feng, W.-H., Delecluse, H.-J., Holley-Guthrie, E., & Kenney, S. C. (2005). Epstein-Barr Virus Lytic Infection Contributes to Lymphoproliferative Disease in a SCID Mouse Model. *Journal of Virology*. https://doi.org/10.1128/JVI.79.22.13993-14003.2005

Höring, E., Podlech, O., Silkenstedt, B., Rota, I. A., Adamopoulou, E., & Naumann, U. (2013). The histone deacetylase inhibitor trichostatin a promotes apoptosis and antitumor immunity in glioblastoma cells. *Anticancer Research*. https://doi.org/33/4/1351

Horst, D., Burmeister, W. P., Boer, I. G. J., van Leeuwen, D., Buisson, M., Gorbalenya, A. E., … Ressing, M. E. (2012). The "Bridge" in the Epstein-Barr Virus Alkaline Exonuclease Protein BGLF5 Contributes to Shutoff Activity during Productive Infection. *Journal of Virology*. https://doi.org/10.1128/JVI.00309-12

Horst, D., Favaloro, V., Vilardi, F., van Leeuwen, H. C., Garstka, M. A., Hislop, A. D., … Wiertz, E. J. H. J. (2011). EBV Protein BNLF2a Exploits Host Tail-Anchored Protein Integration Machinery To Inhibit TAP. *The Journal of Immunology*. https://doi.org/10.4049/jimmunol.1002656

Horst, D., van Leeuwen, D., Croft, N. P., Garstka, M. A., Hislop, A. D., Kremmer, E., … Ressing, M. E. (2009). Specific Targeting of the EBV Lytic Phase Protein BNLF2a to the Transporter Associated with Antigen Processing Results in Impairment of HLA Class I-Restricted Antigen Presentation. *The Journal of Immunology*. https://doi.org/10.4049/jimmunol.0803218

Hsu, C.-L., Kuo, Y.-C., Huang, Y., Huang, Y.-C., Lui, K.-W., Chang, K.-P., … Chang, Y.-S. (2015). Application of a patient-derived xenograft model in cytolytic viral activation therapy for nasopharyngeal carcinoma. *Oncotarget*. https://doi.org/10.18632/oncotarget.5544

Hsu, D. H., de Waal Malefyt, R., Fiorentino, D. F., Dang, M. N., Vieira, P., de Vries, J., … Moore, K. W. (1990). Expression of interleukin-10 activity by Epstein-Barr virus protein BCRF1. *Science (New York, N.Y.)*. https://doi.org/10.1126/science.2173142

Hsu, W. L., Chen, J. Y., Chien, Y. C., Liu, M. Y., You, S. L., Hsu, M. M., … Chen, C. J. (2009). Independent effect of EBV and cigarette smoking on nasopharyngeal carcinoma: A 20-year follow-up study on 9,622 males without family history in Taiwan. *Cancer Epidemiology Biomarkers and Prevention*. https://doi.org/10.1158/1055-9965.EPI-08-1175

Hu, H., Luo, M.-L., Desmedt, C., Nabavi, S., Yadegarynia, S., Hong, A., … Wulf, G. M. (2016). Epstein–Barr Virus Infection of Mammary Epithelial Cells Promotes Malignant Transformation. *EBioMedicine*. https://doi.org/10.1016/j.ebiom.2016.05.025

Huang, W. T., & Lin, C. W. (2014). EBV-encoded miR-BART20-5p and miR-BART8 inhibit the IFN-γ-STAT1 pathway associated with disease progression in nasal NK-cell lymphoma. *American Journal of Pathology*. https://doi.org/10.1016/j.ajpath.2013.12.024

Huang, Y. T., Sheen, T. S., Chen, C. L., Lu, J., Chang, Y., Chen, J. Y., & Tsai, C. H. (1999). Profile of cytokine expression in nasopharyngeal carcinomas: a distinct expression of interleukin 1 in tumor and CD4+ T cells. *Cancer Res*, *59*, 1599–1605. Retrieved from http://www.ncbi.nlm.nih.gov/pubmed/10197635

Huang, Fang, C. Y., Tsai, C. H., Chang, Y., Takada, K., Hsu, T. Y., & Chen, J. Y. (2010). N-methyl-N'-nitro-N-nitrosoguanidine induces and cooperates with 12-O-tetradecanoylphorbol-1,3-acetate/sodium butyrate to enhance Epstein-Barr virus reactivation and genome instability in nasopharyngeal carcinoma cells. *Chemico-Biological Interactions*, *188*(3), 623–634. https://doi.org/10.1016/j.cbi.2010.09.020

Huang, Liu, M. Y., Tsai, C. H., & Yeh, T. H. (2010). Upregulation of interleukin-1 by Epstein-Barr virus latent membrane protein 1 and its possible role in nasopharyngeal carcinoma cell growth. *Head Neck*, *32*(7), 869–876. https://doi.org/10.1002/hed.21270

Hughes, D. J., Dickerson, C. a, Shaner, M. S., Sample, C. E., & Sample, J. T. (2011). trans-Repression of protein expression dependent on the Epstein-Barr virus promoter Wp during latency. *Journal of Virology*. https://doi.org/10.1128/JVI.05158-11

Hui, K. F., Cheung, A. K. L., Choi, C. K., Yeung, P. L., Middeldorp, J. M., Lung, M. L., … Chiang, A. K. S. (2016). Inhibition of class I histone deacetylases by romidepsin potently induces Epstein-Barr virus lytic cycle and mediates enhanced cell death with ganciclovir. *International Journal of Cancer*. https://doi.org/10.1002/ijc.29698

Hui, K. F., & Chiang, A. K. S. (2010). Suberoylanilide hydroxamic acid induces viral lytic cycle in Epstein-Barr virus-positive epithelial malignancies and mediates enhanced cell death. *International Journal of Cancer*. https://doi.org/10.1002/ijc.24945

Hui, K. F., Lam, B. H. W., Ho, D. N., Tsao, S. W., & Chiang, A. K. S. (2013). Bortezomib and SAHA Synergistically Induce ROS-Driven Caspase-Dependent Apoptosis of Nasopharyngeal Carcinoma and Block Replication of Epstein-Barr Virus. *Molecular Cancer Therapeutics*. https://doi.org/10.1158/1535-7163.MCT-12-0811

Hui, K. F., Leung, Y. Y., Yeung, P. L., Middeldorp, J. M., & Chiang, A. K. S. (2014). Combination of SAHA and bortezomib up-regulates CDKN2A and CDKN1A and induces apoptosis of Epstein-Barr virus-positive Wp-restricted Burkitt lymphoma and lymphoblastoid cell lines. *British Journal of Haematology*. https://doi.org/10.1111/bjh.13089

Hunziker, A., Jensen, M. H., & Krishna, S. (2010). Stress-specific response of the p53-Mdm2 feedback loop. *BMC Systems Biology*. https://doi.org/10.1186/1752-0509-4-94

IARC Working Group on the Evaluation of Carcinogenic Risks to Humans. (2012). Biological agents. Volume 100 B. A review of human carcinogens. *IARC Monographs on the Evaluation of Carcinogenic Risks to Humans / World Health Organization, International Agency for Research on Cancer*.

IARC Working Group on the Evaluation of Carcinogenic Risks to Humans. (2014). Malaria and Some Polyomaviruses (Sv40, Bk, Jc, and Merkel Cell Viruses). *IARC Monographs on the Evaluation of Carcinogenic Risks to Humans / World Health Organization, International Agency for Research on Cancer*.

Iempridee, T., Das, S., Xu, I., & Mertz, J. E. (2011). Transforming Growth Factor -Induced Reactivation of Epstein-Barr Virus Involves Multiple Smad-Binding Elements Cooperatively Activating Expression of the Latent-Lytic Switch BZLF1 Gene. *Journal of Virology*. https://doi.org/10.1128/JVI.01197-10

Im, H. J., Pittelkow, M. R., & Kumar, R. (2002). Divergent regulation of the growth-promoting gene IEX-1 by the p53 tumor suppressor and Sp1. *Journal of Biological Chemistry*. https://doi.org/10.1074/jbc.M109414200

Inman, G. J., Binné, U. K., Parker, G. A., Farrell, P. J., & Allday, M. J. (2001). Activators of the Epstein-Barr virus lytic program concomitantly induce apoptosis, but lytic gene expression protects from cell death. *Journal of Virology*. https://doi.org/10.1128/JVI.75.5.2400-2410.2001

Isik, S., Sano, K., Tsutsui, K., Seki, M., Enomoto, T., Saitoh, H., & Tsutsui, K. (2003). The SUMO pathway is required for selective degradation of DNA topoisomerase IIβ induced by a catalytic inhibitor ICRF-193. *FEBS Letters*. https://doi.org/10.1016/S0014-5793(03)00637-9

Ismail, I. H., Nyström, S., Nygren, J., & Hammarsten, O. (2005). Activation of ataxia telangiectasia mutated by DNA strand break-inducing agents correlates closely with the number of DNA double strand breaks. *Journal of Biological Chemistry*. https://doi.org/10.1074/jbc.M411588200

Ito, A., Kawaguchi, Y., Lai, C. H., Kovacs, J. J., Higashimoto, Y., Appella, E., & Yao, T. P. (2002). MDM2-HDAC1-mediated deacetylation of p53 is required for its degradation. *EMBO Journal*. https://doi.org/10.1093/emboj/cdf616

Iwahori, S., Murata, T., Kudoh, A., Sato, Y., Nakayama, S., Isomura, H., … Tsurumi, T. (2009). Phosphorylation of p27Kip1 by Epstein-Barr virus protein kinase induces its degradation through SCFSkp2 ubiquitin ligase actions during viral lytic replication. *J Biol Chem*, *284*, 18923–18931. https://doi.org/10.1074/jbc.M109.015123

Iwakiri, D., & Takada, K. (2004). Phosphatidylinositol 3-kinase is a determinant of responsiveness to B cell antigen receptor-mediated Epstein-Barr virus activation. *Journal of Immunology (Baltimore, Md. : 1950)*. https://doi.org/10.4049/jimmunol.172.3.1561

Iyer, S. P., & Foss, F. F. (2015). Romidepsin for the Treatment of Peripheral T-Cell Lymphoma. *The Oncologist*. https://doi.org/10.1634/theoncologist.2015-0043

Izumi, K. M., & Kieff, E. D. (1997). The Epstein-Barr virus oncogene product latent membrane protein 1 engages the tumor necrosis factor receptor-associated death domain protein to mediate B lymphocyte growth transformation and activate NF-kappaB. *Proceedings of the National Academy of Sciences of the United States of America*.

Jain, S., & Zain, J. (2011). Romidepsin in the treatment of cutaneous T-cell lymphoma. *Journal of Blood Medicine*. https://doi.org/10.2147/JBM.S9649

Janz, A., Oezel, M., Kurzeder, C., Mautner, J., Pich, D., Kost, M., … Delecluse, H. J. (2000). Infectious Epstein-Barr virus lacking major glycoprotein BLLF1 (gp350/220) demonstrates the existence of additional viral ligands. *Journal of Virology*. https://doi.org/10.1128/JVI.74.21.10142-10152.2000

Javier, R. T., & Butel, J. S. (2008). The history of tumor virology. *Cancer Research*. https://doi.org/10.1158/0008-5472.CAN-08-3301

Jayasurya, A., Bay, B. H., Yap, W. M., & Tan, N. G. (2000). Lymphocytic infiltration in undifferentiated nasopharyngeal cancer. *Archives of Otolaryngology--Head & Neck Surgery*.

Jenkins, F. J., & Hoffman, L. J. (2000). Overview of Herpesviruses. In J. J. Goedert (Ed.), *Infectious Causes of Cancer: Targets for Intervention* (pp. 33–49). Totowa, NJ: Humana Press. https://doi.org/10.1007/978-1-59259-024-7_2

Jenkins, P. J., Binné, U. K., & Farrell, P. J. (2000). Histone acetylation and reactivation of Epstein-Barr virus from latency. *Journal of Virology*. https://doi.org/10.1128/JVI.74.2.710-720.2000

Jia, W.-H., & Qin, H.-D. (2012). Non-viral environmental risk factors for nasopharyngeal carcinoma: A systematic review. *Seminars in Cancer Biology*. https://doi.org/10.1016/j.semcancer.2012.01.009

Jiang, J. H., Wang, N., Li, A., Liao, W. T., Pan, Z. G., Mai, S. J., … Zeng, Y. X. (2006). Hypoxia can contribute to the induction of the Epstein-Barr virus (EBV) lytic cycle. *Journal of Clinical Virology*. https://doi.org/10.1016/j.jcv.2006.06.013

Jiang, W., Liu, K., Guo, Q., Cheng, J., Shen, L., Cao, Y., … Cai, K. (2017). Tumor-infiltrating immune cells and prognosis in gastric cancer: a systematic review and meta-analysis. *Oncotarget*. https://doi.org/10.18632/oncotarget.17602

Jochum, S., Moosmann, A., Lang, S., Hammerschmidt, W., & Zeidler, R. (2012). The EBV immunoevasins vIL-10 and BNLF2a protect newly infected B cells from immune recognition and elimination. *PLoS Pathogens*. https://doi.org/10.1371/journal.ppat.1002704

Johannsen, E., Luftig, M., Chase, M. R., Weicksel, S., Cahir-McFarland, E., Illanes, D., … Kieff, E. (2004). Proteins of purified Epstein-Barr virus. *Proceedings of the National Academy of Sciences*. https://doi.org/10.1073/pnas.0407320101

Jones, R. B., O'Connor, R., Mueller, S., Foley, M., Szeto, G. L., Karel, D., … Walker, B. D. (2014). Histone deacetylase inhibitors impair the elimination of hiv-infected cells by cytotoxic t-lymphocytes. *PLoS Pathogens*. https://doi.org/10.1371/journal.ppat.1004287

Kaklamani, V. G., & Gradishar, W. J. (2003). Epirubicin versus doxorubicin: Which is the anthracycline of choice for the treatment of breast cancer? *Clinical Breast Cancer*. https://doi.org/10.3816/CBC.2003.s.012

Kalla, M., & Hammerschmidt, W. (2012). Human B cells on their route to latent infection - Early but transient expression of lytic genes of Epstein-Barr virus. *European Journal of Cell Biology*. https://doi.org/10.1016/j.ejcb.2011.01.014

Kalla, M., Schmeinck, A., Bergbauer, M., Pich, D., & Hammerschmidt, W. (2010). AP-1 homolog BZLF1 of Epstein-Barr virus has two essential functions dependent on the epigenetic state of the viral genome. *Proceedings of the National Academy of Sciences*. https://doi.org/10.1073/pnas.0911948107

Kanda, T., Furuse, Y., Oshitani, H., & Kiyono, T. (2016). Highly Efficient CRISPR/Cas9-Mediated Cloning and Functional Characterization of Gastric Cancer-Derived Epstein-Barr Virus Strains. *Journal of Virology*, *90*(9), 4383–4393. https://doi.org/10.1128/JVI.00060-16

Kao, J.-H. (2015). Hepatitis B vaccination and prevention of hepatocellular carcinoma. *Best Practice & Research Clinical Gastroenterology*, *29*(6), 907–917. https://doi.org/10.1016/j.bpg.2015.09.011

Karimi, P., Islami, F., Anandasabapathy, S., Freedman, N. D., & Kamangar, F. (2014). Gastric cancer: descriptive epidemiology, risk factors, screening, and prevention. *Cancer Epidemiology, Biomarkers & Prevention : A Publication of the American Association for Cancer Research, Cosponsored by the American Society of Preventive Oncology*. https://doi.org/10.1158/1055-9965.EPI-13-1057

Karlsson, Q. H., Schelcher, C., Verrall, E., Petosa, C., & Sinclair, A. J. (2008). Methylated DNA recognition during the reversal of epigenetic silencing is regulated by cysteine and serine residues in the Epstein-Barr virus lytic switch protein. *PLoS Pathogens*. https://doi.org/10.1371/journal.ppat.1000005

Kathiravan, M. K., Khilare, M. M., Nikoomanesh, K., Chothe, A. S., & Jain, K. S. (2013). Topoisomerase as target for antibacterial and anticancer drug discovery. *Journal of Enzyme Inhibition and Medicinal Chemistry*. https://doi.org/10.3109/14756366.2012.658785

Kawanishi. (1993a). Epstein-Barr virus induces fragmentation of chromosomal DNA during lytic infection. *Journal of Virology*, *67*(12), 7654–8. Retrieved from http://www.pubmedcentral.nih.gov/articlerender.fcgi?artid=238235&tool=pmcentrez&rendertype=abstract

Kawanishi. (1993b). Topoisomerase I and II activities are required for Epstein-Barr virus replication. *Journal of General Virology*, *74*(10), 2263–2268. https://doi.org/10.1099/0022-1317-74-10-2263

Keating, S., Prince, S., Jones, M., & Rowe, M. (2002). The Lytic Cycle of Epstein-Barr Virus Is Associated with Decreased Expression of Cell Surface Major Histocompatibility Complex Class I and Class II Molecules. *JOURNAL OF VIROLOGY*. https://doi.org/10.1128/JVI.76.16.8179–8188.2002

Kedes, D. H., & Ganem, D. (1997). Sensitivity of Kaposi's sarcoma-associated herpesvirus replication to antiviral drugs. Implications for potential therapy. *J Clin Invest*. https://doi.org/10.1172/JCI119380

Kenney, S. C., & Mertz, J. E. (2014). Regulation of the latent-lytic switch in Epstein-Barr virus. *Seminars in Cancer Biology*. https://doi.org/10.1016/j.semcancer.2014.01.002

Khan, A. N. H., Gregorie, C. J., & Tomasi, T. B. (2008). Histone deacetylase inhibitors induce TAP, LMP, Tapasin genes and MHC class I antigen presentation by melanoma cells. *Cancer Immunology, Immunotherapy*. https://doi.org/10.1007/s00262-007-0402-4

Khan, G., Hashim, M., Parkin, D., Martel, C. De, Ferlay, J., Franceschi, S., … Nabel, G. (2014). Global burden of deaths from Epstein-Barr virus attributable malignancies 1990-2010. *Infectious Agents and Cancer*. https://doi.org/10.1186/1750-9378-9-38

Kieser, A. (2007). Signal transduction by the Epstein-Barr virus oncogene latent membrane protein 1 (LMP1). *Signal Transduction*. https://doi.org/10.1002/sita.200600116

Kim, D. N., Seo, M. K., Choi, H., Kim, S. Y., Shin, H. J., Yoon, A. R., … Lee, S. K. (2013). Characterization of naturally Epstein-Barr virus-infected gastric carcinoma cell line YCCEL1. *Journal of General Virology*. https://doi.org/10.1099/vir.0.045237-0

Kim, Y., Kim, J. H., Ki, C. S., Ko, Y. H., Kim, J. S., & Kim, W. S. (2016a). Epstein-Barr virus reactivation in extranodal natural killer/T-cell lymphoma patients: A previously unrecognized serious adverse event in a pilot study with romidepsin. *Annals of Oncology*, *27*(3), 508–513. https://doi.org/10.1093/annonc/mdv596

Kim, S., Thiessen, P. A., Bolton, E. E., Chen, J., Fu, G., Gindulyte, A., … Bryant, S. H. (2016b). PubChem substance and compound databases. *Nucleic Acids Research*, *44*(D1), D1202–D1213. https://doi.org/10.1093/nar/gkv951

Kirschbaum, M., Frankel, P., Popplewell, L., Zain, J., Delioukina, M., Pullarkat, V., … Newman, E. (2011). Phase II study of vorinostat for treatment of relapsed or refractory indolent non-Hodgkin's lymphoma and mantle cell lymphoma. *Journal of Clinical Oncology : Official Journal of the American Society of Clinical Oncology*. https://doi.org/10.1200/JCO.2010.32.1398

Kirschner, A. N., Omerovic, J., Popov, B., Longnecker, R., & Jardetzky, T. S. (2006). Soluble Epstein-Barr virus glycoproteins gH, gL, and gp42 form a 1:1:1 stable complex that acts like soluble gp42 in B-cell fusion but not in epithelial cell fusion. *Journal of Virology*. https://doi.org/10.1128/JVI.00572-06

Kirschner, A. N., Sorem, J., Longnecker, R., & Jardetzky, T. S. (2009). Structure of Epstein-Barr Virus Glycoprotein 42 Suggests a Mechanism for Triggering Receptor-Activated Virus Entry. *Structure*. https://doi.org/10.1016/j.str.2008.12.010

Klass, C. M., Krug, L. T., Pozharskaya, V. P., & Offermann, M. K. (2005). The targeting of primary effusion lymphoma cells for apoptosis by inducing lytic replication of human herpesvirus 8 while blocking virus production. *Blood*. https://doi.org/10.1182/blood-2004-09-3569

Knipe, D. N., & Howley, P. M. (2013). *Fields' Virology - Sixth Edition*. *Lippincott Williams & Wilkins*. https://doi.org/9781451105636

Kobayashi, Y., Gélinas, C., & Dougherty, J. P. (2017). Histone deacetylase inhibitors containing a benzamide functional group and a pyridyl cap are preferentially effective human immunodeficiency virus-1 latency-reversing agents in primary resting CD4+T cells. *Journal of General Virology*. https://doi.org/10.1099/jgv.0.000716

Kouzarides, T., Packham, G., Cook, A., & J Farrell, P. (1991). *The BZLF1 protein of EBV has a coiled coil dimerisation domain without a heptad leucine repeat but with homology to the C/EBP leucine zipper*. *Oncogene* (Vol. 6).

Kraus, R. J., Perrigoue, J. G., & Mertz, J. E. (2003). ZEB negatively regulates the lytic-switch BZLF1 gene promoter of Epstein-Barr virus. *Journal of Virology*. https://doi.org/10.1128/JVI.77.1.199

Kraus, R. J., Yu, X., Cordes, B. leaf A., Sathiamoorthi, S., Iempridee, T., Nawandar, D. M., … Mertz, J. E. (2017). Hypoxia-inducible factor-1α plays roles in Epstein-Barr virus's natural life cycle and tumorigenesis by inducing lytic infection through direct binding to the immediate-early BZLF1 gene promoter. *PLoS Pathogens*. https://doi.org/10.1371/journal.ppat.1006404

Kroll, J., Li, S., Levi, M., & Weinberg, A. (2011). Lytic and latent EBV gene expression in transplant recipients with and without post-transplant lymphoproliferative disorder. *Journal of Clinical Virology*. https://doi.org/10.1016/j.jcv.2011.06.013

Krug, L. T., Pozharskaya, V. P., Yu, Y., Inoue, N., & Offermann, M. K. (2004). Inhibition of infection and replication of human herpesvirus 8 in microvascular endothelial cells by alpha interferon and phosphonoformic acid. *J Virol.* https://doi.org/10.1128/JVI.78.15.8359-8371.2004

Kruse, J. P., & Gu, W. (2009). Modes of p53 Regulation. *Cell*. https://doi.org/10.1016/j.cell.2009.04.050

Ku, J.-L., Kim, K.-H., Choi, J.-S., Kim, S.-H., Shin, Y.-K., Chang, H. J., … Park, J.-G. (2012). Establishment and characterization of six human gastric carcinoma cell lines, including one naturally infected with Epstein-Barr virus. *Cellular Oncology (Dordrecht)*. https://doi.org/10.1007/s13402-012-0073-9

Kudoh, A., Daikoku, T., Sugaya, Y., Isomura, H., Fujita, M., Kiyono, T., … Tsurumi, T. (2003a). Inhibition of S-Phase Cyclin-Dependent Kinase Activity Blocks Expression of Epstein-Barr Virus Immediate-Early and Early Genes, Preventing Viral Lytic Replication. *Journal of Virology*, *78*(1), 104–115. https://doi.org/10.1128/JVI.78.1.104-115.2004

Kudoh, A., Fujita, M., Kiyono, T., Kuzushima, K., Sugaya, Y., Izuta, S., … Tsurumi, T. (2003b). Reactivation of lytic replication from B cells latently infected with Epstein-Barr virus occurs with high S-phase cyclin-dependent kinase activity while inhibiting cellular DNA replication. *Journal of Virology*. https://doi.org/10.1128/JVI.77.2.851-861.2003

Kudoh, A., Fujita, M., Zhang, L., Shirata, N., Daikoku, T., Sugaya, Y., … Tsurumi, T. (2005). Epstein-Barr virus lytic replication elicits ATM checkpoint signal transduction while providing an S-phase-like cellular environment. *Journal of Biological Chemistry*. https://doi.org/10.1074/jbc.M411405200

Kudoh, A., Daikoku, T., Ishimi, Y., Kawaguchi, Y., Shirata, N., Iwahori, S., … Tsurumi, T. (2006). Phosphorylation of MCM4 at Sites Inactivating DNA Helicase Activity of the MCM4-MCM6-MCM7 Complex during Epstein-Barr Virus Productive Replication. *Journal of Virology*. https://doi.org/10.1128/JVI.00678-06

Kudoh, A., Iwahori, S., Sato, Y., Nakayama, S., Isomura, H., Murata, T., & Tsurumi, T. (2009). Homologous recombinational repair factors are recruited and loaded onto the viral DNA genome in Epstein-Barr virus replication compartments. *J Virol*, *83*, 6641–6651. https://doi.org/10.1128/JVI.00049-09

Kurth, J., Hansmann, M.-L., Rajewsky, K., & Küppers, R. (2003). Epstein-Barr virus-infected B cells expanding in germinal centers of infectious mononucleosis patients do not participate in the germinal center reaction. *Proceedings of the National Academy of Sciences of the United States of America*. https://doi.org/10.1073/pnas.2627966100

Kurth, J., Spieker, T., Wustrow, J., Strickler, G. J., Hansmann, L. M., Rajewsky, K., & Küppers, R. (2000). EBV-infected B cells in infectious mononucleosis: viral strategies for spreading in the B cell compartment and establishing latency. *Immunity*. https://doi.org/10.1016/S1074-7613(00)00048-0

Kvansakul, M., Wei, A. H., Fletcher, J. I., Willis, S. N., Chen, L., Roberts, A. W., … Colman, P. M. (2010). Structural basis for apoptosis inhibition by Epstein-Barr virus bhrf1. *PLoS Pathogens*. https://doi.org/10.1371/journal.ppat.1001236

Laichalk, L. L., & Thorley-Lawson, D. A. (2005). Terminal differentiation into plasma cells initiates the replicative cycle of Epstein-Barr virus in vivo. *J Virol*. https://doi.org/10.1128/JVI.79.2.1296-1307.2005

Larsen, A. K., Escargueil, A. E., & Skladanowski, A. (2003). Catalytic topoisomerase II inhibitors in cancer therapy. *Pharmacology & Therapeutics*. https://doi.org/10.1016/S0163-7258(03)00058-5

Lee, H.-Z., Kwitkowski, V. E., Del Valle, P. L., Ricci, M. S., Saber, H., Habtemariam, B. A., … Pazdur, R. (2015). FDA Approval: Belinostat for the Treatment of Patients with Relapsed or Refractory Peripheral T-cell Lymphoma. *Clinical Cancer Research : An Official Journal of the American Association for Cancer Research*. https://doi.org/10.1158/1078-0432.CCR-14-3119

Lee, J., van Hummelen, P., Go, C., Palescandolo, E., Jang, J., Park, H. Y., … Kim, K. M. (2012). High-throughput mutation profiling identifies frequent somatic mutations in advanced gastric Adenocarcinoma. *PLoS ONE*. https://doi.org/10.1371/journal.pone.0038892

Lerner, M. A., & Beqaj, S. (2012). Abortive lytic Epstein-Barr virus replication in tonsil-B lymphocytes in infectious mononucleosis and a subset of the chronic fatigue syndrome. *Virus Adaptation and Treatment*. https://doi.org/10.2147/VAAT.S36540

Levitskaya, J., Sharipo, A., Leonchiks, A., Ciechanover, A., & Masucci, M. G. (1997). Inhibition of ubiquitin/proteasome-dependent protein degradation by the Gly-Ala repeat domain of the Epstein–Barr virus nuclear antigen 1. *Proceedings of the National Academy of Sciences of the United States of America*, *94*(23), 12616–12621. Retrieved from http://www.ncbi.nlm.nih.gov/pmc/articles/PMC25057/

Li, L., Zhang, Y., Guo, B. B., Chan, F. K. L., & Tao, Q. (2014). Oncogenic induction of cellular high CpG methylation by Epstein-Barr virus in malignant epithelial cells. *Chinese Journal of Cancer*. https://doi.org/10.5732/cjc.014.10191

Li, Q. Q., Hao, J. J., Zhang, Z., Hsu, I., Liu, Y., Tao, Z., … Agarwal, P. K. (2016). Histone deacetylase inhibitor-induced cell death in bladder cancer is associated with chromatin modification and modifying protein expression: A proteomic approach. *International Journal of Oncology*. https://doi.org/10.3892/ijo.2016.3478

Li, Y., & Seto, E. (2016). HDACs and HDAC inhibitors in cancer development and therapy. *Cold Spring Harbor Perspectives in Medicine*. https://doi.org/10.1101/cshperspect.a026831

Lieberman, P. M. (2014). Epstein-Barr virus turns 50. *Science*. https://doi.org/10.1126/science.1252786

Lin, R.-K., Wu, C.-Y., Chang, J.-W., Juan, L.-J., Hsu, H.-S., Chen, C.-Y., … Wang, Y.-C. (2010). Dysregulation of p53/Sp1 Control Leads to DNA Methyltransferase-1 Overexpression in Lung Cancer. *Cancer Research*, *70*(14), 5807. Retrieved from http://cancerres.aacrjournals.org/content/70/14/5807.abstract

Lin, T. C., Liu, T. Y., Hsu, S. M., & Lin, C. W. (2013). Epstein-barr virus-encoded miR-BART20-5p inhibits t-bet translation with secondary suppression of p53 in invasive nasal NK/T-cell lymphoma. *American Journal of Pathology*. https://doi.org/10.1016/j.ajpath.2013.01.025

Lindemann, R. K., Newbold, a, Whitecross, K. F., Cluse, L. a, Frew, a J., Ellis, L., … Johnstone, R. W. (2007). Analysis of the apoptotic and therapeutic activities of histone deacetylase inhibitors by using a mouse model of B cell lymphoma. *Proceedings of the National Academy of Sciences of the United States of America*. https://doi.org/10.1073/pnas.0702294104

Liu, F., & Zhou, Z. H. (2007). Comparative virion structures of human herpesviruses. In M. E. Arvin A, Campadelli-Fiume G (Ed.), *Human Herpesviruses: Biology, Therapy, and Immunoprophylaxis*. Cambridge University Press. https://doi.org/https://www.ncbi.nlm.nih.gov/books/NBK47399/

Liu, P., & Speck, S. H. (2003). Synergistic autoactivation of the Epstein-Barr virus immediate-early BRLF1 promoter by Rta and Zta. *Virology*. https://doi.org/10.1016/S0042-6822(03)00145-4

Liu, S., Liu, P., Borras, A., Chatila, T., & Speck, S. H. (1997). Cyclosporin A-sensitive induction of the Epstein-Barr virus lytic switch is mediated via a novel pathway involving a MEF2 family member. *EMBO Journal*. https://doi.org/10.1093/emboj/16.1.143

Lu, X., Ning, Z., Li, Z., Cao, H., & Wang, X. (2016). Development of chidamide for peripheral T-cell lymphoma, the first orphan drug approved in China. *Intractable and Rare Diseases Research*. https://doi.org/10.5582/irdr.2016.01024

Lucas, C. L., Kuehn, H. S., Zhao, F., Niemela, J. E., Deenick, E. K., Palendira, U., … Uzel, G. (2014). Dominant-activating germline mutations in the gene encoding the PI(3)K catalytic subunit p110delta result in T cell senescence and human immunodeficiency. *Nat Immunol*. https://doi.org/10.1038/ni.2771

Luka, J., Kallin, B., & Klein, G. (1979). Induction of the Epstein-Barr virus (EBV) cycle in latently infected cells by n-butyrate. *Virology*. https://doi.org/10.1016/0042-6822(79)90455-0

Luu, T. H., Morgan, R. J., Leong, L., Lim, D., McNamara, M., Portnow, J., … Somlo, G. (2008). A phase II trial of vorinostat (suberoylanilide hydroxamic acid) in metastatic breast cancer: a California Cancer Consortium study. *Clinical Cancer Research : An Official Journal of the American Association for Cancer Research*. https://doi.org/10.1158/1078-0432.CCR-08-0122

Ma, H. T., & Poon, R. Y. C. (2011). Synchronization of HeLa Cells. In G. Banfalvi (Ed.), *Cell Cycle Synchronization: Methods and Protocols* (pp. 151–161). Totowa, NJ: Humana Press. https://doi.org/10.1007/978-1-61779-182-6_10

Ma, S.-D., Yu, X., Mertz, J. E., Gumperz, J. E., Reinheim, E., Zhou, Y., … Kenney, S. C. (2012). An Epstein-Barr Virus (EBV) Mutant with Enhanced BZLF1 Expression Causes Lymphomas with Abortive Lytic EBV Infection in a Humanized Mouse Model. *Journal of Virology*. https://doi.org/10.1128/JVI.00770-12

Mahdavifar, N., Ghoncheh, M., Mohammadian-Hafshejani, A., Khosravi, B., & Salehiniya, H. (2016). Epidemiology and Inequality in the Incidence and Mortality of Nasopharynx Cancer in Asia. *Osong Public Health and Research Perspectives*. https://doi.org/10.1016/j.phrp.2016.11.002

Mann, B. S., Johnson, J. R., Cohen, M. H., Justice, R., & Pazdur, R. (2007). FDA approval summary: vorinostat for treatment of advanced primary cutaneous T-cell lymphoma. *Oncologist*. https://doi.org/10.1634/theoncologist.12-10-1247

Mansouri, S., Wang, S., & Frappier, L. (2013). A Role for the Nucleosome Assembly Proteins TAF-Iβ and NAP1 in the Activation of BZLF1 Expression and Epstein-Barr Virus Reactivation. *PLoS ONE*, *8*(5). https://doi.org/10.1371/journal.pone.0063802

Mao, Y., Desai, S. D., & Liu, L. F. (2000). SUMO-1 conjugation to human DNA topoisomerase II isozymes. *Journal of Biological Chemistry*. https://doi.org/10.1074/jbc.M001831200

Mao, Y., Sun, M., Desai, S. D., & Liu, L. F. (2000). SUMO-1 conjugation to topoisomerase I: A possible repair response to topoisomerase-mediated DNA damage. *Proceedings of the National Academy of Sciences of the United States of America*. https://doi.org/10.1073/pnas.080536597

Marshall, B. J., Armstrong, J. A., McGechie, D. B., & Glancy, R. J. (1985). Attempt to fulfil Koch's postulates for pyloric campylobacter. *Medical Journal of Australia*.

Marshall, B. J., & Warren, J. R. (1984). UNIDENTIFIED CURVED BACILLI IN THE STOMACH OF PATIENTS WITH GASTRITIS AND PEPTIC ULCERATION. *The Lancet*. https://doi.org/10.1016/S0140-6736(84)91816-6

Martel, C. De, Ferlay, J., Franceschi, S., Vignat, J., Bray, F., Forman, D., & Plummer, M. (2012). Global burden of cancer attributable to infections in 2008: a review and synthetic analysis. *Lancet Oncol*. https://doi.org/10.1016/S1470-2045(12)70137-7

Martin, G. S. (2004). The road to Src. *Oncogene*. https://doi.org/10.1038/sj.onc.1208077

Martin, G. S., Radke, K., Hughes, S., Quintrell, N., Bishop, J. M., & Varmus, H. E. (1979). Mutants of rous sarcoma virus with extensive deletions of the viral genome. *Virology*. https://doi.org/10.1016/0042-6822(79)90109-0

Martin, N. K., Vickerman, P., Dore, G. J., Grebely, J., Miners, A., Cairns, J., … Hickman, M. (2016). Prioritization of HCV treatment in the direct-acting antiviral era: An economic evaluation. *Journal of Hepatology*. https://doi.org/10.1016/j.jhep.2016.02.007

Mascia, C., Vita, S., Zuccalà, P., Marocco, R., Tieghi, T., Savinelli, S., … Lichtner, M. (2017). Changes in inflammatory biomarkers in HCV-infected patients undergoing direct acting antiviral-containing regimens with or without interferon. *PLoS ONE*. https://doi.org/10.1371/journal.pone.0179400

Matsusaka, K., Funata, S., Fukuyo, M., Seto, Y., Aburatani, H., Fukayama, M., & Kaneda, A. (2017). Epstein–Barr virus infection induces genome-wide de novo DNA methylation in non-neoplastic gastric epithelial cells. *Journal of Pathology*. https://doi.org/10.1002/path.4909

Mauser, A., Holley-Guthrie, E., Zanation, A., Yarborough, W., Kaufmann, W., Klingelhutz, A., … Kenney, S. (2002). The Epstein-Barr virus immediate-early protein BZLF1 induces expression of E2F-1 and other proteins involved in cell cycle progression in primary keratinocytes and gastric carcinoma cells. *J Virol*. https://doi.org/10.1128/JVI.76.24.12543

Mauser, A., Saito, S., Appella, E., Anderson, C. W., Seaman, W. T., & Kenney, S. (2002). The Epstein-Barr virus immediate-early protein BZLF1 regulates p53 function through multiple mechanisms. *J Virol*, *76*, 12503–12512. Retrieved from http://www.ncbi.nlm.nih.gov/pubmed/12438576

Mayo, L. D., Seo, Y. R., Jackson, M. W., Smith, M. L., Guzman, J. R., Korgaonkar, C. K., & Donner, D. B. (2005). Phosphorylation of human p53 at serine 46 determines promoter selection and whether apoptosis is attenuated or amplified. *Journal of Biological Chemistry*. https://doi.org/10.1074/jbc.M503026200

McClain, M. S., Shaffer, C. L., Israel, D. A., Peek, R. M. J., & Cover, T. L. (2009). Genome sequence analysis of Helicobacter pylori strains associated with gastric ulceration and gastric cancer. *BMC Genomics*. https://doi.org/10.1186/1471-2164-10-3

McCormack, P. (2006). Quadrivalent Human Papillomavirus (Types 6, 11, 16, 18) Recombinant Vaccine. *Vaccine*.

McDonald, C., Karstegl, C. E., Kellam, P., & Farrell, P. J. (2010). Regulation of the Epstein-Barr virus Zp promoter in B lymphocytes during reactivation from latency. *J Gen Virol*, *91*, 622–629. https://doi.org/10.1099/vir.0.017277-0

Medveczky, M. M., Horvath, E., Lund, T., & Medveczky, P. G. (1997). In vitro antiviral drug sensitivity of the Kaposi's sarcoma-associated herpesvirus. *AIDS (London, England)*.

Meek, D. W., & Anderson, C. W. (2009). Posttranslational modification of p53: cooperative integrators of function. *Cold Spring Harbor Perspectives in Biology*. https://doi.org/10.1101/cshperspect.a000950

Mellinghoff, I., Daibata, M., Humphreys, R. E., Mulder, C., Takada, K., & Sairenji, T. (1991). Early events in Epstein-Barr virus genome expression after activation: Regulation by second messengers of B cell activation. *Virology*. https://doi.org/10.1016/0042-6822(91)90574-U

Meng, Q., Hagemeier, S. R., Fingeroth, J. D., Gershburg, E., Pagano, J. S., & Kenney, S. C. (2010). The Epstein-Barr virus (EBV)-encoded protein kinase, EBV-PK, but not the thymidine kinase (EBV-TK), is required for ganciclovir and acyclovir inhibition of lytic viral production. *J Virol*, *84*, 4534–4542. https://doi.org/10.1128/JVI.02487-09

Mesri, E. A., Feitelson, M. A., & Munger, K. (2014). Human viral oncogenesis: a cancer hallmarks analysis. *Cell Host Microbe*, *15*, 266–282. https://doi.org/10.1016/j.chom.2014.02.011

Minoura-Etoh, J., Gotoh, K., Sato, R., Ogata, M., Kaku, N., Fujioka, T., & Nishizono, A. (2006). Helicobacter pylori-associated oxidant monochloramine induces reactivation of Epstein-Barr virus (EBV) in gastric epithelial cells latently infected with EBV. *Journal of Medical Microbiology*. https://doi.org/10.1099/jmm.0.46580-0

Minucci, S., & Pelicci, P. G. (2006). Histone deacetylase inhibitors and the promise of epigenetic (and more) treatments for cancer. *Nature Reviews Cancer*. https://doi.org/10.1038/nrc1779

Mitchell, D. A., Xie, W. H., Schmittling, R., Learn, C., Friedman, A., McLendon, R. E., & Sampson, J. H. (2008). Sensitive detection of human cytomegalovirus in tumors and peripheral blood of patients diagnosed with glioblastoma. *Neuro-Oncology*. https://doi.org/10.1215/15228517-2007-035

Miyazaki, I., Cheung, R. K., & Dosch, H. M. (1993). Viral interleukin 10 is critical for the induction of B cell growth transformation by Epstein-Barr virus. *J Exp Med*. https://doi.org/10.1084/jem.178.2.439

Mo, Y. Y., Yu, Y., Shen, Z., & Beck, W. T. (2002). Nucleolar delocalization of human topoisomerase I in response to topotecan correlates with sumoylation of the protein. *Journal of Biological Chemistry*. https://doi.org/10.1074/jbc.M108263200

Montalvo, E. A., Cottam, M., Hill, S., & Wang, Y. J. (1995). YY1 binds to and regulates cis-acting negative elements in the Epstein-Barr virus BZLF1 promoter. *Journal of Virology*.

Moore, K. W., Malefyt, R. D. W., Robert, L., & Garra, A. O. (2001). Interleukin 10 and the Interleukin-10 receptor. *Annu. Rev. Immunol.* https://doi.org/10.1146/annurev.immunol.19.1.683

Morgan, D. G., Miller, G., Niederman, J. C., Smith, H. W., & Dowaliby, J. M. (1979). SITE OF EPSTEIN-BARR VIRUS REPLICATION IN THE OROPHARYNX. *The Lancet*. https://doi.org/10.1016/S0140-6736(79)92384-5

Morris, A. J., Ali, M. R., Nicholson, G. I., Perezperez, G. I., & Blaser, M. J. (1991). Long-Term Follow-up of Voluntary Ingestion of Helicobacter-Pylori. *Annals of Internal Medicine*.

Morris, A., & Nicholson, G. (1987). Ingestion of Campylobacter pyloridis Causes Gastritis and Raised Fasting Gastric pH. *The American Journal of Gastroenterology*. https://doi.org/10.1111/j.1572-0241.1987.tb05291.x

Morrison, T. E., & Kenney, S. C. (2004). BZLF1, an Epstein-Barr virus immediate-early protein, induces p65 nuclear translocation while inhibiting p65 transcriptional function. *Virology*. https://doi.org/10.1016/j.virol.2004.07.020

Morrison, T. E., Mauser, A., Klingelhutz, A., & Kenney, S. C. (2004). Epstein-Barr virus immediate-early protein BZLF1 inhibits tumor necrosis factor alpha-induced signaling and apoptosis by downregulating tumor necrosis factor receptor 1. *J Virol*. https://doi.org/10.1128/JVI.78.1.544

Morrison, T. E., Mauser, A., Wong, A., Ting, J. P., & Kenney, S. C. (2001). Inhibition of IFN-gamma signaling by an Epstein-Barr virus immediate- early protein. *Immunity*.

Mullen, M. M., Haan, K. M., Longnecker, R., & Jardetzky, T. S. (2002). Structure of the Epstein-Barr virus gp42 protein bound to the MHC class II receptor HLA-DR1. *Molecular Cell*. https://doi.org/10.1016/S1097-2765(02)00465-3

Murakami, T., Sato, A., Chun, N. A. L., Hara, M., Naito, Y., Kobayashi, Y., … Kobayashi, E. (2008). Transcriptional modulation using HDACi depsipeptide promotes immune cell-mediated tumor destruction of murine B16 melanoma. *Journal of Investigative Dermatology*. https://doi.org/10.1038/sj.jid.5701216

Murata, T., Hotta, N., Toyama, S., Nakayama, S., Chiba, S., Isomura, H., … Tsurumi, T. (2010). Transcriptional repression by sumoylation of Epstein-Barr virus BZLF1 protein correlates with association of histone deacetylase. *Journal of Biological Chemistry*. https://doi.org/10.1074/jbc.M109.095356

Murata, T., Kondo, Y., Sugimoto, A., Kawashima, D., Saito, S., Isomura, H., … Tsurumi, T. (2012). Epigenetic histone modification of Epstein-Barr virus BZLF1 promoter during latency and reactivation in Raji cells. *J Virol*, *86*, 4752–4761. https://doi.org/10.1128/JVI.06768-11

Murata, T., & Tsurumi, T. (2014). Switching of EBV cycles between latent and lytic states. *Rev Med Virol*, *24*, 142–153. https://doi.org/10.1002/rmv.1780

Nakamura, M., Nishikawa, J., Saito, M., Sakai, K., Sasaki, S., Hashimoto, S., … Sakaida, I. (2016). Decitabine inhibits tumor cell proliferation and up-regulates E-cadherin expression in Epstein-Barr virus-associated gastric cancer. *Journal of Medical Virology*. https://doi.org/10.1002/jmv.24634

Nanbo, A., Inoue, K., Adachi-Takasawa, K., & Takada, K. (2002). Epstein-Barr virus RNA confers resistance to interferon-alpha-induced apoptosis in Burkitt's lymphoma. *EMBO J*, *21*, 954–965. https://doi.org/10.1093/emboj/21.5.954

Nandakumar, A., Uwatoko, F., Yamamoto, M., Tomita, K., Majima, H. J., Akiba, S., & Koriyama, C. (2017). Radiation-induced Epstein–Barr virus reactivation in gastric cancer cells with latent EBV infection. *Tumor Biology*, *39*(7), 1010428317717718. https://doi.org/10.1177/1010428317717718

Nawandar, D. M., Wang, A., Makielski, K., Lee, D., Ma, S., Barlow, E., … Kenney, S. C. (2015). Differentiation-Dependent KLF4 Expression Promotes Lytic Epstein-Barr Virus Infection in Epithelial Cells. *PLoS Pathogens*. https://doi.org/10.1371/journal.ppat.1005195

Nemerow, G. R., Wolfert, R., McNaughton, M. E., & Cooper, N. R. (1985). Identification and characterization of the Epstein-Barr virus receptor on human B lymphocytes and its relationship to the C3d complement receptor (CR2). *Journal of Virology*.

Niedermeier, A., Talanin, N., Chung, E. J., Sells, R. E., Borris, D. L., Orenstein, J. M., … Blauvelt, A. (2006). Histone deacetylase inhibitors induce apoptosis with minimal viral reactivation in cells infected with Kaposi's sarcoma-associated herpesvirus. *J Invest Dermatol*. https://doi.org/10.1038/sj.jid.5700438

Ning, S. (2011). Innate immune modulation in EBV infection. *Herpesviridae*. https://doi.org/10.1186/2042-4280-2-1

Ning, S., Hahn, A. M., Huye, L. E., & Pagano, J. S. (2003). Interferon regulatory factor 7 regulates expression of Epstein-Barr virus latent membrane protein 1: a regulatory circuit. *Journal of Virology*. https://doi.org/10.1128/JVI.77.17.9359

Novalić, Z., Verkuijlen, S. A. W. M., Verlaan, M., Eersels, J. L. H., de Greeuw, I., Molthoff, C. F. M., … Greijer, A. E. (2017). Cytolytic virus activation therapy and treatment monitoring for Epstein-Barr virus associated nasopharyngeal carcinoma in a mouse tumor model. *Journal of Medical Virology*. https://doi.org/10.1002/jmv.24870

O'Connor, M. J. (2015). Targeting the DNA Damage Response in Cancer. *Molecular Cell*. https://doi.org/10.1016/j.molcel.2015.10.040

Ocker, M. (2010). Deacetylase inhibitors - focus on non-histone targets and effects. *World Journal of Biological Chemistry*. https://doi.org/10.4331/wjbc.v1.i5.55

Ogbomo, H., Michaelis, M., Kreuter, J., Doerr, H. W., & Cinatl, J. (2007). Histone deacetylase inhibitors suppress natural killer cell cytolytic activity. *FEBS Letters*. https://doi.org/10.1016/j.febslet.2007.02.045

Ogembo, J. G., Kannan, L., Ghiran, I., Nicholson-Weller, A., Finberg, R. W., Tsokos, G. C., & Fingeroth, J. D. (2013). Human Complement Receptor Type 1/CD35 Is an Epstein-Barr Virus Receptor. *Cell Reports*. https://doi.org/10.1016/j.celrep.2013.01.023

Oh, S. T., Seo, J. S., Moon, U. Y., Kang, K. H., Shin, D. J., Yoon, S. K., … Lee, S. K. (2004). A naturally derived gastric cancer cell line shows latency I Epstein-Barr virus infection closely resembling EBV-associated gastric cancer. *Virology*, *320*, 330–336. https://doi.org/10.1016/j.virol.2003.12.005

Orditura, M., Galizia, G., Sforza, V., Gambardella, V., Fabozzi, A., Laterza, M. M., … De Vita, F. (2014). Treatment of gastric cancer. *World Journal of Gastroenterology : WJG*, *20*(7), 1635–1649. https://doi.org/10.3748/wjg.v20.i7.1635

Orem, J., Mbidde, E. K., Lambert, B., de Sanjose, S., & Weiderpass, E. (2007). Burkitt's Lymphoma in Africa, a Review of the Epidemiology and Etiology. *African Health Sciences*. https://doi.org/10.5555/afhs.2007.7.3.166

Oussaief, L., Hippocrate, A., Clybouw, C., Rampanou, A., Ramirez, V., Desgranges, C., … Joab, I. (2009a). Activation of the lytic program of the Epstein-Barr virus in Burkitt's lymphoma cells leads to a two steps downregulation of expression of the proapoptotic protein BimEL, one of which is EBV-late-gene expression dependent. *Virology*. https://doi.org/10.1016/j.virol.2009.02.009

Oussaief, L., Hippocrate, A., Ramirez, V., Rampanou, A., Zhang, W., Meyers, D., … Joab, I. (2009b). Phosphatidylinositol 3-kinase/Akt pathway targets acetylation of Smad3 through Smad3/CREB-binding protein interaction: contribution to transforming growth factor beta1-induced Epstein-Barr virus reactivation. *The Journal of Biological Chemistry*. https://doi.org/10.1074/jbc.M109.036483

Palser, A. L., Grayson, N. E., White, R. E., Corton, C., Correia, S., Ba abdullah, M. M., … Kellam, P. (2015). Genome Diversity of Epstein-Barr Virus from Multiple Tumor Types and Normal Infection. *Journal of Virology*. https://doi.org/10.1128/JVI.03614-14

Park-Sarge, O. K., & Sarge, K. D. (2008). Detection of sumoylated proteins. *Methods in Molecular Biology*. https://doi.org/10.1007/978-1-60327-461-6-14

Paschos, K., Smith, P., Anderton, E., Middeldorp, J. M., White, R. E., & Allday, M. J. (2009). Epstein-Barr virus latency in B cells leads to epigenetic repression and CpG methylation of the tumour suppressor gene Bim. *PLoS Pathogens*. https://doi.org/10.1371/journal.ppat.1000492

Pathmanathan, R., Prasad, U., Sadler, R., Flynn, K., & Raab-Traub, N. (1995). Clonal proliferations of cells infected with Epstein-Barr virus in preinvasive lesions related to nasopharyngeal carcinoma. *The New England Journal of Medicine*. https://doi.org/10.1056/NEJM199509143331103

Patnaik, A., Tolcher, A., Beeram, M., Nemunaitis, J., Weiss, G. J., Bhalla, K., … Zhi, J. (2015). Clinical pharmacology characterization of RG7112, an MDM2 antagonist, in patients with advanced solid tumors. *Cancer Chemotherapy and Pharmacology*. https://doi.org/10.1007/s00280-015-2830-8

Paulson, E. J., & Speck, S. H. (1999). Differential methylation of Epstein-Barr virus latency promoters facilitates viral persistence in healthy seropositive individuals. *Journal of Virology*.

Pellicciotta, I., Cortez-Gonzalez, X., Sasik, R., Reiter, Y., Hardiman, G., Langlade-Demoyen, P., & Zanetti, M. (2008). Presentation of telomerase reverse transcriptase, a self-tumor antigen, is down-regulated by histone deacetylase inhibition. *Cancer Research*. https://doi.org/10.1158/0008-5472.CAN-08-1014

Peng, H., Chen, Y., Gong, P., Cai, L., Lyu, X., Jiang, Q., … Li, X. (2016). Higher methylation intensity induced by EBV LMP1 via NF-κB/DNMT3b signaling contributes to silencing of PTEN gene. *Oncotarget*. https://doi.org/10.18632/oncotarget.9474

Perrine, S. P., Hermine, O., Small, T., Suarez, F., O'Reilly, R., Boulad, F., … Faller, D. V. (2007). A phase 1/2 trial of arginine butyrate and ganciclovir in patients with Epstein-Barr virus-associated lymphoid malignancies. *Blood*. https://doi.org/10.1182/blood-2006-01-024703

Petosa, C., Morand, P., Baudin, F., Moulin, M., Artero, J. B., & Müller, C. W. (2006). Structural basis of lytic cycle activation by the Epstein-Barr virus ZEBRA protein. *Molecular Cell*. https://doi.org/10.1016/j.molcel.2006.01.006

Phan, A. T., Fernandez, S. G., Somberg, J. J., Keck, K. M., & Miranda, J. J. L. (2016). Epstein-Barr virus latency type and spontaneous reactivation predict lytic induction levels. *Biochemical and Biophysical Research Communications*. https://doi.org/10.1016/j.bbrc.2016.04.070

Plummer, M., de Martel, C., Vignat, J., Ferlay, J., Bray, F., & Franceschi, S. (2016). Global burden of cancers attributable to infections in 2012: a synthetic analysis. *The Lancet Global Health*. https://doi.org/10.1016/S2214-109X(16)30143-7

Preciado, M. V., Chabay, P. A., De Matteo, E. N., Gismondi, M. I., Rey, G., & Zubizarreta, P. (2002). Epstein Barr virus associated pediatric nasopharyngeal carcinoma: its correlation with p53 and bcl-2 expression. *Medical and Pediatric Oncology*. https://doi.org/10.1002/mpo.1349

Price, A. M., & Luftig, M. A. (2014). Dynamic epstein-barr virus gene expression on the path to B-cell transformation. *Advances in Virus Research*. https://doi.org/10.1016/B978-0-12-800098-4.00006-4

Quinn, L. L., Williams, L. R., White, C., Forrest, C., Zuo, J., & Rowe, M. (2016). The Missing Link in Epstein-Barr Virus Immune Evasion: the BDLF3 Gene Induces Ubiquitination and Downregulation of Major Histocompatibility Complex Class I (MHC-I) and MHC-II. *Journal of Virology*. https://doi.org/10.1128/JVI.02183-15

Raab-Traub, N. (2002). Epstein-Barr virus in the pathogenesis of NPC. *Seminars in Cancer Biology*. https://doi.org/10.1016/S1044

Raab-Traub, N., & Flynn, K. (1986). The structure of the termini of the Epstein-Barr virus as a marker of clonal cellular proliferation. *Cell*. https://doi.org/10.1016/0092-8674(86)90803-2

Ragoczy, T., Heston, L., & Miller, G. (1998). The Epstein-Barr virus Rta protein activates lytic cycle genes and can disrupt latency in B lymphocytes. *Journal of Virology*.

Ramasubramanyan, S., Osborn, K., Flower, K., & Sinclair, A. J. (2012). Dynamic Chromatin Environment of Key Lytic Cycle Regulatory Regions of the Epstein-Barr Virus Genome. *Journal of Virology*. https://doi.org/10.1128/JVI.06334-11

Ranganathan, P., Clark, P. A., Kuo, J. S., Salamat, S. S., & Kalejta, R. F. (2012). Significant association of multiple human cytomegalovirus genomic Loci with glioblastoma multiforme samples. *Journal of Virology*. https://doi.org/10.1128/JVI.06097-11

Ray-Coquard, I., Blay, J. Y., Italiano, A., Le Cesne, A., Penel, N., Zhi, J., … Bui, B. N. (2012). Effect of the MDM2 antagonist RG7112 on the P53 pathway in patients with MDM2-amplified, well-differentiated or dedifferentiated liposarcoma: An exploratory proof-of-mechanism study. *The Lancet Oncology*. https://doi.org/10.1016/S1470-2045(12)70474-6

Redchenko, I. V, & Rickinson, a B. (1999). Accessing Epstein-Barr virus-specific T-cell memory with peptide-loaded dendritic cells. *Journal of Virology*.

Ressing, M. E., van Gent, M., Gram, A. M., Hooykaas, M. J. G., Piersma, S. J., & Wiertz, E. J. H. J. (2015). Immune Evasion by Epstein-Barr Virus. In C. Münz (Ed.), *Epstein Barr Virus Volume 2: One Herpes Virus: Many Diseases* (pp. 355–381). Cham: Springer International Publishing. https://doi.org/10.1007/978-3-319-22834-1_12

Ressing, M. E., van Leeuwen, D., Verreck, F. A. W., Keating, S., Gomez, R., Franken, K. L. M. C., … Wiertz, E. J. H. J. (2005). Epstein-Barr virus gp42 is posttranslationally modified to produce soluble gp42 that mediates HLA class II immune evasion. *Journal of Virology*. https://doi.org/10.1128/JVI.79.2.841-852.2005

Reusch, J. A., Nawandar, D. M., Wright, K. L., Kenney, S. C., & Mertz, J. E. (2015). Cellular Differentiation Regulator BLIMP1 Induces Epstein-Barr Virus Lytic Reactivation in Epithelial and B Cells by Activating Transcription from both the R and Z Promoters. *Journal of Virology*. https://doi.org/10.1128/JVI.02781-14

Ribeiro, J., Malta, M., Galaghar, A., Silva, F., Afonso, L. P., Medeiros, R., & Sousa, H. (2017). P53 deregulation in Epstein-Barr virus-associated gastric cancer. *Cancer Letters*, *404*, 37–43. https://doi.org/https://doi.org/10.1016/j.canlet.2017.07.010

Rickinson, A. B., Young, L. S., & Rowe, M. (1987). Influence of the Epstein-Barr Virus Nuclear Antigen EBNA 2 on the Growth Phenotype of Virus-Transformed B Cells. *Journal of Virology*.

Roberts, M. L., Luxembourg, A. T., & Cooper, N. R. (1996). Epstein-Barr virus binding to CD21, the virus receptor, activates resting B cells via an intracellular pathway that is linked to B cell infection. *Journal of General Virology*. https://doi.org/10.1099/0022-1317-77-12-3077

Rodriguez, A., Jung, J., & Flemington, E. K. (2001). Cell Cycle Analysis of Epstein-Barr Virus-Infected Cells following Treatment with Lytic Cycle-Inducing Agents. *JOURNAL OF VIROLOGY*. https://doi.org/10.1128/JVI.75.10.4482–4489.2001

Roughan, J. E., & Thorley-Lawson, D. A. (2009). The Intersection of Epstein-Barr Virus with the Germinal Center. *Journal of Virology*. https://doi.org/10.1128/JVI.02609-08

Roughan, J. E., Torgbor, C., & Thorley-Lawson, D. A. (2010). Germinal center B cells latently infected with Epstein-Barr virus proliferate extensively but do not increase in number. *J Virol*. https://doi.org/JVI.01780-09 [pii]\r10.1128/JVI.01780-09

Rous, P. (1911). A sarcoma of the fowl transmissible by an agent separable from the tumor cells. *The Journal of Experimental Medicine*. https://doi.org/10.1097/00000441-191108000-00079

Rowe, D. T., Rowe, M., Evan, G. I., Wallace, L. E., Farrell, P. J., & Rickinson, A. B. (1986). Restricted expression of EBV latent genes and T-lymphocyte-detected membrane antigen in Burkitt's lymphoma cells. *The EMBO Journal*.

Rowe, M., Glaunsinger, B., van Leeuwen, D., Zuo, J., Sweetman, D., Ganem, D., … Ressing, M. E. (2007). Host shutoff during productive Epstein-Barr virus infection is mediated by BGLF5 and may contribute to immune evasion. *Pnas*. https://doi.org/10.1073/pnas.0611128104

Rowe, M., & Zuo, J. (2010). Immune responses to Epstein-Barr virus: molecular interactions in the virus evasion of CD8+T cell immunity. *Microbes and Infection*. https://doi.org/10.1016/j.micinf.2009.12.001

Ruf, I. K., Lackey, K. A., Warudkar, S., & Sample, J. T. (2005). Protection from interferon-induced apoptosis by Epstein-Barr virus small RNAs is not mediated by inhibition of PKR. *Journal of Virology*. https://doi.org/10.1128/JVI.79.23.14562-14569.2005

Saiki, Y., Ohtani, H., Naito, Y., Miyazawa, M., & Nagura, H. (1996). Immunophenotypic characterization of Epstein-Barr virus-associated gastric carcinoma: massive infiltration by proliferating CD8+ T-lymphocytes. *Laboratory Investigation; a Journal of Technical Methods and Pathology*.

Saito, R., Abe, H., Kunita, A., Yamashita, H., Seto, Y., & Fukayama, M. (2017). Overexpression and gene amplification of PD-L1 in cancer cells and PD-L1 + immune cells in Epstein-Barr virus-associated gastric cancer: The prognostic implications. *Modern Pathology*. https://doi.org/10.1038/modpathol.2016.202

Sathiyamoorthy, K., Hu, Y. X., Möhl, B. S., Chen, J., Longnecker, R., & Jardetzky, T. S. (2016). Structural basis for Epstein-Barr virus host cell tropism mediated by gp42 and gHgL entry glycoproteins. *Nature Communications*. https://doi.org/10.1038/ncomms13557

Sato, Kamura, T., Shirata, N., Murata, T., Kudoh, A., Iwahori, S., … Tsurumi, T. (2009a). Degradation of phosphorylated p53 by viral protein-ECS E3 ligase complex. *PLoS Pathogens*, *5*(7). https://doi.org/10.1371/journal.ppat.1000530

Sato, Shirata, N., Kudoh, A., Iwahori, S., Nakayama, S., Murata, T., … Tsurumi, T. (2009b). Expression of Epstein-Barr virus BZLF1 immediate-early protein induces p53 degradation independent of MDM2, leading to repression of p53-mediated transcription. *Virology*, *388*, 204–211. https://doi.org/10.1016/j.virol.2009.03.017

Sato, Y., Shirata, N., Murata, T., Nakasu, S., Kudoh, A., Iwahori, S., … Tsurumi, T. (2010). Transient increases in p53-responsible gene expression at early stages of Epstein-Barr virus productive replication. *Cell Cycle*, *9*, 807–814. https://doi.org/10.4161/cc.9.4.10675

Sato, Y., & Tsurumi, T. (2010). Noise cancellation: Viral fine tuning of the cellular environment for its own genome replication. *PLoS Pathogens*. https://doi.org/10.1371/journal.ppat.1001158

Saxena, A., Nath Prasad, K., Chand Ghoshal, U., Krishnani, N., Roshan Bhagat, M., & Husain, N. (2008). Association of Helicobacter pylori and Epstein-Barr virus with gastric cancer and peptic ulcer disease. *Scandinavian Journal of Gastroenterology*. https://doi.org/10.1080/00365520801909660

Schepers, A., Pich, D., & Hammerschmid, W. (1996). Activation of oriLyt, the lytic origin of DNA replication of Epstein-Barr virus, by BZLF1. *Virology*. https://doi.org/10.1006/viro.1996.0325

Schmittgen, T. D., & Livak, K. J. (2008). Analyzing real-time PCR data by the comparative C T method. *Nature*. https://doi.org/10.1038/nprot.2008.73

Schneider, B. G., Gulley, M. L., Eagan, P., Bravo, J. C., Mera, R., & Geradts, J. (2000). Loss of p16/CDKN2A tumor suppressor protein in gastric adenocarcinoma is associated with Epstein-Barr virus and anatomic location in the body of the stomach. *Hum Pathol*, *31*, 45–50. Retrieved from http://www.ncbi.nlm.nih.gov/pubmed/10665912

Segal, E., & Widom, J. (2009). What controls nucleosome positions? *Trends in Genetics*. https://doi.org/10.1016/j.tig.2009.06.002

Semmes, O. J., Chen, L., Sarisky, R. T., Gao, Z., Zhong, L., & Hayward, S. D. (1998). Mta has properties of an RNA export protein and increases cytoplasmic accumulation of Epstein-Barr virus replication gene mRNA. *Journal of Virology*.

Serio, T. R., Kolman, J. L., & Miller, G. (1997). Late gene expression from the Epstein-Barr virus BcLF1 and BFRF3 promoters does not require DNA replication in cis. *Journal of Virology*.

Seto, E., & Yoshida, M. (2014). Erasers of histone acetylation: The histone deacetylase enzymes. *Cold Spring Harbor Perspectives in Biology*. https://doi.org/10.1101/cshperspect.a018713

Shah, K. M., Stewart, S. E., Wei, W., Woodman, C. B. J., O'Neil, J. D., Dawson, C. W., & Young, L. S. (2009). The EBV-encoded latent membrane proteins, LMP2A and LMP2B, limit the actions of interferon by targeting interferon receptors for degradation. *Oncogene*. https://doi.org/10.1038/onc.2009.249

Shah, M. A. (2015). Update on metastatic gastric and esophageal cancers. *Journal of Clinical Oncology*. https://doi.org/10.1200/JCO.2014.60.1799

Shair, K. H. Y., Bendt, K. M., Edwards, R. H., Bedford, E. C., Nielsen, J. N., & Raab-Traub, N. (2007). EBV latent membrane protein 1 activates Akt, NFkappaB, and Stat3 in B cell lymphomas. *PLoS Pathogens*. https://doi.org/10.1371/journal.ppat.0030166

Shannon-Lowe, C., Baldwin, G., Feederle, R., Bell, A., Rickinson, A., & Delecluse, H. J. (2005). Epstein-Barr virus-induced B-cell transformation: Quantitating events from virus binding to cell outgrowth. *Journal of General Virology*. https://doi.org/10.1099/vir.0.81153-0

Shannon-Lowe, C. D., Neuhierl, B., Baldwin, G., Rickinson, A. B., & Delecluse, H. J. (2006). Resting B cells as a transfer vehicle for Epstein-Barr virus infection of epithelial cells. *Proc Natl Acad Sci U S A*, *103*, 7065–7070. https://doi.org/10.1073/pnas.0510512103

Shannon-Lowe, C., & Rowe, M. (2011). Epstein-Barr Virus Infection of Polarized Epithelial Cells via the Basolateral Surface by Memory B Cell-Mediated Transfer Infection. *PLoS Pathogens*, *7*(5), e1001338. https://doi.org/10.1371/journal.ppat.1001338

Shannon-Lowe, C., & Rowe, M. (2014). Epstein Barr virus entry; Kissing and conjugation. *Current Opinion in Virology*. https://doi.org/10.1016/j.coviro.2013.12.001

Shao, Y., Gao, Z., Marks, P. a, & Jiang, X. (2004). Apoptotic and autophagic cell death induced by histone deacetylase inhibitors. *Pnas*. https://doi.org/10.1073/pnas.0408345102

Shaw, M. M., Gürr, W. K., Watts, P. a, Littler, E., & Field, H. J. (2001). Ganciclovir and penciclovir, but not acyclovir, induce apoptosis in herpes simplex virus thymidine kinase-transformed baby hamster kidney cells. *Antiviral Chemistry & Chemotherapy*.

Shibata, D., & Weiss, L. M. (1992). Epstein-Barr virus-associated gastric adenocarcinoma. *Am J Pathol*, *140*, 769–774. Retrieved from http://www.ncbi.nlm.nih.gov/pubmed/1314023

Shin, S. R., Paik, S. W., Gwak, G.-Y., Choi, M. S., Lee, J. H., Koh, K. C., & Yoo, B. C. (2011). Antiviral therapy in patients after treatment for hepatitis C-related hepatocellular carcinoma. *Gut and Liver*. https://doi.org/10.5009/gnl.2011.5.1.77

Shirley, C. M., Chen, J., Shamay, M., Li, H., Zahnow, C. A., Hayward, S. D., & Ambinder, R. F. (2011). Bortezomib induction of C/EBP?? mediates Epstein-Barr virus lytic activation in Burkitt lymphoma. *Blood*. https://doi.org/10.1182/blood-2011-01-332379

Shope, R. E., & Hurst, E. W. (1933). INFECTIOUS PAPILLOMATOSIS OF RABBITS : WITH A NOTE ON THE HISTOPATHOLOGY. *The Journal of Experimental Medicine*. https://doi.org/10.1084/jem.58.5.607

Shukla, S. K., Prasad, K. N., Tripathi, A., Singh, A., Saxena, A., Chand Ghoshal, U., … Husain, N. (2011). Epstein-Barr virus DNA load and its association with Helicobacter pylori infection in gastroduodenal diseases. *Brazilian Journal of Infectious Diseases*. https://doi.org/10.1016/S1413-8670(11)70255-0

Silva, A. L., Omerovic, J., Jardetzky, T. S., & Longnecker, R. (2004). Mutational analyses of Epstein-Barr virus glycoprotein 42 reveal functional domains not involved in receptor binding but required for membrane fusion. *Journal of Virology*. https://doi.org/10.1128/JVI.78.11.5946-5956.2004

Simõ-Riudalbas, L., & Esteller, M. (2015). Targeting the histone orthography of cancer: Drugs for writers, erasers and readers. *British Journal of Pharmacology*. https://doi.org/10.1111/bph.12844

Sinclair, A. J. (2003). bZIP proteins of human gammaherpesviruses. *Journal of General Virology*. https://doi.org/10.1099/vir.0.19112-0

Singh, S., & Jha, H. C. (2017). Status of Epstein-Barr Virus Coinfection with Helicobacter pylori in Gastric Cancer. *Journal of Oncology*. https://doi.org/10.1155/2017/3456264

Sixbey, J. W., Nedrud, J. G., Raab-Traub, N., Hanes, R. A., & Pagano, J. S. (1984). Epstein-Barr virus replication in oropharyngeal epithelial cells. *N Engl J Med*.

Smith, G. (2012). Herpesvirus Transport to the Nervous System and Back Again. *Annual Review of Microbiology*. https://doi.org/10.1146/annurev-micro-092611-150051

Söderlund, J., Erhardt, S., & Kast, R. E. (2010). Acyclovir inhibition of IDO to decrease Tregs as a glioblastoma treatment adjunct. *Journal of Neuroinflammation*. https://doi.org/10.1186/1742-2094-7-44

Song, X., Tao, Y. G., Deng, X. Y., Jin, X., Tan, Y. N., Tang, M., … Cao, Y. (2004). Heterodimer formation between c-Jun and Jun B proteins mediated by Epstein-Barr virus encoded latent membrane protein 1. *Cellular Signalling*. https://doi.org/10.1016/j.cellsig.2004.03.014

Sripa, B., Bethony, J. M., Sithithaworn, P., Kaewkes, S., Mairiang, E., Loukas, A., … Brindley, P. J. (2011). Opisthorchiasis and Opisthorchis-associated cholangiocarcinoma in Thailand and Laos. *Acta Tropica*. https://doi.org/10.1016/j.actatropica.2010.07.006

Stewart, S., Dawson, C. W., Takada, K., Curnow, J., Moody, C. A., Sixbey, J. W., & Young, L. S. (2004). Epstein-Barr virus-encoded LMP2A regulates viral and cellular gene expression by modulation of the NF-kappaB transcription factor pathway. *Proc Natl Acad Sci U S A*, *101*, 15730–15735. https://doi.org/10.1073/pnas.0402135101

Stoker, S. D., Novalić, Z., Wildeman, M. A., Huitema, A. D. R., Verkuijlen, S. A. W. M., Juwana, H., … de Boer, J. P. (2015). Epstein–Barr virus-targeted therapy in nasopharyngeal carcinoma. *Journal of Cancer Research and Clinical Oncology*. https://doi.org/10.1007/s00432-015-1969-3

Strockbine, L. D., Cohen, J. I., Farrah, T., Lyman, S. D., Wagener, F., DuBose, R. F., … Spriggs, M. K. (1998). The Epstein-Barr virus BARF1 gene encodes a novel, soluble colony-stimulating factor-1 receptor. *Journal of Virology*.

Suárez, A. L., & Van Dyk, L. F. (2008). Endothelial cells support persistent gammaherpesvirus 68 infection. *PLoS Pathogens*. https://doi.org/10.1371/journal.ppat.1000152

Sugano, N., Chen, W., Roberts, M. L., & Cooper, N. R. (1997). Epstein-Barr virus binding to CD21 activates the initial viral promoter via NF-kappaB induction. *The Journal of Experimental Medicine*. https://doi.org/10.1084/jem.186.5.731

Sukawa, Y., Yamamoto, H., Nosho, K., Kunimoto, H., Suzuki, H., Adachi, Y., … Shinomura, Y. (2012). Alterations in the human epidermal growth factor receptor 2-phosphatidylinositol 3-kinase-v-Akt pathway in gastric cancer. *World Journal of Gastroenterology*. https://doi.org/10.3748/wjg.v18.i45.6577

Sun, C. C., & Thorley-Lawson, D. A. (2007). Plasma Cell-Specific Transcription Factor XBP-1s Binds to and Transactivates the Epstein-Barr Virus BZLF1 Promoter. *Journal of Virology*. https://doi.org/10.1128/JVI.01055-07

Swaminathan, S., Hesselton, R., Sullivan, J., & Kieff, E. (1993). Epstein-Barr virus recombinants with specifically mutated BCRF1 genes. *J Virol*.

Swaminathan, S., Tomkinson, B., & Kieff, E. (1991). Recombinant Epstein-Barr virus with small RNA (EBER) genes deleted transforms lymphocytes and replicates in vitro. *Proceedings of the National Academy of Sciences of the United States of America*. https://doi.org/10.1073/pnas.88.4.1546

Sweet, B. H., & Hilleman, M. R. (1960). The Vacuolating Virus, S.V.40 (26128). *Experimental Biology and Medicine*, *105*(26128), 420–427. https://doi.org/10.3181/00379727-105-26128

Swenson, J. J., Holley-Guthrie, E., & Kenney, S. C. (2001). Epstein-Barr Virus Immediate-Early Protein BRLF1 Interacts with CBP, Promoting Enhanced BRLF1 Transactivation. *Journal of Virology*, *75*(13), 6228–6234. https://doi.org/10.1128/JVI.75.13.6228-6234.2001

Takada, K., Horinouchi, K., Ono, Y., Aya, T., Osato, T., Takahashi, M., & Hayasaka, S. (1991). An Epstein-Barr virus-producer line Akata: establishment of the cell line and analysis of viral DNA. *Virus Genes*. https://doi.org/10.1007/BF00571929

Takada, K., & Ono, Y. (1989). Synchronous and sequential activation of latently infected Epstein-Barr virus genomes. *Journal of Virology*.

Tanner, J., Weis, J., Fearon, D., Whang, Y., & Kieff, E. (1987). Epstein-barr virus gp350/220 binding to the B lymphocyte C3d receptor mediates adsorption, capping, and endocytosis. *Cell*. https://doi.org/10.1016/0092-8674(87)90216-9

Tarakanova, V. L., Leung-Pineda, V., Hwang, S., Yang, C. W., Matatall, K., Basson, M., … Virgin IV, H. W. (2007). γ-Herpesvirus Kinase Actively Initiates a DNA Damage Response by Inducing Phosphorylation of H2AX to Foster Viral Replication. *Cell Host and Microbe*. https://doi.org/10.1016/j.chom.2007.05.008

Temple, R. M., Zhu, J., Budgeon, L., Christensen, N. D., Meyers, C., & Sample, C. E. (2014). Efficient replication of Epstein-Barr virus in stratified epithelium in vitro. *Proc Natl Acad Sci U S A*. https://doi.org/10.1073/pnas.1400818111

Ternette, N., Yang, H., Partridge, T., Llano, A., Cedeño, S., Fischer, R., … Hanke, T. (2016). Defining the HLA class I-associated viral antigen repertoire from HIV-1-infected human cells. *European Journal of Immunology*. https://doi.org/10.1002/eji.201545890

Thorley-Lawson, D. A., & Gross, A. (2004). Persistence of the Epstein–Barr Virus and the Origins of Associated Lymphomas. *New England Journal of Medicine*. https://doi.org/10.1056/NEJMra032015

Thust, R., Tomicic, M., Klöcking, R., Wutzler, P., & Kaina, B. (2000). Cytogenetic genotoxicity of anti-herpes purine nucleoside analogues in CHO cells expressing the thymidine kinase gene of herpes simplex virus type 1: comparison of ganciclovir, penciclovir and aciclovir. *Mutagenesis*.

Tierney, R., Nagra, J., Hutchings, I., Shannon-Lowe, C., Altmann, M., Hammerschmidt, W., … Bell, A. (2007). Epstein-Barr virus exploits BSAP/Pax5 to achieve the B-cell specificity of its growth-transforming program. *J Virol*, *81*, 10092–10100. https://doi.org/10.1128/JVI.00358-07

Tikhmyanova, N., Schultz, D. C., Lee, T., Salvino, J. M., & Lieberman, P. M. (2014). Identification of a new class of small molecules that efficiently reactivate latent Epstein-Barr virus. *ACS Chemical Biology*. https://doi.org/10.1021/cb4006326

Tisato, V., Voltan, R., Gonelli, A., Secchiero, P., & Zauli, G. (2017). MDM2/X inhibitors under clinical evaluation: perspectives for the management of hematological malignancies and pediatric cancer. *Journal of Hematology & Oncology*, *10*(1), 133. https://doi.org/10.1186/s13045-017-0500-5

Traynor, A. M., Dubey, S., Eickhoff, J. C., Kolesar, J. M., Schell, K., Huie, M. S., … Schiller, J. H. (2009). Vorinostat (NSC# 701852) in Patients with relapsed non-small cell lung cancer; A wisconsin oncology network phase II study. *Journal of Thoracic Oncology*. https://doi.org/10.1097/JTO.0b013e3181952478

Tsai, C. L., Li, H. P., Lu, Y. J., Hsueh, C., Liang, Y., Chen, C. L., … Chang, Y. S. (2006). Activation of DNA methyltransferase 1 by EBV LMP1 Involves c-Jun NH(2)-terminal kinase signaling. *Cancer Res*, *66*, 11668–11676. https://doi.org/10.1158/0008-5472.CAN-06-2194

Tsai, M. H., Raykova, A., Klinke, O., Bernhardt, K., Gartner, K., Leung, C. S., … Delecluse, H. J. (2013). Spontaneous lytic replication and epitheliotropism define an Epstein-Barr virus strain found in carcinomas. *Cell Rep*, *5*, 458–470. https://doi.org/10.1016/j.celrep.2013.09.012

Tsai, P.-F., Lin, S.-J., Weng, P.-L., Tsai, S.-C., Lin, J.-H., Chou, Y.-C., & Tsai, C.-H. (2011). Interplay between PKC and Sp1 on Histone Deacetylase Inhibitor-Mediated Epstein-Barr Virus Reactivation. *Journal of Virology*. https://doi.org/10.1128/JVI.01602-10

Tsang, C. M., Yip, Y. L., Lo, K. W., Deng, W., To, K. F., Hau, P. M., … Tsao, S. W. (2012). Cyclin D1 overexpression supports stable EBV infection in nasopharyngeal epithelial cells. *Proceedings of the National Academy of Sciences*. https://doi.org/10.1073/pnas.1202637109

Tsurumi, T. (1993). Purification and characterization of the DNA-binding activity of the Epstein-Barr virus DNA polymerase accessory protein BMRF1 gene products, as expressed in insect cells by using the baculovirus system. *J Virol*.

Tu, Y., Hershman, D. L., Bhalla, K., Fiskus, W., Pellegrino, C. M., Andreopoulou, E., … Sparano, J. A. (2014). A phase I-II study of the histone deacetylase inhibitor vorinostat plus sequential weekly paclitaxel and doxorubicin-cyclophosphamide in locally advanced breast cancer. *Breast Cancer Research and Treatment*. https://doi.org/10.1007/s10549-014-3008-5

Tugizov, S. M., Berline, J. W., & Palefsky, J. M. (2003). Epstein-Barr virus infection of polarized tongue and nasopharyngeal epithelial cells. *Nature Medicine*. https://doi.org/10.1038/nm830

Tzellos, S., & Farrell, P. (2012). Epstein-Barr Virus Sequence Variation—Biology and Disease. *Pathogens*. https://doi.org/10.3390/pathogens1020156

UniProt Consortium, T. (2018). UniProt: the universal protein knowledgebase. *Nucleic Acids Research*. https://doi.org/10.1093/nar/gky092

Uozaki, H., & Fukayama, M. (2008). Epstein-Barr Virus and Gastric Carcinoma – Viral Carcinogenesis through Epigenetic Mechanisms. *Int J Clin Exp Pathol*.

Ushiku, T., Chong, J. M., Uozaki, H., Hino, R., Chang, M. S., Sudo, M., … Fukayama, M. (2007). p73 gene promoter methylation in Epstein-Barr virus-associated gastric carcinoma. *Int J Cancer*, *120*, 60–66. https://doi.org/10.1002/ijc.22275

Valentine, R., Dawson, C. W., Hu, C., Shah, K. M., Owen, T. J., Date, K. L., … O'Neil, J. D. (2010). Epstein-Barr virus-encoded EBNA1 inhibits the canonical NF-kappaB pathway in carcinoma cells by inhibiting IKK phosphorylation. *Mol Cancer*, *9*, 1. https://doi.org/10.1186/1476-4598-9-1

Van de Walle, G. R., Jarosinski, K. W., & Osterrieder, N. (2008). Alphaherpesviruses and Chemokines: Pas de Deux Not Yet Brought to Perfection. *Journal of Virology*, *82*(13), 6090–6097. https://doi.org/10.1128/JVI.00098-08

Van Gent, M., Griffin, B. D., Berkhoff, E. G., van Leeuwen, D., Boer, I. G. J., Buisson, M., … Ressing, M. E. (2011). EBV Lytic-Phase Protein BGLF5 Contributes to TLR9 Downregulation during Productive Infection. *The Journal of Immunology*. https://doi.org/10.4049/jimmunol.0903120

Van Gent, M., Gram, A. M., Boer, I. G. J., Geerdink, R. J., Lindenbergh, M. F. S., Jan Lebbink, R., … Ressing, M. E. (2015). Silencing the shutoff protein of Epstein???Barr virus in productively infected B cells points to (innate) targets for immune evasion. *Journal of General Virology*. https://doi.org/10.1099/jgv.0.000021

Vandeven, N., & Nghiem, P. (2014). Pathogen-driven cancers and emerging immune therapeutic strategies. *Cancer Immunology Research*. https://doi.org/10.1158/2326-6066.CIR-13-0179

Vassilev, L. T., Vu, B. T., Graves, B., Carvajal, D., Podlaski, F., Filipovic, Z., … Liu, E. A. (2004). In Vivo Activation of the p53 Pathway by Small-Molecule Antagonists of MDM2. *Science*. https://doi.org/10.1126/science.1092472

Vogelstein, B., Papadopoulos, N., Velculescu, V. E., Zhou, S., Diaz, L. A., & Kinzler, K. W. (2013). Cancer genome landscapes. *Science*. https://doi.org/10.1126/science.1235122

Vrzalikova, K., Vockerodt, M., Leonard, S., Bell, A., Wei, W., Schrader, A., … Murray, P. G. (2011). Down-regulation of BLIMP1α by the EBV oncogene, LMP-1, disrupts the plasma cell differentiation program and prevents viral replication in B cells: Implications for the pathogenesis of EBV-associated B-cell lymphomas. *Blood*. https://doi.org/10.1182/blood-2010-09-307710

Wadler, S., Fuks, J. Z., & Wiernik, P. H. (1986). Phase I and II agents in cancer therapy: I. Anthracyclines and related compounds. *Journal of Clinical Pharmacology*. https://doi.org/10.1002/j.1552-4604.1986.tb02942.x

Wallin, K.-L., Wiklund, F., Ångström, T., Bergman, F., Stendahl, U., Wadell, G., … Dillner, J. (1999). Type-Specific Persistence of Human Papillomavirus DNA before the Development of Invasive Cervical Cancer. *New England Journal of Medicine*. https://doi.org/10.1056/NEJM199911253412201

Wang'Ondu, R., Teal, S., Park, R., Heston, L., Delecluse, H., & Miller, G. (2015). DNA damage signaling is induced in the absence of Epstein - Barr virus (EBV) Lytic DNA replication and in response to expression of ZEBRA. *PLoS ONE*. https://doi.org/10.1371/journal.pone.0126088

Wang, B., Fang, L., Zhao, H., Xiang, T., & Wang, D. (2012). MDM2 inhibitor Nutlin-3a suppresses proliferation and promotes apoptosis in osteosarcoma cells. *Acta Biochimica et Biophysica Sinica*. https://doi.org/10.1093/abbs/gms053

Wang, P., Rennekamp, A. J., Yuan, Y., & Lieberman, P. M. (2009). Topoisomerase I and RecQL1 Function in Epstein-Barr Virus Lytic Reactivation. *Journal of Virology*. https://doi.org/10.1128/JVI.02379-08

Wang, Y., Li, H., Tang, Q., Maul, G. G., & Yuan, Y. (2008). Kaposi's Sarcoma-Associated Herpesvirus ori-Lyt-Dependent DNA Replication: Involvement of Host Cellular Factors. *Journal of Virology*. https://doi.org/10.1128/JVI.01319-07

Ward, M. H., Pan, W. H., Cheng, Y. J., Li, F. H., Brinton, L. A., Chen, C. J., … Hildesheim, A. (2000). Dietary exposure to nitrite and nitrosamines and risk of nasopharyngeal carcinoma in Taiwan. *International Journal of Cancer*. https://doi.org/10.1002/(SICI)1097-0215(20000601)86:5<603::AID-IJC1>3.0.CO;2-H

Weigel, R., Fischer, D. K., Heston, L., & Miller, G. (1985). Constitutive expression of Epstein-Barr virus-encoded RNAs and nuclear antigen during latency and after induction of Epstein-Barr virus replication. *Journal of Virology*, *53*(1), 254–259. Retrieved from http://www.ncbi.nlm.nih.gov/pmc/articles/PMC255024/

Westphal, E. M., Blackstock, W., Feng, W., Israel, B., & Kenney, S. C. (2000). Activation of lytic Epstein-Barr virus (EBV) infection by radiation and sodium butyrate in vitro and in vivo: A potential method for treating EBV-positive malignancies. *Cancer Research*.

Wieczorek, M., Abualrous, E. T., Sticht, J., Alvaro-Benito, M., Stolzenberg, S., Noe, F., & Freund, C. (2017). Major histocompatibility complex (MHC) class I and MHC class II proteins: Conformational plasticity in antigen presentation. *Frontiers in Immunology*. https://doi.org/10.3389/fimmu.2017.00292

Wildeman, M. A., Novalić, Z., Verkuijlen, S. A. W. M., Juwana, H., Huitema, A. D. R., Tan, I. B., … Greijer, A. E. (2012). Cytolytic virus activation therapy for Epstein-Barr virus-driven tumors. *Clinical Cancer Research*, *18*(18), 5061–5070. https://doi.org/10.1158/1078-0432.CCR-12-0574

Wille, C. K., Nawandar, D. M., Panfil, A. R., Ko, M. M., Hagemeier, S. R., & Kenney, S. C. (2013). Viral genome methylation differentially affects the ability of BZLF1 versus BRLF1 to activate Epstein-Barr virus lytic gene expression and viral replication. *J Virol*, *87*, 935–950. https://doi.org/10.1128/JVI.01790-12

Wilstermann, A. M., Bender, R. P., Godfrey, M., Choi, S., Anklin, C., Berkowitz, D. B., … Graves, D. E. (2007). Topoisomerase II-drug interaction domains: Identification of substituents on etoposide that interact with the enzyme. *Biochemistry*. https://doi.org/10.1021/bi700272u

Woellmer, A., Arteaga-Salas, J. M., & Hammerschmidt, W. (2012). BZLF1 Governs CpG-Methylated Chromatin of Epstein-Barr Virus Reversing Epigenetic Repression. *PLoS Pathogens*. https://doi.org/10.1371/journal.ppat.1002902

Wood, V. H. J., O'Neil, J. D., Wei, W., Stewart, S. E., Dawson, C. W., & Young, L. S. (2007). Epstein-Barr virus-encoded EBNA1 regulates cellular gene transcription and modulates the STAT1 and TGFβ signaling pathways. *Oncogene*. https://doi.org/10.1038/sj.onc.1210496

Woods, D., & Turchi, J. J. (2013). Chemotherapy induced DNA damage response: Convergence of drugs and pathways. *Cancer Biology & Therapy*, *14*(5), 379–389. https://doi.org/10.4161/cbt.23761

Wu, C. C., Li, T. K., Farh, L., Lin, L. Y., Lin, T. S., Yu, Y. J., … Chan, N. L. (2011). Structural basis of type II topoisomerase inhibition by the anticancer drug etoposide. *Science*. https://doi.org/10.1126/science.1204117

Wu, F. Y., Chen, H., Wang, S. E., ApRhys, C. M. J., Liao, G., Fujimuro, M., … Hayward, G. S. (2003). CCAAT/enhancer binding protein alpha interacts with ZTA and mediates ZTA-induced p21(CIP-1) accumulation and G(1) cell cycle arrest during the Epstein-Barr virus lytic cycle. *Journal of Virology*. https://doi.org/10.1128/JVI.77.2.1481

Wu, T., Wang, Y., & Yuan, Y. (2014). Antiviral activity of topoisomerase II catalytic inhibitors against Epstein-Barr virus. *Antiviral Research*. https://doi.org/10.1016/j.antiviral.2014.05.003

Wu, Y., Maruo, S., Yajima, M., Kanda, T., & Takada, K. (2007). Epstein-Barr Virus (EBV)-Encoded RNA 2 (EBER2) but Not EBER1 Plays a Critical Role in EBV-Induced B-Cell Growth Transformation. *Journal of Virology*, *81*(20), 11236–11245. https://doi.org/10.1128/JVI.00579-07

Wycisk, A. I., Lin, J., Loch, S., Hobohm, K., Funke, J., Wieneke, R., … Tampé, R. (2011). Epstein-barr viral BNLF2a protein hijacks the tail-anchored protein insertion machinery to block antigen processing by the transport complex TAP. *Journal of Biological Chemistry*. https://doi.org/10.1074/jbc.M111.237784

Xia, T., O'Hara, A., Araujo, I., Barreto, J., Carvalho, E., Sapucaia, J. B., … Harrington, W. J. (2008). EBV microRNAs in primary lymphomas and targeting of CXCL-11 by ebv-mir-BHRF1-3. *Cancer Research*. https://doi.org/10.1158/0008-5472.CAN-07-5126

Yang, F., Kemp, C. J., & Henikoff, S. (2015). Anthracyclines induce double-strand DNA breaks at active gene promoters. *Mutation Research - Fundamental and Molecular Mechanisms of Mutagenesis*. https://doi.org/10.1016/j.mrfmmm.2015.01.007

Yang, P. W., Chang, S. S., Tsai, C. H., Chao, Y. H., & Chen, M. R. (2008). Effect of phosphorylation on the transactivation activity of Epstein-Barr virus BMRF1, a major target of the viral BGLF4 kinase. *Journal of General Virology*. https://doi.org/10.1099/vir.0.83546-0

Yang, G. Da, Huang, T. J., Peng, L. X., Yang, C. F., Liu, R. Y., Huang, H. B., … Huang, B. J. (2013). Epstein-Barr Virus_Encoded LMP1 Upregulates MicroRNA-21 to Promote the Resistance of Nasopharyngeal Carcinoma Cells to Cisplatin-Induced Apoptosis by Suppressing PDCD4 and Fas-L. *PLoS ONE*. https://doi.org/10.1371/journal.pone.0078355

Yin, Y., Manoury, B., & Fåhraeus, R. (2003). Self-Inhibition of Synthesis and Antigen Presentation by Epstein-Barr Virus-Encoded EBNA1. *Science*, *301*(5638), 1371. Retrieved from http://science.sciencemag.org/content/301/5638/1371.abstract

Yip, W. K., Abdullah, M. A., Yusoff, S. M., & Seow, H. F. (2009). Increase in tumour-infiltrating lymphocytes with regulatory T cell immunophenotypes and reduced zeta-chain expression in nasopharyngeal carcinoma patients. *Clinical and Experimental Immunology*, *155*(3), 412–422. https://doi.org/10.1111/j.1365-2249.2008.03793.x

Yoshioka, M., Kikuta, H., Ishiguro, N., Endo, R., & Kobayashi, K. (2003). Latency pattern of Epstein-Barr virus and methylation status in Epstein-Barr virus-associated hemophagocytic syndrome. *Journal of Medical Virology*. https://doi.org/10.1002/jmv.10411

You, J. S., & Jones, P. A. (2012). Cancer Genetics and Epigenetics: Two Sides of the Same Coin? *Cancer Cell*. https://doi.org/10.1016/j.ccr.2012.06.008

Younes, A., Oki, Y., Bociek, R. G., Kuruvilla, J., Fanale, M., Neelapu, S., … Martell, R. E. (2011). Mocetinostat for relapsed classical Hodgkin's lymphoma: An open-label, single-arm, phase 2 trial. *The Lancet Oncology*. https://doi.org/10.1016/S1470-2045(11)70265-0

Young, L. S., Dawson, C. W., Brown, K. W., & Rickinson, A. B. (1989). Identification of a human epithelial cell surface protein sharing an epitope with the C3d/epstein-barr virus receptor molecule of B lymphocytes. *International Journal of Cancer*. https://doi.org/10.1002/ijc.2910430508

Young, L. S., & Murray, P. G. (2003). Epstein-Barr virus and oncogenesis: from latent genes to tumours. *Oncogene*, *22*, 5108–5121. https://doi.org/10.1038/sj.onc.1206556

Young, L. S., & Rickinson, A. B. (2004). Epstein-Barr virus: 40 years on. *Nat Rev Cancer*, *4*, 757–768. https://doi.org/10.1038/nrc1452

Young, K. A., Chen, X. S., Holers, V. M., & Hannan, J. P. (2007a). Isolating the Epstein-Barr virus gp350/220 binding site on complement receptor type 2 (CR2/CD21). *Journal of Biological Chemistry*. https://doi.org/10.1074/jbc.M706324200

Young, L. S., Arrand, J. R., & Murray, P. G. (2007b). EBV gene expression and regulation. In *Human Herpesviruses*. https://doi.org/10.1017/CBO9780511545313.028

Young, K. a, Herbert, A. P., Barlow, P. N., Holers, V. M., & Hannan, J. P. (2008). Molecular basis of the interaction between complement receptor type 2 (CR2/CD21) and Epstein-Barr virus glycoprotein gp350. *Journal of Virology*. https://doi.org/10.1128/JVI.01673-08

Young, L. S., Yap, L. F., & Murray, P. G. (2016). Epstein–Barr virus: more than 50 years old and still providing surprises. *Nature Reviews Cancer*. https://doi.org/10.1038/nrc.2016.92

Yu, X., Wang, Z., & Mertz, J. E. (2007). ZEB1 regulates the latent-lytic switch in infection by Epstein-Barr virus. *PLoS Pathogens*. https://doi.org/10.1371/journal.ppat.0030194

Zalani, S., Holley-Guthrie, E., & Kenney, S. (1996). Epstein-Barr viral latency is disrupted by the immediate-early BRLF1 protein through a cell-specific mechanism. *Proceedings of the National Academy of Sciences of the United States of America*, *93*(17), 9194–9. https://doi.org/10.1073/pnas.93.17.9194

Zeng, Y., Middeldorp, J., Madjar, J. J., & Ooka, T. (1997). A major DNA binding protein encoded by BALF2 open reading frame of Epstein-Barr Virus (EBV) forms a complex with other EBV DNA-binding proteins: DNAase, EA-D, and DNA polymerase. *Virology*. https://doi.org/10.1006/viro.1997.8891

Zhang, H., Li, Y., Wang, H.-B., Zhang, A., Chen, M.-L., Fang, Z.-X., … Zeng, M.-S. (2018). Ephrin receptor A2 is an epithelial cell receptor for Epstein–Barr virus entry. *Nature Microbiology*, *3*(2), 164–171. https://doi.org/10.1038/s41564-017-0080-8

Zhang, N., Chen, J., Xiao, L., Tang, F., Zhang, Z., Zhang, Y., … Shao, C. (2016). Accumulation Mechanisms of CD4+CD25+FOXP3+ Regulatory T Cells in EBV-associated Gastric Carcinoma. *Scientific Reports*. https://doi.org/10.1038/srep18057

Zhang, Q., Gutsch, D., & Kenney, S. (1994). Functional and physical interaction between p53 and BZLF1: implications for Epstein-Barr virus latency. *Mol Cell Biol*, *14*, 1929–1938. Retrieved from http://www.ncbi.nlm.nih.gov/pubmed/8114724

Zhang, Q., Hong, Y., Dorsky, D., Holley-Guthrie, E., Zalani, S., Elshiekh, N. A., … Kenney, S. (1996). Functional and physical interactions between the Epstein-Barr virus (EBV) proteins BZLF1 and BMRF1: Effects on EBV transcription and lytic replication. *Journal of Virology*.

Zhang, X.-P., Liu, F., & Wang, W. (2011). Two-phase dynamics of p53 in the DNA damage response. *Proceedings of the National Academy of Sciences*. https://doi.org/10.1073/pnas.1100600108

Zhao, J., Liang, Q., Cheung, K. F., Kang, W., Lung, R. W., Tong, J. H., … Yu, J. (2013). Genome-wide identification of Epstein-Barr virus-driven promoter methylation profiles of human genes in gastric cancer cells. *Cancer*, *119*, 304–312. https://doi.org/10.1002/cncr.27724

Zhao, Y., Lu, S., Wu, L., Chai, G., Wang, H., Chen, Y., … Zhu, W. (2006). Acetylation of p53 at Lysine 373 / 382 by the Histone Deacetylase Inhibitor Depsipeptide Induces Expression of p21 Waf1 / Cip1. *Molecular and Cellular Biology*. https://doi.org/10.1128/MCB.26.7.2782

Zhou, X., Lin, W., Tan, F. K., Assassi, S., Fritzler, M. J., Guo, X., … Arnett, F. C. (2011). Decreased catalytic function with altered sumoylation of DNA topoisomerase I in the nuclei of scleroderma fibroblasts. *Arthritis Research and Therapy*. https://doi.org/10.1186/ar3435

Zhou, Y., Shi, D., Miao, J., Wu, H., Chen, J., Zhou, X., … Xie, C. (2017). PD-L1 predicts poor prognosis for nasopharyngeal carcinoma irrespective of PD-1 and EBV-DNA load. *Scientific Reports*, *7*, 43627. https://doi.org/10.1038/srep43627

Zhu, H., Huang, M., Yang, F., Chen, Y., Miao, Z.-H., Qian, X.-H., … Ding, J. (2007). R16, a novel amonafide analogue, induces apoptosis and G2-M arrest via poisoning topoisomerase II. *Molecular Cancer Therapeutics*. https://doi.org/10.1158/1535-7163.MCT-06-0584

Zuo, J., Currin, A., Griffin, B. D., Shannon-Lowe, C., Thomas, W. A., Ressing, M. E., … Rowe, M. (2009). The Epstein-Barr virus G-protein-coupled receptor contributes to immune evasion by targeting MHC class I molecules for degradation. *PLoS Pathogens*. https://doi.org/10.1371/journal.ppat.1000255

zur Hausen, H. (2009). The search for infectious causes of human cancers: Where and why (Nobel Lecture). *Angewandte Chemie - International Edition*. https://doi.org/10.1002/anie.200901917

Appendix

Appendix tables

Appendix Table 1: Extended SGC compound library information. Information was provided by the SGC, Oxford. SGC – Structural Genomics Consortium, Oxford.

Target	Compound	Dose to achieve IC50-IC90, µM of in-cell 'biochemical' activity
BAZ2A/B	GSK2801	0.1–1
BAZ2A/B	BAZ2-ICR	0.5–1
BRPF1B	PFI-4	0.5–1
BRPF1-3	OF-1	0.5–1
BRPF1-3	NI-57	0.5–1
BET	JQ1	0.001–1
BET	PFI-1	0.001–1
BRD7/9	LP99	0.5–1
BRD9/7	BI-9564	0.2–1
CBP/EP300 bromo	SGCCBP30	0.1–1
CBP/EP300 bromo	ICBP112	0.1–1
Demethylases 2OG dependent	IOX1	0.5–50
DNMTs	5-azacytidine	N/A
Dot1L	SGC0946	0.1–1
EZH2	UNC1999	0.1–3
EZH2	GSK343	0.1–3
G9a	UNC0638	0.1–1
G9a	UNC0642	0.1–1
G9a	A366	0.1–1
HDAC	Chidamide	N/A
HDAC	CXD101	N/A
HDAC	Panobinostat	N/A
HDAC	PXD101	N/A
HDAC	Romidepsin	N/A
HDAC	SAHA	N/A
HDAC	TSA	N/A
JMJD3	GSK J4	0.1–10
L3MBTL3	UNC1215	0.1–1
LSD1	GSKLSD1	0.001–0.005
PAD4	GSK484	0.5–10
pan-BRD	Bromosporine	0.1–1
PARP	Olaparib	N/A

PHD2	IOX2	250
PRMT3	SGC 707	0.5–1
SETD7	PFI-2	0.1–1
Smarca2/4	PFI-3	0.5–1
SMYD2	LLY-507	0.1–1
SMYD2	BAY-598	0.1–1
SUV420H1/H2	A-196	0.2–1
WDR5	OICR-9429	0.5–3

Appendix Table 2: Biochemical inhibition of HDAC1-9 by HDACis (Ki [nM]). Based on Bradner *et al.*, 2010.

Name	HDAC1	HDAC2	HDAC3	HDAC4	HDAC5	HDAC6	HDAC7	HDAC8	HDAC9
CI-994	50	190	550	-	-	-	-	-	-
Chidamide	not reported								
CXD101	not reported								
Dinaline	not reported								
Entinostat	22	65	36	-	-	-	-	-	-
LAQ824	0.55	1.4	4.2	2,250	420	9.5	9,500	340	9,000
Mocetinostat	9	34	265	-	-	-	-	-	-
Panobinostat	1	0.65	1.1	550	80	1.5	4,550	105	3,200
PXD101	0.85	0.85	1.5	380	175	1.6	75	25	25
Romidepsin	0.0015	0.038	0.15	20.5	550	9.5	1,250	0.15	1,100
SAHA	1.3	1.6	5	-	3600	1.6	-	480	-
Trichostatin A	28	42	275	17,000	1,500	16	8,500	170	-

Appendix Table 3: Additional compounds of the extended FDA-approved library. FDA - Food and Drug Administration.

Compounds in the expanded oncology drug set		
Galiellalactone	SR1 HCl	Clomifene citrate
VER 155008	BAY 73-4506_Regorafenib	Tetramisole HCl
RDEA119_Refametinib	Brivanib	1-methyl-D-tryptophan, 95%
GSK2126458	MGCD0103_Mocetinostat	CUDC-101
BIBF 1120_Nintedanib	FK 506_Tacrolimus	Tubastatin A HCl
RD162	4-hydroxytamoxifen	CHIR-258 (Dovitinib)
AVN944	PF-04708671	Nelarabine
AV-951 (Tivozanib)	Camptothecin	(R)-Flurbiprofen (Tarenflurbil)
AZD1480	Docetaxel	Busulfan
MLN8237_Alisertib	Finasteride	Quinacrine HCl
Ridaforolimus	YM155	Aspirin (Acetylsalicylic Acid)
BIRB 796 (Doramapimod)	PHA-739358 (Danusertib)	Iniparib (BSI-201, IND-71677)
VX-11e	PCI-32765_Ibrutinib	TGX-221
ABT-263 (Navitoclax)	CPI-613	ABT-751
BI 2536	GSK 269962	PF4800567 hydrochloride
MDV3100_Enzaluamide	Prednisone	Tandutinib
AZD8055	Enzastaurin	Pemetrexed
OSI-027	Rapamycin (sirolimus)	Arsenic(III) oxide
MK-4827, HCl salt	HA-1077 (Fasudil)	Masitinib
PIK-75 HCl	Flutamide	Bicalutamide
PX-866_Sonolisib	I-BET151 (GSK1210151A)	Rofecoxib (Vioxx)
MK1775	Motesanib Diphosphate (AMG-706)	FG-4592
Epothilone B (Patupilone)	LY2603618_Rabusertib	GSK 650394
AT9283	ABT-869_Linifanib	XAV-939
RAF265	AT 101	Pravastatin
FK-866 HCl_Daporinad	Estramustine sodium phosphate	Valproic acid
AZD4547	Bexarotene	Olaparib
PF-04691502	Lapatinib, di-p-toluenesulfonate salt	CYT-387_Momelotinib
AC220_Quizartinib	Dasatinib	Roscovitine_Selicilib
PLX4032_Vemurafenib	Pilocarpine	Amonafide
LY 333531 mesylate_Ruboxistaurin	Lestaurtinib	Lomeguatrib
Plerixafor	LY2784544_Gandotinib	Indibulin
Everolimus	KX2-391	Prednisolone
XL880 (Foretinib)	LY2157299	Chloroquine diphosphate
MGCD-265	PF 431396	Vismodegib
Bimatoprost	Goserelin acetate	OSI-906_Linsitinib

Dacomitinib (monohydrate) (PF-00299804)	Cisplatin aq	Tasocitinib_Tofacitinib
BMS-754807	Axitinib	17-DMAG (Alvespimycin)
INK128	Nilutamide	Stattic
NVP-LDE225 (Diphosphate salt)	Metformin hydrochloride aq	Vatalanib
Sotrastaurin	Panobinostat	Deferoxamine mesylate
ABT-199	AZD2014	Methylprednisolone
PKC412_Midostaurin	AS703026_Pimasertib	AP24534 (Ponatinib)
LY2228820 (CP868569)	JNJ 26854165 (Serdemetan)	CAL-101
TAK-901	AZ 3146	Bosutinib
2-methoxyestradiol (Panzem)	Doxorubicin	ABT-888 (Veliparib)
EMD1214063	NVP-BEZ235_Dactolisib	Belinostat (PXD101)
GSK2636771	Irinotecan	ZSTK474
INCB018424 (free base, Ruxolitinib)	AZD6244 (Selumetinib)	Thio-TEPA
Atorvastatin Ca	S-trityl-L-cysteine, 40 mM	Melphalan
AG-014699_Rucaparib	Canertinib	Tipifarnib (Zarnestra)
Tubacin	PF-2341066 (Crizotinib)	Dinaciclib (SCH727965)
Homoharringtonine	Obatoclax Mesylate (GX15-070)	GDC-0941_Pictilisib
Nutlin-3	BIIB021	Decitabine (Dacogen)
TAK-733	PF670462	Entinostat
DCC-2036_Rebastinib	Idarubicin HCl	Hydroxyurea
XL184_Cabozantinib	Simvastatin	Aminoglutethimide
MLN4924	CI-994_Tacedinaline	PF-3845
Dabrafenib Mesylate	Abitrexate/Methotrexate	Varespladib
NVP-AUY922	Vorinostat	PAC-1
PF 477736	Lasofoxifene	17-AAG (Tanespimycin, Geldanamycin)
Carfilzomib	Crenolanib	Prima-1 Met
Toremifene citrate	Vincristine Sulfate (Oncovin)	Pazopanib
AT-406	UCN-01	Sorafenib
(5Z)-7-Oxozeaenol	CHR 2797_Tosedostat	Dexamethasone (Decadron)
GDC-0980	PD-0332991	Capecitabine
MK-2206	Anagrelide	GDC-0068
BMS-911543	Nilotinib	ARQ 197_Tivantinib
GSK1120212_Trametinib	Clafen (Cyclophosphamide, Endoxan)	NVP-BGJ398
ARRY-162_MEK-162	Gefitinib	XL-147
AZD 7762 hydrochloride	BIBW2992 (Tovok)_Afatinib	Mithramycin A

BI 6727_Volasertib	MK-0752	Perifosine aq/PBS
R406_Tamatinib	BKM-120_Buparlisib	JNJ-26481585_Quisinostat
SB 743921	Auranofin	AZD1152-HQPA

Appendix Table 4: Complete list of screening hits alone or in combination with chidamide treatment. Compounds were considered as hits with a Z-score ≥ 1.96, Zebra expression levels ≥ 5% and more than 1000 cells per well after treatment. Hits are sorted based on their Zebra expression levels.

Library alone	With chidamide
Pyrvinium pamoate	Daunorubicin
Acrisorcin	Decitabine
Daunorubicin	Quniacrine HCl
Entinostat	Mitoxantrone hydrochloride
PIK-75 HCl	Teniposide
Topotecan	Epirubicin
Nonoxynol-9	Mycophenolate mofetil
Acriflavinium hydrochloride	Topotecan
Teniposide	Thiram
Dichlorophen	Podofilox
Cyclosporine	Paclitaxel
Proflavine hemisulfate	Tioxolone
Amlodipine besylate	Vincristine sulfate
Oxyphenbutazone	Floxuridine
Adapalene	Pentamidine isethionate
Mitoxantrone hydrochloride	Albendazole
Aminacrine	Bufexamac
Ciclopirox olamine	Metitepine maleate
Methylbenzethonium chloride	Acetarsol
Pimozide	Glafenine
Triflupromazine hydrochloride	Chlorpyrifos
Abamectin	
Fluvastatin	
Homidium bromide	
Spiperone	
Alexidine hydrochloride	
Retinyl acetate	
Suxibuzone	
Bleomycin	
Idoxuridine	

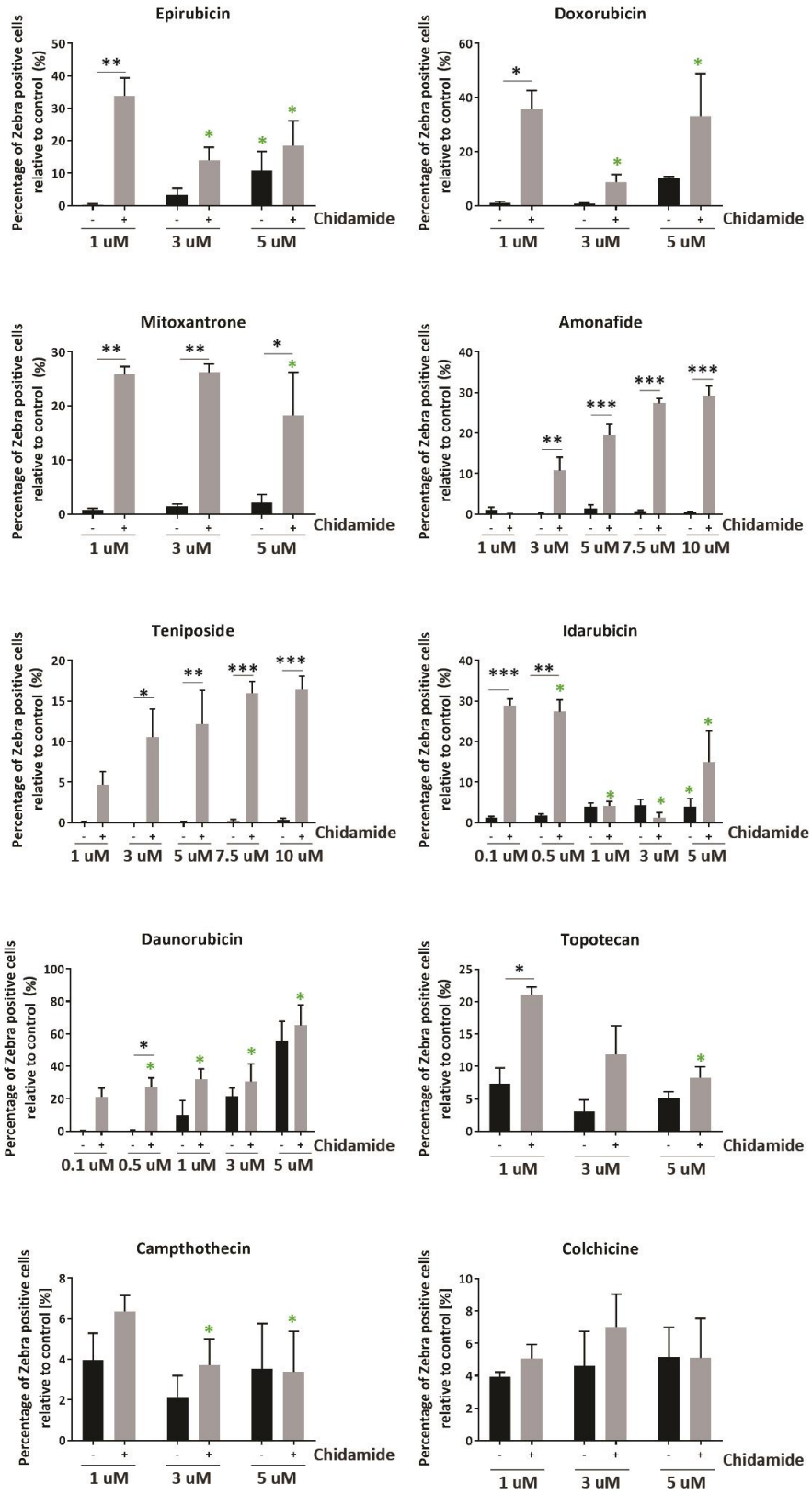
Appendix Table 5: Complete list of all topoisomerase inhibitors included in the extended FDA library. Compound classifications were determined based on the information contained in their PubChem database entry according to (Kim *et al.*, 2016b). Analysis courtesy of Dr Felix Zhou (University of Oxford).

Topoisomerase inhibitors included in extended FDA library		
Amonafide	Erythromycin	Nalidixic acid
Amphotericin B	Etoposide	Norfloxacin
Camptothecin	Flumequine	Novobiocin sodium
Capecitabine	Gatifloxacin	Orbifloxacin
Cinoxacin	Gemifloxacin mesylate	Oxolinic acid
Ciprofloxacin	Genistein	Pefloxacine mesylate
Colchicine	Homoharringtonine	Phenazopyridine
Daunorubicin	Hydrocortisone	Propanolol (+/-)
Deflazacort	Idarubicin	Prulifloxacin
Difloxacin	Irinotecan	Rufloxacin
Docetaxel	Levofloxacin	Sarafloxacin
Doxifluridine	Lomefloxacin	Sparfloxacin
Doxorubicin	Mitoxantrone	Teniposide
Enoxacin	Moxifloxacin	Topotecan
Epirubicin	Nadifloxacin	Vanomycin

Appendix Table 6: *TP53* status in different cell lines. The cDNA of the indicated cell lines was determined as described in Chapter 2.2.3. WT – wild-type.

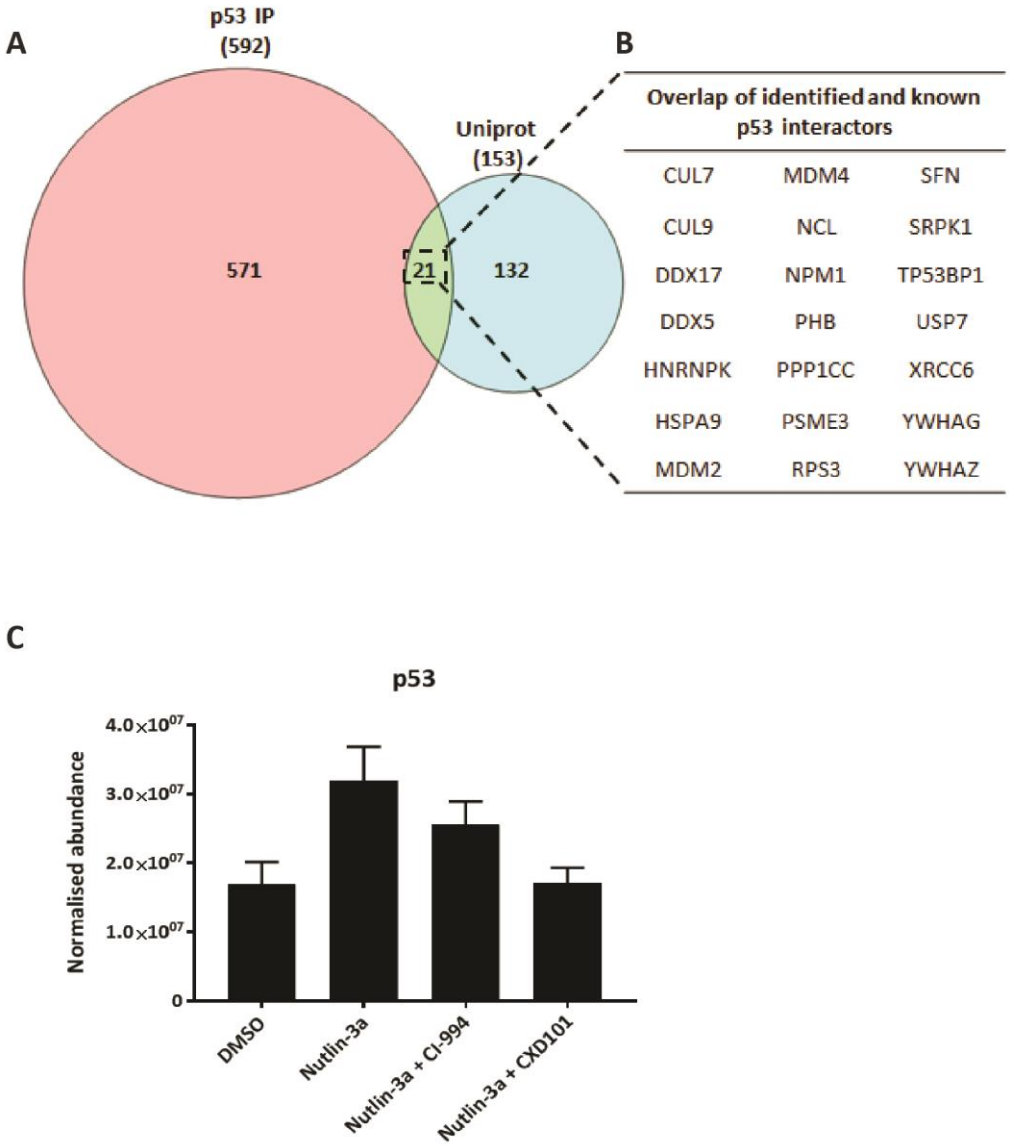
Cell line	TP53 status
AGS rEBV-GFP	WT
SNU719	WT
YCCEL1	WT
NCC-24	R273H
C666.1	WT

Appendix figures



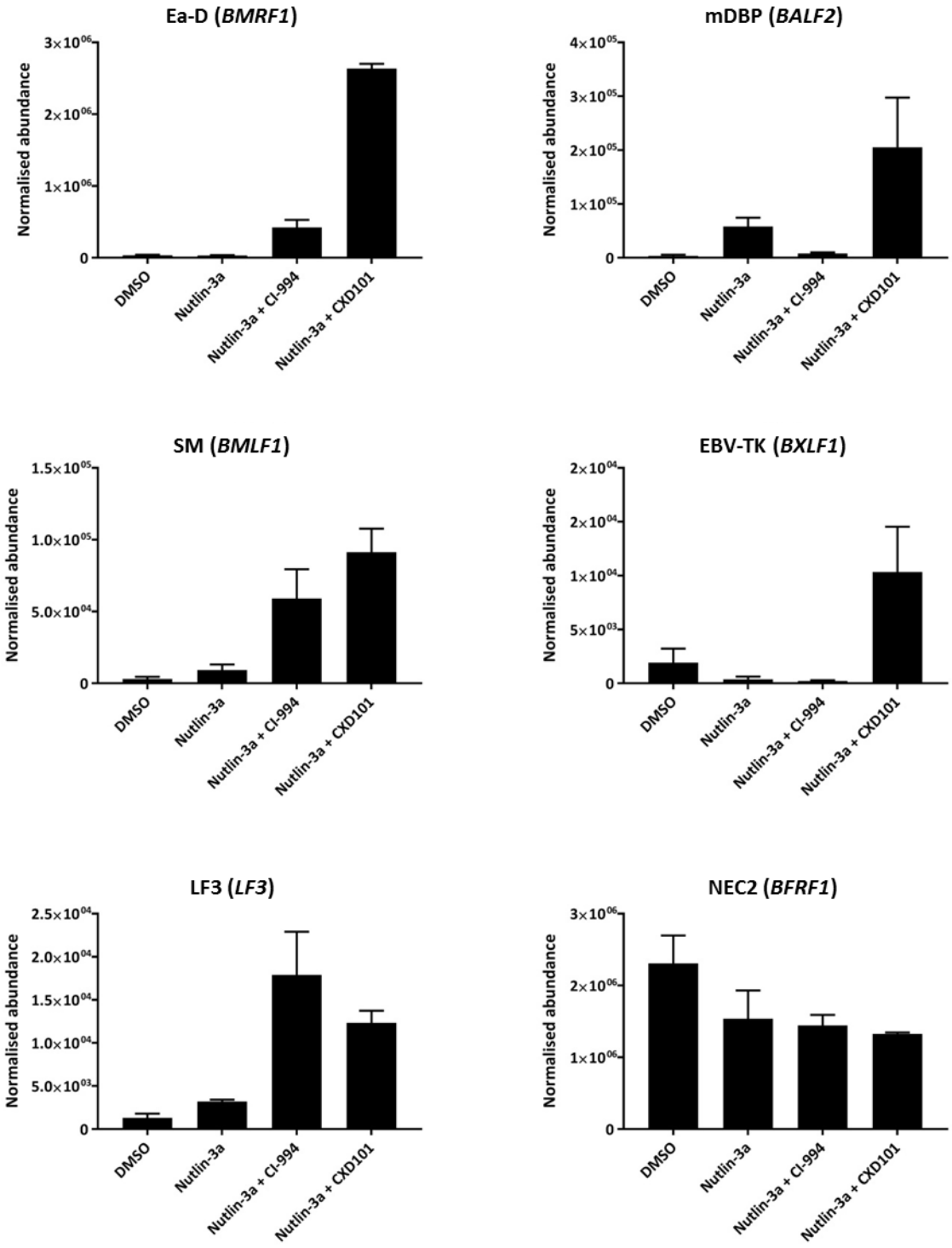
Appendix Figure 1: Percentage of Zebra-expressing cells induced by topoisomerase inhibitor treatment at different concentrations. YCCEL1 cells were treated for 48 h with 2.5 µM chidamide in

combination with the stated topoisomerase inhibitors. Immunofluorescence imaging and analysis by an ImageJ macro (provided by Mark Shipman, University of Oxford) was used to identify the percentage of Zebra-expressing cells. Bars represent the average of three independently performed experiments. *n* = 3, error bars ± SEM. *P** ≤ 0.05; *P*** ≤ 0.01; *P**** ≤ 0.005. Significance was calculated using Sidak's multiple comparison test relative to single compound treatment.



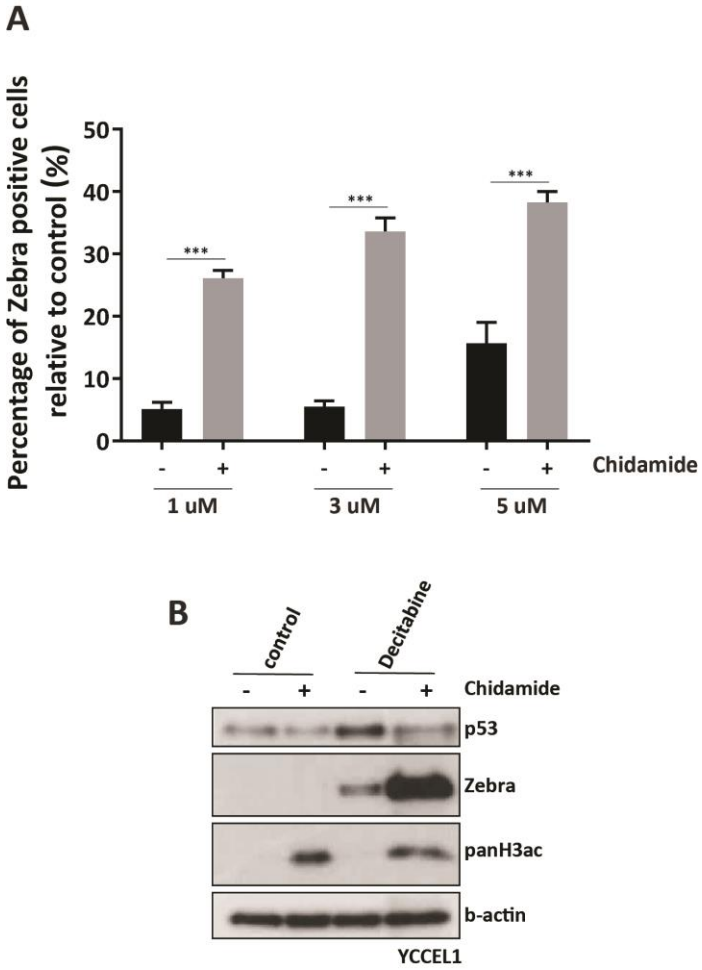
Appendix Figure 2: Comparison of identified and previously reported p53 interactors with examples of their detected abundance. YCCEL1 cells were treated for 48 hours with either DMSO, 5 µM Nutlin-3a, 5 µM Nutlin-3a with 5 µM CI-994 or 5 µM Nutlin-3a with 5 µM CXD101. The subsequent preparation for MS was performed as stated in chapter 2.2.4. A) Venn diagram of all p53 interactors identified by mass spectrometry of a p53 immunoprecipitation experiment in differently treated YCCEL1 cells and known p53 interactors stated on the proteins UniProt entry (UniProt Consortium, 2018). B) Proteins were identified with PEAKS8.5 using the human and EBV database, and quantification was performed with Progenesis using label-free quantification of all identified proteins with the top three peptides of

each identified protein. Bars represent the average of three independently performed experiments. Figures courtesy of Dr Thomas Leissing (University of Oxford). *n* = 3, error bars ± SEM.



Appendix Figure 3: EBV proteins identified to bind p53 after 48 hours of compound treatment and their normalised abundance. YCCEL1 cells were treated for 48 hours with either DMSO, 5 µM Nutlin-3a, 5 µM Nutlin-3a with 5 µM CI-994 or 5 µM Nutlin-3a with 5 µM CXD101. The subsequent preparation for MS was performed as stated in chapter 2.2.4. Proteins identified with PEAKS8.5 using the human and EBV database and quantification was performed with Progenesis using label-free quantification of

all identified proteins with the top three peptides of each identified protein. Bars represent the average of three independently performed experiments and the names in brackets the gene names of the identified proteins. Figures courtesy of Dr Thomas Leissing (University of Oxford). *n* = 3, error bars ± SEM. Ea-D – early antigen diffuse component; EBV-TK – Epstein-Barr virus thymidine kinase; mDBP – major DNA-binding protein; NEC2 – nuclear egress protein 2.



Appendix Figure 4: Percentage of Zebra-expressing cells induced by decitabine treatment at different concentrations. YCCEL1 cells were treated for 48 h with 2.5 µM chidamide in combination with the indicated concentrations of decitabine (3 µM for western blotting). A) Immunofluorescence imaging and analysis by an ImageJ macro (provided by Mark Shipman, University of Oxford) was used to identify the percentage of Zebra-expressing cells. Bars represent the average of three independently performed experiments. *n* = 3, error bars ± SEM. *P** ≤ 0.05; *P*** ≤ 0.01; *P**** ≤ 0.005. Significance was calculated using Sidak's multiple comparison test relative to single compound treatment. B) Western blot analysis of Zebra expression in YCCEL1 cells. Results are representative of three independent repeats of this experiment. panH3ac – acetylated histone H3.

ImageJ macro for the quantification of the Zebra signal per cell

```
run("Set Measurements...", "area integrated redirect=None decimal=3");
var x=100;
var y=10000;
run("Colors...", "foreground=black background=black selection=white");
dir1 = getDirectory("Choose Source Directory ");
dir2 = getDirectory("Choose Destination Directory ");
list = getFileList(dir1);
setBatchMode(false);
notice = "converted: \n";
x = getNumber("Enter minimum object area:", x);
y = getNumber("Enter maximum object area:", y);
for (i=0; i<list.length; i++)
{
showProgress(i+1, list.length);
open(dir1+list[i]);
run("Split Channels");
wait(140);
rename("A546");
wait(140);
run("Put Behind [tab]");
wait(140);
rename("DAPI");
wait(140);
selectWindow("DAPI");
wait(140);
run("Enhance Contrast...", "saturated=0.4 normalize process_all use");
wait(140);
```

```
selectWindow("DAPI");

wait(140);

run("Gaussian Blur...", "sigma=2 stack");

wait(140);

run("8-bit");

run("8-bit");

run("Auto Local Threshold...", "method=Phansalkar radius=15 parameter_1=0 parameter_2=0 white
stack");

wait(140);

selectWindow("A546");

run("Duplicate...", "title=A546-mask duplicate");

rename("A546-mask");

selectWindow("A546-mask");

run("Gaussian Blur...", "sigma=2 stack");

run("Enhance Contrast...", "saturated=0.1 normalize process_all use");

run("8-bit");

run("8-bit");

setAutoThreshold("MaxEntropy dark");

setOption("BlackBackground", true);

run("Convert to Mask", "method=MaxEntropy background=Dark calculate black");

imageCalculator("Add create stack", "DAPI","A546-mask");

////////////////////////////////////////////////////////////////////////////////////////////////////

 n = nSlices();

 for (k=1; k<=n; k++) {

   showProgress(k, n);

wait(140);

selectWindow("Result of DAPI");

wait(140);

setSlice(k);
```

```
run("Select None");
run("Analyze Particles...", "size=x-y show=Nothing clear add slice");
wait(140);
selectWindow("A546");
wait(140);
setSlice(k);
roiManager("Measure");
roiManager("Show None");
roiManager("Show All");
wait(140);
run("Enhance Contrast...", "saturated=0.4 normalize process_slice");
wait(140);
run("Flatten", "slice");
wait(140);
selectWindow("A546-1");
wait(140);
saveAs("Jpeg", dir2+list[i]+"_"+k+"_overlay.jpg");
wait(140);
close();
wait(140);
selectWindow("Results");
wait(140);
saveAs("Measurements", dir2+list[i]+"_"+k+"_nuclear.xls");
wait(140);
selectWindow("Results");
wait(140);
run("Clear Results");
wait(140);
```

```
roiManager("Delete");
wait(140);
   }
////////////////////////////////////////////////////////////////////////////////////////
close();
wait(140);
close();
wait(140);
close();
wait(140);
close();
wait(140);
}
print(notice);
print("min object area=");
print (x);
print("um^2");
print("max object area=");
print (y);
print("um^2");
selectWindow("Log");
saveAs("Text", dir2+"Log.txt");
exit();
```